Melarsoprol Cyclodextrin Inclusion Complexes for the Treatment of Human African Trypanosomiasis

Amy Jones

BSc (Hons) Veterinary Science

University of Glasgow

Submitted in fulfilment of the requirements for the Degree of Doctor of Philosophy

Institute of Infection, Immunity and Inflammation
School of Medical, Veterinary and Life Sciences

April 2011

Abstract

Human African trypanosomiasis (HAT) is a parasitic disease caused by the protozoan parasites *T. b. rhodesiense* and *T. b. gambiense*. The disease is currently endemic in 36 sub-Saharan countries with an estimated 60 million people at risk from the infection. The disease progresses through two stages; an early or haemolymphatic stage where the parasites are confined to the peripheral compartment and a late or encephalitic stage where the parasites penetrate the blood-brain barrier (BBB) and invade the CNS. Without treatment the disease is invariably fatal but at present chemotherapy is reliant on a small handful of drugs. Pentamidine and suramin are available for the treatment of the early stage of the disease while the CNS stage of the disease is treated with a combination of nifurtimox and eflornithine known as NECT therapy or melarsoprol. NECT therapy is only effective in the treatment of *T. b. gambiense* infections meaning treatment of *T. b. rhodesiense* infections is completely dependent on the trivalent arsenical melarsoprol. Melarsoprol is an extremely toxic compound, the administration of which is extremely painful and associated with numerous adverse reactions. The most serious of which is a post treatment reactive encephalopathy (PTRE). The PTRE occurs in up to 10% of all patients given melarsoprol. Half of all patients who develop the PTRE will die as a result of the compliciation. This gives melarsoprol chemotherapy an overall fatality rate of 5% which is unacceptably high. There is therefore an urgent need for new, safe and easily administrable trypanocides.

To improve the physiochemical and pharmacokinetic properties of melarsoprol the drug was complexed with two cyclodextrin molecules, hydroxypropyl-β-cyclodextrin (HPβCD) and randomly methylated-β-cyclodextrin (RAMβCD) to produce; mel/HPβCD and mel/RAMβCD. Cyclodextrins are cyclic oligosaccharides, widely used within the pharmaceutical industry to improve the solubility and oral bioavailability of poorly soluble lipophilic drugs. In this study, the trypanocidal activity of the melarsoprol cyclodextrin complexes was investigated *in-vitro* and in an *in-vivo* CNS stage model of *T. b. brucei* infection. *In-vitro* studies showed that the trypanocidal activity of melarsoprol is retained following its complexation with HPβCD and RAMβCD. The *in-vitro* trypanocidal activity of the melarsoprol cyclodextrin complexes against bloodstream *T. b.*

brucei trypanosomes was comparable to that of contemporary melarsoprol. Furthermore, in an *in-vivo* murine model of CNS stage *T. b. brucei* the melarsoprol cyclodextrin complexes, mel/HPβCD and mel/RAMβCD produced 100% cure rates when administered orally at a dose of 0.05 mmol/kg, daily, for seven consecutive days. Contemporary melarsoprol when administered by the same route and schedule only cured 33.3% of the animals. The cyclodextrins HPβCD and RAMβCD thus increase the oral bioavailability of melarsoprol whilst retaining the compounds trypanocidal activity. An oral administrable, water soluble formulation of melarsoprol instantly eliminates the problems associated with the intravenous administration of conventional melarsoprol. Furthermore, an orally available formulation would be of great benefit in the resource poor, isolated settings in which HAT occurs as patients would not require hospitalisation during treatment thus alleviating the pressure on local hospitals.

In the current investigation quantitative taqman PCR was utilised to investigate the rate of parasite clearance from the CNS during complexed melarsoprol treatment. Both mel/HPβCD and mel/RAMβCD were rapidly trypanocidal. Twenty-four hours after administration of one dose the number of trypanosomes within the brain was reduced by greater than 80% and all trypanosomes were eliminated from the brain by twenty-four hours after administration of four doses of mel/HPβCD and five doses of mel/RAMβCD. The elimination of all trypanosomes from the CNS following four doses of mel/HPβCD and five doses of mel/RAMβCD, indicates that it may be possible to reduce the dosage schedule from seven daily doses to four daily doses of mel/HPβCD and five doses of mel/RAMβCD. A short, simple, easily administrable treatment protocol is an essential requirement of any new trypanocide as if the treatment schedule is prolonged and complicated patients are unlikely to comply.

CNS stage trypanosome infection is associated with a breakdown of the blood-brain barrier (BBB). Ideally following successful chemotherapy BBB function should be restored. In this investigation the effect of a curative mel/HPβCD treatment regime on the BBB was investigated in a murine model of CNS *T. b. brucei* infection using small bore MRI analysis. Mel/HPβCD treatment results in a rapid restoration of BBB function as by twenty-four hours after the completion of mel/HPβCD therapy the integrity of the BBB was fully restored. However, a very

mild neuroinflammatory reaction persisted in the brain for up to fifteen days after completion of chemotherapy. This suggests that the BBB damage observed in trypanosome infection may be due to either the parasites directly or their secretory products and not as a result of the ongoing neuroinflammatory reaction.

Despite melarsoprol being in use for over 60 years its pharmacokinetics are poorly understood and a sensitive assay by which to quantify the concentration of arsenic reaching tissues following administration of the compound is not available. In this study a gas chromatography mass spectrometry (GC-MS) technique was developed to quantify the concentration of arsenic reaching the plasma and brain following oral and intravenous administration of the melarsoprol cyclodextrin complexes, mel/HPβCD and mel/RAMβCD. The GC-MS assay had a limit of detection of 5ng/ml and a precision (expressed as the inter-day coefficient of variation) of 13.2%. The concentration of arsenic within the brain following the oral and intravenous administration of mel/HPβCD was below the limit of quantification of the assay. The pharmacokinetics of mel/HPβCD and mel/RAMβCD could therefore not be determined in the present study.

This study demonstrates that the melarsoprol cyclodextrin complexes mel/HPβCD and mel/RAMβCD are highly trypanocidal with no overt signs of toxicity and more importantly are orally available. Following the oral administration of mel/HPβCD or mel/RAMβCD the melarsoprol is slowly released over a prolonged period of time from the cyclodextrin cavity. Patients are therefore not exposed to a 'bolus' of the drug as is the case in the intravenous administration of contemporary melarsoprol. The slow and sustained release of melarsoprol from the cyclodextrins should result in less adverse reactions and a decreased incidence of the PTRE. Furthermore, the complexed melarsoprol treatment protocol is shorter than the currently used 10 day concise melarsoprol treatment schedule therefore the total amount of melarsoprol administered to patients will be reduced. Patients should therefore experience fewer adverse reactions. In conclusion the results from this study demonstrate that the melarsoprol cyclodextrin complexes mel/HPβCD and mel/RAMβCD are promising oral candidates for the treatment of HAT.

“Our greatest glory is not in never falling, but in rising every time we fall”

Confucius

Dedicated to mum, my shining light and inspiration x

Acknowledgements

First and foremost I would to thank my supervisors Dr Jean Rodgers and Prof. Peter Kennedy for their unwavering support and encouragement over the last three and a half years. I am eternally grateful to Jean for her constant guidance, reassurance and patience, especially over the last few months while writing up, without which I would never have reached the end. I would also like to acknowledge Barbara Bradley for all her help and support both in the lab and outside. Without her help and patience, long days in the unit would have turned into even longer nights. Thank you.

A proportion of this work would not have been completed without the contributions of several collaborators. I am extremely grateful to Dr Stèphane Gibaud, of Nancy Universitè for developing the melarsoprol cyclodextrin complexes and for making me feel extremely welcome in his laboratory. At the University of Strathclyde, Department of Pharmacy I would like to thank Prof. Alex Mullen for all his helpful, enthusiastic and animated discussions and also Dr Fitsum Araya for showing me the 'ropes' in the laboratory. I would also like to acknowledge Prof. George Gettinby for assisting with the statistical analysis conducted in this thesis. With the help of tea and biscuits he made the world of statistics seem a less daunting place.

I would also like to thank all the past and present members of the trypanosomiasis group and the department of veterinary parasitology for making the laboratory and department a pleasure to work in, and for providing an endless supply of cakes!

I would like to thank all my friends and family for being a constant source of support and encouragement both through the good times and the bad. I would especially like to thank Lesley for always being no more than a phone call away. Her kind words and reassurances saw me through the low points. Finally, I would like to thank my Dad for his endless and unconditional love, support, encouragement and constant belief in me over the last few years, without which I would not be where I am today.

Declaration

I declare that this thesis and the results presented within it are entirely my own work.

No part of this thesis has been previously submitted for a degree at any other institution.

Amy Jones

Supporting oral presentations

Jones, A., Rodgers, J., Bradley, B., Barrett, M. P. and Kennedy (2010). Complex melarsoprol; a possible oral therapy for the treatment of human African trypanosomiasis. *Nanotryp consortium meeting*. 23rd September 2010 Paris, France

Jones, A., Rodgers, J., Bradley, B., Barrett, M. P. and Kennedy (2010). Complex melarsoprol; a possible oral therapy for the treatment of human African trypanosomiasis. *X11th International Congress of Parasitology*. 15th – 20th August 2010 Melbourne.

Jones, A., Rodgers, J., Bradley, B., Barrett, M.P. and Kennedy, P.G.E (2010) Complex melarsoprol: a promising candidate in the treatment of human African trypanosomiasis. *Faculty of Biomedical and Life Sciences Seminar Series*.

Jones, A., Rodgers, J., Bradley, B., Kennedy, P.G.E (2009). Melarsoprol cyclodextrin inclusion complexes. *Faculty of Veterinary Medicine, Division of Infection and Immunity Seminar Series*.

Jones, A., Rodgers, J., Bradley, B., Kennedy, P.G.E (2009). Novel approaches to chemotherapy in a murine model of human African trypanosomiasis. *Faculty of Veterinary Medicine Annual Postgraduate Pfizer Prize*.

Supporting poster presentations

Jones, A., Rodgers, J., Bradley, B., Barrett, M.P. and Kennedy, P.G.E. (2010). Complex melarsoprol: A promising candidate in the treatment of human African trypanosomiasis. *British Society for Parasitology Spring and Trypanosomiasis and Leishmaniasis meeting*. 29th March -1st April 2010 Cardiff.

Jones, A., Rodgers, J., Bradley, B., Barrett, M.P. and Kennedy, P.G.E. (2009). Oral Melarsoprol cures CNS stage *Trypanosoma brucei brucei* infection in a murine model of human African trypanosomiasis P139. *British Society for Parasitology Spring and Malaria meeting*. 5th-8th April 2009 Edinburgh.

Jones, A., Rodgers, J., Bradley, B. and Kennedy, P.G.E. (2008) Novel forms of oral melarsoprol cure CNS stage *Trypanosoma brucei brucei* infection in a murine model of human African trypanosomiasis. *Infectious disease of the nervous system: Pathogenesis and worldwide impact*. 10-13th September 2008 Paris, France. Published in; BMC proceedings 2008, 2 (Suppl 1):P28.

Abbreviations

AAS	Atomic absorption spectrometry
AE	Elution buffer
ALT	Alanine aminotransferase
AP	Alkaline phosphatase
APES	3-aminopropyltriethoxysilane
APL	Acute promyeloctic leukaemia
ASPT1	Adenosine sensitive pentamidine transporter
AST	Aspartate
ATP	Adenosine triphosphate
BBB	Blood-brain barrier
BMECs	Brain microvascular endothelial cells
BSA	Bovine serum albumin
CaM	Calmodulin
CATT	Card agglutination test for trypanosomiasis
CCK	Cholecystokinin
CD	Cyclodextrin
cDNA	Complementary deoxyribonucleic acid

CGTase	Cyclodextrin glycosyl transferase
C_{max}	Maximum concentration
CNS	Central nervous system
CSF	Cerebrospinal fluid
DAB	3, 3' diaminobenzidine
DALYs	Disability adjusted life years
DB289	Pafuramidine maleate
DFMO	Eflornithine
DMEβCD	Dimethyl β cyclodextrin
DMSO	Dimethyl sulfoxide
DNA	Deoxyribonucleic acid
DNDi	Drugs for neglected diseases initiative
DRC	Democratic Republic of Congo
DRC-ICP-MS	Dynamic reaction cell inductively coupled mass spectrometry
ED	Effective concentration
EI	Electron impact
ELISA	Enzyme-linked immunosorbent assay
FAM	6-carboxyfluorescine
FDA	Food and Drug administration

FITC	Fluorescein isothiocyanate
FOV	Field of view
GC-MS	Gas chromatography mass spectrometry
GI	Gastrointestinal tract
GLDH	Glutamate dehydrogenase
GLM	General linear model
GOT	Glutamic oxaloacetic
GPT	Glutamic pyruvic
HAPT1	High affinity pentamidine transporter
HAT	Human African trypanosomiasis
H&E	Haematoxylin and eosin
HIV	Human immunodeficiency virus
HPβCD	Hydroxyproyl β cyclodextrin
HPLC	High performance liquid chromatography
HRP	Horseradish peroxidise
IC	Inhibitory concentration
ICCT	Institute for Combat and Control of trypanosomiasis
ICP-MS	Inductively coupled plasma mass spectrometry
I.V.	Intravenous

JPC	Japanese Pharmaceutical codex
LAPT1	Low affinity pentamidine transporter
LC	Liquid chromatography
LD	Lethal dose
mAECT	Mini anion exchange centrifugation technique
Mel Cy	Cymelarsan
Mel W	Trimelarsen
MHCT	Micro haematocrit centrifugation technique
MIC	Minimum inhibitory concentration
MLCK	Myosin light chain kinase
mRNA	Messenger ribonucleic acid
MS	Multiple sclerosis
M_t	Transverse magnetization
MTT	Tetrazolium salt method
M_z	Longitudinal magnetization
NBT/BCIP	5-bromo-4-chloro-3-indolyl phosphate/nitro blue tetrazolium
NECT	Nirfurtimox eflornithine combination therapy
NFOH	Hydroxymethylnitrofurazone
NMR	Nuclear magnetic resonance

NMT	N-myristoyltransferase
NOAEL	No observed adverse effect level
NSAID	Non steroidal anti-inflammatory drug
NSHS	Normal sheep serum
NVU	Neurovascular unit
NWV	Net magnetization
OCT	Ornithine carbamoyl transferase
OD	Optical density
ODC	Ornithine decarboxylase
OVA	Ovalbumin
PAP	Peroxidase anti-peroxidase
PAR	Protease activated receptor
PBS	Phosphate buffered saline
PCR	Polymerase chain reaction
PFR	Paraflagella rod
PGBS	Phosphate glucose buffered saline
PgMET	Plasmodium tRNA methionine
Ph.Eur.	European Pharmacopoeia
PPM	Parts per million

PTRE	Post treatment reactive encephalopathy
QBC	Quantitative buffy coat
QPCR	Quantitative polymerase chain reaction
RAMβCD	Randomly-methylated β cyclodextrin
RARE	Rapid acquisition with relaxation enhancement
RBC	Red blood cells
RF	Radiofrequency
RNA	Ribonucleic acid
RNA_i	Ribonucleic acid interference
RPM	Revolutions per minute
SBEβCD	Sulfobutylether β cyclodextrin
SIM	Single ion mode
SSC	Salt sodium citrate
$t_{1/2}$	Terminal elimination half-life
TAMRA	6-carboxy-tetramethyl-rhodamine
TE	Echo time
TEER	Transendothelial electrical resistance
TMβCD	Trimethyl β cyclodextrin
TR	Repetition time

tRNA	Transfer ribonucleic acid
TSA	Tyramdie signal amplification
USP/NF	US Pharmacopoeia
$V_{D\beta}$	Volume of distribution
VSG	Variable surface glycoprotein
WHO	World health organisation
w.t.	Wild type

Table of contents

List of figures ..... **xxviii**
List of tables ..... **xxxi**
List of equations ..... **xxxiii**

Chapter 1: Introduction **1**

1.1 The Trypanosomiases 2
1.1.1 Classification 2
1.1.2 Parasite biology 2
1.1.2.1 Antigenic variation 6
1.1.3 Trypanosomes of veterinary importance 6
1.1.4 Trypanosomes of medical importance 7
1.1.4.1 American 7
1.1.4.2 African 7
1.1.5 African trypanosomes 9
1.1.5.1 History 9
1.1.5.2 Geographical distribution 11
1.1.5.3 The vector 13
1.1.5.4 Life cycle 13
1.1.6 Trypanosomiasis in man 14
1.1.6.1 Current situation of HAT 14
1.1.6.2 Pathogenesis 16
1.1.6.2.1 Haemolymphatic 16
1.1.6.2.2 Specific organ damage 17
1.1.6.2.3 Central nervous system pathology 18
1.1.6.3 Clinical signs 19
1.1.6.3.1 Haemolymphatic manifestations 19
1.1.6.4 Central nervous system manifestations 21
1.1.6.5 Diagnosis 22
1.1.7 Chemotherapy 26
1.1.7.1.1 Haemolymphatic infection 26
1.1.7.1.2 Suramin 26
1.1.7.1.3 Pentamidine 27
1.1.7.2 CNS infection 29

1.1.7.2.1 Melarsoprol 29
1.1.7.2.2 Eflornithine (α difluoromethylornithine) (DFMO) 33
1.1.7.2.3 Nifurtimox 35
1.1.7.2.4 Nifurtimox and eflornithine combination therapy (NECT) .. 36
1.1.7.3 Emerging treatments 37
1.1.7.3.1 DB289 37
1.1.7.3.2 Fexinidazole 38
1.1.7.3.3 N-myristoyltransferase inhibitors 39
1.1.7.3.4 Oxaborole 6-carboxamides 40
1.1.7.4 The future of HAT chemotherapy 40
1.2 Cyclodextrins: Enabling excipients 41
1.2.1 History 41
1.2.2 Structure 42
1.2.3 Physicochemical properties 44
1.2.4 Production 45
1.2.4.1 Enzymology 45
1.2.4.1.1 The cyclization reaction 46
1.2.4.2 Industrial production 46
1.2.4.2.1 The solvent process 48
1.2.4.2.2 The non-solvent process 48
1.2.5 Cyclodextrin derivatives 49
1.2.5.1 Production of cyclodextrin derivatives 50
1.2.5.1.1 Methylated cyclodextrins 51
1.2.5.1.2 Hydroxypropyl β cyclodextrin (HPβCD) 51
1.2.6 Cyclodextrin Complexes 52
1.2.6.1 Mechanism of inclusion 52
1.2.6.2 The driving force of complex formation 53
1.2.6.2.1 Release of high enthalpy water molecules 53
1.2.6.2.2 Release of ring strain 54
1.2.6.2.3 Van der Waals forces 54
1.2.7 Toxicity of cyclodextrins 54
1.2.7.1 Cytotoxicity 54
1.2.7.2 Parenteral toxicity 55
1.2.7.2.1 Alpha (α) cyclodextrin 55
1.2.7.2.2 Beta (β) cyclodextrin 55

1.2.7.2.3 Gamma (γ) cyclodextrin 56
1.2.7.2.4 Hydroxypropyl β cyclodextrin (HPβCD) 56
1.2.7.3 Oral toxicity 57
1.2.7.3.1 Alpha (α) cyclodextrin 57
1.2.7.3.2 Beta (β) cyclodextrin 58
1.2.7.3.3 Gamma (γ) cyclodextrin 59
1.2.7.3.4 Hydroxypropyl β cyclodextrin (HPβCD) 59
1.2.7.3.5 Di-methyl β cyclodextrin (DMβCD) 61
1.2.8 Pharmacological uses of cyclodextrins 61
1.2.8.1 Decreasing toxicity 61
1.2.8.2 Stability 62
1.2.9 Current regulatory status 63

Chapter 2: General methods 65

2.1 Trypanosomes 66
2.1.1 The history of T. brucei brucei stabilate GVR35 66
2.2 The murine model of *T. b. brucei* 66
2.2.1 Animals 67
2.2.2 Establishing trypanosome infection 67
2.2.3 Monitoring of parasitaemia 68
2.3 Complexed melarsoprol 68
2.3.1 Preparation of complexed melarsoprol 68
2.3.2 Characterisation of melarsoprol cyclodextrin complexes 70
2.3.3 Calculation of complexed melarsoprol doses for oral administration 70
2.3.4 Calculation of volume of melarsoprol cyclodextrin complexes to be orally administered 71
2.3.5 Calculation of complexed melarsoprol dose for intravenous administration 71
2.3.6 Calculation of the volume of mel/HPβCD to be intravenously administered 72
2.3.7 Preparation of melarsoprol cyclodextrin complexes for administration 72
2.3.8 Oral administration of melarsoprol cyclodextrin complexes 73

2.3.9 Intravenous administration of mel/HPβCD 73

Chapter 3: Establishing the inhibitory concentration and minimum curative dose of complexed melarsoprol 74

3.1 Introduction 75
3.1.1 Melarsoprol 75
3.1.1.1 Melarsoprol derivatives 75
3.1.2 The pharmacological uses of cyclodextrins 77
3.1.2.1 Increasing solubility 77
3.1.2.1.1 A-type profiles 78
3.1.2.1.2 B-type profiles 78
3.1.2.2 Increasing bioavailability 79
3.1.3 Melarsoprol cyclodextrin complexes 83
3.2 Methods 85
3.2.1 Assessing the inhibitory concentration of complexed melarsoprol 85
3.2.1.1 Preparation of stock solutions 85
3.2.1.2 Preparation of working solutions 85
3.2.1.3 Culturing of trypanosomes 85
3.2.1.4 Alamar blue assay 86
3.2.1.4.1 Preparation of Alamar blue solution 86
3.2.1.4.2 Alamar blue assay 86
3.2.1.5 Statistical analysis 88
3.2.2 Determining the in-vivo trypanocidal activity of complexed melarsoprol and melarsoprol compounds 88
3.2.2.1 Establishing *T. b. brucei* infection in mice 88
3.2.2.2 Preparation of compounds for oral administration 88
3.2.2.3 Preparation of Mel/HPβCD for intravenous administration . 89
3.2.2.4 Chemotherapy schedules 89
3.2.2.4.1 Oral administration of compounds 89
3.2.2.4.2 Intravenous administration of mel/HPβCD 89
3.2.2.5 Assessing the effectiveness of chemotherapy 90
3.2.3 Determining the hepatic toxicity of complexed melarsoprol 91

3.2.3.1 Chemotherapy schedules 91
3.2.3.2 Collection of samples 91
3.2.3.3 Preparation of samples for histopathology analysis 91
3.2.3.4 Histopathological analysis 91
3.3 Results 93
3.3.1 Inhibitory concentration (IC_{50}) of complexed melarsoprol.. 93
3.3.2 The minimum oral curative dose of complexed melarsoprol.. 93
3.3.3 The minimum intravenous curative dose of mel/HPβCD.... 96
3.3.4 *In-vivo* trypanocidal activity of melarsoprol compounds ... 96
3.3.5 Hepatotoxicity of complexed melarsoprol 98
3.3.5.1 Immediately following completion of the treatment regime.. 98
3.3.5.2 Seven days after completion of chemotherapy..... 98
3.3.5.3 Fourteen days after completion of chemotherapy..... 99
3.3.5.4 Twenty-one days after completion of chemotherapy 100
3.4 Discussion 101

Chapter 4: Detection of trypanosomes within the brain 108

4.1 Introduction 109
4.1.1 Location of trypanosomes in the brain 109
4.1.2 In-situ hybridization 112
4.1.2.1 Detection of *Trypanosoma cruzi*.....112
4.1.3 Quantitative PCR (QPCR) 113
4.1.3.1 Principles of taqman real-time PCR.....113
4.1.3.2 Current uses of QPCR.....116
4.1.3.2.1 Diagnostics.....116
4.1.3.2.2 Assessing efficacy of chemotherapy 117
4.1.4 Melarsoprol resistance 117
4.2 Methods 119
4.2.1 Melarsoprol resistant (GVR35/M14) T. b. brucei strain 119
4.2.2 Establishing infection with GVR35/M14 119
4.2.3 Establishing infection with GVR35/C1.9.....119
4.2.4 Confirmation of trypanosome infection 120

4.2.5 Preparation of melarsoprol cyclodextrin complexes 120
4.2.6 Administration of complexes.....120
4.2.7 In-situ hybridization 121
4.2.7.1 Treatment schedule 121
4.2.7.2 Collection of samples 121
4.2.7.3 Preparation of samples for in-situ hybridization 121
4.2.7.4 In-situ hybridization procedure 122
4.2.7.4.1 Oligonucleotide probe.....122
4.2.7.4.2 Dewaxing and rehydration of the tissue sections 122
4.2.7.4.3 Permeabilisation of the tissue sections.....123
4.2.7.4.4 Fixation of tissue sections 124
4.2.7.4.5 Denaturation of the target sequence 124
4.2.7.4.6 Hybridization 124
4.2.7.4.7 Post-hydridization washes 124
4.2.7.4.8 Visualisation 125
4.2.7.4.9 Tyramide signal amplification system (TSA™ PerkinElmer) ... .126
4.2.8 Quantitative PCR.....127
4.2.8.1 Treatment schedule 127
4.2.8.2 Collection of samples 128
4.2.8.3 DNA extraction 128
4.2.8.4 Quantification of DNA 129
4.2.8.5 Identification of gene of interest.....129
4.2.8.6 Generation of a plasmid containing the PFR2 gene.....130
4.2.8.7 Resuspension of plasmids 130
4.2.8.8 Transformation of cells with PFR2 plasmid 131
4.2.8.9 Purification of the plasmid 131
4.2.8.10 Quantification of purified plasmid DNA 132
4.2.8.11 Calculation of the plasmid copy number contained within ... the purified plasmid DNA 132
4.2.8.12 Preparation of standard dilutions for the standard curve .133
4.2.8.13 Preparation of primers and probe 133
4.2.8.14 QPCR reaction 133
4.2.8.15 Statistical analysis 134
4.3 Results.....135

4.3.1 In-situ hybridization 135
4.3.2 QPCR 135
4.3.2.1 *T. b. brucei* melarsoprol sensitive strain (GVR 35/C1.9) ... 135
4.3.2.1.1 The effect of mel/HPβCD treatment on CNS parasite load 135
4.3.2.1.2 The effect of mel/RAMβCD treatment on CNS parasite load 136
4.3.2.1.3 Comparison of mel/HPβCD and mel/RAMβCD treatment .. 138
4.3.2.2 *T. b. brucei* melarsoprol resistant strain (GVR35/M14) 141
4.3.2.2.1 The effect of mel/HPβCD treatment on CNS parasite load 141
4.3.2.2.2 The effect of mel/RAMβCD chemotherapy on CNS parasite .. load 141
4.3.2.2.3 Comparison of mel/HPβCD and mel/RAMβCD treatment .. 142
4.3.2.3 Comparison of the melarsoprol sensitive and resistant strains 144
4.4 Discussion 149

Chapter 5: Visualisation of the changes in permeability of the blood-brain barrier following complexed melarsoprol chemotherapy 157

5.1 Introduction 158
5.1.1 Barriers of the CNS 158
5.1.1.1 The blood-brain barrier 158
5.1.1.2 The blood–CSF barrier 160
5.1.1.3 Arachnoid barrier 160
5.1.2 Trypanosomes and the blood-brain barrier 162
5.1.2.1 Trypanosome traversal of the BBB 162
5.1.2.1.1 *In-vitro* blood-brain barrier studies 162
5.1.2.1.2 *In-vivo* blood-brain barrier studies 163
5.1.2.2 Breakdown of the blood-brain barrier during trypanosome infection 164
5.1.3 Magnetic resonance imaging 166
5.1.3.1 Principles of magnetic resonance imaging 166
5.1.3.2 The use of contrast agents 168
5.1.3.3 Magnetic resonance imaging of the CNS in disease 168
5.1.3.3.1 Multiple sclerosis 169

5.1.3.3.2 Cerebral malaria 169
5.1.3.3.3 Human African trypanosomiasis..... 170
5.2 Methodology 174
5.2.1 Trypanosome infection..... 174
5.2.2 Confirmation of trypanosome infection 174
5.2.3 Preparation of complexed melarsoprol for administration 174
5.2.4 The treatment schedule employed..... 174
5.2.5 Magnetic resonance imaging 175
5.2.5.1 Preparation of animals..... 175
5.2.5.2 Magnetic resonance imaging parameters..... 175
5.2.5.3 Analysis of magnetic resonance images 176
5.2.6 Collection of samples for analysis of inflammatory reaction.. 176
5.2.7 Preparation of samples for analysis of inflammatory reaction 176
5.2.8 Analysis of inflammatory reaction 177
5.2.9 Statistical analysis..... 177
5.3 Results..... 179
5.3.1 MRI 179
5.3.1.1 Comparison of the signal change detected on day 21 post-infection and in uninfected animals 179
5.3.1.2 Comparison of the percentage signal change detected on day 21 post-infection and following completion of mel/HPβCD chemotherapy 181
5.3.1.3 Comparison of the percentage signal change detected 24 hours, 8 and 15 days after completion of mel/HPβCD chemotherapy 183
5.3.2 Neuropathological reaction 185
5.4 Discussion 189

Chapter 6: Investigating the pharmacokinetic properties of complexed melarsoprol 194

6.1 Introduction 195
6.1.1 Pharmacokinetics of melarsoprol..... 195

6.1.1.1 Original bioassay 195
6.1.1.2 ELISA 196
6.1.1.3 Long-term bioassay 197
6.1.1.4 Automated biological assay 201
6.1.1.5 High performance liquid chromatography assay 202
6.1.1.6 Comparing bioassay and HPLC approaches 203
6.1.2 Melarsoprol metabolites 204
6.1.3 Pharmacokinetics of complexed melarsoprol 206
6.2 Methods 208
6.2.1 Establishing *T. b. brucei* infection 208
6.2.2 Confirmation of trypanosome infection 208
6.2.3 Preparation of complexed melarsoprol for oral administration 208
6.2.4 Preparation of mel/HPβCD for intravenous administration 208
6.2.5 Oral administration of complexed melarsoprol 209
6.2.6 Intravenous administration of mel/HPβCD 209
6.2.7 Treatment schedule 209
6.2.7.1 Oral administration 209
6.2.7.2 Intravenous administration 209
6.2.8 Collection of samples 210
6.2.9 Determining the arsenic content of tissue samples by gas chromatography mass spectrometry 211
6.2.9.1 Digestion of tissues 211
6.2.9.2 Resuspension of digestion residue 211
6.2.9.3 Gas chromatography mass spectrometry analysis 212
6.2.9.4 Assay validation 213
6.2.9.4.1 Constructing an arsenic standard curve 213
6.2.9.4.2 Determining the precision (repeatability) of the assay 213
6.2.9.4.3 Extraction recovery 213
6.3 Results 215
6.3.1 Chromatograms 215
6.3.2 Calibration curve 215
6.3.3 Precision of the assay 218
6.3.4 Extraction recovery 218
6.3.5 Concentration of arsenic within the brain 219

6.3.6 Concentration of arsenic within the plasma 219
6.4 Discussion 222

Chapter 7: General Discussion 229

7.1 The trypanocidal activity of mel/HPβCD and mel/RAMβCD 230
7.2 The effect of mel/HPβCD chemotherapy on the integrity of . the blood-brain barrier 235
7.3 Future work 236
7.4 Conclusions 238
Appendix 1 241
Appendix 2 244
Appendix 3 249
References 253

List of figures

Figure 1-1: The systematic classification of trypanosomes in use today..... 4
Figure 1-2: A diagram of the trypomastigote intermediate bloodstream form of *T. b. rhodesiense* 5
Figure 1-3: A map illustrating the geographical distribution of the human infective trypanosomes *T. b. gambiense* and *T. b. rhodesiense*. 12
Figure 1-4: The life cycle of *Trypanosoma brucei* spp..... 15
Figure 1-5: The chemical structure of suramin 26
Figure 1-6: The chemical structure of pentamidine 28
Figure 1-7: The chemical structure of melarsoprol 30
Figure 1-8: The chemical structure of eflornithine 34
Figure 1-9: The chemical structure of nifurtimox..... 36
Figure 1-10: The chemical structure of fexinidazole..... 39
Figure 1-11: The truncated cone and chemical structure of β cyclodextrin... 44
Figure 1-12: Schematic representation of the cyclization reaction..... 47
Figure 1-13: The mechanism of inclusion complex formation 52
Figure 2-1: The grading scale used to score the level of parasitaemia in the experimental animals..... 69
Figure 3-1: The possible phase-solubility profiles obtained following complexation of a guest molecule with a cyclodextrin..... 79
Figure 3-2: The absorption of a drug from an inclusion complex following oral administration. 82
Figure 3-3: The flow process used in the Alamar blue assay 87
Figure 3-4: The treatment schedule used 91
Figure 3-5: The IC_{50} of the compounds against wild type (s427) *T. b. brucei* trypanosomes 94
Figure 3-6: The number of animals relapsed at each dose after receiving mel/HPβCD, mel/RAMβCD, HPβCD or RAMβCD 97
Figure 3-7: The *in-vivo* trypanocidal activity of melarsoprol compounds in murine CNS stage *T. b. brucei* model 97
Figure 3-8: The histopathological changes observed in the liver immediately after administration of HPβCD 98

Figure 3-9: The histopathological changes observed in the liver 7 days after completion of mel/HPβCD (A), RAMβCD (B), HPβCD (C) and mel/RAMβCD (D) chemotherapy 99
Figure 3-10: The histopathological changes observed in the liver 14 days after completion of mel/HPβCD (A) and RAMβCD (B) chemotherapy .100
Figure 3-11: The histological changes observed within the liver 21 days after completion of treatment.....100
Figure 4-1: A schematic representation of the Taqman PCR reaction 114
Figure 4-2: Amplification plots illustrating how the Ct value is calculated .116
Figure 4-3: The treatment schedule used 121
Figure 4-4: The chemotherapy regime used in the quantitative PCR (QPCR) experiment.....127
Figure 4-5: The number of copies of the PFR2 gene present within 100ng of DNA prepared from approximately 25mg of brain tissue taken from whole brain homogenate, of mice infected with *T. b. brucei* (GVR35/C1.9) following chemotherapy with A) Mel/HPβCD and B) Mel/RAMβCD. 137
Figure 4-6: Interaction plots comparing the mean [log(x+1)] PFR2 copy number detected after administration of each dose of mel/HPβCD or mel/RAMβCD with number of doses.....138
Figure 4-7: The number of copies of the PFR2 gene present within 100ng of DNA prepared from approximately 25mg of brain tissue taken from whole brain homogenate from mice infected with *T. b. brucei* (GVR35/M14) following chemotherapy with A) Mel/HPβCD and B) Mel/RAMβCD.....143
Figure 4-8: Interaction plots comparing the mean [log(x+1)] PFR2 copy number detected after administration of each dose of mel/HPβCD or mel/RAMβCD with number of doses.....145
Figure 4-9: Interaction plots demonstrating the interactions in the mean [log(x+1)] PFR2 copy number detected between the two melarsoprol cyclodextrin complexes, mel/HPβCD and mel/RAMβCD and the number of doses and also between the melarsoprol sensitive (GVR35/C1.9) and resistant (GVR35/M14) *T. b. brucei* stabilates 146

Figure 5-1: The blood-brain barrier 159
Figure 5-2: The blood-CSF barrier 160
Figure 5-3: The arachnoid barrier 161
Figure 5-4: The treatment schedule employed in the MRI study.....175
Figure 5-5: The signal enhancement maps generated following magnetic resonance imaging 182
Figure 5-6: The percentage signal change detected by MRI in mice infected with *T. b. brucei* 184
Figure 5-7: Coronal sections through the brain of a mouse 21 days after infection with *T. b. brucei* (A and C) and a mouse killed 15 days after completion of mel/HPβCD chemotherapy (B and D) 186
Figure 6-1: The oral treatment schedule employed 210
Figure 6-2: The intravenous treatment schedule employed 210
Figure 6-3: The chromatogram obtained from brain tissue spiked with 250ng As 216
Figure 6-4: The chromatogram obtained from normal brain tissue.....216
Figure 6-5: The As calibration curve for concentrations ranging from 1000ng/ml to 100ng/ml 217
Figure 6-6: The As calibration curve for concentrations ranging from 50ng/ml to 5ng/ml.....217
Figure 6-7: The chromatogram obtained from a brain sample taken 1 hour after the oral administration of 0.05mmol/kg mel/HPβCD 220
Figure 6-8: The chromatogram obtained from a brain sample taken 4 hours after the oral administration of 0.05mmol/kg mel/HPβCD 221
Figure 6-9: The chromatogram obtained from a plasma sample taken 30 seconds after the I.V. administration of 0.03 mmol/kg mel/HPβCD 221

List of tables

Table 1-1: The pathogenic trypanosomes of veterinary importance 8

Table 1-2: Registered pharmaceutical products containing cyclodextrins... 43

Table 1-3: The physicochemical properties of α, β and γ cyclodextrin 45

Table 1-4: The physicochemical properties of cyclodextrin derivatives of pharmaceutical importance 50

Table 2-1: The amount of melarsoprol contained within 1g of each complex as determined by HPLC..... 70

Table 2-2: The amount of each complex required per ml in order to give the required doses 71

Table 2-3: The volume of complexed melarsoprol solution administered depending upon the weight of the animal..... 71

Table 2-4: The volume of mel/HPβCD solution administered I.V. to animals in order to achieve a dose of 0.03mmol/kg 72

Table 3-1: The amount of each compound required in mg per ml in order to give a dose of 0.05mmol/kg 89

Table 3-2: The sixteen treatment groups used in the experiment..... 90

Table 3-3: Comparison of the inhibitory concentration (IC_{50}) of the mel/HPβCD, mel/RAMβCD, melarsoprol, diminazene aceturate, HPβCD and RAMβCD..... 95

Table 3-4: The number of animals cured in each treatment group..... 96

Table 4-1: The sequence data for the oligonucleotide probes used in the in-situ hybridization procedure 122

Table 4-2: The combination of enzyme concentrations, incubation times and temperatures used to identify the optimal degree of digestion for the tissue sections. 123

Table 4-3: Sequence data for the primers and probe used to identify *T. b. brucei* by QPCR analysis. 130

Table 4-4: Comparison of the number of copies of the PFR2 gene detected within 100ng of DNA prepared from approximately 25mg of whole brain homogenate from mice infected with melarsoprol sensitive *T. b. brucei* trypanosomes following mel/HPβCD chemotherapy ... .139

Table 4-5: Comparison of the number of copies of the PFR2 gene detected within 100ng of DNA prepared from approximately 25mg of whole brain homogenate from mice infected with melarsoprol sensitive *T. b. brucei* trypanosomes following mel/RAMβCD chemotherapy 140
Table 4-6: Comparison of the number of copies of the PFR2 gene detected within 100ng of DNA prepared from approximately 25mg of whole brain homogenate from mice infected with melarsoprol resistant *T. b. brucei* trypanosomes following mel/HPβCD chemotherapy ... .147
Table 4-7: Comparison of the number of copies of the PFR2 gene detected within 100ng of DNA prepared from approximately 25mg of whole brain homogenate from mice infected with melarsoprol resistant *T. b. brucei* trypanosomes following mel/RAMβCD chemotherapy 148
Table 5-1: Neuropathological grading scale 178
Table 5-2: The MRI scans completed in each animal.....180
Table 5-3: Comparison of the percentage signal change detected within the brain, prior to mel/HPβCD chemotherapy commencing on day 21 post-infection and 24 hours, 8 and 15 days (corresponding to days 28, 35 and 42 post-infection respectively) after completion of the treatment regime and in uninfected, untreated animals 187
Table 5-4: Comparison of the percentage signal change detected in the brain 24 hours, 8 and 15 days (corresponding to days 28, 35 and 42 post-infection respectively) after completion of mel/HPβCD chemotherapy to untreated, uninfected control animals.....188
Table 6-1: The treatment protocol employed in the Daloa region, Ivory Coast 199
Table 6-2: The schedule used to digest the tissue samples 212
Table 6-3: The schedule used to completely digest all tissue elements and heat the samples to dryness.....212
Table 6-4: The concentration of As detected by GC-MS in brain tissues spiked with 25ng/ml As 218
Table 6-5: The concentration of arsenic detected by GC-MS in solutions containing 25ng/ml of As 219

List of equations

Equation 1-1: The complexation process 52
Equation 3-1: Determination of the stability constant of complex formation .. 78
Equation 4-1: The equation used to calculate the change in reporter fluorescence normalised to that of the quencher.....115
Equation 4-2: The equation used in order to calculate the number of copies of the PFR2 gene fragment present within the sample of purified DNA.....133
Equation 5-1: The equation used to generate signal enhancement maps 176
Equation 6-1: The equation used to calculate the melarsoprol content of samples analysed using the bioassay 197
Equation 6-2: The equation used to calculate the melarsoprol content of samples analysed using the automated bioassay 201

Chapter 1: Introduction

1.1 The Trypanosomiases

1.1.1 Classification

The genus *Trypanosoma* was first created in 1843 by Gruby with all trypanosome species grouped together. The first attempt to distinguish the trypanosomes was made in 1912 by Laveran and Mesnil who classified the trypanosomes as either pathogenic or non-pathogenic. In 1913, the pathogenic African trypanosomes were further divided into three groups, based on their mode of development in the tsetse fly vector, by Duke and Roubaud independently (Hoare, 1970b). This classification was extended to the non-pathogenic trypanosomes in 1921 by Knuth and Du Toit. In 1926, Wenyon divided the mammalian trypanosomes into two major groups, the Stercoraria and the Salivaria based on their site of development in the vector. Species comprising the Stercoraria typical develop in the hindgut of the vector and are transmitted by contamination while species comprising the Salivaria develop in the anterior of the vector and are transmitted by inoculation (Hoare, 1970b). These two major divisions were further subdivided into groups and subgroups based on the morphology and biology of the trypanosomes. In 1964, Hoare simplified the classification system (Hoare, 1964). The two major subdivisions, Stercoraria and Salivaria, were retained while related trypanosome species were rearranged into subgenera to give the classification system in use today (Figure 1-1).

1.1.2 Parasite biology

Trypanosomes are unicellular eukaryotic parasites ranging in size from 12μm to 70μm (Hoare, 1970b; Stevens and Brisse, 2004). The body takes the shape of a flattened spindle which is usually curved in shape but this can vary between species (Hoare, 1970b) (Figure 1-2). The anterior portion of the body is usually drawn out to a fine point while the posterior portion is usually broader and tapers more abruptly or terminates in a blunt or rounded tip (Hoare, 1972). A network of microtubules extending from one end of the cell body to the other serves as the cytoskeleton, maintaining the overall shape of the organism (Hoare, 1972). The cell body is enclosed by a strong and resistant envelope consisting of three layers known as the pellicle. At certain regions along the

body the pellicle membrane is thrown into folds forming an undulating membrane (Hoare, 1970b; Hoare, 1972).

Locomotion is by means of a single flagella which runs the entire length of the body along the undulating membrane. Once the flagella reaches the anterior of the body it either terminates at the end of the membrane or continues forming a free portion. The flagella is composed of microtubules which are enclosed by the flagellar sheath. The flagella originates behind the nucleus in the posterior portion of the cell body at the basal body which forms the base of the flagellum. From the basal body the flagella emerges to the surface through an invagination of the membrane known as the flagellar pocket (Hoare, 1970b; Hoare, 1972).

The kinetoplast is a distinctive feature in trypanosomes and the other members of the order Kinetoplastida. In trypanosomes it accounts for 10 to 20% of the total DNA content (Melville, Majiwa and Tait, 2004). It always lies in close proximity to the basal body accompanying the latter as it migrates during development of the trypanosome (Hoare, 1970b). The position of the kinetoplast within the body along with its size and shape are characteristic of certain species of trypanosome and can be used to identify certain species (Hoare, 1972). Trypanosomes have a single nucleus containing a large central achromatic karyosome. The nucleus is usually round or elongated in appearance and is situated in different positions depending upon the life-cycle stage of the parasite. In bloodstream forms it is normally located in the central or anterior position. Between the nucleus and the flagella pocket lies the golgi apparatus. In addition to the major structural elements trypanosomes also contain numerous cytoplasmic inclusions (Hoare, 1970b; Hoare, 1972).

Trypanosomes are primarily diploid organisms however there are certain regions of the genome which are not diploid, for example the VSG genes, their expression sites and the mini-chromosomes (Melville, Majiwa and Tait, 2004). Three classes of chromosomes have been identified in the trypanosome genome; mega chromosomes (≥ 1Mb), intermediate chromosomes (>100kb), and mini chromosomes (30-100kb). Trypanosomes possess approximately 8 to 10 mega

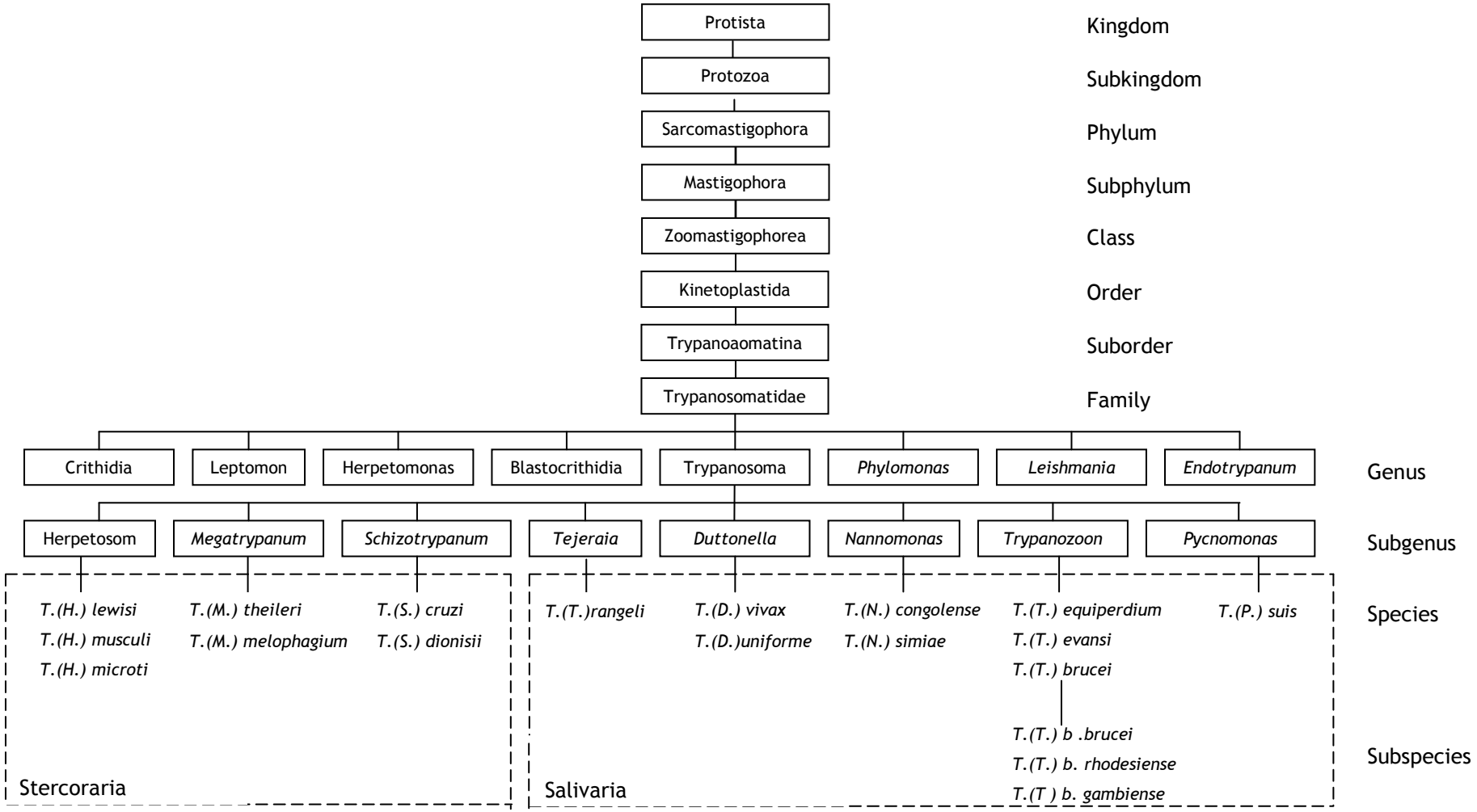

Figure 1-1: The systematic classification of trypanosomes in use today

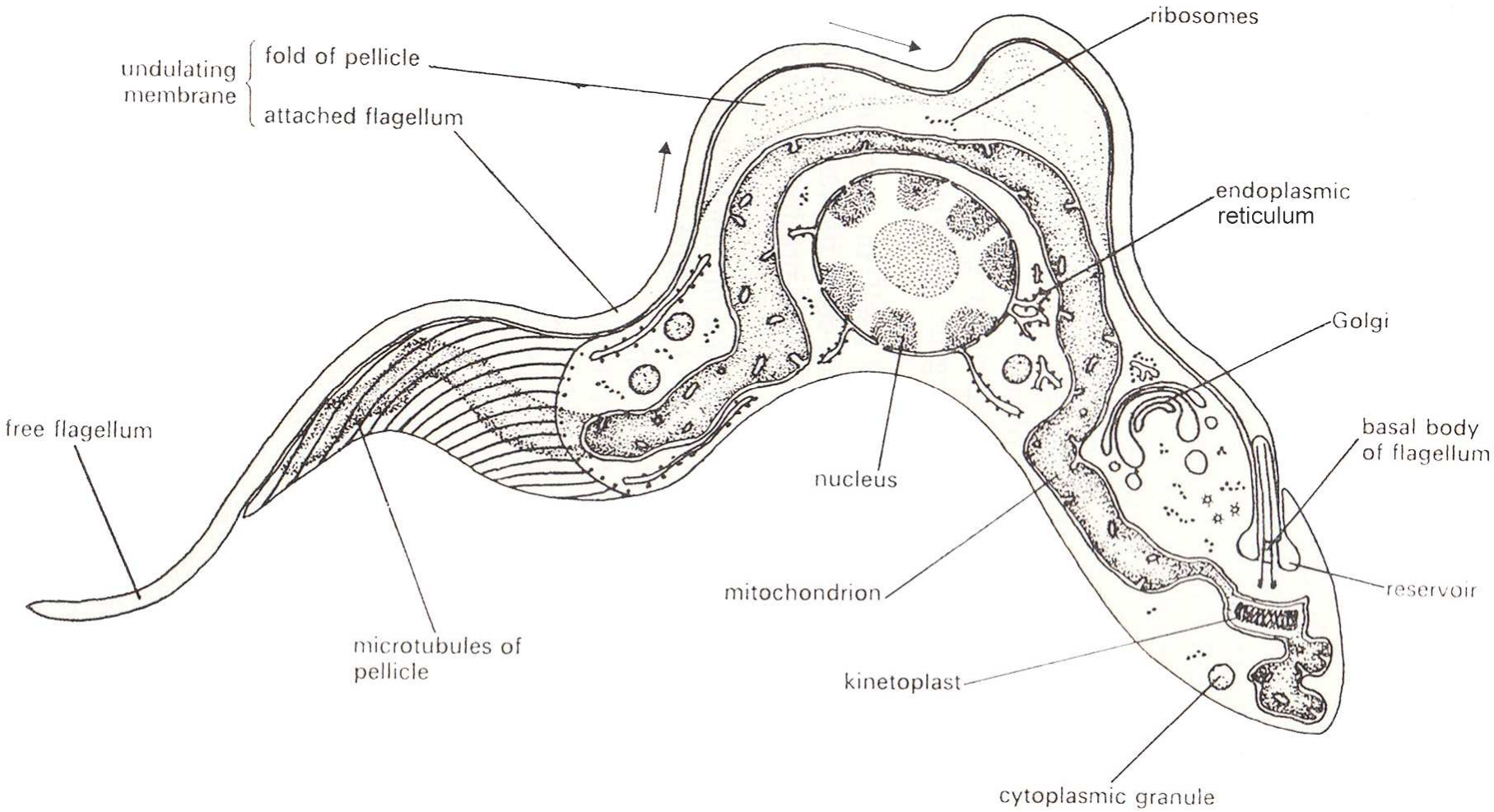

Figure 1-2: A diagram of the trypomastigote intermediate bloodstream form of *T. b. rhodesiense*
Seen at the level of the electron microscope (Vickerman, 1970).

chromosomes, a 100 mini chromosomes and varying numbers of intermediate chromosomes (Melville, Majiwa and Tait, 2004; World Health Organisation, 1998).

1.1.2.1 Antigenic variation

Trypanosomes evade the host immune system by undergoing antigenic variation. The entire surface of bloodstream and metacyclic trypanosomes consists of a variable surface glycoprotein (VSG) coat. The VSG is very immunogenic eliciting an immune response in the host that results in the production of antibodies which are lytic to the trypanosome (Barry and Carrington, 2004). In order to persist within the host individual trypanosomes spontaneously switch to a different antigenically distinct VSG coat. Thus while the trypanosomes displaying the original VSG are lysed by antibodies, the few trypanosomes displaying the antigenically distinct VSG are able to persist and proliferate, generating the next wave of parasitaemia. This cycle is repeated continuously giving rise to the characteristic fluctuating parasitaemia associated with trypanosome infections.

Antigen switching is rapid, occurring at an average rate of one switch in every 100 trypanosome doublings (Barry and Carrington, 2004). The repertoire of VSGs is extensive with each trypanosome containing >1500 VSG genes (Barry, Marcello, Morrison, Read *et al.*, 2005; Berriman, Ghedin, Hertz-Fowler, Blandin *et al.*, 2005).

1.1.3 Trypanosomes of veterinary importance

The trypanosome species of importance in sub-Saharan Africa are listed in Table 1-1. The species *T. evansi*, *T. congolense*, *T. vivax* and *T. b. brucei* show a lack of host specificity infecting a wide range of mammals including cattle, horses, sheep and goats. Infection results in a disease known locally as ‘nagana’, the zulu word for 'low spirits' and is characterised by fever, anaemia and cachexia. In addition hind limb paralysis may also occur in infections involving *T. b. brucei* and *T. vivax* (Hoare, 1970a). In contrast to the other African trypanosomes the species *T. suis*, *T. simiae* and *T. equiperdum* are host specific. *T. suis* and *T. simiae* are primarily parasites of wild and domestic pigs producing rapid onset and fatal infections in the latter (Hoare, 1970a). Although, there have been

isolated reports of *T. simiae* infections occurring in cattle, horses and camels (Culwick and Fairbairn, 1947; Hoare, 1972; Killickkendrick and Godfrey, 1963). *T. equiperdum* occurs exclusively in equines producing veneral disease or dourine. Infection is characterised by an initial oedema of the genitalia followed by neurological sequelae (Hoare, 1970a).

1.1.4 Trypanosomes of medical importance

1.1.4.1 American

Chagas disease (American trypanosomiasis) is the most important parasitic infection in Latin America (Miles, Yeo and Gaunt, 2004). The causative agent, *Trypanosoma cruzi* belongs to the sterocoraria division and is transmitted by blood feeding reduviid bugs of the subfamily Triatominae. Infection occurs when triatominae faeces, containing the infective metacyclic trypanosomes, is rubbed into the bite wound, an existing wound or the conjunctiva of the eye (Cox, 1993). The initial phase of the disease, characterised by the presence of the parasites in the blood, is often asymptomatic. In approximately 90% of infected individuals the infection will resolve spontaneously without treatment with trypanocidal drugs. Approximately 60% to 70% of these patients will never develop clinical apparent disease. They are classed as having the indeterminate form of chronic Chagas disease characterised by seropositivity for *T. cruzi* accompanied by normal electrocardiagram and radiographs of the chest, oesophagus and colon (Rassi Jr, Rassi and Marin-Neto, 2010). The remaining 30 to 40% of patients will go on to develop a chronic form of the disease 10 to 30 years after initial infection. Chronic chagas disease can take one of three forms, cardiac, digestive (megacolon or megaoesphagus) or cardiodigestive (Rassi Jr, Rassi and Marin-Neto, 2010).

1.1.4.2 African

The only African trypanosomes infective to man are *T. b. gambiense* and *T. b. rhodesiense*. Cases of human trypanosomiasis as a result of infection with

Subgenus	Species	Mammalian hosts	Distribution
Duttonella	*T. vivax*	Bovines, sheep, goats, equines, dogs, antelopes	Tropical Africa
	T. uniforme	Bovines, sheep, goats, antelopes	East and central Africa, Angola
Nannomonas	*T. congolense*	Bovines, sheep, goats, equines, pigs, dogs, antelopes	Tropical Africa
	T. simiae	Pigs, warthogs, possibly bovines, equines and camels	Tropical Africa
Trypanozoon	*T. b. brucei*	All domestic mammals and antelopes	Tropical Africa
	T. b. rhodesiense	Man, bovines, goats, antelopes	East Africa
	T. b. gambiense	Man, bovines, goats, pigs and a variety of wild animals[1]	Tropical Africa
	T. evansi	Bovines, equines, camels, dogs	North and north west Africa, Sudan, Somalia, Philippines, Spain, Tunisia, Vietnam, Burkino Faso, India, Indonesia, Iran, Israel, Jordon, Afghanistan, Pakistan, South America[2]
	T. equiperdum	Equines	North, south and south west Africa, Iran, Pakistan, Russia
Pycnomonas	*T. suis*	Pigs, warthogs, bush pigs	Tanzania, Burundi

Table 1-1: The pathogenic trypanosomes of veterinary importance
Modified from (Hoare, 1970a; Stevens and Brisse, 2004). [1]*T. b. gambiense* has been isolated from a wide range of wild mammals including the giant rat, porcupine, civets, duikers and monkeys (Herder, Simo, Nkinin and Njiokou, 2002; Massussi, Massussi, Mbida Mbida, Djieto-Lordon *et al.*, 2010). [2]The South American countries where cases of *T. equiperdum* have been reported include Bolivia and Argentina.

T. evansi have occasionally been reported in the literature but are exceptionally rare and unusual (Joshi, Shegokar, Powar, Herder *et al.*, 2005). The African trypanosomes will now be discussed in further detail.

1.1.5 African trypanosomes

1.1.5.1 History

The first account of sleeping sickness was recorded in 1721 by the naval surgeon John Atkins. He described the disease as ‘the sleepy distemper’ of blacks and thought that the disease only occurred in black people, in particular slaves, as a result of excess phlegm or serum in the brain, poor diet and a natural weakness of the brain (Cox, 2004). Unaware of Atkins's previous report on sleeping sickness, Thomas Winterbottom a physician working in Sierra Leone in 1803 described a new disease he named 'negro lethargy'. It was characterised by enlargement of the posterior cervical lymph nodes. This is now know to be a common clinical sign of human African trypanosomiasis (HAT) and is known as Winterbottom’s sign (Cox, 2004; Maudlin, 2006). Although both Atkins and Winterbottom had described human African trypanosomiasis and the clinical signs associated with it, neither had any real idea about the nature of the disease or how it occurred.

The first report of trypanosomes was in the blood of frogs in 1842 by Gluge. This was followed by similar independent reports by Mayer and Gruby in 1843 (Cox, 2004). In the same year Gruby devised the genus *Trypanosoma*, deriving the name from the greek word for borer 'trupanon' based on the cork screw like movement of the parasites (Cox, 2004). Evans was the first to identify trypanosomes in domestic animals in 1880. He observed what is now known as *T. evansi* in the blood of camels, horses and mules suffering from a wasting disease called 'surra' in the Punjab (Evans, 1881). Although Evans was able to associate the trypanosomes with the disease he was not able to identify the source of the disease and thought the parasites were acquired from drinking water.

Bruce, a British colonial medical officer stationed in South Africa was the first to identify the source of the disease in 1894 (Bruce, 1895). Bruce had been sent to Africa in order to investigate an outbreak of 'nagana', a wasting disease of cattle

also known as 'fly disease'. In the blood of the stricken animals Bruce discovered trypanosomes and named them *T. brucei*. He noticed that they closely resembled the trypanosomes that had previously been identified by Evans in camels and horses suffering from surra in the Punjab. Bruce was certain that the trypanosomes were the cause of nagana and suspected that the tsetse fly was responsible for its transmission as he noted that infected cattle had spent time in tsetse fly infested areas (Bruce, 1895). In order to confirm his suspicions Bruce arranged for healthy cattle to be sent to areas where tsetse flies were present. Upon their return the cattle were found to be infected with trypanosomes (Cox, 2004). Bruce thought that transmission of trypanosomes by the tsetse fly was purely mechanical (Bruce and Nabarro, 1903), it was not until 1909 that the cyclical transmission of trypanosomes was demonstrated by Kleine (Kleine, 1909). Kleine suggested that a sexual stage of development existed in the tsetse fly vector. However, when the lifecycle was reviewed by Bruce, it was concluded that trypanosomes could only undergo asexual development and the sexual stage was removed from the lifecycle (Bruce, 1914). It was not until 1986 that sexual development was demonstrated experimentally in *T. b. brucei* (Jenni, Marti, Schweizer, Betschart *et al.*, 1986). Sexual recombination takes place in the salivary glands of the tsetse fly and it is thought that the unattached epimastigote represents the sexual stage (Gibson, Peacock, Ferris, Williams *et al.*, 2008). However, mating is not mandatory and it is unclear how frequently genetic exchange occurs in natural trypanosome infections (Hide, Welburn, Tait and Maudlin, 1994; Smith, Smith, O'Rourke and Spratt, 1993; Sternberg, Turner, Wells, Ranford-Cartwright *et al.*, 1989; Tait, 1980; Tibayrenc, Kjellberg and Ayala, 1990).

The first report of trypanosomes in man was in 1901 by Forde, a British Colonial surgeon, who observed them in the blood of an Englishman who had been working on the River Gambia (Forde, 1902). Forde did not realise the significance of his discovery and showed them to Dutton who identified them as trypanosomes and named them *T. gambiense* (Dutton, 1902). In 1902, concerned about an epidemic that was sweeping through east Africa, the British government requested that the Royal Society establish a sleeping sickness commission to investigate the problem. The commission consisted of a young Italian named Aldo Castellani who incorrectly concluded that the disease was

caused by a bacterial Streptococcus infection. Castellani submitted a paper detailing his conclusions to the Proceedings of the Royal Society but its publication was blocked by Bruce who doubted the data presented (Cox, 2004). Frustrated with the lack of progress the Royal Society sent out a second sleeping sickness commission in 1903 consisting of Bruce and David Nabarro. By the time of Bruce's arrival in Africa, Castellani had already identified trypanosomes in the blood and cerebrospinal fluid (CSF) of patients suffering from sleeping sickness (Castellani, 1903) but it is the subject of much controversy as to whether Castellani alone identified trypanosomes as the cause of sleeping sickness or if he was assisted by Bruce. In 1903 Bruce submitted a report identifying *T. b. gambiense* as the causative agent of sleeping sickness in Uganda and indicated the tsetse fly *G. palpalis* as the vector responsible for transmission of the disease (Bruce, Nabarro and Grieg, 1903).

The causative agent of the more acute east African sleeping sickness was not identified until 1910 by Stephens and Fantham (Stephens and Fantham, 1910). Noting a number of differences between their parasite and that previously described by Dutton (Dutton, 1902) they concluded that they had identified a new species of human trypanosome and named it *T. b. rhodesiense* (Stephens and Fantham, 1910). Game animals were subsequently confirmed as reservoir hosts of *T. b. rhodesiense* in 1912 (Kinghorn and Yorke, 1912) but it was not until the end of the twentieth century that domestic animals were identified as possible reservoir hosts of *T. b. gambiense* (World Health Organisation, 1998).

1.1.5.2 Geographical distribution

The dependence on an insect vector for transmission means the African trypanosomes are restricted to sub-Saharan Africa where their tsetse fly vector resides (Hoare, 1970b). The tsetse fly belt currently extends across 10 million km^2 of the African continent spanning 38 countries. However, the species *T. vivax*, *T. evansi* and *T. equiperdum* have been able to extend their distribution beyond the African continent by evolving non-cyclical or mechanical methods of transmission. *T. vivax and T. evansi* are transmitted by biting flies primarily of the genera *Tabanus* while *T. equiperdum* is transmitted by direct contact during coitus between mares and stallions (Hoare, 1970a). Through the exportation of infected animals *T. vivax*, *T. evansi* and *T. equiperdum* are now found in

multiple foci around the world (Table 1-1). The African trypanosomes of animals *T. vivax*, *T. simiae*, *T. b. brucei* and *T. suis* are widely distributed throughout Africa occurring in areas where tsetse flies are present. In contrast the geographical distribution of the African trypanosomes infective to humans *T. b. gambiense* and *T. b. rhodesiense* is very distinct. *T. b. gambiense* is located in west and central Africa while *T. b. rhodesiense* is present in east Africa (Figure 1-3). The geographical divide between the two subspecies roughly follows that of the Rift Valley (Welburn, Fevre, Coleman, Odiit *et al.*, 2001).

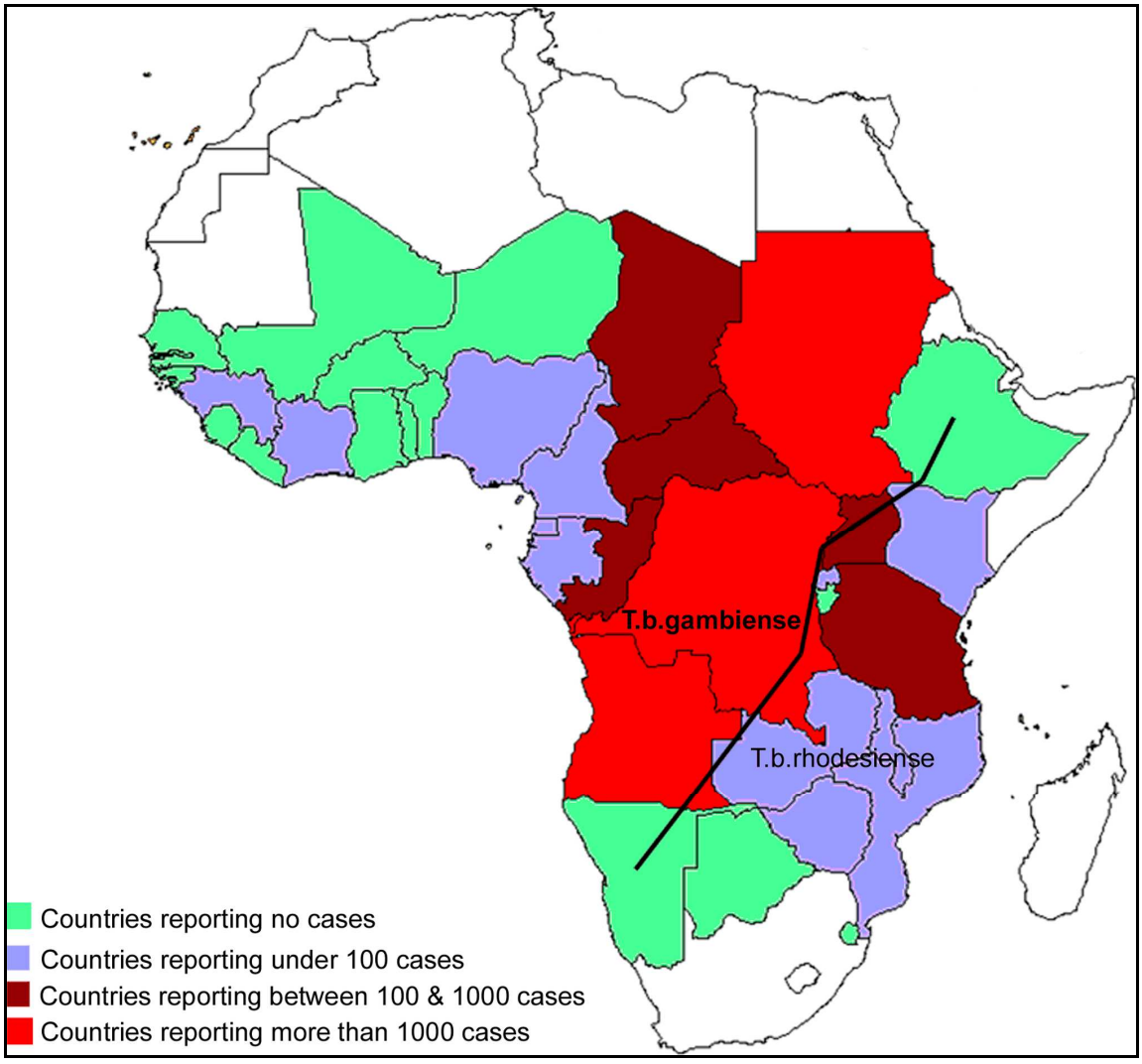

Figure 1-3: A map illustrating the geographical distribution of the human infective trypanosomes *T. b. gambiense* and *T. b. rhodesiense.*
T. b. gambiense is located in west and central Africa while *T. b. rhodesiense* is present in east Africa. The black line represents the division between the two subspecies (Simarro, Jannin and Cattand, 2008).

Currently the only country where both subspecies of the parasite exists is Uganda with *T. b. gambiense* located in the north-west and *T. b. rhodesiense* to the south-east (Maudlin, 2006). Although both subspecies currently exist in

Uganda they are geographically separate but there is a concern that the parasites are moving towards each other and that one day their distribution will overlap (Picozzi, Fevre, Odiit, Carrington *et al.*, 2005). This will cause problems in the diagnosis and treatment of the disease as will be discussed later.

1.1.5.3 The vector

African trypanosomes are transmitted by tsetse flies of the genus *Glossina*. Over 30 species comprise the genus which is separated into three subgenera *Glossina*, *Nemorhina* and *Austenina* based on the morphology of the male and female genitalia and the karyotype (Newstead, 1911). Only *Nemorhina* and *Glossina* subgenera are involved in the transmission of human African trypanosomiasis. Transmission of *T. b. rhodesiense* is mainly by four species of savannah tsetse flies belonging to the morsitans group. *G. m. morsitans* and *G. m. centralis* in east Africa, *G. pallidipes* in east and southern Africa and *G. swynnertoni* in Kenya and Tanzania (Pepin and Meda, 2001). One species belonging to the palpalis group, *G. f. fuscipes* has also been implicated in the transmission of *T. b. rhodesiense* in central and east Africa (World Health Organisation, 1998). The vectors of *T. b. gambiense* mainly belong to the palpalis group with the species responsible for transmission varying depending upon the vegetation present. In the forests of west and central Africa *G. palpalis palpalis* is the principal vector while *G. p. gambiensis*, *G. tachinoides* and *G. fuscipes fuscipes* are the main vectors in savannah regions. The only species of the morsitans group to act as vectors of *T. b. gambiense* are *G. pallidipes* and *G. morsitans* (Pepin and Meda, 2001).

1.1.5.4 Life cycle

The life cycle of the trypanosome commences with the inoculation of metacyclic trypanosomes into the mammalian host by the tsetse fly (Figure 1-4). Following inoculation the metacyclic trypanosomes enter the bloodstream and lymphatic vessels where they multiply by binary fission, transforming into long slender trypomastigotes (Vickerman, 1985). The long slender trypomastigotes give rise to non-dividing short stumpy forms, which are taken up by the tsetse fly when it feeds on the host. Once ingested by the tsetse fly the stumpy forms pass into the

midgut of the fly where they transform into procyclics (Vickerman, 1985). Upon transformation to procyclics there is a switch in the main energy source from glucose to proline and the variable surface glycoprotein coat is lost (Steiger, 1973; Vickerman, 1985). The procyclics multiply extensively in the lumen of the gut and invade the ectoperitrophic space through penetration of the peritrophic membrane (Evans and Ellis, 1983; Vickerman, Tetley, Hendry and Turner, 1988). From the ectoperitrophic space the trypanosomes gradually migrate forward to the proventriculus where they cease dividing and assume the proventricular mesocyclic form (Vickerman, 1985). The proventricular trypanosomes reinvade the endotrophic space and migrate via the oesophagus, probosics lumen and hypopharynx to the salivary glands (Vickerman *et al.,* 1988; Vickerman, 1985). In the salivary glands the proventricular forms are transformed into epimastigotes, which attach to the microvilli of the wall of the salivary gland. Transition from the epimastigote form into the infective metacyclic form occurs through two intermediary stages. Initially the epimastigotes transform into uncoated trypomastigotes (premetacyclics) which are still capable of division (Vickerman, 1985). Subsequently, the premetacyclics acquire the variable surface glycoprotein (VSG) coat and cease dividing. They are now known as metacyclics and are discharged into the mammalian host via the fly's saliva during feeding (Vickerman, 1985). The complete cycle in the vector takes between 3 to 5 weeks (Vickerman *et al.,* 1988).

1.1.6 Trypanosomiasis in man

1.1.6.1 Current situation of HAT

Human African trypanosomiasis (HAT) is currently prevalent in 36 countries throughout sub-Saharan Africa. It is estimated that 60 million people are at risk from the disease but only 4 million are under adequate health surveillance (World Health Organisation, 1998). In 2009 9,878 cases of HAT were reported to the World Health Organisation (WHO) (World Health Organisation, 2010). Due to the remote areas in which HAT occurs and the lack of adequate disease screening programmes many cases go unreported therefore the true number of cases is likely to be considerably higher than this figure. In 2004, 1.6 million

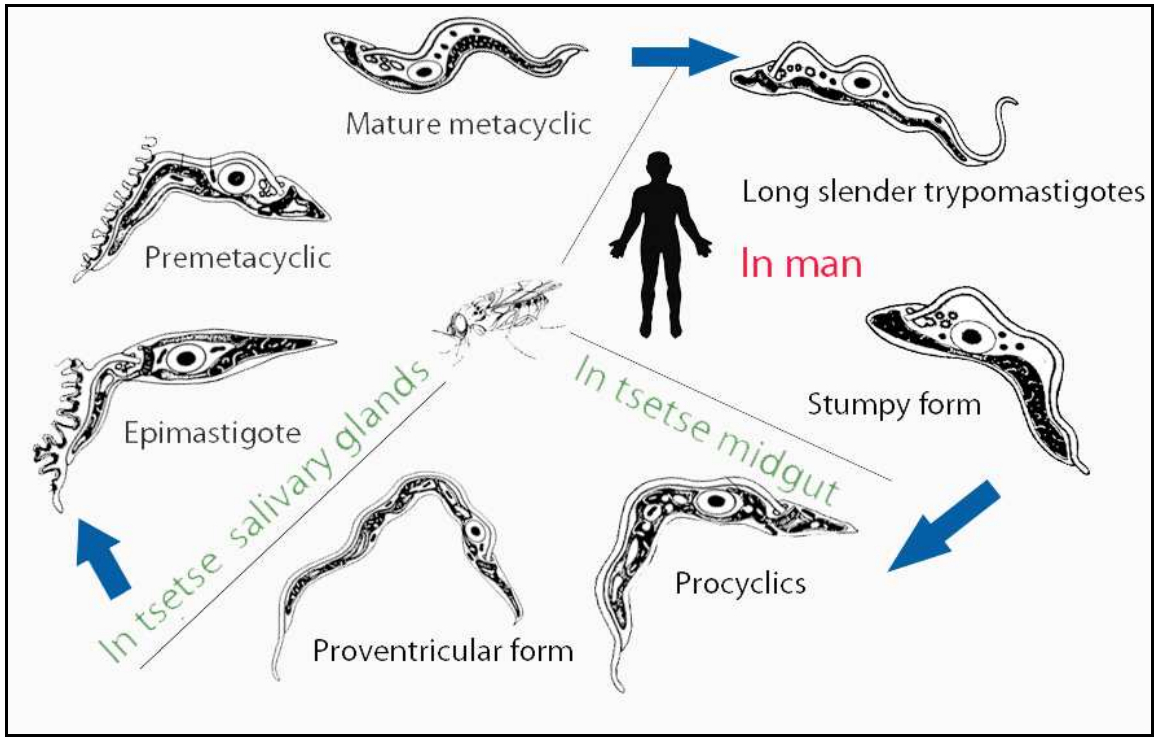

Figure 1-4: The life cycle of *Trypanosoma brucei* spp
The lifecycle commences when metacyclic trypanosomes are inoculated into the mammalian host by the tsetse fly. The metacyclic trypanosomes multiply by binary fission in the blood and lymphatic systems of the host giving rise to long slender trypomastigotes. The long slender trypomastigotes give rise to stumpy forms which are taken up by the tsetse fly when it feeds on the host. In the midgut of the tsetse fly the stumpy forms transform into procyclics. The procyclics multiply extensively in the lumen of the gut and migrate to the proventriculus where they assume the proventricular form. The proventricular forms migrate to the salivary glands where they are transformed into epimastigotes. Transition from the epimastigote form to the infective metacyclic occurs through two stages. Initially the epimastigotes transform into uncoated trypomastigotes (premetacyclics). The premetacyclics subsequently acquire the variable surface glycoprotein coat and are now known as metacyclics.

DALYs (disability adjusted life years) were lost due to HAT (World Health Organisation, 2004). At the turn of the twentieth century HAT was endemic in sub-Saharan Africa with over 60,000 cases reported in 1930 (Simarro, Jannin and Cattand, 2008). The introduction of mass screening programmes and control measures by the colonial powers brought the disease under control and by 1960 the disease had almost being eradicated (Simarro, Jannin and Cattand, 2008). However, when countries gained their independence screening programmes and control measures were abandoned or disrupted by civil war. As a result the incidence of HAT began to increase reaching a peak in 1998 with over 37,000 cases reported (Simarro, Jannin and Cattand, 2008). In 1997 the World Health Organisation (WHO) expressed concern at the growing problem of HAT in sub-Saharan Africa. This resulted in the reintroduction of screening programmes and control measures and gradually the number of cases of HAT began to decline. The disease once again appears to be largely under control in many countries (Simarro, Jannin and Cattand, 2008). In 2009 the number of reported cases fell below 10,000 for the first time in 50 years (World Health Organisation, 2010). It is hoped that one day HAT will be eliminated from the African continent but this goal is a long way off and some are sceptical as to whether elimination can ever be achieved.

1.1.6.2 Pathogenesis

The pathogenesis of HAT is poorly understood. The clinical manifestations associated with the haemolymphatic stage of the disease are often non-specific, irregular and inconsistent. Data from human patients is limited as *post mortem* examinations are not routinely conducted in Africa. Most of the information regarding the pathogenesis of the disease has therefore come from animal models.

1.1.6.2.1 Haemolymphatic

Anaemia is a prominent feature in trypanosome infections with the severity depending upon the host and species of trypanosome present. In *T. b. rhodesiense* infections severe anaemia is frequently observed while in *T. b. gambiense* infections it is not a significant clinical finding (Greenwood and Whittle, 1980). The anaemia is thought to arise due to the extravascular

destruction of red blood cells (RBC) but the mechanisms by which erythrophagocytosis is induced are not fully understood with numerous hypotheses suggested. It has been proposed that trypanosomal antigens bind to the surface of the RBC making the cells a target for circulating anti-trypanosomal antibodies. As a result the RBC become susceptible to phagocytosis. Phagocytosis of the RBC may also be initiated through alterations in the RBC surface membranes which occur as a result of the cells becoming ATP depleted due to having to compete with the trypanosomes for essential metabolites (Jennings, 1976). Trypanosomes may also produce a haemolytic factor which causes the direct lysis of circulating RBC. This hypothesis was supported by the observation that trypanosomes produce a low molecular weight protein which when incubated with normal RBC induced lysis (Jennings, 1976).

1.1.6.2.2 Specific organ damage

A generalised lymphadenopathy is commonly observed in trypanosome infections. In *T. b. gambiense* infections enlargement of the lymph nodes in the posterior cervical triangle frequently occurs and is referred to as Winterbottom's sign after the physician who first described the reaction (Apted, 1970a). Enlargement of the posterior cervical lymph nodes is not a common occurrence in *T. b. rhodesiense* infections where involvement of the axillary and epitrochlear glands is more common. However, the degree and sites of lymphodenopathy varies greatly between geographical locations and outbreaks (Apted, 1970a). Histological examination of the enlarged lymph nodes reveals follicular hyperplasia, sinus histiocytosis and perivascular infiltrations consisting of plasma and morular cells. As the infection progresses the affected lymph nodes become atrophic and depleted of lymphoid cells with capsular and trabecular fibrosis occurring in the most advanced cases (Greenwood and Whittle, 1980; Poltera, 1985).

Splenic enlargement proportional to the degree of anaemia is a frequent occurrence in trypanosome infections. In the early stages of infection the sinusoids are packed with active macrophages and the Malpighian corpuscles increase in size. Histological examination of the Malpighian corpuscles reveals changes analogous to those observed in the lymph glands with the

transformation of small inactive lymphocytes into plasma cells. Fibrosis of the spleen is not observed until the latter stages of the disease (Ormerod, 1970).

In the early stages of *T. b. rhodesiense* infections the heart is considered the organ most at risk (Ormerod, 1970). In a histological study conducted in a patient who had died as a result of HAT, a pancarditis involving all cardiac layers including the valves and conducting system was observed (Poltera, Cox and Owor, 1976). Cardiac involvement is not restricted to *T. b. rhodesiense* infections, sclerotic endocarditis and periarterial myocarditis have been reported in patients suffering from *T. b. gambiense* infections (Ormerod, 1970). Cardiac involvement has also been clearly demonstrated in animal models of trypanosome infection involving a range of species. In one study conducted in a murine model of *T. b. brucei*, parasites were observed in the endocardium of all chambers of the heart. Following the infiltration of parasites an inflammatory response consisting of mononuclear cells was observed. In advanced infections dilation of the lymphatic channels and marginal sinuses was also observed (Poltera, 1980).

1.1.6.2.3 Central nervous system pathology

The central nervous system (CNS) pathology observed in trypanosome infections was first described in 1906 by Mott who examined material from humans and experimental animals infected with *T. b. gambiense* (Mott, 1906). The pathological information from patients mostly relates to the advanced/terminal stages of the disease. Animal models have therefore played an important role in understanding the earlier pathological events associated with infection.

Trypanosomal invasion of the CNS is characterised by a meningo-encephalitis. Inflammation occurs in the pia–arachnoid which becomes thickened due to the infiltration of lymphocytes in particular B cells, plasma cells and morular cells (Mott, 1906). Morular cells are a prominent feature in trypanosome infections and are often referred to as Mott cells after F. W. Mott, who was the first to describe the cells in the CNS lesions of trypanosomiasis. The cellular infiltrate extends along the Virchow-Robin spaces surrounding the blood vessels that enter the brain (Greenwood and Whittle, 1980). The blood vessels become surrounded by inflammatory cells in particular Mott cells producing a lesion known as a

perivascular cuff (Mott, 1906). Perivascular cuffing is more commonly observed in the Gambiense form of the disease as death due to cardiac manifestations frequently occurs in *T. b. rhodesiense* infections before CNS lesions become apparent (Ormerod, 1970). Activated astrocytes and microglia are frequently found surrounding the blood vessels and within the brain parenchyma (Pentreath, 1989). In some cases the lesions take the form of a severe haemorrhagic leukencephalopathy (Adams, Haller, Boa, Doua *et al.*, 1986). Surprisingly in trypanosome infections there is little neuronal damage. Neuronal deterioration has only been reported in the most advances cases of the disease, in the region of the basal ganglia (Greenwood and Whittle, 1980).

1.1.6.3 Clinical signs

1.1.6.3.1 Haemolymphatic manifestations

The first sign of trypanosome infection is often the development of a lesion at the site of the tsetse fly bite known as the chancre. Chancre development usually occurs within five to fifteen days of the initial bite although longer and shorter time periods have been reported (Apted, 1970a). Initially the chancre appears as a round inflamed area with a red spot in the centre. Over the next 48 hours it rapidly develops into a painful round puritic nodule reaching up to three centimetres in diameter. Following its expansion the chancre gradually subsides over a two week period leaving an area of scaly desquamation (Apted, 1970a). The frequency with which the chancre occurs varies, it is more frequently reported in *T. b. rhodesiense* infections and in Europeans (Apted, 1970a).

One to three weeks after the initial infective bite patients develop a fever due to the trypanosomes invading the blood stream. The fever is often high and is frequently accompanied by temporal or frontal headaches and occasionally vomiting and rigors (Apted, 1970a). The fever persists for up to seven days after which it subsides before returning in intermittent bouts punctuated with periods of remissions during which the patient feels well (Atouguia and Kennedy, 2000). The fever is more pronounced and occurs more frequently in *T. b. rhodesiense* than *T. b. gambiense* infections (Apted, 1970a; World Health Organisation, 1998). In the initial stage of *T. b. gambiense* infections, enlargement of the lymph nodes in the posterior cervical triangle frequently occurs and is known as

Winterbottom's sign. The glands are discrete, freely movable and non-tender (Apted, 1970a). Enlargement of the cervical lymph nodes is characteristic of *T. b. gambiense* infections as enlargement of the glands is not frequently observed in *T. b. rhodesiense* infections where lymphadenopathy tends to be more generalised (World Health Organisation, 1998).

Six to eight weeks after the onset of the illness an irregular, evanescent annular rash may appear on the trunk, shoulders and thighs. The rash takes the form of large scattered circinate, erythematous patches often reaching three to four centimetres in diameter (Apted, 1970a). It is most frequently observed in light skinned people as it is invisible in the dark skin of Africans but even in fair skinned people the rash is often difficult to locate. This may be due to the tendency of the rash to fade frequently and reappear over a period of weeks (Apted, 1970a). Pruritus is a common complaint in patients with first stage sleeping sickness being reported in 40% to 50% of cases (Atouguia and Kennedy, 2000).

The major organs involved in the first stage of infection are the liver, spleen and heart. The liver and spleen both become enlarged and are easily palpable (World Health Organisation, 1998). In some patients cardiac involvement is present from the onset of infection and tachycardia without fever is suggested to be one of the earliest signs of infection (Apted, 1970a; Ormerod, 1970). Although cardiac involvement is more common in the acute rhodesiense form of the disease cardiac manifestations have also been reported in *T. b. gambiense* infections (Ormerod, 1970). Cardiac manifestations common in the first stage of infection include lower intensity heart sounds, murmurs (Buchanan, 1929), myocarditis with congestive heart failure (Duggan and Hutchins, 1966; Koten and De Raadt, 1969; Manson-Bahr and Charters, 1963), pericardial effusions (De Raadt, 2005; Hawking and Greenfield, 1941; Manson-Bahr and Charters, 1963), and pancarditis (Atouguia and Kennedy, 2000). Abnormalities in the cardiac rhythm are often detected by electrocardiograph (Atouguia and Kennedy, 2000) and radiographic imaging frequently reveals cardiomegaly due to pericardial effusion and dilation of the cardiac cavities (Buscher and Lejon, 2004; Manson-Bahr and Charters, 1963).

Abnormalities in the endocrine system become apparent in the first stages of the disease. In women endocrine dysfunction manifests itself as a cessation of the menstrual cycle and sterility. In pregnant women who become infected, low birth weights, still or premature births and abortion are common occurrences (Apted, 1970a). In men a loss of libido and impotence are the most frequently reported clinical manifestations (Apted, 1970a).

An infrequent clinical manifestation of trypanosome infection is a deep hyperaesthesia known as Kérandel's sign. The sensation occurs following the compression of soft tissues and the pain experienced is completely out of proportion to the force applied. The pain is felt a few seconds after the compression occurs and rapidly becomes severe before subsiding and disappearing after a few minutes (Apted, 1970a). When it is present Kérandel's sign is almost diagnostic of trypanosome infection but it occurs very infrequently being reported in only 29 out of 109 European patients examined and it appears to be even rarer in Africans (Apted, 1970a; Duggan and Hutchins, 1966).

1.1.6.4 Central nervous system manifestations

As the disease progresses central nervous system (CNS) involvement becomes more apparent. The clinical manifestations observed depend upon which area of the brain is damaged (Apted, 1970a). Damage to the extra-pyramidal area is a common occurrence resulting in tremors of the hands, fasciculation of the muscles of the limbs, face, lips and tongue and an increase in muscle tonicity (Apted, 1970a). Paralysis of whole muscle groups can occur due to focal lesions or the effects of pressure within the brain. The paralysis mainly effects the lower limbs and is occasionally transient but more frequently it is permanent (Apted, 1970a; Atouguia and Kennedy, 2000). Its occurrence varies throughout Africa being more common in certain regions (Apted, 1970a). The speech of patients is also affected becoming slow and difficult to understand as the disease progresses (Kellersberger, 1933).

Mental disturbances are a common occurrence in patients with CNS stage disease. Initial changes may be subtle involving alterations in behaviour and personality (Atouguia and Kennedy, 2000; Gelfand, 1947). As the disease progresses patients experience irritability, anxiety, indifference, agitation and

manic episodes sometimes with euphoria, uncontrolled sexual impulses, violent moods, delirium and hallucinations (Apted, 1970a; Atouguia and Kennedy, 2000).

The most characteristic sign of CNS involvement is the day time somnolence from which the disease derives its name although hypersomnia is not a feature of HAT (Apted, 1970a; Lundkvist, Kristensson and Bentivoglio, 2004). Instead there is a disruption of the sleep-wake pattern with patients developing uncontrollable urges to sleep during the day which alternate with night time insomnia (Bentivoglio, Grassi-Zucconi, Olsson and Kristensson, 1994; Lundkvist, Kristensson and Bentivoglio, 2004). In the latter stages of the disease the uncontrollable urge to sleep is almost continuous and patients frequently fall into sleep while talking or in the middle of a task (Atouguia and Kennedy, 2000; Duggan and Hutchins, 1966; Kellersberger, 1933). As the disease enters its final stages there is a progressive deterioration in the mental state of the patient. The patient becomes indifferent to their environment developing an intolerable pruritus and becomes emaciated (Apted, 1970a; Atouguia and Kennedy, 2000). Eventually the patient enters a coma and death ensues either from the disease itself, intercurrent infections or malnutrition (Apted, 1970a; Kellersberger, 1933).

1.1.6.5 Diagnosis

As the clinical signs of HAT are non-specific diagnostic tests have to be performed for a definitive diagnosis to be obtained (Kennedy, 2004). Most patients infected with *T. b. gambiense* are detected during mass screening programs. The most commonly used test for screening populations in areas where *T. b. gambiense* occurs is the card agglutination test for trypanosomiasis (CATT). The CATT test was developed in 1978 and is a fast and simple way of detecting the presence of *T. b. gambiense* specific antibodies in the blood, plasma or serum of patients (Magnus, Van Meirvenne and Vervoort, 1978). The test detects the presence of antibodies against the dominant variable antigen LiTat 1.3. The patients' blood is combined with a reagent containing whole, fixed and stained trypanosomes expressing the antigen on the card and is shaken for 5 minutes on a rotor. In patients who have been exposed to *T. b. gambiense*, agglutination is clearly visible (Magnus, Van Meirvenne and Vervoort, 1978). The sensitivity and specificity of the CATT test has been estimated to lie between

92-100% and 90-95% respectively (Bafort, Schutte and Gathiram, 1986; Jamonneau, Truc, Garcia, Magnus *et al.*, 2000; Noireau, Gouteux and Duteurtre, 1987; Zillmann and Albiez, 1986). False negatives can occur in patients infected with trypanosome strains which lack the LiTat 1.3 antigen (Dukes, Gibson, Gashumba, Hudson *et al.*, 1992; Enyaru, Matovu, Akol, Sebikali *et al.*, 1998) and false positives have been reported in patients with malaria and other parasitic infections (Magnus, Van Meirvenne and Vervoort, 1978). In all patients with a positive CATT, the parasite must be demonstrated in biological fluids in order for the diagnosis to be confirmed (Kennedy, 2004). However, this is often difficult in *T. b. gambiense* infections as the parasite is present in very low numbers in the peripheral circulation (Atouguia and Kennedy, 2000). Individuals who are CATT positive but negative for the presence of trypanosomes are subject to follow up investigations until parasites are visualised or the individual becomes CATT negative (Simarro, Ruiz, Franco and Josenando, 1999). The CATT test is only effective in the diagnosis of *T. b. gambiense* infections (Enyaru, Odiit, Winyi-Kaboyo, Sebikali *et al.*, 1999). In individuals where *T. b. rhodesiense* infection is suspected the only way to obtain a definitive diagnosis is by direct visualisation of the parasites in biological fluids.

Biological fluids commonly examined for the presence of trypanosomes are blood, lymph node aspirates and cerebrospinal fluid. Thick, thin or wet blood films can be used to detect the parasite in the blood. In wet blood films a drop of the patients blood is placed on a slide and directly examined under a microscope for the presence of trypanosomes (World Health Organisation, 1998). The technique has a low sensitivity with a limit of detection of approximately 10,000 trypanosomes per ml of blood but it is still widely used in the field due to its low cost, simplicity and immediate results (Chappuis, Loutan, Simarro, Lejon *et al.*, 2005a). Trypanosomes are more easily visualised in the blood of patients with *T. b. rhodesiense* infections as the density of circulating parasites is higher than in *T. b. gambiense* infections (Atouguia and Kennedy, 2000). Sensitivity can be improved by using a concentration technique. The most widely used concentration technique is the microhaematocrit centrifugation technique (MHCT) which was developed over 30 years ago (Woo, 1970; Woo, 1971; World Health Organisation, 1998). Capillary tubes containing anticoagulant are filled three quarters full with the patients' blood and sealed with plasticine before

being centrifuged at high speed. The trypanosomes are concentrated at the level of the white blood cells between the plasma and erythrocytes and can be directly visualised at low magnification. By examining more than one capillary tube per patient less than 500 trypanosomes per ml of blood can be detected. However, visualisation of the smaller trypanosomes is often impeded by the presence of the larger microfilariae when co-infections occur (Chappuis *et al.*, 2005a). A second technique which can be used to enhance the visualisation of trypanosomes in blood samples is the mini anion exchange centrifugation technique (mAECT) (Lumsden, Kimber, Evans and Doig, 1979; Zillmann, Konstantinov, Berger and Braun, 1996). As trypanosomes are less negatively charged than blood cells they can be separated from venous blood by anion exchange chromatography. The trypanosomes are then concentrated at the bottom of a glass tube by low speed centrifugation where they can be visualised by microscopy. The technique is very sensitive with a detection limit of less than 100 trypanosomes per ml of blood but the technique is quite tedious and time consuming, limiting its use in the field (Chappuis *et al.*, 2005a). An alternative to the microhaematocrit and mini anion exchange centrifugation techniques is the quantitative buffy coat (QBC) technique (Bailey and Smith, 1992; Levine, Wardlaw and Patton, 1989). The technique concentrates the parasites by high speed centrifugation and utilises acridine orange to stain the nucleus and kinetoplast. The fluorescent trypanosomes can then be visualised by ultraviolet light between the white blood cells in the expanded buffy coat. The technique is very sensitive and robust with a sensitivity of 95% for trypanosome concentrations of 450 per ml of blood. Despite this, production of QBC kits has recently ceased (Buscher and Lejon, 2004).

In addition to blood samples, chancre and lymph node aspirates can also be examined for the presence of trypanosomes (World Health Organisation, 1998). The examination of lymph node aspirates is frequently used in the diagnosis of *T. b. gambiense* infections due to its low cost and simplicity (Buscher and Lejon, 2004). Enlarged lymph nodes are punctured and the fresh aspirate is examined under the microscope for the presence of motile trypanosomes. The sensitivity of the technique varies between 40 and 80% depending upon the parasite strain, the prevalence of other diseases causing lymphadenopathy in the area and the stage of the disease, with sensitivity being higher during the first stage

(Chappuis *et al.*, 2005a; Simarro, Louis and Jannin, 2003). Trypanosomes can be detected in the chancre two days earlier than in the blood but this technique is seldomly used in the field as most patients present late in infection when the chancre has resolved (Apted, 1970a).

Once a definitive diagnosis has been obtained the stage of the disease must be determined due to the high toxicity of the drugs used to treat the second stage of the disease. The stage of the disease is determined by lumbar puncture and examination of the cerebrospinal fluid (CSF). The criteria for second stage disease as determined by WHO is the presence of one of the following in the cerebrospinal fluid; trypanosomes, an elevated leukocyte count (>5 cells/μl) or an increase in the protein content (>37mg/100ml as measured by the dye binding protein assay) (World Health Organisation, 1998). At present there is disagreement about the cut off point used to differentiate between first and second stage disease (Kennedy, 2008). Many believe that the cut off point for first stage disease should be raised to 10 or 20 cells/μl of CSF (Bisser, Lejon, Preux, Bouteille *et al.*, 2002; Lejon, Reiber, Legros, Dje *et al.*, 2003; Miezan, Meda, Doua, Yapo *et al.*, 1998). This is due to studies conducted in Côte d'Ivoire where patients with 6 to 20 cells/μl of CSF were successfully treated with the first stage drug pentamidine (Doua, Miezan, Singaro, Yapo *et al.*, 1996) while in a further study in Angola the relapse rate after pentamidine treatment was similar in patients with 0 to 5 cells/μl or 6 to 10 cell/μl of CSF (Ruiz, Simarro and Josenando, 2002). In Angola and Côte d'Ivoire the cut off point for first stage disease has already been raised to 20 cells/μl of CSF (Doua *et al.*, 1996; Pepin and Milord, 1994). The quantification of protein in the CSF for stage determination of HAT is no longer recommended (Chappuis *et al.*, 2005a).

Research into the development of new diagnostic tests for HAT that are simple to carry out in the field and allow accurate staging of the disease is currently in progress.

1.1.7 Chemotherapy

1.1.7.1.1 Haemolymphatic infection

1.1.7.1.2 Suramin

Suramin is a polysulphonated naphthyl urea (Figure 1-5) that was first used in the treatment of HAT in 1922 (Voogd, Vansterkenburg, Wilting and Janssen, 1993). It was developed following the observation that two closely related naphthalene dyes, trypan red and trypan blue, exhibited trypanocidal activity. Suramin is effective against both *T. b. rhodesiense* and *T. b. gambiense* early stage infections but pentamidine is preferred for treatment of *T. b. gambiense* infections due to its easier administration schedule (Apted, 1970b). The compound is supplied as a white powder which is readily soluble in water. Administration consists of a test dose of 5mg/kg body weight on day one followed by five injections of 20mg/kg body weight every three to seven days (World Health Organisation, 1998). Administration is via slow intravenous infusions as intramuscular administration results in an intense local irritation at the injection site (Williamson, 1970).

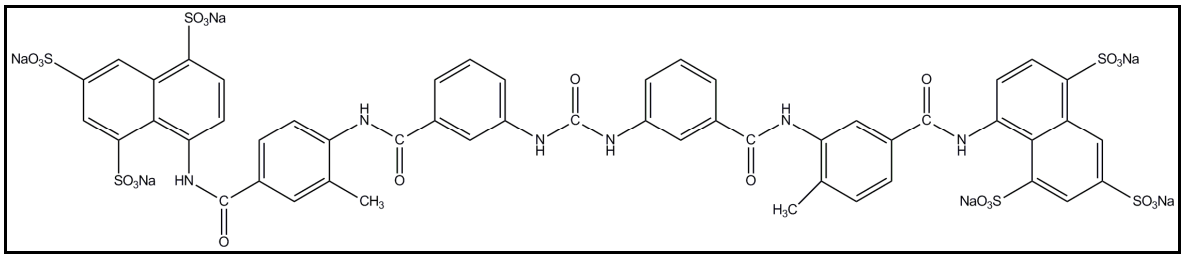

Figure 1-5: The chemical structure of suramin

Following administration over 99.7% of the drug becomes bound to plasma proteins resulting in the drug being eliminated very slowly (Pepin and Milord, 1994; World Health Organisation, 1998). It can be found in the blood up to three months after administration (Pepin and Milord, 1994). The main route of elimination is through the kidneys with approximately 80% of the administered dose being excreted in the urine (World Health Organisation, 1998). The kidneys are the main organ of accumulation of the drug and can therefore be a site of toxicity (World Health Organisation, 1998). Renal toxicity in the form of a mild proteinuria is often observed therefore patients' urine is frequently checked

throughout treatment in order to detect any renal impairment (Apted, 1970b). Severe adverse reactions to the drug are rare. Adverse reactions which have been reported following suramin administration include nausea, vomiting, urticaria, loss of consciousness, fever, photophobia, lacrimation, exfoliative dermatitis and haemolytic anaemia (Apted, 1970b; Burri, Stich and Brun, 2004).

Suramin is slowly trypanocidal killing trypanosomes 12 to 36 hours after administration (Hawking, 1978). It is suspected that the drug gradually accumulates within the trypanosome via endocytosis bound to low-density lipoproteins (Vansterkenburg, Coppens, Wilting, Bos *et al.*, 1993). Despite many years of research the trypanocidal mechanism of suramin remains obscure. The drug carries six negative charges that enable the compound to bind to many enzymes by electrostatic interactions. Enzymes inhibited by suramin include L-α-glycerophosphate oxidase, glyceraldehyde-3-phosphate dehydrogenase, RNA polymerase and kinases, thymidine kinase, dihydrofolate reductase, urease and hexokinase (Chello and Jaffe, 1972; Fairlamb and Bowman, 1977; Jaffe, Meymaria and Mccormac, 1972; Willson, Callens, Kuntz, Perie *et al.*, 1993). However, it is unclear whether trypanocidal activity occurs as a direct result of enzyme inhibition.

At present no resistance to suramin has been reported in the field.

1.1.7.1.3 Pentamidine

Pentamidine is an aromatic diamidine (Figure 1-6) that was introduced for the treatment of sleeping sickness in 1940 (Sands, Kron and Brown, 1985). It was developed after it was observed that a related compound synthalin, which induces hypoglycaemia in mammals, had pronounced anti-trypanocidal activity. Pentamidine is also used to treat antimony refractory leishmaniasis and *Pneumocystis carni* pneumonia (Drake, Lampasona, Nicks and Schwarzmann, 1985). Pentamidine is used in the treatment of first stage *T. b. gambiense* infections. It is administered as an intramuscular injection at a dose of 4mg/kg body weight daily or on alternate days for 7 to 10 days (World Health Organisation, 1998). The drug is generally well tolerated with only minor adverse reactions occurring which are usually reversible. Immediately following administration hypotension accompanied by dizziness and collapse of the patient

has been reported in 9.6% of patients administered the drug (Burri, Stich and Brun, 2004). At the site of administration local reactions including pain, sterile abscesses and necrosis can occur (World Health Organisation, 1998). Systemic reactions which have been reported following pentamidine treatment include leucopenia, abnormal liver function tests, hypoglycaemia and hyperglycaemia (Burri, Stich and Brun, 2004).

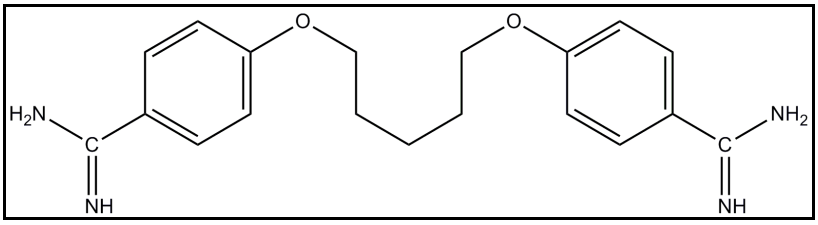

Figure 1-6: The chemical structure of pentamidine

Pentamidine has a large volume of distribution of 11,850l after a single dose and 35,000l after multiple doses (Burri, Stich and Brun, 2004). As 70-80% of the drug is bound to plasma proteins its half-life is very long, varying between 7 and 48 days (World Health Organisation, 1998). The drug's long half life led to it being used in mass prophylaxis campaigns by the French, Belgian and Portuguese colonial health authorities (Williamson, 1970). Despite being highly successful in controlling *T. b. gambiense* the prophylactic use of pentamidine is no longer recommended (Van Hoof, Henrard and Peel, 1944). Of the administered dose approximately 5% is recovered unchanged in the urine (Bronner, Gustafsson, Doua, Ericsson *et al.*, 1995). In rat liver homogenates and microsomes the majority of the administered dose is metabolised to at least 7 primary metabolites by the cytochrome P450 dependant oxygenases before being eliminated via the urine (Bronner, Ericsson, Nordin, Wikstrom *et al.*, 1995).

Uptake of pentamidine into trypanosomes is carrier mediated. The primary carrier is the P2 aminopurine permease transporter (ASPT1) but at least two other transporters are involved in the uptake of pentamidine, a high affinity pentamidine transporter (HAPT1) and a low affinity pentamidine transporter (LAPT1) (de Koning and Jarvis, 2001). The mechanism of action of pentamidine is poorly understood. As a di-cation pentamidine interacts electrostatically with cellular polyanions (Denise and Barrett, 2001). Binding to nucleic acid, disruption of kinetoplast DNA, inhibition of mRNA trans-splicing and inhibition of RNA-editing have all been suggested as possible mechanisms of action but to

date none have been confirmed (Wang, 1995). As the drug accumulates to very high levels within the trypanosome it is possible that its toxic effects arise due to inhibition of multiple cellular targets (Carter, Berger and Fairlamb, 1995; Denise and Barrett, 2001).

1.1.7.2 CNS infection

1.1.7.2.1 Melarsoprol

Melarsoprol, a melaminophenyl based organic arsenical (Figure 1-7) was introduced for the treatment of sleeping sickness in 1949 (Friedheim, 1949). The drug is insoluble in water so it is prepared as a 3.6% solution dissolved in propylene glycol. Various administration schedules have been used since its introduction. Until recently a schedule consisting of a series of 3-4 injections of increasing melarsoprol concentration separated by a drug free period of 7 to 10 days was the most frequently used schedule (World Health Organisation, 1998). Recent pharmacokinetic investigations demonstrated that a concise regime consisting of 10 daily injections of 2.2 mg/kg was as effective and no more toxic than the prolonged schedule (Burri, Nkunku, Merolle, Smith *et al.*, 2000; Schmid, Nkunku, Merolle, Vounatsou *et al.*, 2004; Schmid, Richer, Bilenge, Josenando *et al.*, 2005). This condensed schedule is now used in the field for the treatment of *T. b. gambiense* infections. The efficacy of the concise schedule against the more acute rhodesiense form of the disease has yet to be assessed. The prolonged schedule is therefore still recommended for the treatment of *T. b. rhodesiense* infections (Schmid *et al.*, 2005). The mechanism by which melarsoprol exerts its trypanocidal effect is unknown. Trypanosomes exposed to melarsoprol rapidly lyse. It was suggested that inhibition of glycolysis and the subsequent loss of ATP could be responsible for the lysis observed but it appears that lysis occurs before there is a significant depletion of ATP within the parasite (Van Schaftingen, Opperdoes and Hers, 1987). A second possible target of melarsoprol is the thiol trypanothione. Trypanothione is a key, low molecular weight thiol comprising of two glutathione molecules conjugated with spermidine. It is responsible for most of the tasks carried out by glutathione in mammalian cells (Fairlamb and Cerami, 1992). Arsenic forms very stable conjugates with trypanothione therefore it has been proposed as a possible target of melarsoprol (Fairlamb, Henderson and Cerami, 1989). However, at the

point of arsenical induced lysis only a small proportion of the drug is conjugated with trypanothione therefore it is unclear whether trypanothione is the target of the drug (Fairlamb, Smith and Hunter, 1992).

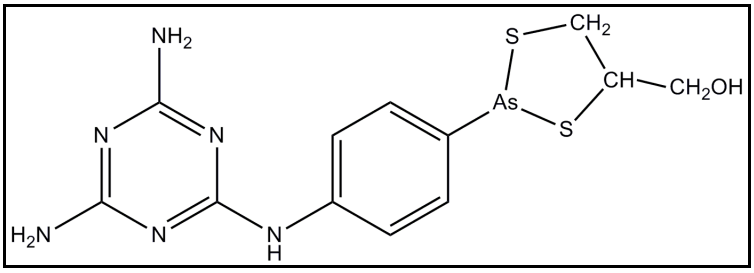

Figure 1-7: The chemical structure of melarsoprol

Resistance to melarsoprol in the field has now reached 30% in certain areas of Uganda (Legros, Evans, Maiso, Enyaru *et al.*, 1999). The mechanisms behind this resistance are not fully understood. Melarsoprol uptake into trypanosomes is mediated by the P2 aminopurine transporter (Carter and Fairlamb, 1993; Delespaux and de Koning, 2007; Maser, Sutterlin, Kralli and Kaminsky, 1999). The P2 transporter is encoded by the TbAT1 gene (Maser *et al.*, 1999). Disruption of the TbAT1 gene in bloodstream *T. b. brucei* parasites *in-vitro* results in limited arsenical resistance suggesting that different or additional mechanisms for high level arsenical resistance exist (Matovu, Stewart, Geiser, Brun *et al.*, 2003). One mechanism that has been suggested is the over expression of ABC transporters. ABC transporters have already been implicated in drug resistance in multiple protozoan parasites (Jones and George, 2005; Klokouzas, Shahi, Hladky, Barrand *et al.*, 2003). Three ABC transporter genes have been identified in *T. b. brucei* (Maser and Kaminsky, 1998). The over expression of one of these, TbMRPA resulted in a ten fold increase in melarsoprol resistance *in-vitro* (Shahi, Krauth-Siegel and Clayton, 2002). The TbMRPA transporter is thought to extrude the melarsoprol-trypanothione conjugate from the parasite rather than the drug itself. However, *in-vivo* over expression of TbMRPA did not lead to a reduced sensitivity to melarsoprol and there is no evidence of TbMRPA over expression in clinical isolates (Alibu, Richter, Voncken, Marti *et al.*, 2006). It can therefore be concluded that over expression of ABC transporters is unlikely to contribute to melarsoprol resistance in the field (de Koning, 2008).

Research to find an alternative transport mechanism by which melarsoprol enters trypanosomes led to the discovery that the high affinity pentamidine

transporter (HAPT) also mediates the uptake of melaminophenyl arsenicals (Bridges, Gould, Nerima, Maser *et al.*, 2007; Matovu *et al.*, 2003). It is thought that concomitant loss of both the P2 and HAPT transporters in trypanosomes could result in high level melarsoprol resistance. The hypothesis was tested *in-vitro* with a cell line in which the P2 and HAPT transporter had been lost (Bridges *et al.*, 2007). The cell line was highly resistant to melarsen oxide confirming the suspicion that high level melarsoprol resistance could occur due to loss of both the P2 and HAPT transporter (Bridges *et al.*, 2007). However, the physiological function of HAPT is currently unknown. *In-vivo* a high inoculum of the P2/HAPT deficient line was required to establish a parasitaemia and the infection appeared to be self curing (Bridges *et al.*, 2007). It is therefore possible that HAPT performs a function vital for trypanosomal survival *in-vivo* but not *in-vitro* (de Koning, 2008). The definitive mechanism by which high level melarsoprol resistance occurs is still to be elucidated.

Melarsoprol chemotherapy is associated with numerous adverse reactions. Pyrexia, headache and general malaise occur in nearly all patients to which the drug is given (Burri, Stich and Brun, 2004). Other adverse reactions occasionally reported include peripheral motoric or sensorial neuropathy, renal dysfunction (proteinuria and hypertension), abdominal pains, myocardial damage, vomiting and diarrhoea (Blum and Burri, 2002). In less than 1% of patients a severe skin reaction, exfoliative dermatitis, has been reported upon completion of treatment (World Health Organisation, 1998). Care has to be taken when administering the drug as leakage of the propylene glycol solvent into the surrounding tissues results in chemical cellulitis and necrosis at the site of injection (Pepin and Milord, 1994).

The most severe adverse reaction to melarsoprol treatment is a post treatment reactive encephalopathy (PTRE). The PTRE occurs in up to 10% of patients treated with the drug of which 50% will die from the complication (Kennedy, 2004; Pepin and Milord, 1994). It most frequently occurs at the end of the first series of injections, during the interval between the first and second series of injections or during the second series of injections (Haller, Adams, Merouze and Dago, 1986). Patients experience fever, headaches, dizziness, tremors and slurred speech followed by mental dullness and confusion, staggering gait or restlessness (Haller *et al.*, 1986; World Health Organisation, 1998). There is

usually a rapid deterioration in the patients condition with patients frequently experiencing seizures and a loss of consciousness, often progressing to a deep coma (Atouguia and Kennedy, 2000; Pepin and Milord, 1994; World Health Organisation, 1998).

The mechanisms behind the occurrence of the PTRE are not fully understood and many hypotheses have been put forward. Jennings *et al.* proposed that administration of melarsoprol results in a rapid clearance of trypanosomes from the bloodstream but not the CNS (Jennings, McNeil, Ndungu and Murray, 1989). As a result the trypanosomes within the brain become the sole focus of the activated immune system resulting in an exacerbation of the pre-existing meningoencephalitis (Jennings *et al.,* 1989). Pepin and Milord agreed that the PTRE was an immune mediated event but proposed an alternative mechanism for its occurrence (Pepin and Milord, 1991). They suggested that melarsoprol treatment results in the formation of immune complexes and the release of trypanosomal antigens which bind to glial cells and become a target for antibodies and T lymphocytes (Pepin and Milord, 1991). Based on this theory it was suggested that very aggressive treatment schedules could result in the rapid release of immune complexes or trypanosomal antigens thus increasing the likelihood of the PTRE occurring. This theory was investigated by Jennings *et al.* in a murine model of the disease (Jennings, Hunter, Kennedy and Murray, 1993). A rapidly curative treatment regime was administered to mice with early CNS stage disease, in which low numbers of trypanosomes are present within the CNS and also to mice suffering from relapse infections in which large numbers of trypanosomes are present within the CNS. In both instances the existing meningoencephalitis was rapidly resolved, indicating that it is the presence of living trypanosomes within the CNS and not trypanosomal antigens which are responsible for the PTRE (Jennings *et al.,* 1993). The speed at which trypanosomes were killed had little effect on the development of the meningoencephalitis suggesting that aggressive treatment regimes which eliminate all trypanosomes from the CNS are less likely to result in the PTRE (Jennings *et al.,* 1993).

The development of the PTRE is not exclusively associated with HAT patients as it was also observed in patients with acute promyelocytic leukaemia (APL) who were given melarsoprol (Soignet, Tong, Hirschfeld and Warrell, 1999). It was

suggested that the CNS toxicity observed was due to a direct toxic effect of the compound (Soignet *et al.*, 1999). However, information from HAT patients suggests that the PTRE is not a result of direct arsenical toxicity as patients who survived the PTRE could receive additional doses of melarsoprol without the PTRE reoccurring (Pepin, Guern, Ethier, Milord *et al.*, 1989). Furthermore, incidences of encephalopathy have also been reported following the administration of the trypanocidal drugs eflornithine and suramin (Burri and Blum, 1996; Chappuis, Udayraj, Stietenroth, Meussen *et al.*, 2005b).

The administration of the corticosteriod prednisolone prior to and during the administration of melarsoprol has been suggested to prevent the development of the PTRE. Pepin *et al.* reported a decrease in the incidence of the PTRE in patients when 1mg/kg of prednisolone was administered orally, concurrently with melarsoprol (Pepin *et al.*, 1989). However, other authors are more sceptical about the potential benefits of corticosteroids in preventing the PTRE. In one study involving patients infected with *T. b. rhodesiense*, the co-administration of corticosteroids with melarsoprol had no effect on the incidence of the PTRE (Orlando and Arroz, 1987).

In patients who develop the PTRE, melarsoprol treatment is suspended and the symptoms of the PTRE are managed. Patients are given 5% isotonic glucose intravenously, body temperature and convulsions are controlled with antipyretics and antiepileptic drugs respectively. The cerebral oedema is treated with hypertonic solutions, diuretics, adrenaline and corticosteroids (World Health Organisation, 1986). If the symptoms resolve melarsoprol therapy can be restarted and interestingly the PTRE does not recur (Pepin *et al.*, 1989).

1.1.7.2.2 Eflornithine (α difluoromethylornithine) (DFMO)

Eflornithine (Figure 1-8) is the most recent drug to be recommended for the treatment of second stage HAT being registered in 1990 and 1991 in the USA and Europe respectively (Kuzoe, 1993). It was originally developed as a potential antineoplastic agent however it has still not being registered for this purpose (Barrett, Boykin, Brun and Tidwell, 2007; Barrett and Barrett, 2000; Singh and Lippman, 1998). The drug was originally recommended for the treatment of melarsoprol refractory CNS stage *T. b. gambiense* infections but it has recently

been approved as a first line treatment for CNS stage T. *b. gambiense* infections in combination with nifurtimox (NECT therapy) (Pepin and Milord, 1994; World Health Organisation, 2009). As a monotherapy the drug is administered at a dose of 400mg/kg body weight per day given over four slow intravenous infusions every six hours for 14 days (World Health Organisation, 1998). Commonly reported adverse reactions include suppression of bone marrow activity with anaemia, leukopenia and thrombocytopenia being reported in 44, 27 and 7% of patients respectively (World Health Organisation, 1998). Diarrhoea, vomiting, fever and convulsions have also been reported following administration of eflornithine (Chappuis *et al.,* 2005b). Generally adverse reactions are reversible upon cessation of treatment (Burri, Stich and Brun, 2004). Following administration eflornithine does not bind significantly to plasma proteins and approximately 80% of the administered dose is excreted unchanged in the urine within 24 hours (Burri and Brun, 2003).

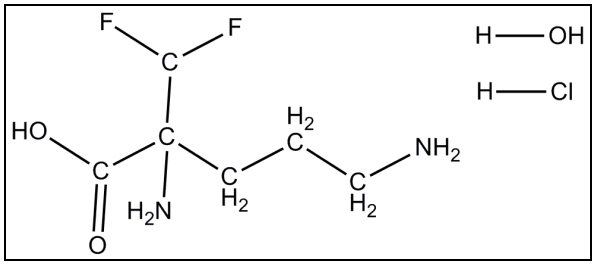

Figure 1-8: The chemical structure of eflornithine

Eflornithine is an irreversible inhibitor of the enzyme ornithine decarboxylase (ODC) (Mamont, Duchesne, Grove and Bey, 1978). ODC catalyses the conversion of ornithine to putrescine which is the first rate limiting step in the synthesis of the polyamines spermidine and spermine (Bacchi, Nathan and Hutner, 1980). Polyamines are essential for the growth and multiplication of all eukaryotic cells (Pegg and Mccann, 1982). Selectivity arises as the ODC of *T. b. gambiense* is replenished much more slowly than in mammalian cells (Ghoda, Phillips, Bass, Wang *et al.*, 1990). Upon exposure to eflornithine trypanosomes are transformed into non-dividing stumpy forms which are then cleared by the immune system (Bitonti, McCann and Sjoerdsma, 1986). A fully functioning immune system is therefore essential in order for eflornithine chemotherapy to be effective. Eflornithine is not effective in the treatment of CNS stage *T. b. rhodesiense* infections as the ODC enzyme of *T. b. rhodesiense* is replenished more rapidly than in *T. b. gambiense* (Iten, Mett, Evans, Enyaru *et al.*, 1997).

Resistance to eflornithine has been induced *in-vitro* in procyclic *T. b. brucei* lines (Bellofatto, Fairlamb, Henderson and Cross, 1987; Phillips and Wang, 1987). Accumulation of the drug was decreased in the parasites but it is not known if this is a result of reduced uptake or due to an active drug extrusion mechanism. Resistance to eflornithine is yet to be reported in the field, if resistance did emerge it would have disastrous consequences for the treatment of HAT.

One of the main limitations to the widespread use of eflornithine is its prolonged treatment schedule. The need for the drug to be infused every six hours for 14 days means large quantities of infusion solutions are required, which are often not available in the resource poor settings where HAT occurs. Furthermore, patients must be hospitalised for the duration of the treatment and this places a massive strain on already stretched health services. In an attempt to reduce the administration schedule of eflornithine, the drug was recently combined with the orally available nitroimidazole nifurtimox to produce a combination therapy known as NECT. (Discussed in detail below).

1.1.7.2.3 Nifurtimox

Nifurtimox (Figure 1-9) was introduced in the 1960's for the treatment of Chagas disease which is caused by the American trypanosome *T. cruzi* (Brener, 1979). At present nifurtimox is not licensed for use in sleeping sickness, it is only used on compassionate grounds for the treatment of melarsoprol refractory infections (World Health Organisation, 1998). When nifurtimox is administered alone it is not very effective in the treatment of CNS stage *T. b. gambiense* infections with cure rates of between 40 and 80% (Janssens and Demuynck, 1977; Moens, Dewilde and Ngato, 1984; Pepin, Milford, Meurice, Ethier *et al.*, 1992; Pepin and Milord, 1994; Pepin, Milord, Mpia, Meurice *et al.*, 1989). Its efficacy improves greatly when it is combined with eflornithine in a combination therapy known as NECT (See below).

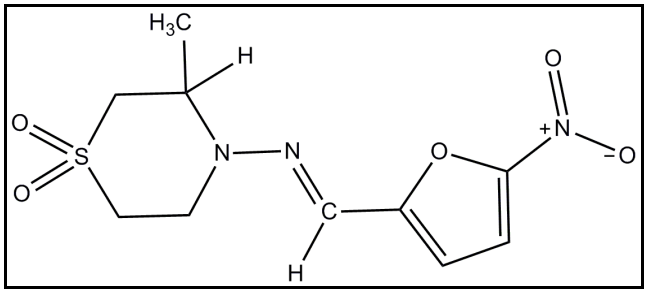

Figure 1-9: The chemical structure of nifurtimox

Nifurtimox is given orally but it is not well tolerated with two thirds of patients experiencing adverse reactions (Burri, Stich and Brun, 2004). The drug is toxic to the peripheral and central nervous system with convulsions, psychotic reactions, nystagmus and vertigo frequently occurring. In addition, gastrointestinal tract disturbances and skin rashes have been reported (World Health Organisation, 1998). The mode of action of nifurtimox is not fully understood. The drug is a nitroheterocycle and is composed of a nitro group linked to an aromatic ring (Figure 1-9) (Grunberg and Tisworth, 1973). Like most nitroheterocycles, nirfurtimox is as a pro-drug and the active metabolite is generated through reduction of the nitro group. In trypanosomes, reduction of nirfurtimox is catalysed by type I nitroreductases. The reaction generates an unsaturated open-chain nitrile which has pronounced trypanocidal and cytotoxic properties (Hall, Bot and Wilkinson, 2011). It is thought that selectivity arises as type I nitroreductases are predominately expressed in trypanosomes but not in eukaryotic cells. The cellular target of the open-chain nitrile is currently unknown but as the metabolite displays equivalent trypanocidal and cytotoxic activity, it is possible that its cellular target is common to both trypanosomes and eukaryotic cells (Hall, Bot and Wilkinson, 2011).

1.1.7.2.4 Nifurtimox and eflornithine combination therapy (NECT)

A phase III randomised open-label multi-centre trial of nifurtimox and eflornithine combination therapy (NECT) has recently been completed in the Republic and Democratic Republic of Congo (Priotto, Kasparian, Mutombo, Ngouama *et al.*, 2009). In the trial patients were either given the standard eflornithine regime of 400mg/kg per day given by slow intravenous infusion every six hours for 14 days or eflornithine 400mg/kg per day by slow intravenous infusion every 12 hours for 7 days plus nifurtimox 15mg/kg per day orally every 8 hours for 10 days. NECT therapy was found to be as effective as eflornithine

monotherapy with cure rates of 96.5 to 97.9% compared to 91.6 to 92.3% for eflornithine monotherapy. A lower frequency of diarrhoea, hypotension, infections, dysphagia, skin rashes, pruritus, fever and neutropenia was observed in patients receiving the NECT therapy compared to eflornithine alone. However, nausea, vomiting, anorexia and tremors occurred more frequently in patients receiving NECT therapy than eflornithine monotherapy. Neutropenia and anaemia were the most prominent haematological reactions in both treatment groups although the frequency of neutropenia was significantly reduced in patients receiving NECT therapy. From the clinical trial it can be concluded that eflornithine in combination with nifurtimox is safe and effective in the treatment of CNS stage *T. b. gambiense* infections (Priotto *et al.,* 2009). NECT therapy has many advantages over eflornithine monotherapy. The simpler and shorter administration schedule of NECT means fewer resources are required and the hospitalisation time of patients is greatly reduced. This makes NECT therapy more feasible in the resource poor settings where HAT occurs. In 2009, NECT therapy was added to the WHO List of Essential Medicines for the treatment HAT and is now the first line drug for the treatment of *T. b. gambiense* infections (World Health Organisation, 2009). The efficacy of NECT therapy in the treatment of *T. b. rhodesiense* CNS infections has not been assessed and it is therefore not recommended for the treatment of *T. b. rhodesiense* infections (Priotto *et al.,* 2009).

1.1.7.3 Emerging treatments

Due to the high toxicity of melarsoprol and the difficulty and cost involved in the administration of eflornithine there is a desperate need for the development of new trypanocides. Any new trypanocides must be safe, easy to administer and cheap to produce. In recent years a few candidates have emerged as possible trypanocides but none have gained approval.

1.1.7.3.1 DB289

DB289 (pafuramidine maleate) is a recently synthesised methamidoxime prodrug. *In-vitro* DB289 is inactive with an ED_{50} > 3000ng/ml but following oral administration it is converted to the active compound DB75 by a series of O-demethylation and dehydroxylation reactions (Yeates, 2003). In a *Cynomolgus*

monkey model of acute *T. b. rhodesiense* infection cures were obtained when DB289 was administered orally at 10mg/kg daily for 5 days (Yeates, 2003). A phase I clinical safety trial was conducted in healthy volunteers. Volunteers were given a single DB289 treatment at doses ranging from 25 to 600mg or as multiple daily doses ranging from 25 to 100mg. The compound was well tolerated and no significant adverse effects were observed during the trial (Yeates, 2003). The success of the phase I trial led to a phase II trial being conducted in patients infected with *T. b. gambiense* in Angola and the Democratic Republic of Congo (DRC). Patients were treated with DB289 orally for 10 days at 100mg twice a day (Barrett, 2010). The compound was well tolerated and at 24 months the post-treatment efficacy was 85%, which is comparable to that of pentamidine. However, due to the initial phase I trial being conducted in Caucasian patients the US Food and Drug Administration (FDA) requested a second retrospective phase I trial be completed in healthy indigenous African patients. In the study DB289 was given to the patients orally, twice a day, for 14 days at dose of 100mg (Yeates, 2003). In approximately 25% of the patients, elevated liver enzymes were observed following treatment but these levels returned to normal. However, approximately 8 weeks after administration of the last dose of the drug, five patients developed acute renal toxicity (Barrett, 2010). This resulted in the development of DB289 being discontinued. At present research continues into the trypanocidal activity of DB75 and two additional aza analogues. Although DB75 and its aza analogues have been shown to be effective in murine and monkey models they have not yet entered into clinical trials (Wenzler, Boykin, Ismail, Hall *et al.*, 2009).

1.1.7.3.2 Fexinidazole

Fexinidazole is a 5-nitroimidazole (Figure 1-10) whose trypanocidal activity was first demonstrated in 1980, but concerns about its genotoxicity led to it being abandoned as a potential trypanocide (Jennings and Urquhart, 1983). However the discovery that different nitroheterocycles display varying degrees of genotoxicity and the recent introduction of novel nitroheterocycles into clinical trials for tuberculosis, anaerobic protozoan and helminth infections (Anderson and Curran, 2007; Stover, Warrener, VanDevanter, Sherman *et al.*, 2000) led to a renewed interest in fexinidazole as a potential trypanocide by the Drugs for Neglected Disease initiative (DNDi).

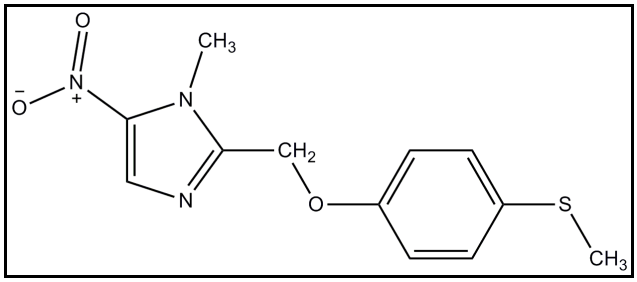

Figure 1-10: The chemical structure of fexinidazole

Fexinidazole displays a good *in-vitro* trypanocidal activity with an inhibitory concentration (IC_{50}) of 2.57μM and 1.14μM against *T. b. rhodesiense* and *T. b. gambiense* respectively. In an acute murine model of *T. b. rhodesiense* infection total cures were obtained following the oral administration of fexinidazole at doses of 100mg/kg once daily and 50mg/kg twice daily for 4 days. In a chronic CNS stage murine model of *T. b. brucei* infection, fexinidazole, administered orally at a dose of 200mg/kg/day for five consecutive days cured 87.5% (7/8) of the animals (Torreele, Bourdin, Tweats, Kaiser *et al.*, 2010). Toxicological studies completed in the rat and dog raised no issues with the no observed adverse effect level (NOAEL) determined to be 200mg/kg/day for both species. These promising results led to fexinidazole entering phase I clinical trials in healthy African volunteers in 2009 to allow the bioavailability, pharmaco-kinetics and tolerability of the compound to be assessed. The trials are currently ongoing but it is hoped that if the compound successfully completes all pre-clinical and clinical developmental stages it will be registered for the treatment of HAT by 2014 (Torreele *et al.*, 2010).

1.1.7.3.3 N-myristoyltransferase inhibitors

N-myristoyltransferase (NMT) is a ubiquitous eukaryotic co- and post-translational modification which is essential for the biological activity and membrane targeting of numerous important proteins (Farazi, Waksman and Gordon, 2001; Resh, 2006). Frearson *et al*. recently identified a potent inhibitor of NMT in *T. b. brucei* named DDD85646 (Frearson, Brand, McElroy, Cleghorn *et al.*, 2010). DDD85646 is highly trypanocidal *in-vitro* with the number of motile trypanosomes reduced to below detectable levels within 48 hours of exposure. *In-vivo* studies in an acute *T. b. brucei* murine model determined the minimum curative oral dose of DDD85646 to be 12.5mg/kg twice a day for 4 days.

Complete cures were also achieved with shorter oral dosing schedules of 100mg/kg twice a day for 1 day and 25mg/kg twice a day for two days (Frearson *et al.*, 2010). The compound is currently undergoing optimization in order to improve its CNS penetration and selectivity.

1.1.7.3.4 Oxaborole 6-carboxamides

Recently a class of boron containing compounds, oxaborole carboxamides were identified which show potent *in-vitro* trypanocidal activity against *T. b. brucei, T. b. gambiense* and *T. b. rhodesiense* (Nare, Wring, Bacchi, Beaudet *et al.*, 2010). The trypanocidal activity of two of the compounds AN3520 and SCYX-6759 was investigated in more detail. For both compounds complete cures were achieved in an acute *T. b. brucei* murine model following intraperitoneal (i.p.) and oral administration (p.o.). In a CNS *T. b. brucei* murine model SCYX-6759 displayed a superior activity achieving 100% and 83% cure rates following i.p. and p.o. administration respectively (Nare *et al.*, 2010). In comparison, i.p. administration of AN3520 only resulted in partial cure rates of 78% (Nare *et al.*, 2010). Adverse toxicological reactions were not observed following the administration of either compound and the compounds displayed favourable physiochemical profiles (Nare *et al.*, 2010).

The studies conducted to date suggest that oxaborole carboxamides are promising lead compounds and their potential to serve as trypanocidal agents is currently being investigated.

1.1.7.4 The future of HAT chemotherapy

New trypanocides, which are easily administrable, non-toxic and cheap to produce, are urgently required. Despite extensive research over the last few years, only one new compound, fexinidazole, is currently in clinical trials for the treatment of HAT. Melarsoprol is a very effective trypanocide. However, the drug's high toxicity and difficult administration schedule mean that the compound is no longer used as the first line drug for the treatment of CNS stage *T. b. gambiense* infections. If the solubility of melarsoprol could be increased so that the compound is soluble in water, oral dosing could become a possibility, thereby eliminating the problems associated with administration of the drug.

Furthermore, if the toxicity of the drug could be reduced without its trypanocidal activity being compromised it could once again be used as a first line therapy for the treatment of HAT. One possible mechanism of improving the properties of melarsoprol is to utilise the drug in conjunction with cyclodextrins.

1.2 Cyclodextrins: Enabling excipients

1.2.1 History

Cyclodextrin chemistry began in 1891 with the discovery of a crystalline like substance in the bacterial digest of starch, by the French scientist Villiers (Brewster and Loftsson, 2007; Villiers, 1891). The compound displayed a similar profile to cellulose, being resistant to acid hydrolysis and lacking any reducing powers. As a result Villiers named the compound 'cellulosine' (Loftsson and Duchene, 2007). No progress was made in the field until twelve years later, when an Austrian microbiologist, Schardinger, described two different crystalline compounds in the bacterial digest of potato starch (Brewster and Loftsson, 2007; Schardinger, 1903). The two compounds isolated from the digest displayed similar properties to the 'cellulosine' previously described by Villiers. Schardinger named the compounds crystalline dextrins and subsequently α dextrin and β dextrin (Loftsson and Duchene, 2007). Today these compounds are referred to as α and β cyclodextrins.

Cyclodextrin research continued to progress in the following years with the identification of γ cyclodextrin by Freudenberg and Jacobi in 1935 (Freudenberg and Jacobi, 1935). The basic structural and physiochemical properties of α, β, and γ were described by Cramer in 1954 (Cramer, 1954; Loftsson and Duchene, 2007). This work described the chemical structure, cavity size, solubility and reactivity of the cyclodextrins, in addition to their complexing ability and the effect of complextion on the stability of the included guest molecule. Although the full chemical structure and complexing abilities of cyclodextrins were well characterised by the end of the 1950's, the compounds were only available as rare, impure chemicals in small quantities (Loftsson and Duchene, 2007). This severely restricted the use of cyclodextrins and their full potential as pharmaceutical agents remained unexplored.

Cyclodextrins are produced by the enzyme cyclodextrin glycosyltransferase (CGTase). The development of genetically modified CGTases, with increased activity and specificity enabled pure cyclodextrins to be produced in large quantities. The availability of high grade cyclodextrins finally allowed their potential use as pharmaceutical excipients to be investigated and in 1976 the world's first pharmaceutical preparation containing cyclodextrins; prostaglandin E2/βCD (Prostarmon E^{TM}) was launched in Japan (Loftsson and Duchene, 2007). In the same year α and β cyclodextrin were officially approved as food additives in Japan. It was a further twelve years before the first cyclodextrin based product piroxicam/βCD was licensed in Europe. This was followed by the licensing of itraconazole/2-HPβCD in the United States of America (USA) in 1997. Today, worldwide 30 - 40 cyclodextrin based pharmaceutical products are available. A selection of the most commonly used preparations are detailed in Table 1-2.

1.2.2 Structure

Cyclodextrins are cyclic oligosaccharides consisting of at least six glucopyranose units linked by α-1, 4 glycosidic bonds. Steric hinderances prevent the formation of cyclodextrins with fewer than six glucopyranose units, while larger ring cyclodextrins, containing more than nine dextran units, are rarely used in pharmaceutical products since they remain poorly characterised and are difficult to produce in a pure form (Loftsson and Brewster, 1996). The cyclodextrins of greatest pharmaceutical relevance consist of either six, seven or eight glucopyranose units and are designated α, β and γ respectively. Cyclodextrins take the shape of a truncated cone or torus rather than a perfect cylinder (Figure 1-11). Each glucopyranose unit contains three hydroxyl groups; one primary and two secondary. The secondary hydroxyls are located on the C-2 and C-3 atoms of the unit, while the primary hydroxyl is positioned on the C-6 atom. As a result, all the secondary hydroxyls are situated on the interior of the torus, while all the primary hydroxyls are located on the outer edge of the torus (Bekers, Uijtendaal, Beijnen, Bult *et al.*, 1991).

Cyclodextrin	Drug	Trade name	Formulation	Company (country)
α cyclodextrin (α CD)	Alprostadil	Caverject dual	I. V. solution	Pfizer (Europe)
	Cefotiam-hexetil	Pansporin	Tablet	Takeda (Japan)
	OP-1206	Opalmon	Tablet	Ono (Japan)
	PGE_1	Prostavastin	Parenteral solutions	Schwarz (Europe)
β-Cyclodextrin (βCD)	Benexate HCl	Ulgut, Lonmiel	Capsule	Teikoku (Japan)
	Cephalosporin	Meiact	Tablet	Meiji Seika (Japan)
	Cetirizine	Cetrizin	Chewing tablet	Losan Pharma (Germany)
	Chlordiazepoxide	Transillium	Tablet	Gador (Argentina)
	Dexamethasone	Glymesason	Ointment, tablet	Fujonaga (Japan)
	Meloxicam	Mobitil	Tablet and suppository	Medical Union Pharmaceuticals (Egypt)
	Nicotine	Nicorette	Sublingual tablet	Pfizer (Europe)
	Nitroglycerin	Nitropen	Sublingual tablet	Nihon Kayaku (Japan)
	PGE_2	Prostarmon E	Sublingual tablet	Ono (Japan)
2-Hydroxypropyl-β-CD (HPβCD)	Indomethacin	Indocid	Eye drop solution	Chauvin (Europe)
	Itraconazole	Sporanox	Oral and I. V. infusion	Janssen (Europe, USA)
	Mitomycin	MitoExtra Mitozytrex	I. V. infusion	Novartis (Europe)
Sulfobutylether-β- CD (SBEβCD)	Aripiprazole	Abilify	I.M. solution	Bristol-Myers Squibb (USA); Otsuka Pharm. (USA)
	Maropitant	Cerenia	Parenteral solution	Pfizer Animal Health (USA)
Randomly methylated β-CD(RAMβCD)	17β-Estradiol	Aerodiol	Nasal Spray	Servier (Europe)
	Chloramphenicol	Clorocil	Eye drop solution	Oftalder (Europe)

Table 1-2: Registered pharmaceutical products containing cyclodextrins
(Loftsson, Brewster and Masson, 2004; Loftsson, Jarho, Masson and Jarvinen, 2005; Szejtli, 2004) www.cyclodex.com/SafetyandRegulatoryStatus.html.

This configuration gives rise to the truncated cone shape, with secondary hydroxyls forming the wider edge and primary hydroxyls forming the narrow edge (Uekama, Hirayama and Irie, 1998). The positioning of the primary hydroxyl groups results in the exterior of the torus being hydrophilic in character. In contrast, the interior of the cavity is hydrophobic since it is lined by a ring of C(3) – H and C(5) – H hydrogens and a ring of glucosidic oxygens (Bekers *et al.*, 1991; Uekama, Hirayama and Irie, 1998).

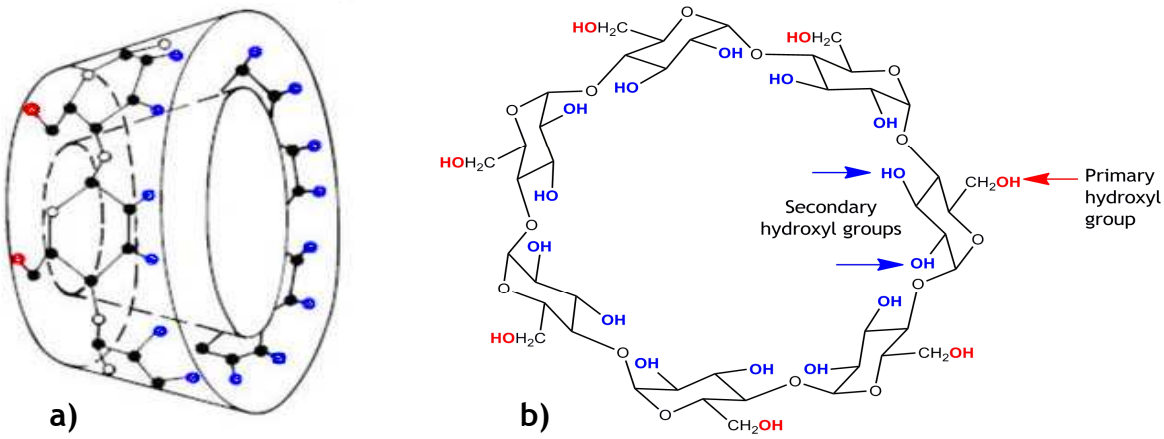

Figure 1-11: The truncated cone and chemical structure of β cyclodextrin
a) Cyclodextrins take the shape of a truncated cone, with an inner cavity. The secondary hydroxyl groups (blue) are situated on the interior of the torus, while the primary hydroxyls (red) are located on the outer edge. As a result the interior of the cavity is hydrophobic while the exterior is hydrophilic b) The chemical structure of β cyclodextrin, showing the position of the primary (red) and secondary (blue) hydroxyl groups. Modified from (Loftsson and Brewster, 1996).

1.2.3 Physicochemical properties

The physicochemical properties of each cyclodextrin vary according to the number of glucopyranose units present in their structure (Table 1-3). The structure and physiochemical properties of a cyclodextrin influence its ability to form an inclusion complex. For example, the small cavity diameter of α cyclodextrin severely limits the variety of guest molecules which are able to enter into it and form complexes. In β cyclodextrin, hydrogen bonding between the C2-OH group of one glucopyranose unit and the C3-OH group of an adjacent unit, results in the cyclodextrin having a very low water solubility which severely restricts its use (Brewster, Simpkins, Hora, Stern *et al.*, 1989; Szejtli, 1988). Cyclodextrins with more desirable characteristics can be produced by substituting one or more of the hydrogen atoms on either the primary or

secondary hydroxyls with an alternative chemical moiety. Common substitutions include hydroxyl, methyl, acetyl or sulfobutylether groups (Loftsson and Duchene, 2007; Thompson, 1997).

	α	β	γ
Number of glucopyranose units	6	7	8
Molecular weight	973	1135	1297
Cavity diameter (nm)	0.47 – 0.53	0.6 – 0.66	0.75 – 0.83
Cavity height (nm)	0.79	0.79	0.79
Cavity volume (ml mol^{-1})	174	262	472
Solubility (mg ml^{-1} at 25°)	130	18.5	300

Table 1-3: The physicochemical properties of α, β and γ cyclodextrin
Modified from (Loftsson and Brewster, 1996; Loftsson and Duchene, 2007; Shimpi, Chauhan and Shimpi, 2005; Thompson, 1997).

1.2.4 Production

1.2.4.1 Enzymology

Cyclodextrins are produced from starch by the actions of the enzyme, cyclodextrin glycosyltransferase (CGTase) (Biwer, Antranikian and Heinzle, 2002). The enzyme has been identified in nearly 30 species of bacteria. A large proportion of these bacteria belong to the genus *Bacillus* but certain species of *Paenibacillus, Klebsiella, Thermoanaerobacterium, Thermoanaerobacter* and *Actinomycetes* also produce CGTase (Abelian, Afyan, Avakian, Melkumyan *et al.*, 1995; Bahl, Burchhardt, Spreinat, Haeckel *et al.*, 1991; Binder, Huber and Bock, 1986; Fiedler, Pajatsch and Bock, 1996; Larsen, Duedahl-Olesen, Christensen, Mathiesen *et al.*, 1998; Wind, Uitdehaag, Buitelaar, Dijkstra *et al.*, 1998). CGTase enzymes produce a mixture of α, β and γ cyclodextrin (van der Veen, Uitdehaag, Dijkstra and Dijkhuizen, 2000). The ratio of α, β and γ cyclodextrin

produced varies depending upon the bacterial species from which the enzyme was isolated. For example, the CGTase from *Bacillus agaradhaerens* and *Bacillus obhensis* mainly produces β cyclodextrin, while α cyclodextrin is the main cyclic product of the CGTase isolated from *Bacillus macerans* and *Klebsiella pneumoniae* (Binder, Huber and Bock, 1986; Qi and Zimmermann, 2005; Sin, Nakamura, Kobayashi, Masaki *et al.*, 1991; Takano, Fukuda, Monma, Kobayashi *et al.*, 1986).

CGTase are members of the transferase group of enzymes. They catalyse various transglycosylation reactions including cyclization, disproportionation, coupling and also hydrolysis of starch (Biwer, Antranikian and Heinzle, 2002; Kobayashi, 1996). The cyclization reaction is of greatest interest here as this reaction ultimately results in the formation of cyclodextrins.

1.2.4.1.1 The cyclization reaction

The cyclization reaction consists of three stages: cleavage of the substrate, circularization of the linear intermediate and the formation of a new glycosidic bond to maintain the cyclic conformation (Figure 1-12). The reaction commences with the CGTase enzyme cleaving a α 1, 4 glycosidic bond in the starch, producing a covalent α 1, 4 linked glycosyl-enzyme intermediate (Mosi, He, Uitdehaag, Dijkstra *et al.*, 1997). In the subsequent circularization step, the linear glycosyl-enzyme intermediate assumes a cyclic formation (Uitdehaag, Mosi, Kalk, van der Veen *et al.*, 1999). Finally, a new α 1, 4 glycosidic bond is formed between the adjacent glucopyranose units to maintain the cyclic conformation (Uitdehaag, Kalk, van der Veen, Dijkhuizen *et al.*, 1999). Upon formation of the glycosidic bond the CGTase is released and is free to participate in further reactions.

1.2.4.2 Industrial production

In the industrial setting cyclodextrins can be produced by two different methodologies. The solvent method makes use of a complexing agent, usually an organic solvent, to selectively precipitate the desired cyclodextrin, which is then easily separated from the reaction mixture (Biwer, Antranikian and Heinzle, 2002). In the non-solvent method no complexing agent is used and a mixture of

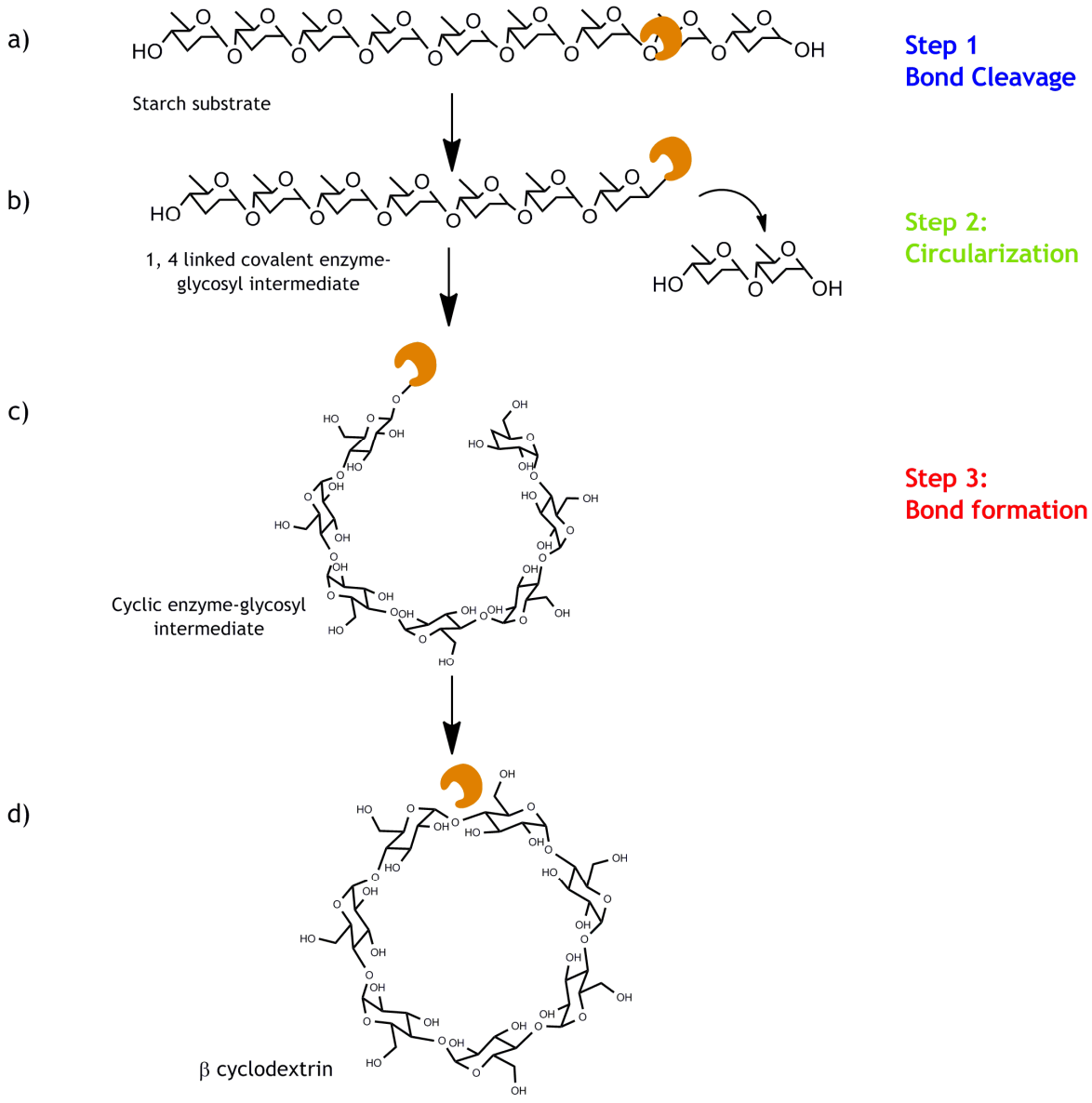

Figure 1-12: Schematic representation of the cyclization reaction
a) The CGTase enzyme cleaves a α 1, 4 linked bond in the starch substrate to produce b) a covalent α 1, 4 linked glycosyl-enzyme intermediate. c) The glycosyl-enzyme intermediate, subsequently assumes a cyclic conformation and in the final step d) a new glycosidic bond is formed to maintain the cyclic conformation.

cyclodextrins is produced (Biwer, Antranikian and Heinzle, 2002). The desired cyclodextrin is subsequently separated from the reaction mixture by crystallisation.

1.2.4.2.1 The solvent process

The process begins with the liquefaction of the substrate in order to reduce its viscosity. This is achieved by partially hydrolysing the starch with either thermostable α amylases, acids or by mechanical disintegration (Biwer, Antranikian and Heinzle, 2002). Over hydrolysis of the starch is detrimental to the process and results in decreased cyclodextrin yields. If α amylases are used for hydrolysis, they must be inactivated by heat treatment before the reaction can progress to the next stage. Following liquefaction, the starch is cooled to the temperature at which the CGTase is active and the enzyme, along with the complexing agent, is added to the reaction. Upon addition of the CGTase the cyclization reaction commences and cyclic products begin to be produced (Biwer, Antranikian and Heinzle, 2002). As the desired cyclodextrin is formed, it interacts with the complexing agent, producing an insoluble complex. Upon cessation of the reaction, the insoluble complex containing the cyclodextrin and complexing agent is separated from the remaining reaction mixture by centrifugation or filtration (Hedges, 1992). The remaining unconverted starch can be re-used in alternative fermentation processes such as the production of alcohols and antibiotics (Schmid, 1996). The recovered complex is washed and the complexing agent is separated from the cyclodextrin by steam distillation. The remaining solution containing the cyclodextrin is concentrated by vacuum distillation and the cyclodextrin subsequently precipitated and filtered. In the final step the cyclodextrin is washed and dried ready for packaging (Biwer, Antranikian and Heinzle, 2002).

1.2.4.2.2 The non-solvent process

The non-solvent method was developed by Horikoshi and co-workers in the early 1970's as a way of producing β cyclodextrin without the use of organic solvents (Horikoshi, 1979; Matzuzawa, Kawano, Nakamura and Horikoshi, 1975). As in the solvent method the process begins with the liquefaction of starch. In the non-solvent method a 15% suspension of potato starch containing 10mM $CaCl_2$ is used

as the substrate. Following liquefaction, the substrate is cooled and the pH adjusted to 8.4 by the addition of $Ca(OH)_2$ (Schmid, 1996). The cyclization reaction and the formation of the cyclodextrin commences with the addition of the CGTase. During the cyclization reaction, the temperature of the substrate is maintained at 60ºC (Schmid, 1996). The reaction is allowed to progress for 30 hours with continuous agitation, after which, the CGtase is inactivated by raising the reaction temperature to 100 - 120ºC. Following cessation of the reaction, the enzyme glucoamylase is added to the reaction mixture, to hydrolyse any remaining, unconverted starch and non-cyclic dextrins (Biwer, Antranikian and Heinzle, 2002). The resulting solution is filtered and concentrated under reduced pressure. The β cyclodextrin is recovered from the concentrated solution by crystallisation followed by centrifugation. The recovered cyclodextrin is then washed, recrystallised, dried and packaged, with the final product containing a minimum of 98% cyclodextrin (Hedges, 1992).

The solvent method of cyclodextrin production is favoured over the non-solvent method as it produces a higher yield, fewer by products and consists of simpler reactions. The non-solvent method is mainly used in Japan to produce β cyclodextrin for use as a food additive (Schmid, 1996).

1.2.5 Cyclodextrin derivatives

The complexing ability and aqueous solubility of the parent (α, β, γ) cyclodextrins is considerably improved by substituting one or more of the primary and/or secondary hydroxyl groups with a chemical moiety (Uekama, 1985). This effect is greatest in β cyclodextrin. The randomly methylated β cyclodextrin (RAMβCD), in which 14 of the 21 hydroxyl groups have been substituted with a methyl moiety, has a solubility of 57g/100ml. In contrast, the parent β cyclodextrin has a solubility of only 1.8g/100ml (Thompson, 1997). This increase in solubility occurs as modification of the hydroxyl groups disrupts the intramolecular hydrogen bonding around the torus, destabilising the crystalline lattice. As a result more hydroxyl groups are available to interact with the surrounding water molecules resulting in an increased solubility (Albers and Muller, 1995).

Functional groups commonly incorporated into the cyclodextrin torus include ethers, esters, aminos and azidos. In addition to substitution of the hydroxyl groups, the primary hydroxyls can also be oxidised to carboxy derivatives (Szejtli, 1996). As the parent cyclodextrins contain 18, 21 and 24 (α, β and γ) substitutable hydroxyl groups respectively, the possible number of cyclodextrin derivatives is extensive. To date more than 1500 cyclodextrin derivatives have been synthesized but only a small fraction are available as pharmaceutical excipients (Szejtli, 1998). The cyclodextrin derivatives of pharmaceutical importance and their physicochemical properties are listed in Table 1-4.

	HPβCD[1]	RAMβCD[2]	SBEβCD[3]
Number of glucopyranose units	7	7	7
Molecular weight	1400	1312	2163
Solubility (mg ml^{-1} at 25°C)	>600	>500	>500

Table 1-4: The physicochemical properties of cyclodextrin derivatives of pharmaceutical importance
[1]Hydroxpropyl-β-cyclodextrin, [2]Randomly methylated-β-cyclodextrin, [3]Sulfobutylether-β-cyclodextrin (Loftsson and Duchene, 2007).

1.2.5.1 Production of cyclodextrin derivatives

The hydroxyl groups of the cyclodextrin torus differ in their degree of reactivity. The sterically exposed primary hydroxyl groups located at C(6) are the most reactive followed by the hydroxyls at positions C(2) and C(3) (Fromming and Szejtli, 1994). However, the difference in reactivity is quite small and selective substitution of the hydroxyl groups is mainly achieved through alteration of the reaction conditions. Despite the ability to selectively substitute hydroxyl groups, randomly substituted cyclodextrins are often preferred over defined, symmetrical modified cyclodextrins as they are less susceptible to recrystallisation (Fromming and Szejtli, 1994).

1.2.5.1.1 Methylated cyclodextrins

Methyl substituents are introduced onto the cyclodextrin torus by an alkylation reaction (Thompson, 1997). β cyclodextrin contains 21 hydroxyl groups which can be substituted. A wide range of methyl derivatives with varying degrees of substitution can therefore be produced. Substitution of all 21 hydroxyl groups results in a fully methylated derivative (2, 3, 6-tri-O-methyl-β-cyclodextrin). Partial selective substitution of the C(2) and C(6) or C(3) and C(6) hydroxyls groups results in the dimethyl derivatives 2, 6-di-O-methyl-β-CD and 3, 6-di-O-methyl-β-CD respectively (Thompson, Toosy and Ciccarelli, 2010). Although fully and partially substituted dimethylated derivatives of β cyclodextrin can be produced, they are of little pharmaceutical use as they are very difficult to purify. The methylated derivative of β cyclodextrin which is of most pharmaceutical use is randomly methylated (RAMβCD). RAMβCD has an average degree of substitution of 1.8 methyl groups per glucopyranose unit (Aman, Reuscher, Wimmer and Hirsenkorn, 1995; Szente and Szejtli, 1999).

1.2.5.1.2 Hydroxypropyl β cyclodextrin (HPβCD)

Condensation of β cyclodextrin with propylene oxide under alkaline conditions results in the hydroxyl groups of the cyclodextrin being substituted with a 2-hydroxypropyl group, producing 2-hydroxypropyl-β-cyclodextrin (2-HPβCD) (Pitha, Szabo and Fales, 1987). The 2-hydroxypropyl function is able to insert onto any of the 21 hydroxyl groups of β cyclodextrin, in any combination, the reaction therefore generates an amorphous mixture of geometric and optical isomers. For 2-HPβCD it has been calculated that there are approximately 130,000 possible derivatives and if the optically active centre of the 2-hydroxypropyl function is taken into account this number is even greater (Loftsson and Brewster, 1996). Selective substitution of the hydroxyl groups can be achieved by adjusting the reaction conditions. A strong basic solution favours substitution of the primary hydroxyl groups, while a weak basic solution leads to substitution of the more acidic secondary hydroxyl groups (Pitha, Rao, Lindberg and Seffers, 1990). The 2-HPβCD's of commercial and pharmaceutical value have an average degree of substitution of 4 or 8 hydroxypropyl groups per glucopyranose unit (Thompson, 1997).

1.2.6 Cyclodextrin Complexes

1.2.6.1 Mechanism of inclusion

Cyclodextrins are able to form inclusion complexes with a variety a polar and a-polar guest molecules. The minimum requirement for inclusion complex formation is that the guest molecule must fit entirely or at least partially into the cyclodextrin cavity (Hirayama and Uekama, 1987). If the molecule is too small, it will fall out of the cavity, while large, bulky molecules are unable to enter into the cavity (Bekers *et al.*, 1991). Usually 1:1 inclusion complexes are formed but if a molecule is too large to be entirely accommodated by one cyclodextrin cavity and the free uncomplexed section of the molecule is amenable to complex formation 1:2 complexes can be formed. Similarly, if the molecule is small, two molecules may enter into the cyclodextrin cavity to form a 2:1 complex (Thompson, 1997).

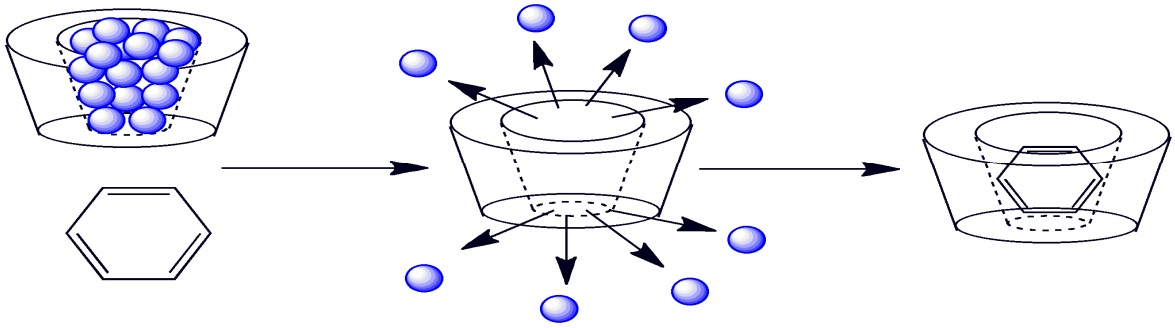

Figure 1-13: The mechanism of inclusion complex formation
Water molecules within the cyclodextrin cavity are replaced with a guest molecule.

Complex formation involves the substitution of the water molecules included within the cyclodextrin cavity by a guest molecule (Figure 1-13). The process can be depicted by Equation 1-1 assuming a 1:1 complex is formed.

$$CD + G \underset{K_D}{\overset{K_R}{\rightleftharpoons}} CD.G \qquad K = K_D / K_R$$

Equation 1-1: The complexation process
An inclusion complex (CD.G) is formed following the interaction between a guest molecule (G) and a cyclodextrin (CD). The binding constant (K) is equal to the rate of dissociation (K_D) / the rate of recombination (K_R).

The guest molecules encapsulated within the cyclodextrin cavities are in equilibrium with the free guest molecules in the solution (Bekers *et al.,* 1991). The overall stability of the complex is determined by two parameters, the rate of dissociation and the rate of recombination. Rates of dissociation and recombination vary widely depending upon the cyclodextrin and guest molecule (Thompson, 1997).

1.2.6.2 The driving force of complex formation

The 'driving force' behind complex formation is not fully understood but it is known that complexation occurs due to the interplay of numerous factors. Factors thought to play a role in complex formation include the replacement of the high enthalpy water molecules from within the cavity with a less polar guest molecule (Szejtli, 1999), the release of ring strain upon complexation (Clarke, Coates and Lincoln, 1988; Saenger, Noltemeyer, Manor, Hingerty *et al.*, 1976) and van der waals forces (Cramer, 1956; Nishijo and Nagai, 1991).

1.2.6.2.1 Release of high enthalpy water molecules

The water molecules contained within the cyclodextrin cavity cannot form their full complement of hydrogen bonds like those in the bulk of the solution due to steric restrictions. They are therefore regarded as molecules of enhanced energy or enthalpy. It is postulated that the release of these enthalpy rich water molecules acts as a driving force for complex formation (Szejtli, 1999). This theory is supported by the observation that the driving force of complexation decreases as the cavity size of the cyclodextrin increases. This is due to the larger cavities being able to accommodate numerous water molecules. As a result the properties of the water molecules within the cavity resemble those in the bulk solvent i.e. they are of low energy. Consequently the driving force of complexation is decreased (Szejtli, 1999). The nine membered δ cyclodextrin is a weak complexing agent and it is predicted that the even larger cyclodextrins (ε,η) will be of no use as complexing agents (Miyazawa, Ueda, Nagase, Endo *et al.*, 1995).

1.2.6.2.2 Release of ring strain

Prior to complex formation, α cyclodextrin is in a strained high energy conformation as one of the glucopyranose units is rotated inwards. On complex formation the two water molecules inside the cavity are displaced by the guest molecule and the α cyclodextrin molecule undergoes a conformational change to a relaxed state of minimum energy. It is this transformation from a strained to a relaxed state that is thought to drive complex formation (Saenger *et al.*, 1976). The effect is only relevant in the case of α cyclodextrin as the higher order β and γ cyclodextrins do not occur in a strained, distorted form.

1.2.6.2.3 Van der Waals forces

The entry of a guest molecule into the cyclodextrin cavity brings about changes in the enthalpy and entropy of the cyclodextrin. The negative change in enthalpy and the positive change in entrophy frequently observed upon complex formation are characteristic of Van der Waals forces, suggesting they may play a role in formation of the complex (Nishijo and Nagai, 1991). Further evidence for the possible role of Van der Waals forces in complex formation has come from molecular modelling studies. Matsui and Mochida in their work evaluating the binding forces contributing to the complexation of alcohols with α and β cyclodextrins, found Van der Waals interactions to be of primary importance in the inclusion process and in stabilisation of the resulting complexes (Matsui and Mochida, 1979).

1.2.7 Toxicity of cyclodextrins

1.2.7.1 Cytotoxicity

In-vitro, cyclodextrins induce the lysis of human erythrocytes by altering the cell membrane (Irie, Otagiri, Sunada, Uekama *et al.*, 1982). The degree of disruption depends upon which cyclodextrin the erythrocytes are exposed to. In the presence of α and γ cyclodextrins, the erythrocytes undergo progressive shape changes before eventually lysing (Ohtani, Irie, Uekama, Fukunaga *et al.*, 1989). In contrast, erythrocytes exposed to β cyclodextrin, immediately swell and lyse

without undergoing shape changes (Ohtani *et al.*, 1989). Haemolysis occurs as the cyclodextrins induce the release of essential components such as cholesterol, phospholipids and proteins from the cell membrane. As a result the erythrocyte membrane becomes more fluid and prone to lysis (Irie *et al.*, 1982).

1.2.7.2 Parenteral toxicity

1.2.7.2.1 Alpha (α) cyclodextrin

The LD_{50} of α cyclodextrin following intravenous injection in the rat is 1000mg/kg (Frank, Gray and Weaver, 1976). Parenteral administration of α cyclodextrin is associated with the onset of severe nephrosis. The nephrotoxicity of α cyclodextrin was investigated in the rat by Frank *et al*. (Frank, Gray and Weaver, 1976). The cyclodextrin was given I.V. as 1, 2, 4 or 7 daily injections, at doses of 0.1g/kg or 1.0g/kg. At the lower dose of 0.1g/kg no nephrotoxicity was observed but the highest dose of 1.0g/kg, induced severe nephrosis. The nephrosis was characterised by the presence of giant lysosomes and an increase in the number of apical vacuoles in the proximal convoluted tubules of the kidney (Frank, Gray and Weaver, 1976). The mechanisms responsible for the nephrosis observed following the parenteral administration of α cyclodextrin are not fully understood.

1.2.7.2.2 Beta (β) cyclodextrin

With an LD_{50} of 788mg/kg, β cyclodextrin is the most toxic of the parent cyclodextrins (Frank, Gray and Weaver, 1976). Parenteral administration of the cyclodextrin is associated with the onset of severe nephrosis. Structural changes become apparent in the convoluted segments of the proximal tubule of the kidney following a single subcutaneous dose of 670mg/kg (Frank, Gray and Weaver, 1976). If the cyclodextrin is repeatedly administered over 7 days at a dose of 450mg/kg, severe nephrosis is induced in the kidney. This nephrosis is similar to that observed following the I.V. administration of α cyclodextrin. Alterations in the vacuolar organelles of the proximal convoluted tubules of the kidney become apparent. The number of large and small apical vesicles increases and lysosomes also appear at perinuclear and basal locations and are

often distorted by the presence of needle-like micro-crystals, which protrude into the membranes (Frank, Gray and Weaver, 1976).

Nephrosis occurs as β cyclodextrin has a high affinity for cholesterol resulting in the formation of cholesterol-inclusion complexes following its parenteral administration (Frijlink, Franssen, Eissens, Oosting *et al.*, 1991). The cholesterol-inclusion complexes are filtered by the glomerular basement membrane and enter the urine. The lower concentration of cholesterol in the urine, leads to the cyclodextrin/cholesterol complex dissociating. The free cholesterol then re-enters the cells of the proximal convoluted tubule or loop of Henle where it recombines with the cyclodextrin. The resulting complex crystallises within the kidney and it is these intracellular crystals which cause most of the cellular damage (Frijlink *et al.*, 1991).

1.2.7.2.3 Gamma (γ) cyclodextrin

Gamma is the most toxicologically benign of the three parent cyclodextrins with a LD_{50} >2,400 mg/kg in the rat (Matsuda, Mera, Segawa, Uchida *et al.*, 1983). This is 2.5 and 3 times higher than the LD_{50} of α and β cyclodextrin respectively. Sub-chronic toxicity studies, in the rat, have demonstrated that γ cyclodextrin can be administered I.V., daily, for 30 days, at doses of up to 200mg/kg with no adverse effects (Donaubauer, Fuchs, Langer and Bar, 1998). Furthermore, in chronic long-term, dosing studies, no remarkable adverse effects were observed when the cyclodextrin was administered I.V., daily at 120mg/kg to rats (Donaubauer *et al.*, 1998). This lack of toxicity, in comparison to the other parent cyclodextrins, may be due to γ cyclodextrin having a higher intrinsic aqueous solubility and a lower affinity for endogenous lipids (Irie and Uekama, 1997).

1.2.7.2.4 Hydroxypropyl β cyclodextrin (HPβCD)

Hydroxyalkylation of β cyclodextrin has been shown to decrease its parenteral toxicity. A single I.V. dose of 2000mg/kg in mice was not lethal, in contrast a single I.V. dose of 1820mg/kg of the parent, β cyclodextrin was 100% lethal in rats (Frank, Gray and Weaver, 1976). In sub-acute toxicity studies no treatment

related effects were observed in rats and *Cynomolgus* monkeys receiving 200mg/kg HPβCD every second day for 90 days (Brewster, Estes and Bodor, 1990). Furthermore, in a second, sub-chronic dosing study, administration of HPβCD at 50mg/kg/day in rats and 100mg/kg/day in dogs for 90 days, resulted in no adverse effects (Coussement, Vancauteren, Vandenberghe, Vanparys *et al.*, 1990). HPβCD is less toxic than the parent β cyclodextrin, due to its higher aqueous solubility (Irie and Uekama, 1997). Toxicology studies of HPβCD have been completed in humans. In one study HPβCD was administered by single I.V. infusion at doses ranging from 0.5 to 3g. No significant pathophysiological changes were observed in any of the volunteers and there was no alteration in haematological or clinical parameters. In addition, no impairment of renal function was observed (Seiler, Szathmary, Huss, Decoster *et al.*, 1990).

1.2.7.3 Oral toxicity

Acute LD_{50} values cannot be determined for the parent cyclodextrins following oral administration as the highest possible doses do not result in animal mortality (Szejtli, 1996). It can only be concluded that the acute LD_{50} of β cyclodextrin is greater than 12.5g/kg for mice, 18.8g/kg for rats and more than 5g/kg for dogs (Gergely, Sebestyen and Virag, 1982; Szejtli and Sebestyen, 1979). The acute LD_{50} of γ cyclodextrin is greater than 16g/kg for mice and 8g/kg for dogs (Matsuda *et al.,* 1983).

1.2.7.3.1 Alpha (α) cyclodextrin

Acute and sub-chronic toxicity studies have been completed for α cyclodextrin in rats and dogs (Lina and Bar, 2004a; Lina and Bar, 2004b). In the acute toxicity study, α cyclodextrin was well tolerated in the rat, when administered at concentrations of 1.5, 5 and 20% via the diet for 13 weeks. The only notable treatment related effects were soft stools and infrequent, mild diarrhoea in animals receiving the 20% diet (Lina and Bar, 2004b). No significant treatment related changes were also observed in dogs fed diets containing 5, 10 or 20% α cyclodextrin, for 13 weeks (Lina and Bar, 2004a). In common with the rat study, the only treatment related effect was diarrhoea, which was observed in all treatment groups. Following completion of treatment, increased caecal weights

were observed in rats receiving the 5 and 20% diets and in dogs receiving the 10 and 20% α cyclodextrin diets. However, an increase in caecal weight is a physiological response to the ingestion of low digestible yet fermentable carbohydrates. It is commonly observed following the ingestion of sugar alcohols and lactose and is considered to be of little toxicology importance in humans (Newberne, Conner and Estes, 1988; World Health Organisation, 1987).

1.2.7.3.2 Beta (β) cyclodextrin

In an oral toxicity study in rats, β cyclodextrin was administered via a stomach tube at doses of 200, 400 or 600mg/kg for either three or six months (Gergely, Sebestyen and Virag, 1982). For both time periods no treatment related alterations were observed in the bio-chemical blood values. Furthermore, gross pathology and histopathology analysis did not reveal any abnormalities. This lack of toxicity was also observed in a 6 month study conducted in the dog, in which β cyclodextrin was administered daily at doses of 100, 250 or 500mg/kg (Szejtli, 1996). Occasional vomiting and loose stools or diarrhoea were observed in dogs fed a diet containing 10% β cyclodextrin for 90 days, however, no other treatment related effects were found (Hirayama and Uekama, 1987).

The effects of prolonged oral administration of β cyclodextrin has also been investigated in rats and dogs (Bellringer, Smith, Read, Gopinath *et al.*, 1995). Rats were fed diets containing 12,500, 25,000 or 50,000ppm β cyclodextrin (equivalent to 654, 1313 or 2655mg/kg/day for males and 864, 1743 or 3614mg/kg/day for females). Dogs received diets containing 6,200, 12,500 or 50,000ppm (equivalent to 229, 456 or 1831mg/kg/day for males and 224, 476 or 1967mg/kg/day for females). The diets were fed for a period of 52 weeks. No treatment related effects were observed in rats receiving the 12,500ppm diet and in dogs receiving the 12,500 and 50,000ppm diets. In rats receiving the 25,000 and 50,000ppm diets, the plasma levels of liver enzymes were elevated. When the livers of these animals were analysed histopathologicaly, hepatic changes and portal inflammatory cell infiltration, consistent with increased plasma liver enzyme levels were detected. In dogs an increased incidence of diarrhoea was observed in all treatment groups. Elevated urinary protein and calcium levels were also detected in dogs receiving the 50,000ppm diet.

However, no histopathological changes were detected in any treatment group therefore the minor treatment alterations observed in the dog study were considered to be of no toxicological importance (Bellringer *et al.*, 1995).

1.2.7.3.3 Gamma (γ) cyclodextrin

In an acute oral toxicity study rats were fed diets containing 5, 10, 15 and 20% γ cyclodextrin for 2 weeks (Lina and Bar, 1998). In common with other studies in which cyclodextrins were administered orally, the cyclodextrin was generally well tolerated. The only notable treatment related effect was an increased incidence of soft faeces in treatment groups receiving the 10, 15 and 20% diets. This lack of toxicity was also observed in a 13 week sub-chronic study conducted in rats and dogs (Lina and Bar, 1998; Til and Bar, 1998). Rats were fed diets containing 1.5, 5 or 20% γ cyclodextrin while dogs received diets containing 5, 10 or 20% γ cyclodextrin. An increased incidence of diarrhoea was observed in dogs in all treatment groups and in rats receiving the 20% diet. Male rats receiving the 20% diet also showed significantly reduced mean body weights but this was not observed in female rats or dogs. In female dogs receiving the 20% γ cyclodextrin diet a decreased urine pH was detected but urinary parameters were normal in all other animals. Haematological and histopathological analysis, revealed no abnormalities in any treatment groups for both species (Lina and Bar, 1998; Til and Bar, 1998). In common with previous studies in which large amounts of cyclodextrin was administered orally, an increased caecal weight was observed at the end of the treatment period, in female rats receiving the 20% diet and in female dogs receiving the 10 and 20% γ cyclodextrin diets (Lina and Bar, 1998; Lina and Bar, 2004a; Til and Bar, 1998). As in previous studies, this effect was considered to be a physiological response to the ingestion of low digestible, yet fermentable carbohydrates and was considered of little toxicological importance.

1.2.7.3.4 Hydroxypropyl β cyclodextrin (HPβCD)

Multiple studies have been conducted into the oral toxicity of HPβCD. In an acute 7 day study 4,500mg/kg/day HPβCD was administered to rats (Gould and Scott, 2005). Changes were observed in the plasma alanine aminotransferase

(ALT), aspartate (AST) and glutamate dehydrogenase (GLDH) levels but these changes were not accompanied by any histopathological changes. Alterations in AST and ALT plasma levels were also detected in a second oral toxicity study in which rats were administered HPβCD at doses of 2,250 or 4,500mg/kg/day for 7 days. As in the previous study, the elevations in plasma liver enzymes were not accompanied by any histopathological changes (Gould and Scott, 2005). The effects of longer term HPβCD administration were investigated in a one month toxicity study in rats. The rats were administered HPβCD at doses of 450 or 4,500mg/kg/day. Loose faeces was observed in rats receiving the highest dose from day 13 onwards. At 4,500mg/kg/day increased platelet counts, reduced reticulocyte numbers and lowered haematocrit values were also observed in males. In all treatment groups elevated plasma liver enzymes were detected. However, as is in the previous acute HPβCD toxicology study, the increased levels of plasma liver enzymes were not accompanied by any histopathological changes (Gould and Scott, 2005).

The toxicity of long-term, chronic HPβCD administration was investigated in a 12 month rat study (Gould and Scott, 2005). Rats were fed diets containing 500, 2,000 or 5,000mg/kg/day HPβCD. Although elevated plasma liver enzymes were detected in a previous toxicology study, in which HPβCD was administered at a dose of 450mg/kg/day for a month, no toxicological effects were observed in the present study in animals fed a diet containing 500mg/kg HPβCD for 12 months. When the dietary concentration of HPβCD was increased to 2,000mg/kg/day, elevated plasma levels of liver enzymes were detected and urine pH and volume were decreased (Gould and Scott, 2005). In previous, short-term toxicological studies, elevated plasma liver enzymes were not associated with any histopathological changes. However, in the chronic dosing study, the increased plasma levels of liver enzymes observed following administration of 2,000mg/kg/day HPβCD were accompanied by histopathological alterations. Swollen epithelial cells were detected in the urinary tract and centrilobular swelling in the liver and focal hyperplasia in the pancreas were also observed. At doses of 5,000mg/kg/day, these treatment related changes were more pronounced. In addition, white blood cell counts were elevated, thrombocytes and lipids were reduced and occult urinary blood was observed. At necropsy the

weight of the pancreas, kidney and lungs were increased and histopathology revealed an infiltration of foamy cells in the lungs (Gould and Scott, 2005).

Clinical trials of HPβCD have been conducted in humans. No toxicological effects were observed in patients administered 4-8g of HPβCD orally, daily for 1 to 2 weeks (De Beule, 1996). However, in a second study in which volunteers were administered 16-24g of HPβCD orally, daily for 14 days, soft stools and diarrhoea were observed (Irie and Uekama, 1997).

1.2.7.3.5 Di-methyl β cyclodextrin (DMβCD)

Limited data is available on the toxicity of the methylated cyclodextrins. In one study DMβCD was administered orally in aqueous solution at doses up to 3000mg/kg to mice, with no adverse effect (Bekers *et al.*, 1991).

1.2.8 Pharmacological uses of cyclodextrins

Cyclodextrins are of great interest to the pharmaceutical industry as they can alter the physical and chemical properties of the included guest molecule thus producing a compound with more desirable characteristics. Complexation is commonly used to improve the solubility and bioavailability of poorly soluble drugs, decrease toxicity, disguise unpleasant odours and tastes, increase stability and modify the release rate of drugs.

1.2.8.1 Decreasing toxicity

Complexation can prevent drug molecules from coming into direct contact with biological membranes. As a result local irritation and tissue damage caused by a drug can be reduced following complexation (Nagai and Ueda, 1996). Cyclodextrins have therefore been widely used to decrease the gastrointestinal toxicity of numerous drugs (Nambu, Kikuchi, Kikuchi, Takahashi *et al.*, 1978; Santucci, Fiorucci, Chiucchiu, Sicilia *et al.*, 1992). Santucci *et al.* reported a significant decrease in the number of acute gastric lesions in patients receiving the non-steroidal anti-inflammatory drug (NSAID) piroxican as a complex with β cyclodextrin, compared to the drug alone (Santucci *et al.*, 1992). The ulcer inducing effect of indomethacin was also significantly reduced following

complexation of the drug with β cyclodextrin (Nambu *et al.,* 1978). Cyclodextrins can also be used to reduce the haemolytic activity of amphiphatic drugs (Irie, Sunada, Otagiri and Uekama, 1983; Uekama, Irie, Sunada, Otagiri *et al.*, 1981a; Uekama, Irie, Sunada, Otagiri *et al.*, 1981b). The haemolytic effects of chlorpromazine and flufenamic, in an isotonic solution, were inhibited by the addition of cyclodextrins. The haemolytic activity of both drugs was decreased by cyclodextrins in the order of β>γ>α, with haemolysis almost completely inhibited by β cyclodextrin (Uekama *et al.,* 1981a; Uekama *et al.,* 1981b). Uptake of both drugs by the erythrocytes was reduced following addition of the cyclodextrins. This suggests that protection from haemolysis is due to a reduction in the effective drug concentration upon complexation and not due to the direct action of the cyclodextrins on the erythrocyte membrane (Uekama *et al.,* 1981b). In addition to inhibiting the haemolysis of erythrocytes *in-vitro*, complexation of chlorpromazine with β cyclodextrin also alleviates the local tissue irritation observed following intramuscular administration of the drug (Irie, Kuwahara, Otagiri, Uekama *et al.*, 1983).

Cyclodextrins can also be utilised for detoxification. Pitha and Szente administered dimethyl-β-cyclodextrin (DMβCD) to animals suffering from retinoic acid induced, hypervitaminosis A (Pitha and Szente, 1983). In animals given the cyclodextrin, the survival rate increased from 39% to 69%, and symptoms resolved. The DMβCD formed inclusion complexes with the retinoic acid, decreasing its free concentration and thus reducing its toxicity (Pitha and Szente, 1983).

1.2.8.2 Stability

Cyclodextrins are able to accelerate or decelerate many reactions including, hydrolysis, oxidation, decarboxylation, photodecomposition and degradation (Bekers *et al.,* 1991; Uekama, Hirayama and Irie, 1998). The ability of a cyclodextrin to either enhance or prevent the degradation of a drug depends upon the cyclodextrin used, the nature of the drug and the stability constant of the resulting complex. In the pharmaceutical industry, the stabilisation effect of cyclodextrins is of most interest.

In the harsh acidic environment of the gastrointestinal tract many drugs are susceptible to hydrolysis. The resulting hydrolysis products are often inactive or display a decreased therapeutic efficiency. Cyclodextrins can be used to inhibit or suppress this rate of hydrolysis. In an acidic environment the cardiac glycoside digoxin is susceptible to hydrolysis with one of the hydrolysis products digoxigenin displaying one-tenth the cardio activity of the parent compound (Uekama, Fujinaga, Hirayama, Otagiri *et al.*, 1982). Complexation of digoxin with cyclodextrins decreases its rate of hydrolysis in the order of $\beta>\gamma>\alpha$, with hydrolysis almost completely inhibited by β cyclodextrin (Uekama *et al.,* 1982). By reducing the rate of hydrolysis, cyclodextrins enable digoxin to be given orally without a concurrent loss in activity.

Many drugs are susceptible to degradation in the presence of light. The degradation products are often inactive and in some instances may even be toxic. Complexation with cyclodextrins can protect light sensitive compounds from this form of degradation. Tomono *et al*. investigated the effects of β cyclodextrin and its derivatives on the decomposition of photosensitive drugs. (Tomono, Gotoh, Okamura, Ueda *et al.*, 1988). The photodecomposition of pyridoxine hydrochloride, in the solid state was reduced by 50.6% following complexation with trimethyl-β-cyclodextrin (TM-β-CD). β cyclodextrin and its dimethyl and trimethyl derivatives, also decreased the photodecomposition of nifedipine, hydrochlorothiazide, clofibrate and retinol acetate (Tomono *et al.*, 1988). By preventing photodecomposition, cyclodextrins are able to extend the shelf life of many light sensitive drugs and inhibit the formation of undesirable degradation products.

1.2.9 Current regulatory status

The regulatory status of cyclodextrins varies from country to country and is continually evolving. In Japan, all three parent cyclodextrins are approved food additives and are included in the Japanese Pharmaceutical codex (JPC) (Loftsson and Duchene, 2007). In Europe, only two of the parent cyclodextrins, α and β are listed in the European Pharmacopoeia (Ph.Eur.). In addition to the two parent cyclodextrins, the modified hydroxypropyl derivative of β cyclodextrin, HPβCD is also included in the Ph.Eur. In the US, the only parent cyclodextrin to

be listed in the US Pharmacopoeia (USP/NF) is β cyclodextrin. However, HPβCD is cited in the US food and drug administration's (FDA) list of inactive pharmaceutical ingredients (Loftsson and Duchene, 2007).

Cyclodextrins which are not listed in a pharmacopoeia or registered as inactive pharmaceutical ingredients may still be used in pharmaceutical preparations. The modified cyclodextrins SBEβCD and RAMβCD are not included in any pharmacopoeia or list of inactive pharmaceutical ingredients, yet numerous pharmaceutical products containing these cyclodextrins have been approved by the regulating authorities (Table 1-2).

Chapter 2: General methods

General methods

The methods described in this chapter are used repeatedly throughout the thesis. If alterations are made to the techniques described here to suit the needs of a particular experiment they are detailed in the methods section of the chapter concerned. The recipes of solutions and the sources of all chemicals used in the work are detailed in appendices 2 and 3 respectively.

2.1 Trypanosomes

2.1.1 The history of T. brucei brucei stabilate GVR35

T. b. brucei trypanosomes were isolated from an infected wildebeest in the Serengeti National park in 1966. The trypanosomes were subsequently transferred to the London School of Hygiene and Tropical Medicine and serially passaged through rats to produce the stabilate LUMP 22. Serial passage of the LUMP 22 stabilate through mice resulted in the stabilate LUMP 1001 being produced. In 1977 a clone of this stabilate was obtained by Dr Frank Jennings at the University of Glasgow. A clone of the stabilate was produced by passaging the trypanosomes through sub-lethally irradiated mice. The resulting clone was designated GVR35/C1 and was stored in liquid nitrogen. Working stabilates are produced from the GVR35/C1 reserve stabilate as required through passage in mice. The *T. b. brucei* trypanosomes used throughout this study were from the working stabilate GVR35/C1.9.

2.2 The murine model of *T. b. brucei*

The GVR35 experimental murine model was used throughout this study in order to evaluate the trypanocidal activity of the melarsoprol cyclodextrin inclusion complexes mel/HPβCD and mel/RAMβCD. The model was developed at the University of Glasgow Veterinary school by Dr Frank Jennings. The model is very well characterised and has been used extensively for evaluating the effectiveness of new chemotherapy regimes (Atouguia, Jennings and Murray, 1995; Jennings, 1987; Jennings, 1992; Jennings, 1993; Jennings *et al.*, 1993).

Infection of CD-1 mice with the GVR35/C1.9 *T. b. brucei* stabilate establishes a trypanosome infection in the animals. During the first 14 days of the infection, the trypanosomes are confined to the peripheral systems and there is no CNS involvement. Between days 14 and 21 post-infection the trypanosomes penetrate the blood-brain barrier (BBB) and CNS stage infection is established in the animals (Jennings and Gray, 1983). Animals sacrificed at this time point display a mild CNS inflammatory reaction, characterised by a slight increase in the level of astrocyte activation and the presence of small numbers of inflammatory cells in the meninges. Without treatment the disease continues to advance and most animals generally succumb to the disease approximately 30 days after infection. As this study is concerned with the ability of complexed melarsoprol to cure CNS stage trypanosome infections, all chemotherapy regimes commenced on day 21 post-infection when a CNS stage infection is known to be established in the animals.

2.2.1 Animals

Female CD-1 mice were purchased from Charles River Ltd, Margate, England. Animals were approximately 6 to 8 weeks in age and weighed between 28 and 35 grams. The mice were allowed to acclimatise in the animal unit at the University of Glasgow Veterinary School for a period of at least one week before undergoing any scientific procedures. The mice were housed in groups of six in standard caging and food and water was provided *ad libitum* throughout. The animals were maintained under a 12 hour light/dark cycle at a temperature of 19 to 23ºC and at a humidity of 55 ± 10%.

2.2.2 Establishing trypanosome infection

The working stabilate GVR35/C.1.9 was initially passaged in a donor animal in order to obtain the number of trypanosomes required to inoculate larger batches of experimental animals. A small section of the frozen GVR35/C1.9 stabilate was removed and diluted in phosphate glucose buffered saline (PGBS) pH 8 until a suspension containing 2 trypanosomes per field when viewed by light microscope at a magnification of 400 was obtained. This equates to approximately 2 x 10^4 trypanosomes/0.1ml. A 0.2ml aliquot of the suspension was injected

intraperitoneally into a mouse. The development of the parasitaemia in the animal was monitored by examining a wet blood film prepared from tail blood under a light microscope (described below). When the first parasitaemic peak was reached the animal was euthanised by exposure to increasing concentrations of carbon dioxide and exsanguinated by cardiac puncture. The blood was diluted in PGBS pH 8 as described above. A 0.1ml aliquot of the trypanosome suspension was then inoculated intraperitoneally in order to establish infection in the experimental animals.

2.2.3 Monitoring of parasitaemia

To confirm that the trypanosome infection had established successfully in the experimental animals, the parasitaemia was checked in all infected mice prior to the administration of any trypanocidal compounds. A 1mm section from the very tip of the animal's tail was removed with scissors and a drop of blood expressed onto a glass microscope slide. A 7x22 mm coverslip was placed over the blood to produce a wet blood film and the slide was viewed under a light microscope at a magnification of 400. The number of trypanosomes present per visual field was estimated and scored according to the scale in Figure 2-1.

2.3 Complexed melarsoprol

2.3.1 Preparation of complexed melarsoprol

The melarsoprol cyclodextrin complexes were prepared by Dr S. Gibaud of Nancy Universitè, France, according to the method previously described in Gibaud *et al*. 2005 (Gibaud, Zirar, Mutzenhardt, Fries *et al*., 2005). Briefly 1mmol of melarsoprol was added to an aqueous solution containing 2mmol of either HPβCD or RAMβCD. The solution was incubated under constant stirring at 25ºC for 14 hours. Following filtration through a 0.22µm filter, the solutions were freeze-dried to obtain dry powders. The resulting melarsoprol complexes were stored at room temperature and protected from the light until use.

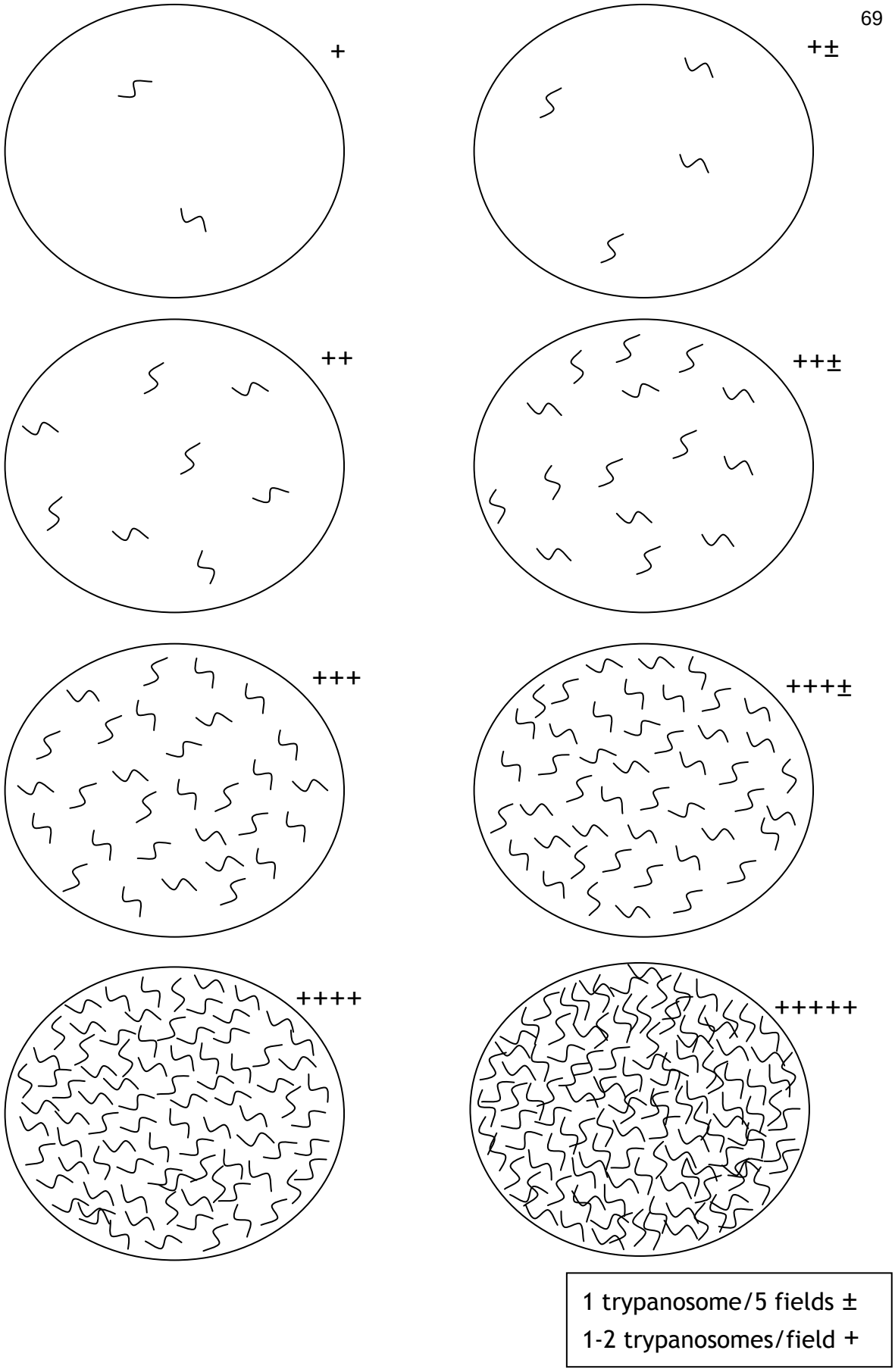

Figure 2-1: The grading scale used to score the level of parasitaemia in the experimental animals

A wet blood film was examined under a light microscope at a magnification of 400.The number of trypanosomes present within each visual field was estimated and graded based on the scale above.

2.3.2 Characterisation of melarsoprol cyclodextrin complexes

The quantity of melarsoprol incorporated into each cyclodextrin was determined by high-performance liquid chromatography (HPLC) (Gibaud *et al.*, 2005). The ratio of melarsoprol to cyclodextrin for each complex was subsequently calculated (Table 2-1).

Complex	Amount of melarsoprol contained within 1g of complex (mg)	Melarsoprol to cyclodextrin ratio
Mel/HPβCD	59	1:17
Mel/RAMβCD	71	1:14

Table 2-1: The amount of melarsoprol contained within 1g of each complex as determined by HPLC.

2.3.3 Calculation of complexed melarsoprol doses for oral administration

The amount of each complex required in order to give a melarsoprol dose of 0.05mmol/kg was calculated. This dose is equivalent to 0.05µmols of melarsoprol per gram body weight. This means that 10 grams equates to 0.5µmols, therefore the amount of complex required to prepare a solution containing 0.5µmols of melarsoprol in 0.1ml was calculated. 0.5µmols of melarsoprol in 0.1ml is equivalent to 5mmols per litre. To give a concentration of 5mmols per litre 1.99g of melarsoprol is required which equates to 2mg of melarsoprol per ml (See appendix 1 for full calculations). This value relates to standard melarsoprol, in order to calculate the amount of each complex required to give a melarsoprol concentration of 5mmols the ratio of melarsoprol to cyclodextrin within the complex needs to be taken into account. The ratio of melarsoprol to cyclodextrin in the mel/HPβCD complex is 1:17 this means that for every 17 grams of the complex only 1 gram is melarsoprol. Therefore to obtain a melarsoprol concentration of 5mmols the quantity giving 5mmols of melarsoprol (i.e. 2mg/ml) must be multiplied by 17. Similarly the ratio of melarsoprol to cyclodextrin in the mel/RAMβCD complex is 1:14 therefore the quantity of melarsoprol giving 5mmols (i.e. 2mg/ml) must be multiplied by 14 in order to obtain the correct quantity of melarsoprol. This means that to obtain a dose of 0.05mmol/kg, 34mg/ml of mel/HPβCD and 28mg/ml of mel/RAMβCD is

required. From these doses the amount of each complex required to obtain the other doses was calculated (Table 2-2).

	Amount of complex required per ml (mg)	
Dose (mmol/kg)	Mel/HPβCD	Mel/RAβCD
0.0125	8.5	7
0.025	17	14
0.05	34	28
0.1	68	56
0.2	136	112

Table 2-2: The amount of each complex required per ml in order to give the required doses

2.3.4 Calculation of volume of melarsoprol cyclodextrin complexes to be orally administered

All drug solutions were prepared to allow their administration at 0.1ml/10g body weight. The volume of solution administered according to the weight of the mouse is detailed in Table 2-3.

Animal weight (grams)	Volume of drug to be administered (ml)
18.0 - 22.4	0.20
22.5 - 27.4	0.25
27.5 - 32.4	0.30
32.5 - 37.4	0.35
37.5 - 42.4	0.4
42.5 - 47.4	0.45
47.5 - 52.0	0.50

Table 2-3: The volume of complexed melarsoprol solution administered depending upon the weight of the animal

2.3.5 Calculation of complexed melarsoprol dose for intravenous administration

The amount of mel/HPβCD required to achieve a melarsoprol dose of 0.03mmol/kg was calculated. This dose is equivalent to 0.03µmols of melarsoprol per gram body weight. This means that 10 grams equates to 0.3µmols, therefore the amount of complex required to prepare a solution containing 0.3µmols of melarsoprol in 0.05ml was calculated. 0.3µmols of melarsoprol in 0.05ml is equivalent to 6mmols per litre. To give a concentration of 6mmols per litre 2.388g of melarsoprol is required which equates to 2.388mg

of melarsoprol per ml (See appendix 1 for full calculations). This value relates to standard melarsoprol, in order to calculate the amount of mel/HPβCD required to give a melarsoprol concentration of 6mmols the ratio of melarsoprol to cyclodextrin within the complex needs to be taken into account. The ratio of melarsoprol to cyclodextrin in the mel/HPβCD complex is 1:17 this means that for every 17 grams of the complex only 1 gram is melarsoprol. Therefore to obtain a melarsoprol concentration of 6mmols the quantity giving 6mmols of melarsoprol (i.e. 2.388mg/ml) must be multiplied by 17. This means that to obtain a dose of 0.03mmol/kg, 40.6mg of mel/HPβCD is required per ml.

2.3.6 Calculation of the volume of mel/HPβCD to be intravenously administered

For intravenous administration, the mel/HPβCD solution was prepared to allow administration at 0.05ml/10g of body weight. The volume of the solution given according to the weight of the mouse is detailed in Table 2-4.

Animal weight (grams)	Volume to be administered (ml)
18.0 – 22.45	0.1
22.5 – 27.45	0.125
27.5 – 32.45	0.15
32.5 – 37.45	0.175
37.5 – 42.45	0.2
42.5 – 47.0	0.225

Table 2-4: The volume of mel/HPβCD solution administered I.V. to animals in order to achieve a dose of 0.03mmol/kg

2.3.7 Preparation of melarsoprol cyclodextrin complexes for administration

The melarsoprol cyclodextrin complexes are supplied as fine white powders. The amount of each complex required to give the appropriate doses were weighed out on a fine balance and placed in a sterile falcon tube. The complexes were subsequently dissolved in the corresponding amount of sterile water in order to obtain the desired concentration. The total volume required was calculated based on an average body weight of 40g therefore for oral administration 0.4ml

was prepared per mouse, while for I.V. administration 0.2ml was prepared per mouse. An additional 1ml was allowed to accommodate the volume lost in the gavage needle and syringe hub. As the stability of the melarsoprol cyclodextrin complexes in solution is not known, the solutions were prepared fresh each day immediately prior to administration.

2.3.8 Oral administration of melarsoprol cyclodextrin complexes

The melarsoprol cyclodextrin complexes were administered orally as a solution. The animals were weighed and the appropriate volume of the complexed melarsoprol solution taken up in a 1ml syringe. A 20 gauge x 25mm gavage needle was place on the syringe. Mice were restrained by grasping the scruff of the animals' neck between the thumb and forefinger and securing the tail between the third and fourth fingers. The gavage needle was carefully inserted into the intradental space and then slowly into the oesophagus. The complexed melarsoprol solution was subsequently administered. Following administration the gavage needle was immediately withdrawn and the animal released.

2.3.9 Intravenous administration of mel/HPβCD

Animals were anaesthetised with isoflurane delivered as a mixture of 3% isoflurane and 50% oxygen. The animals were placed on a heat mat in order to dilate the caudal veins and the mel/HPβCD solution was administered, slowly and carefully into the tail vein using a 30 gauge insulin syringe. Anaesthesia was maintained throughout the procedure.

Chapter 3: Establishing the inhibitory concentration and minimum curative dose of complexed melarsoprol

3.1 Introduction

3.1.1 Melarsoprol

Melarsoprol is a very lipophilic and poorly water soluble drug with a log P of 2.53 and a solubility of 6mg/l at 25°C (Gibaud *et al.*, 2005). The compound's limited solubility means that it has to be dissolved in the solvent propylene glycol to produce a 3.6% solution. This is the only formulation of melarsoprol currently available. The formulation is far from ideal with the propylene glycol solvent posing numerous problems. Administration is extremely painful and the solution has to be administered very carefully and slowly, as if the solvent leaks into the tissues surrounding the vein, necrosis and chemical cellulitis can occur (Pepin and Milord, 1994). Administration of the solution is not the only problem associated with this drug. Melarsoprol is very toxic with patients experiencing numerous side effects following its administration (Blum and Burri, 2002; Burri, Stich and Brun, 2004; World Health Organisation, 1998). The most serious adverse event reported following the administration of melarsoprol is a post treatment reactive encephalopathy (PTRE). This reaction has been reported in up to 10% of patients receiving the drug, of which 50% will die as a result of the complication (Kennedy, 2004; Pepin and Milord, 1994). This gives melarsoprol an overall fatality rate of 5%, which is unacceptably high. The mechanisms behind the development of the PTRE are discussed in detail in chapter 1. Despite the problems associated with melarsoprol chemotherapy, the drug is a highly effective trypanocide and trypanosomes exposed to melarsoprol *in-vitro* lyse very rapidly. Furthermore, melarsoprol is still the only treatment available for CNS stage *T. b. rhodesiense* infections.

3.1.1.1 Melarsoprol derivatives

The high trypanocidal activity of melarsoprol led researchers to attempt to develop derivatives which were less toxic and water soluble yet retained the trypanocidal activity of melarsoprol. One melarsoprol derivative which was developed in the early 1960's as a possible replacement for melarsoprol is trimelarsen (mel W). In an initial study conducted in six patients with late stage *T. b. gambiense* infection, mel W was found to be as effective as melarsoprol

when administered intramuscularly or subcutaneously as two series consisting of four daily injections of 1 to 5mg/kg separated by a 7 day drug free interval (Friedheim and De Jongh, 1959). No adverse reactions were observed and no trypanosomes were detected in the CSF following completion of the treatment regime. Following the success of this initial trial a larger scale study was conducted in 24 patients with intermediate or late stage CNS *T. b. gambiense* infection. Patients were administered mel W daily, for 3 consecutive days at 4mg/kg, following a drug free period of 7 to 10 days patients received an additional four doses of mel W at 4mg/kg once per day (Watson, 1962). Initial results obtained 11 months after completion of mel W treatment indicated the drug was as effective as melarsoprol. In all patients the CSF cell count had decreased or returned to normal. However, at a second follow-up 2 years after completion of treatment, the CSF protein count had risen in four patients suggesting mel W may not be as effective as initially thought (Watson, 1965). An earlier study conducted by Roberston in CNS stage *T. b. rhodesiense* patients, also reported high treatment failure rates following mel W chemotherapy (Robertson, 1963). In the study 17 patients were given mel W as three series of four injections at doses ranging from 25 to 300mg/kg. Each series was separated by a drug free period of 3 to 11 days (Robertson, 1963). Adverse reactions were a common occurrence, with all but four patients developing febrile reactions and six patients developing CNS reactions (Robertson, 1963). Follow-up, 16 months after completion of treatment, revealed that nine patients had relapsed. The results obtained by Watson (Watson, 1965) and Robertson (Robertson, 1963) indicate that mel W is not as effective as melarsoprol in the treatment of CNS stage *T. b. gambiense* and *T. b. rhodesiense* infections. Furthermore, it may be more toxic than melarsoprol. As a result the use of mel W in the treatment of HAT was abandoned.

The following years have seen little progress in the way of new trypanocides. Recently DB75, N-myristoyltransferase inhibitors and oxaborole 6-carboxamides have been identified as potential trypanocides and fexinidazole entered phase I clinical trials in September 2009 (further details are contained in chapter 1) (Frearson *et al.,* 2010; Nare *et al.,* 2010; Torreele *et al.,* 2010; Wenzler *et al.,* 2009). However, there is still an urgent need for the development of new trypanocides or the reformulation of existing ones. If the toxicity of melarsoprol

could be reduced and its solubility increased so that oral dosing was possible, without a concurrent lost in trypanocidal activity, melarsoprol could once again be used as a first line therapy for the treatment of HAT. One possible mechanism of improving the properties of contemporary melarsoprol is to utilise the drug in conjunction with cyclodextrins.

3.1.2 The pharmacological uses of cyclodextrins

Cyclodextrins are of great interest to the pharmaceutical industry as through complex formation they can alter the physical and chemical properties of the included guest molecule thus producing a compound with more desirable characteristics. Complexation is commonly used to improve the solubility and bioavailability of poorly soluble drugs, decrease toxicity, disguise unpleasant odours and tastes, increase stability and modify the release rate of drugs.

3.1.2.1 Increasing solubility

One of the most important features of cyclodextrins is their ability to increase the aqueous solubility of poorly soluble drugs. Upon complexation the hydrophobic molecule enters into the cyclodextrin cavity where it is sheathed by the exterior hydrophilic hydroxyl groups of the cyclodextrin. This results in an increase in the apparent aqueous solubility of the enclosed molecule. The changes in solubility observed upon complexation can be investigated by phase-solubility analysis (Higuchi and Connons, 1965).

Phase-solubility analysis allows the stability constant of the complex to be calculated and also gives an insight into the stoichiometry of the complex. The technique was developed by Higuchi and Connons in 1965 (Higuchi and Connons, 1965). An excess of the drug of interest is added to solutions of increasing cyclodextrin concentration. The solutions are agitated until equilibrium is established, filtered and then the total drug concentration determined analytically (Brewster and Loftsson, 2007). A phase-solubility plot can then be constructed by plotting the solubility of the guest molecule as a function of the cyclodextrin concentration. A number of different solubility profiles are obtained depending upon the type of complex formed (Figure 3-1).

3.1.2.1.1 A-type profiles

A-type solubility profiles indicate water soluble complexes are being formed which have a higher solubility than the free uncomplexed drug (Brewster and Loftsson, 2007; Higuchi and Connons, 1965). Three subtypes of A-type profiles have been defined: A_L, A_P and A_N (Higuchi and Connons, 1965). In A_L profiles the solubility of the drug increases linearly as a function of cyclodextrin concentration. Although, it is assumed that 1:1 complexes are being formed in this situation, higher order complexes in which multiple drug molecules enter into the cyclodextrin cavity can also give rise to A_L type profiles. In A_P profiles a greater solubilisation of the drug is obtained at higher cyclodextrin concentrations, suggesting that more than one cyclodextrin molecule is encapsulating the drug. In A_N type profiles the opposite effect is seen, as the cyclodextrin concentration increases, solubilisation of the drug becomes less effective. Numerous mechanisms have been proposed for the occurrence of A_N type profiles including alterations in the viscosity, surface tension and conductivity of the solution (Brewster and Loftsson, 2007).

For complexes displaying an A_L type profile where there is a 1:1 complexation, the stability constant (K_C) of the complex can be determined from the slope and intercept of the initial straight-linear phase of the phase-solubility plot and is described by Equation 3-1:

$$K_C = \frac{(S_t - S_0)}{S_0 \{ [CD]_t - (S_t - S_0) \}}$$

Equation 3-1: Determination of the stability constant of complex formation
Where S_0 is the intrinsic solubility of the drug in the absence of the cyclodextrin, S_t refers to the total aqueous solubility of the drug in the presence of a given cyclodextrin concentration $(CD)_t$ (Higuchi and Connons, 1965).

3.1.2.1.2 B-type profiles

B-type solubility profiles indicate the formation of complexes with limited water solubility and can be divided into to two types; B_I and B_S (Higuchi and Connons, 1965). In B_S profiles the solubility of the drug initially increases linearly as a function of cyclodextrin concentration. However, as the maximum solubility of

the drug is reached a plateau occurs. If cyclodextrin continues to be added once the maximum solubility of the drug is reached precipitation of the complex occurs. Finally, when addition of cyclodextrin results in insoluble complexes, the solubility is said to follow a B_I type profile (Brewster and Loftsson, 2007; Higuchi and Connons, 1965).

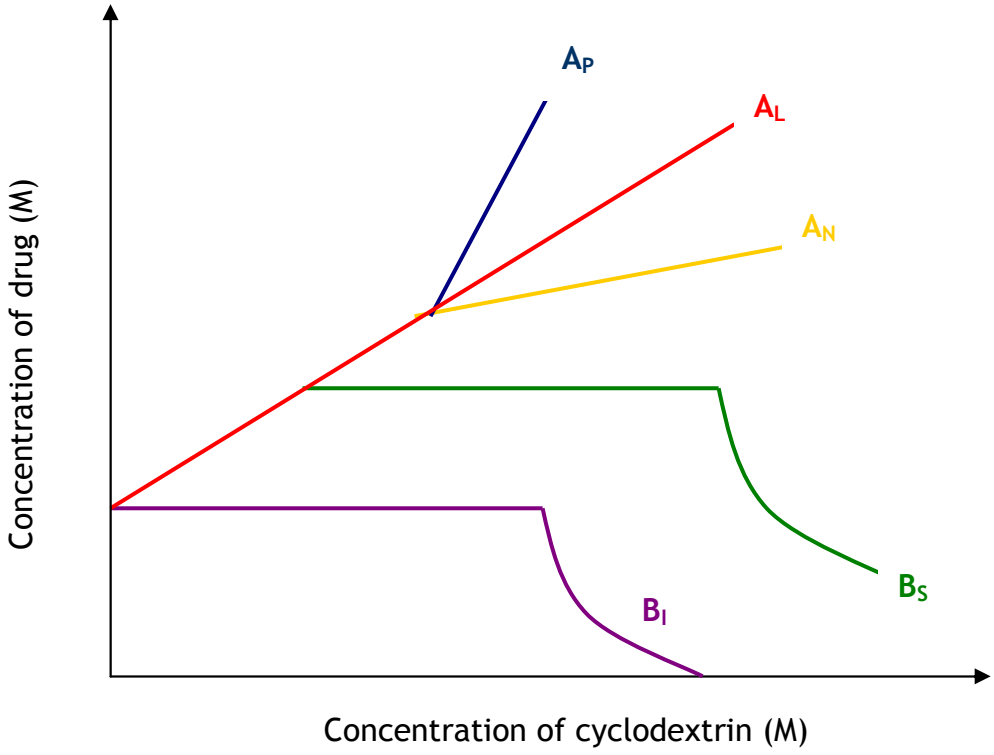

Figure 3-1: The possible phase-solubility profiles obtained following complexation of a guest molecule with a cyclodextrin.
Profiles A_N, A_L and A_P indicate very soluble complexes are formed where as B_S type profiles indicate a complex of limited solubility is formed. B_I profiles indicate an insoluble complex is formed.

3.1.2.2 Increasing bioavailability

Following oral administration the amount and rate at which a drug appears within the bloodstream is dependant upon a number of factors including the solubility, dissolution rate and the rate of intestinal absorption of the drug (Nagai and Ueda, 1996). If the rate-limiting step in the process is dissolution of the compound rather than permeation through the intestinal membrane then cyclodextrins can be used to increase the bioavailability of the drug (Carrier, Miller and Ahmed, 2007; Hirayama and Uekama, 1999; Uekama and Otagiri, 1987). In this case cyclodextrins can lead to an increase in bioavailability by acting as a temporary carrier and delivering the drug to the intestinal membrane (Figure 3-2) (Uekama, Hirayama and Irie, 1998). Following oral administration

the complex is dissolved in the intestinal fluids and dissociation of the complex occurs at the intestinal membrane (Stella, Rao, Zannou and Zia, 1999). Absorption is rapid from unstable complexes displaying a high dissolution rate, while for more stable complexes the rate of absorption is lower as the equilibrium is shifted towards complex formation resulting in a lower free drug concentration (Uekama and Otagiri, 1987). This effect can be overcome by administering a competing agent at the same time as the complex. The competing agent competes with the drug molecule for access to the cyclodextrin cavity resulting in an increase in the free concentration and hence bioavailability of the drug. A classical example of this is the complex formed by β cyclodextrin and the antihistamine cinnarizene (Tokumura, Ueda, Tsushima, Kasai *et al.*, 1984). Although complexation increased the dissolution rate of cinnarizine by a factor of 30 no increase in bioavailability was observed following oral administration of the complex (Tokumura, Tsushima, Tatsuishi, Kayano *et al.*, 1985; Tokumura *et al.*, 1984). Complexation failed to increase the bioavailability of cinnarizene due to the relatively high ($6200M^{-1}$) stability constant of the complex (Tokumura *et al.*, 1985). Tokumura *et al*. attempted to increase the bioavailability of cinnarizene from its β cyclodextrin complex by simultaneously administering the competing agent DL-phenylalanine (Tokumura, Nanba, Tsushima, Tatsuishi *et al.*, 1986). This approach resulted in a clear increase in the plasma concentration of cinnarizene. DL-phenylalanine did not act as an absorption promoter to cinnarizene directly, as no increase in bioavailability was observed when cinnarizene alone was administered with DL-phenylalanine. The amino acid therefore acts a competing agent, when administered with cinnarizene-β-cyclodextrin, increasing the free concentration and hence bioavailability of cinnarizene (Tokumura *et al.*, 1986).

A further example where cyclodextrins have been used successfully to increase the bioavailability of a compound is the antifungal agent itraconazole. Itraconazole is a highly efficacious broad–spectrum triazole antifungal agent (Willems, Van der Geest and de Beule, 2001). However, its use is limited by its poor pharmacokinetic properties. The drug is very lipophilic and poorly soluble in water with an estimated solubility of 1ng/ml at pH 7 (Brewster, Neeskens and Peeters, 2007). Numerous formulations have been trialled in an attempt to improve the pharmacological performance of the drug. The first oral formulation

of the drug was based on a solid dispersion system. Inert sugar spheres were coated with a solvent containing the drug and hydroxypropylmethylcellulose to produce capsules (Gilis, De Conde, Vandecruys and [Anon], 2003). Following oral administration the capsules dissolve within the stomach to give a supersaturated solution of the drug (Leuner and Dressman, 2000). However, absorption of the drug is highly variable. The low pK_a of itraconazole means dissolution and absorption of the drug occur more effectively at a low pH (Vanpeer, Woestenborghs, Heykants, Gasparini *et al.*, 1989). Absorbance of the drug is therefore improved by administering the capsules simultaneously with food, which stimulates the production of gastric secretions (Grant, 2000). However, in HIV patients who are frequently administered the drug in order to prevent opportunistic fungal infections, gastric secretions are usually reduced due to hypochlorhydia (Welage, Carver, Revankar, Pierson *et al.*, 1995). As a result the oral bioavailability of itraconazole is reduced in these patients and therapeutic levels are often difficult to maintain (Cartledge, Midgely and Gazzard, 1997; Peeters, Neeskens, Tollenaere, Van Remoortere *et al.*, 2002). In an attempt to improve the oral bioavailability of itraconazole, an aqueous oral formulation was developed through the use of cyclodextrins.

Itraconazole was complexed with HPβCD to produce an aqueous formulation. In the presence of HPβCD the solubility of itraconoazole was increased, with concentrations of 1.45, 2.21 and 4.0mg/ml obtained at pH 7, 4 and 2 respectively (Peeters *et al.*, 2002). The bioavailability of itraconazole was also increased following its complexation. In a comparative study, healthy volunteers were administered 200mg of itraconazole in the new oral formulation or as capsules lacking HPβCD. The bioavailability of itraconazole was increased by up to 37% with the oral formulation compared to the capsules (Barone, Moskovitz, Guarnieri, Hassell *et al.*, 1998). Additionally, in HIV patients significantly higher plasma concentrations of itraconazole were obtained following administration of the oral itraconazole/HPβCD complex compared to the capsules (Cartledge, Midgely and Gazzard, 1997). This indicates that the absorption of itraconazole is enhanced following its complexation with HPβCD.

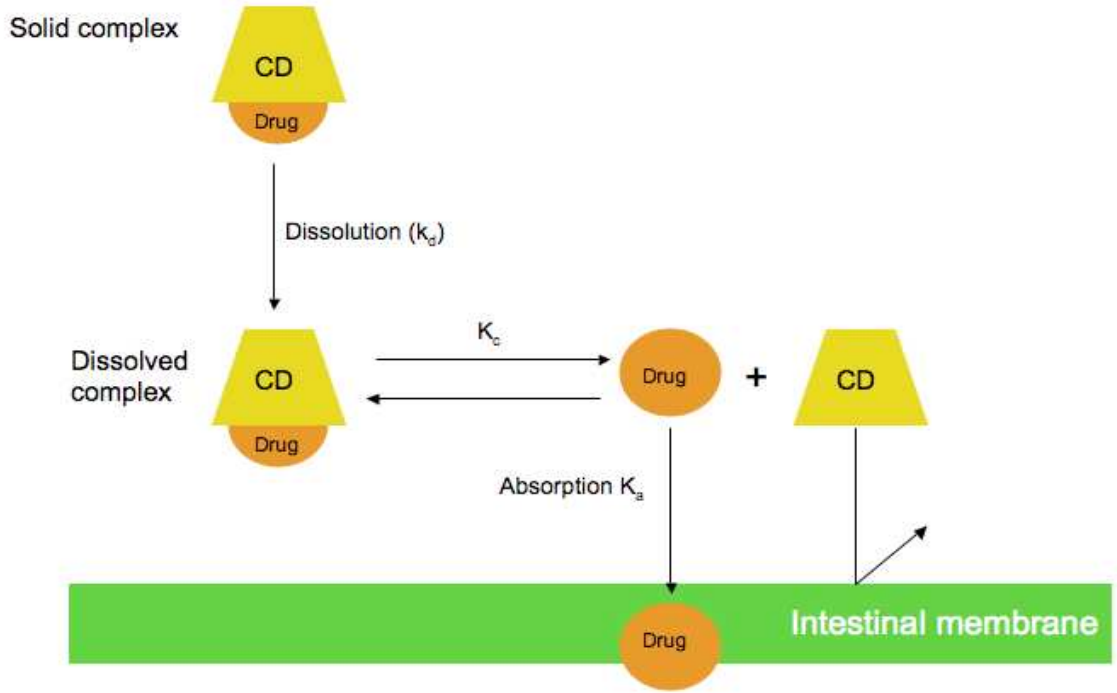

Figure 3-2: The absorption of a drug from an inclusion complex following oral administration.
Dissolution (Kd) of the complex occurs followed by dissociation at the intestinal membrane. An equilibrium is established between the dissociated drug, empty cyclodextrin and the complex. Following dissociation the free drug is able to be absorbed across the intestinal membrane. The cyclodextrin owing to its large size is unable to cross the intestinal membrane. Absorption of the drug is dependant on dissolution (K_d) and dissociation (K_C) of the complex (Stella *et al.,* 1999).

The lack of toxicity and the improvement in the absorption and bioavailability of itraconazole following its complexation with HPβCD led to the complex being approved by the US Food and Drug Administration. The oral formulation was registered in 1997 in the US and was subsequently followed by an I.V. formulation in 1999 (Peeters *et al.*, 2002). The product is marketed as Sporanox®.

The example of itraconazole indicates that the solubility and bioavailability of poorly soluble lipophilic drugs can be improved through complexation with cyclodextrins. Furthermore, it demonstrates that the licensing and regulating bodies do approve formulations containing cyclodextrins.

3.1.3 Melarsoprol cyclodextrin complexes

Cyclodextrin chemistry was utilised in an attempt to produce an aqueous formulation of melarsoprol suitable for oral or intravenous administration. An aqueous solution of melarsoprol which could be administered either orally or parenterally would not only improve the tolerability and safety of the drug but would also be highly advantageous in the remote settings were HAT occurs. Patients could receive treatment in local health centres from community health workers and hospitalisation would not be required, thus strain would not be put on already stretched resources and patients would not become a burden on their families while receiving treatment.

Initially four different melarsoprol cyclodextrin complexes were produced using the cyclodextrins α, β, HPβCD and RAMβCD (Gibaud *et al.*, 2005). The complexes were produced by placing 1mmol of melarsoprol in an aqueous solution of the appropriate cyclodextrin. The suspensions were stirred for 14 hours at 25°C before being filtered and freeze dried. Each complex was then assessed for its ability to solubilise melarsoprol. The solubility of melarsoprol was not improved by complexation with α cyclodextrin (Gibaud *et al.*, 2005). The failure of α cyclodextrin to increase the solubility of melarsoprol is most likely due to the cavity of the cyclodextrin being too small for adequate complexation to occur. The amount of melarsoprol which could be solubilised by β cyclodextrin was limited by the poor solubility of β cyclodextrin as at higher cyclodextrin

concentrations precipitation of the complex occurred (Gibaud *et al.*, 2005). The best solubilisation of melarsoprol was achieved with the modified cyclodextrins HPβCD and RAMβCD. With both cyclodextrins an A_L type phase solubility plot was obtained indicating that the solubility of melarsoprol increases linearly as a function of cyclodextrin concentration (Gibaud *et al.*, 2005; Higuchi and Connons, 1965). The solubility of melarsoprol was increased by a factor of $7.2x10^3$ following complexation with HPβCD or RAMβCD. The stability constants (K_a) of the complexes were 56,077 ± 4205M for mel/RAMβCD, and 54,168 ± 5350M for mel/HPβCD. These are within the range considered suitable for pharmacological use. As a result mel/HPβCD and mel/RAMβCD were selected for further investigation.

In this chapter the inhibitory concentration (IC_{50}) of mel/HPβCD and mel/RAMβCD against *T. b. brucei* bloodstream trypanosomes will be determined *in-vitro* to confirm that the melarsoprol has retained its trypanocidal activity following complexation with HPβCD and RAMβCD. Additionally, the minimum curative dose of the complexes will be determined in a murine model of CNS stage *T. b. brucei* infection.

3.2 Methods

3.2.1 Assessing the inhibitory concentration of complexed melarsoprol

3.2.1.1 Preparation of stock solutions

Mel/HPβCD and mel/RAMβCD are supplied as fine white powders with the ratio of cyclodextrin to melarsoprol quantified for each batch. The ratio of cyclodextrin to melarsoprol for the complexes used in this thesis has already been stated in chapter two. Using these ratios the amount of mel/HPβCD and mel/RAMβCD required to give stock solutions of 100mM were calculated and the solutions prepared in DMSO. Stock solutions of melarsoprol and diminazene aceturate were also prepared at a concentration of 100mM. Stock solutions of the empty cyclodextrins HPβCD and RAMβCD were prepared at a melarsoprol equivalent concentration of 100mM. The stock solutions of the cyclodextrin complexes mel/HPβCD and mel/RAMβCD and the empty cyclodextrins HPβCD and RAMβCD were freshly prepared prior to each assay as no information is available regarding their stability in solution and at -20°C. Melarsoprol and diminazene aceturate are stable at -20°C, so the stock solutions of these compounds were stored at -20°C until use.

3.2.1.2 Preparation of working solutions

The 100mM stock solutions of each compound were diluted in HMI-9 culture medium supplemented with 10% foetal calf serum and β mercaptoethanol to give working solutions of 200μM. Working solutions were freshly prepared prior to each assay.

3.2.1.3 Culturing of trypanosomes

Bloodstream forms of *T. b. brucei* S427 were cultivated in HMI-9 medium containing 10% foetal calf serum and β mercaptoethanol at 37°C in a humidified environment at a 5% carbon dioxide (CO_2) concentration. Trypanosomes were allowed to proliferate until a cell density of 1-2x10^6 cells/ml was reached. Upon

reaching the required density an 8-10µl sample of the culture was removed from the flask and placed in the chambers of a haemocytometer. The haemocytometer was viewed at x10 magnification and the number of trypanosomes within 1mm^2 of the ruled grid area counted. The total number of trypanosomes per ml was subsequently derived and adjusted to 4x10^4 trypanosomes/ml by the addition of HMI-9 culture medium. This served as the seed stock in the Alamar blue assay.

3.2.1.4 Alamar blue assay

3.2.1.4.1 Preparation of Alamar blue solution

A 0.49mM Alamar blue solution was prepared by the addition of 12.5mg Alamar blue to 100ml of 1 x PBS, pH 7.4. The solution was subsequently sterilised through a 0.22µm syringe filter inside a laminar flow hood. Following preparation the solution was stored at 4˚C and protected from the light until use.

3.2.1.4.2 Alamar blue assay

A modification of the Alamar blue assay previously described by Raz *et al*. was used (Raz, Iten, GretherBuhler, Kaminsky *et al.*, 1997). 200µl of the working drug solutions were added to every second well in the first column of a 96 well plate, while 100µl of HMI-9 culture medium was added to the remaining wells. In order to obtain serial dilutions of the compounds across the plate, 100µl of the working drug solution from well A1 was transferred into well A2 and mixed thoroughly. 100µl from well A2 was then transferred into well A3. This process was repeated along the length of the first and second rows of the plate. The last well of the second row was left drug free and served as a negative control. To every well 100µl of the trypanosome seed stock containing 4 x 10^3 trypanosomes was added. This resulted in final drug concentrations ranging from 100µM to 24pM. The plates were subsequently incubated for 48 hours at 37˚C under 5% CO_2.

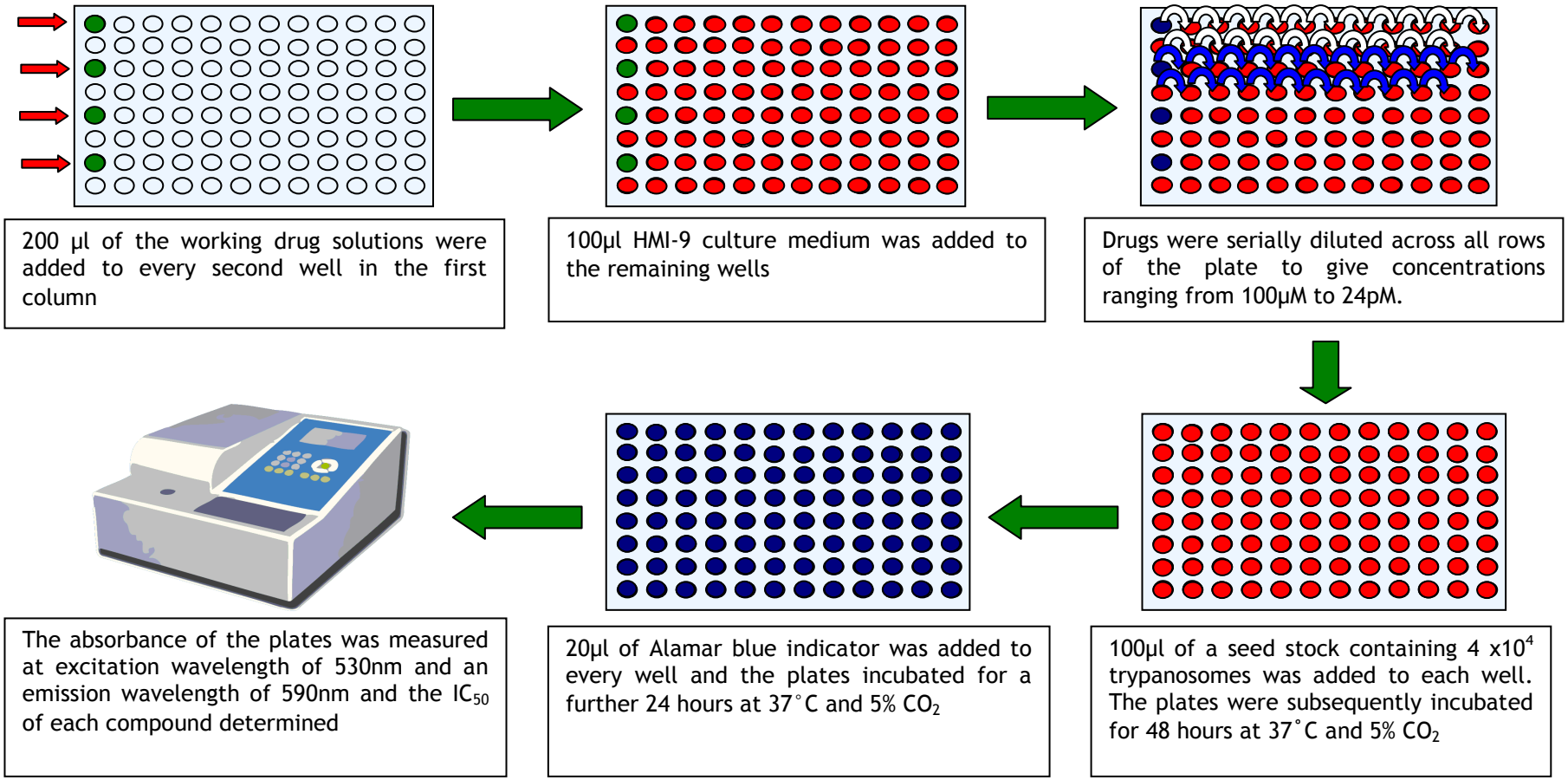

Figure 3-3: The flow process used in the Alamar blue assay

After the incubation period 20µl of Alamar blue solution was added to each well. The plates were then incubated for a further 24 hours at 37˚C and 5% CO_2. Following the second incubation period the absorbance was measured using a Fluo Star fluorescence spectrometer at an excitation wavelength of 530nm and an emission wavelength of 590nm using the program Optima. The assay was performed in duplicate for each compound on three separate occasions.

3.2.1.5 Statistical analysis

The change in fluorescence was plotted as a function of drug concentration for each compound using GraphPad Prism 5 software and the inhibitory concentration (IC_{50}) of each compound derived. Data was analysed using analysis of variance methods, in particular the General Linear Model (GLM) in Minitab 16. This provides a method for investigating main effect differences. To adjust for any zero values, the [log(x+1)] transformation was applied prior to analysis. Significance was measured using the p value at the 5% significance level. Effect sizes were further investigated using 95% confidence intervals for the differences between means.

3.2.2 Determining the in-vivo trypanocidal activity of complexed melarsoprol and melarsoprol compounds

3.2.2.1 Establishing *T. b. brucei* infection in mice

Female CD-1 mice approximately 6 to 8 weeks in age were infected with 2 $x10^4$ *T. b. brucei* trypanosomes of stabilate GVR 35/C1.9. Infection was confirmed in all animals prior to chemotherapy commencing by examining a wet blood film prepared from tail blood for the presence of trypanosomes. These procedures are described in detail in chapter 2.

3.2.2.2 Preparation of compounds for oral administration

Five solutions of mel/HPβCD and mel/RAMβCD were prepared at concentrations of 0.0125, 0.025, 0.05, 0.1 and 0.2mmol/kg. The full details regarding the preparation of the complexes are detailed in chapter 2. In order to assess the

in-vivo trypanocidal activity of conventional melarsoprol formulations, 0.05mmol/kg solutions of trimelarsen (mel W), cymelarsan (mel Cy) and a fine suspension of melarsoprol were prepared (Table 3-1). All solutions were freshly prepared at the start of each day in sterile water.

Compound	Amount of compound required (mg) per ml to give a dose of 0.05mmol/kg
Melarsoprol	2
Trimelarsen	2.66
Cymelarsan	2.51

Table 3-1: The amount of each compound required in mg per ml in order to give a dose of 0.05mmol/kg

3.2.2.3 Preparation of Mel/HPβCD for intravenous administration

A 0.03mmol/kg solution of mel/HPβCD was prepared by the addition of 40.45mg of mel/HPβCD to sterile pyrogen free saline. The full details regarding the calculation of the dose are provided in chapter 2.

3.2.2.4 Chemotherapy schedules

Following infection mice were randomly assigned to one of sixteen treatment groups (Table 3-2). Each group consisted of six animals. Twenty-one days after infection, during the CNS stage of the disease, chemotherapy commenced.

3.2.2.4.1 Oral administration of compounds

The compounds were administered by oral gavage, daily, for seven consecutive days. Animals were appropriately restrained, the gavage needle (20 gauge x 25mm) inserted directly into the oesophagus and the drugs slowly administered directly into the stomach.

3.2.2.4.2 Intravenous administration of mel/HPβCD

The drug was administered once at a dose of 0.03mmol/kg into the caudal vein. The full procedure is described in chapter 2.

	Dose (mmol/kg)					
			Oral			I.V.
Drug	0.0125	0.025	0.05	0.1	0.2	0.03
Mel/HPβCD	√	√	√	√	√	√
Mel/RAMβCD	√	√	√	√	√	
Melarsoprol			√			
Trimelarsen			√			
Cymelarsan			√			
HPβCD				√		
RAMβCD				√		

Table 3-2: The sixteen treatment groups used in the experiment
Each treatment group consisted of six animals. The compounds were administered orally, daily, for 7 consecutive days. Mel/HPβCD was also administered as a single I.V. dose of 0.03mmol/kg.

3.2.2.5 Assessing the effectiveness of chemotherapy

Following completion of chemotherapy, each regime was evaluated for its ability to cure CNS stage *T. b. brucei* infection. A wet blood film prepared from tail blood was observed weekly for 60 days for the presence of trypanosomes (Full procedure is detailed in chapter 2). Animals remaining parasitaemic for two consecutive weeks were culled and the chemotherapy regime deemed unsuccessful. Mice aparasitaemic at the end of the 60 day observation period were sacrificed and the brain removed. The brain was homogenised in 5ml of PGBS and injected intraperitoneally into normal recipient mice. A wet blood film prepared from tail blood of the recipient mice was examined on a weekly basis for 60 days for the presence of trypanosomes. Animals parasitaemic for two consecutive weeks were culled and the chemotherapy regime deemed unsuccessful. Recipient animals aparasitaemic at the end of the 60 day observation period were considered cured and the chemotherapy regime deemed successful.

3.2.3 Determining the hepatic toxicity of complexed melarsoprol

3.2.3.1 Chemotherapy schedules

Mel/HPβCD, mel/RAMβCD, HPβCD or RAMβCD were administered by oral gavage, daily, for seven consecutive days at a dose of 0.05mmol/kg (melarsoprol concentration) to normal mice. Immediately after completion of chemotherapy three animals were sacrificed from each treatment group (Figure 3-4). An additional three animals from each treatment group were sacrificed 7, 14 and 21 days after completion of chemotherapy.

								7		14		21
M	M	M	M	M	M	M	>		>		>	
						K		K		K		K

Figure 3-4: The treatment schedule used
Female CD-1 mice were administered (M) mel/HPβCD, mel/RAMβCD, HPβCD or RAMβCD daily, for 7 consecutive days, at a dose of 0.05mmol/kg. Three animals from each treatment group were sacrificed (K), immediately, 7, 14 and 21 days after completion of the treatment regime.

3.2.3.2 Collection of samples

Animals were culled by exposure to increasing levels of carbon dioxide. Following sacrifice the liver was carefully excised and placed in 4% neutral buffered formalin.

3.2.3.3 Preparation of samples for histopathology analysis

The liver was removed from the neutral buffered formalin and processed to paraffin blocks. From the paraffin blocks 3µm thick sections were cut and mounted onto glass microscope slides. The sections were stained with haematoxylin and eosin (H&E) in order to identify any abnormalities.

3.2.3.4 Histopathological analysis

The liver sections were viewed by light microscopy and any regions of abnormality, consistent with toxicity identified. This assessment was conducted

under guidance from Prof. Hal Thompson, Veterinary Pathology, University of Glasgow Veterinary School.

3.3 Results

3.3.1 Inhibitory concentration (IC_{50}) of complexed melarsoprol

The change in fluorescence as a function of drug concentration was measured for mel/HPβCD, mel/RAMβCD, HPβCD, RAMβCD, melarsoprol and diminazene aceturate and the IC_{50} of each compound subsequently determined (Figure 3-5). The IC_{50} of melarsoprol (6.933nM) was not significantly different to that of mel/HPβCD (21.62nM, P = 0.267) or mel/RAMβCD (8.80nM, P = 0.200). The cyclodextrins alone HPβCD and RAMβCD had no trypanocidal activity. The IC_{50} of HPβCD (0nM) was significantly higher than the IC_{50} of melarsoprol (6.933nM, P=0.001), mel/HPβCD (21.62nM, P < 0.0001) and mel/RAMβCD (8.80nM, P=0.0007). No significant difference (P = 1.000) was detected between the IC_{50} of HPβCD and RAMβCD. The IC_{50} of diminazene aceturate (100.6nM) was significantly higher than the IC_{50} of melarsoprol (6.933nM, P = 0.0002), mel/HPβCD (21.62nM, P = 0.0086) and mel/RAMβCD (8.80nM, P = 0.0003). Summary statistics are detailed in Table 3-3.

3.3.2 The minimum oral curative dose of complexed melarsoprol

At the lowest dose of 0.0125mmol/kg neither mel/HPβCD nor mel/RAMβCD produced any cures in the murine CNS stage model of trypanosomiasis (Figure 3-6). Although all animals were aparasitaemic following completion of the chemotherapy regime, they relapsed to parasitaemia within two weeks of the treatment ending. When the dose was doubled to 0.025mmol/kg mel/HPβCD had a cure rate of 50% (3/6 animals cured) while mel/RAMβCD had a cure rate of 66.6% (4/6 animals cured). The lowest dose at which a 100% cure rate (6/6 animals cured) was obtained for both complexes was 0.05mmol/kg. 100% cure rates (6/6 animals cured) were also obtained at doses of 0.1 and 0.2mmol/kg (Table 3-4). HPβCD and RAMβCD had no trypanocidal activity up to doses of 0.2mmol/kg. Animals receiving HPβCD or RAMβCD remained parasitaemic throughout the study.

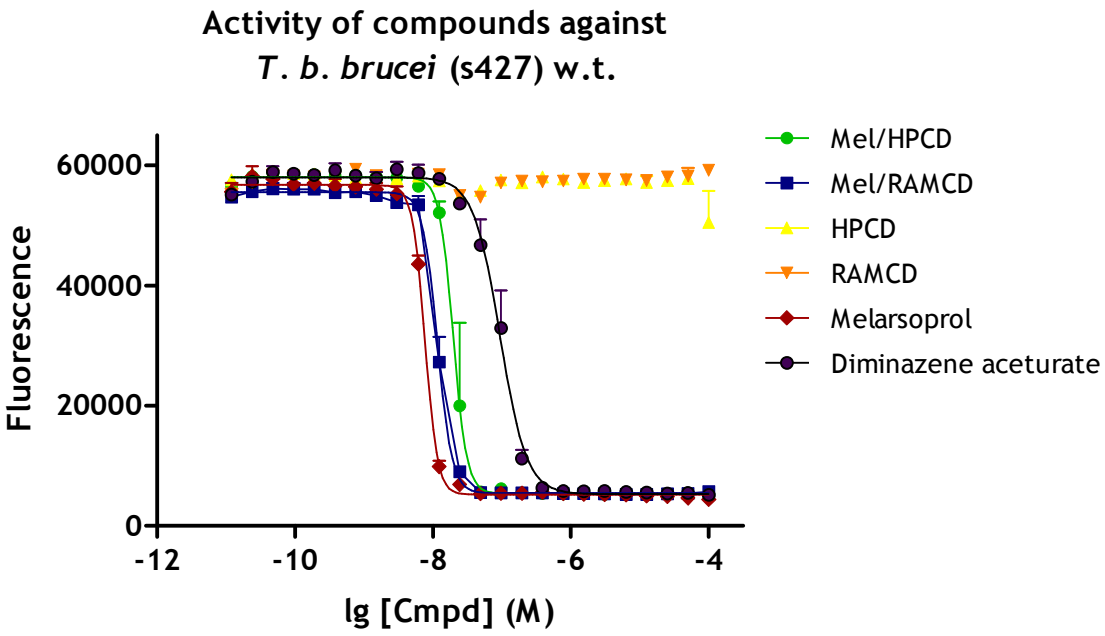

	IC_{50} (nM)
Mel/HPCD	19.7
Mel/RAMCD	11.65
HPCD	
RAMCD	
Melarsoprol	7.684
Diminazene aceturate	94.22

Figure 3-5: The IC_{50} of the compounds against wild type (s427) *T. b. brucei* trypanosomes
The IC_{50} of mel/HPβCD, mel/RAMβCD, melarsoprol, diminazene aceturate, HPβCD and RAMβCD against wild type (s427) *T. b. brucei* trypanosomes was determined by Alamar blue assay.

	Diminazene aceturate	HPβCD	Mel/HPβCD	Mel/RAMβCD	Melarsoprol	RAMβCD
HPβCD	P < 0.0001 (-5.757, -3.346)					
Mel/HPβCD	P = 0.0086 (-2.786, -0.375)	P < 0.0001 (1.766, 4.177)				
Mel/RAMβCD	P = 0.0003 (-3.610, -1.198)	P = 0.0007 (0.942, 3.353)	P = 0.2674 (-2.029, 0.382)			
Melarsoprol	P = 0.0002 (-3.681, -1.270)	P = 0.001 (0.870, 3.281)	P = 0.2002 (-2.101, 0.310)	P = 0.9999 (-1.277, 1.1340)		
RAMβCD	P < 0.0001 (-5.757, -3.345)	P = 1.000 (-1.205, 1.206)	P < 0.0001 (-4.176, -1.765)	P = 0.0007 (-3.352, -0.9412)	P = 0.001 (-3.281, -0.8696)	
Mean ± SE N	100.6 ± 23.6 3	0.00 ± 0.00 3	21.62 ± 8.64 3	8.80 ± 3.00 3	6.983 ± 0.308 3	0.00 ± 0.00 3

Table 3-3: Comparison of the inhibitory concentration (IC_{50}) of the mel/HPβCD, mel/RAMβCD, melarsoprol, diminazene aceturate, HPβCD and RAMβCD
The IC_{50} of each compound was determined against wild type S427 *T. b. brucei* trypanosomes by Alamar blue assay. The figures in the body of the table demonstrate the comparisons, in terms of statistical significance, between the IC_{50} (nM) of each compound, shown in the row and column headings. The p-values and 95% confidence intervals for differences are based on analysis using the logarithmic transformation [log(x+1)] of the IC_{50}. The mean IC_{50} value ± the standard error (mean ± SE) and the number of repeats are also shown.

3.3.3 The minimum intravenous curative dose of mel/HPβCD

The administration of 0.03mmol/kg mel/HPβCD intravenously resulted in a cure rate of only 16.6% (1/6 animals cured) in a CNS stage murine model of *T. b. brucei*.

3.3.4 In-vivo trypanocidal activity of melarsoprol compounds

The ability of three conventional melarsoprol compounds trimelarsen, cymelarsan and melarsoprol to cure CNS stage murine trypanosome infection was investigated (Figure 3-7). Trimelarsen and cymelarsan were unable to produce cures when administered orally at a dose of 0.05mmol/kg, daily, for 7 consecutive days. All animals receiving trimelarsen and cymelarsan were aparasitaemic following completion of chemotherapy but relapsed to parasitaemia within three weeks of treatment ending. A cure rate of 33.3% (2/6 animals cured) was obtained following the administration of melarsoprol (Table 3-4).

	Dose (mmol/kg)					
	Oral					I.V.
	0.0125	0.025	0.05	0.1	0.2	0.03
	Number of animals cured					
Mel/HPβCD	0/6	3/6	6/6	6/6	6/6	1/6
Mel/RAMβCD	0/6	4/6	6/6	6/6	6/6	-
Melarsoprol	-	-	2/6	-	-	-
Trimelarsen	-	-	0/6	-	-	-
Cymelarsan	-	-	0/6	-	-	-
HPβCD	-	-	-	-	0/6	-
RAMβCD	-	-	-	-	0/6	-

Table 3-4: The number of animals cured in each treatment group
Animals were infected with $2x10^4$ *T. b. brucei* GVR35/C1.9 trypanosomes. On day 21 post-infection, chemotherapy commenced. The compounds were administered orally, daily, for 7 consecutive days. Mel/HPβCD was also administered I.V. at single dose of 0.03mmol/kg.

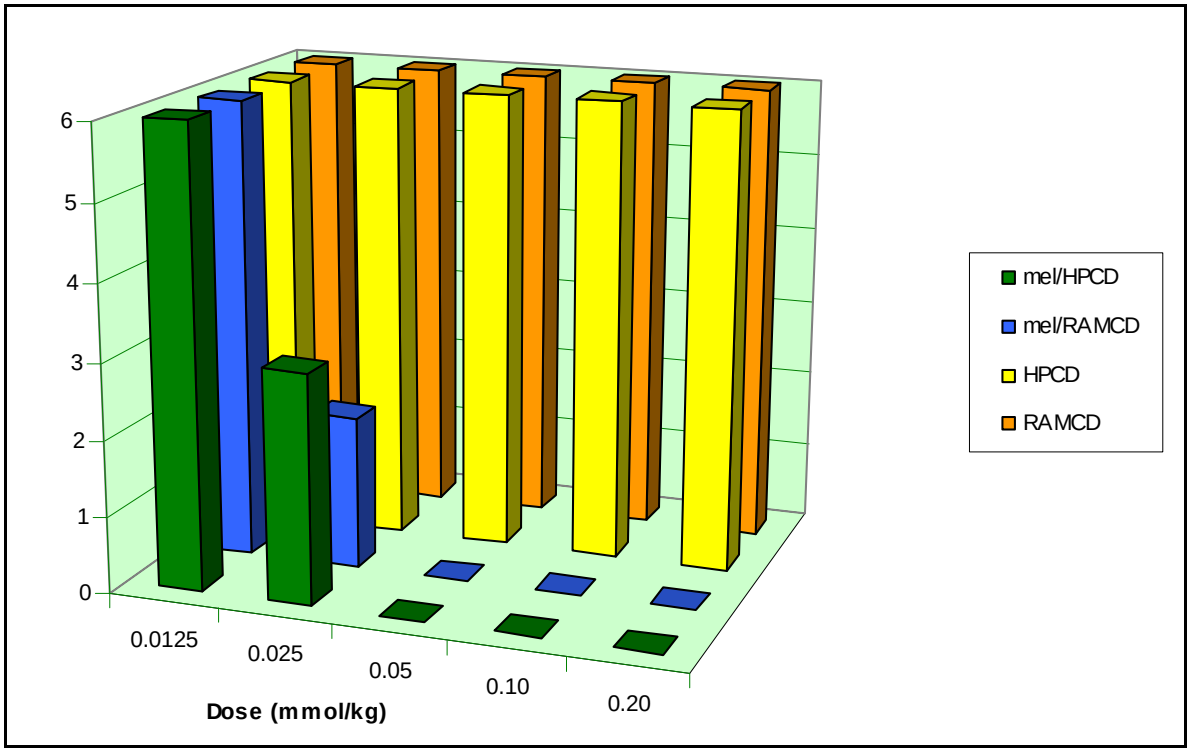

Figure 3-6: The number of animals relapsed at each dose after receiving mel/HPβCD, mel/RAMβCD, HPβCD or RAMβCD
Animals were infected with 2 x10^4 *T. b. brucei* trypanosomes. On day 21 post-infection when CNS stage trypanosome infection is established animals received mel/HPβCD, mel/RAMβCD, HPβCD or RAMβCD at doses ranging from 0.0125 to 0.20mmol/kg. All compounds were administered by oral gavage, daily, for seven consecutive days.

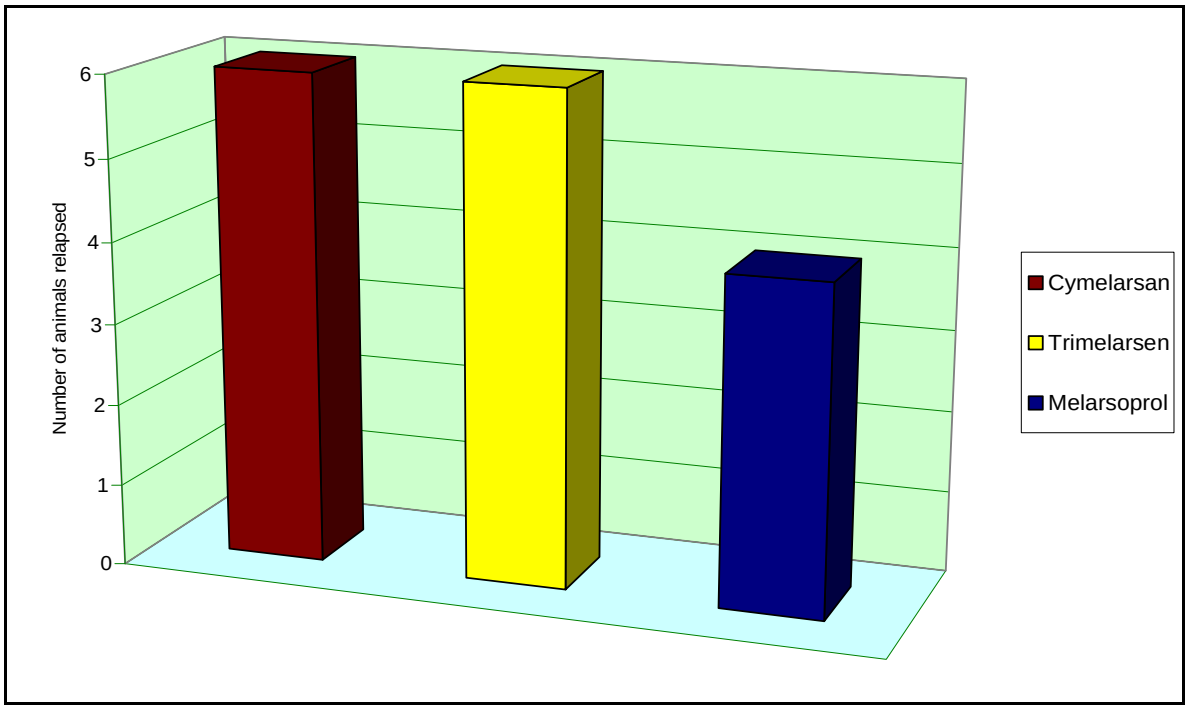

Figure 3-7: The *in-vivo* trypanocidal activity of melarsoprol compounds in murine CNS stage *T. b. brucei* model
All compounds were administered at a dose of 0.05mmol/kg, daily, by oral gavage, for seven consecutive days.

3.3.5 Hepatotoxicity of complexed melarsoprol

The hepatotoxicty of complexed melarsoprol and the cyclodextrins HPβCD and RAMβCD following oral administration was assessed by histopathological analysis.

3.3.5.1 Immediately following completion of the treatment regime

Pathological changes were detected in one animal receiving HPβCD at a dose of 0.05mmol/kg. In this animal pyknotic cells were observed around the blood vessels (Figure 3-8). These changes could be the result of a vascular event, in which cellular blood flow was disrupted, resulting in damage to the hepatocytes. Histopathological changes were not detected in any other animal.

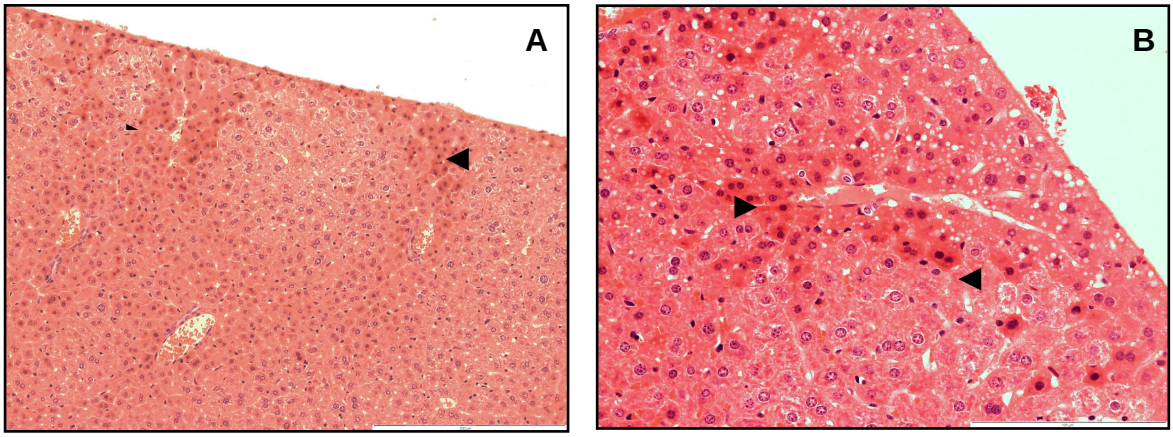

Figure 3-8: The histopathological changes observed in the liver immediately after administration of HPβCD
HPβCD was administered orally, for seven consecutive days at a dose of 0.05mmol/kg. Animals were sacrificed immediately after completion of the treatment regime. Pyknotic cells were observed around the blood vessels (A and B) (arrow heads).

3.3.5.2 Seven days after completion of chemotherapy

Small isolated foci of lymphocytes were observed within the liver parenchyma of one animal receiving mel/HPβCD (Figure 3-9, panel A) and also in one animal receiving RAMβCD therapy (Figure 3-9, panel B). Apart from these small isolated focuses the rest of the liver was histologically normal. In one animal receiving HPβCD (Figure 3-9, panel C), a small focus of necrotic cells, consisting of dead hepatocytes, lymphocytes and neutrophils was observed above the central vein (CV). The remainder of the liver was normal and these changes were not observed in any other treatment group. Vacuolated cytoplasm was observed in

two animals receiving mel/RAMβCD therapy (Figure 3-9, panel D). This may be due to the storage of glycogen within the hepatocytes.

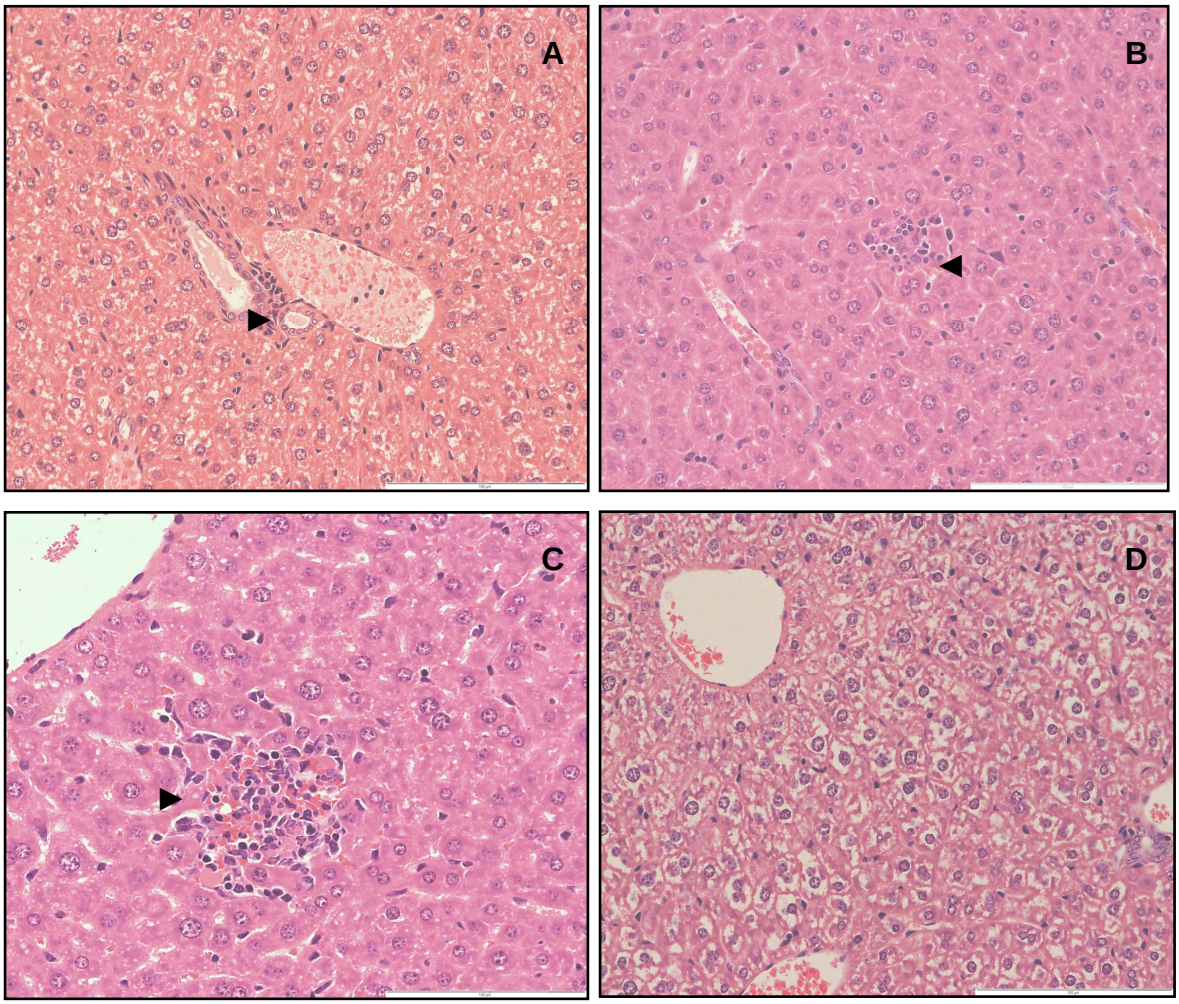

Figure 3-9: The histopathological changes observed in the liver 7 days after completion of mel/HPβCD (A), RAMβCD (B), HPβCD (C) and mel/RAMβCD (D) chemotherapy
Mel/HPβCD, RAMβCD, HPβCD or mel/RAMβCD was administered orally, for 7 consecutive days at a dose of 0.05mmol/kg. 7 days after completion of chemotherapy animals were sacrificed. Small isolated foci of lymphocytes (arrow heads) were observed in animals administered mel/HPβCD (A) and RAMβCD (B). In one animal receiving HPβCD (C), a small foci of necrotic cells (arrow head) consisting of dead hepatocytes, lymphocytes and neutrophils was observed. Vacuolated cytoplasm (D) was observed in two animals administered mel/RAMβCD.

3.3.5.3 Fourteen days after completion of chemotherapy

Fourteen days after the completion of chemotherapy, a small isolated focus of neutrophils was observed in one animal receiving mel/HPβCD (Figure 3-10, panel A). In two animals receiving RAMβCD, and in one animal receiving HPβCD, a mild focal hepatitis was observed (Figure 3-10, panel B). No histological changes were detected in animals receiving mel/RAMβCD.

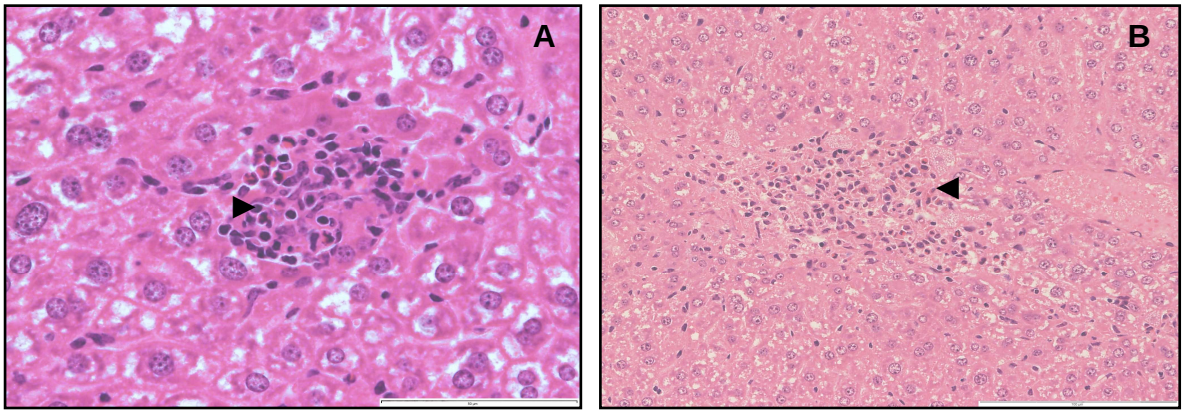

Figure 3-10: The histopathological changes observed in the liver 14 days after completion of mel/HPβCD (A) and RAMβCD (B) chemotherapy
Mel/HPβCD or RAMβCD were administered orally, daily, for 7 consecutive days. Animals were sacrificed 14 days after completion of treatment. A small isolated focus of neutrophils (arrow head) was observed in the liver parenchyma of one animal receiving mel/HPβCD treatment (A). Focal hepatitis (arrow head) was observed in animals receiving the empty cyclodextrins HPβCD and RAMβCD (B).

3.3.5.4 Twenty-one days after completion of chemotherapy

Twenty-one days after the completion of treatment, histological changes were observed in all treatment groups. The alterations were characterised by a focal hepatitis within the liver parenchyma. The reaction was present in one animal from the mel/HPβCD, mel/RAMβCD and RAMβCD treatment groups and in two animals receiving HPβCD. All other animals were histologically normal.

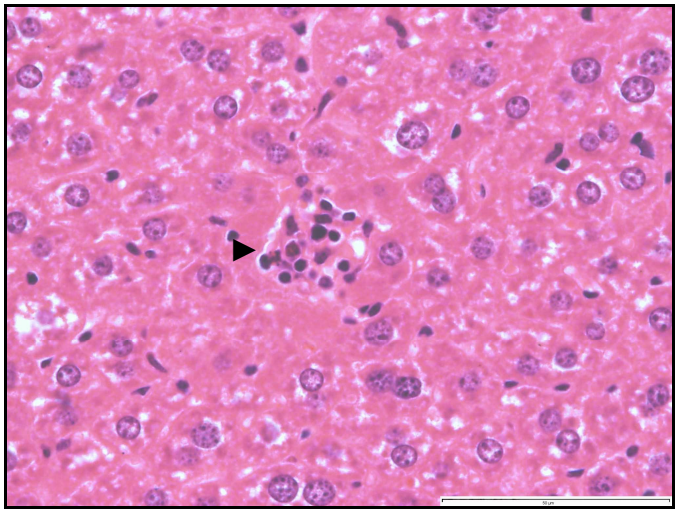

Figure 3-11: The histological changes observed within the liver 21 days after completion of treatment
Mel/HPβCD, mel/RAMβCD, HPβCD and RAMβCD were administered orally, for 7 consecutive days, at a dose of 0.05mmol/kg. Histopathological changes in the form of focal hepatitis (arrow head) were observed in all treatment groups.

3.4 Discussion

For a novel formulation of melarsoprol to be considered as a new drug candidate in the treatment of HAT its trypanocidal activity must be comparable to that of the current formulation and it should display a reduced toxicity. The *in-vitro* trypanocidal activity of the melarsoprol cyclodextrin compounds mel/HPβCD and mel/RAMβCD against bloodstream *T. b. brucei* trypanosomes was determined by means of an Alamar blue assay. The complexation of melarsoprol to the cyclodextrins HPβCD or RAMβCD did not significantly reduce the *in-vitro* trypanocidal activity of melarsoprol. Of the two melarsoprol cyclodextrin complexes mel/RAMβCD displayed the greatest *in-vitro* trypanocidal activity against bloodstream *T. b. brucei* trypanosomes with an IC_{50} of 8.80nM compared to that of 21.62nM for mel/HPβCD but this difference was not significant.

In the present study the *in-vitro* activity of melarsoprol was not significantly reduced following its complexation to HPβCD and RAMβCD. This is in contrast to the study by Zirar *et al*. who reported a significant reduction in the *in-vitro* activity of melarsoprol following its complexation with HPβCD (Zirar, Gibaud, Camut and Astier, 2007). In the study, erythroleukemia (K562) and myelomonocytic leukaemia (U937) cells lines were exposed to melarsoprol or mel/HPβCD at concentrations ranging from 0.01μM to 1mM (melarsoprol concentration). The cells were incubated for two or three days before cell viability was determined by the tetrazolium salt method (MTT test) (Hansen, Nielsen and Berg, 1989). The cytotoxicity of melarsoprol was retained following its complexation with HPβCD but the level of cytotoxicity observed was significantly reduced in both cell lines compared to free melarsoprol. For mel/HPβCD IC_{50} values of 9.3 ± 1.2 and 8.9 ± 7.2μM were obtained in the K562 and U937 lines respectively compared to 2.65 ± 0.08 and 2.40 ± 0.02μM for free melarsoprol (Zirar *et al.,* 2007). The cytotoxicity of mel/RAMβCD was not determined.

The discrepancy between the present study and that of Zirar *et al*. could be due to different cells lines the two assays were conducted on. In the present study, the IC_{50} of the melarsoprol cyclodextrin complexes was determined for wild type S427 *T. b. brucei* trypanosomes. Trypanosomes are very sensitive to melarsoprol,

rapidly lysing in the presence of the drug. The IC_{50} of melarsoprol in trypanosomes therefore lies in the nano gram range. In the study conducted by Zirar *et al*. the cytoxicity of the melarsoprol cyclodextrin complexes was determined in erythroleukemia (K562) and myelomonocytic leukaemia (U937) cells lines. The cells lines are not as sensitive to melarsoprol as trypanosomes with the IC_{50} lying in the micro gram range. Melarsoprol is an unstable compound and rapidly undergoes an acid-base catalysed hydrolysis in which the dithiarsolane ring is opened resulting in the formation of the metabolite melarsen oxide (Keiser and Burri, 2000). *In-vivo* melarsoprol is rapidly metabolised to melarsen oxide (Keiser, Ericsson and Burri, 2000). This was demonstrated in a study investigating the metabolites of melarsoprol. The half-life of melarsoprol by HPLC analysis was determined to be less than 30 minutes in the plasma. The metabolite melarsen oxide was rapidly formed reaching maximum plasma levels (C_{max}) after 15 minutes (Keiser, Ericsson and Burri, 2000). In *in-vitro* assays melarsoprol is also rapidly hydrolysed to melarsen oxide. When melarsoprol is complexed with the cyclodextrins HPβCD and RAMβCD the dithiarsolane ring is contained within the hydrophobic cyclodextrin cavity and is therefore inaccessible to water molecules so hydrolysis is prevented. The inability of melarsoprol to undergo hydrolysis while contained within the cyclodextrin cavity has been confirmed by stability studies (Gibaud *et al.,* 2005). The degradation kinetics of melarsoprol are significantly reduced when the compound is contained within the cyclodextrin cavity as opposed to being free. By forming an inclusion complex the stability half-life of the compound is doubled. In order for hydrolysis to occur the melarsoprol molecule must first dissociate from the cyclodextrin cavity. Upon dissociation, water molecules are able to access the dithiarsolane ring and the active metabolite, melarsen oxide is formed. However, the newly formed melarsen oxide can also form complexes with the empty cyclodextrins resulting in a decrease in the free melarsen oxide concentration. The increased stability obtained by complexation and the ability of the active metabolite, melarsen oxide, to re-enter the cyclodextrin cavity means the amount of free melarsen oxide is decreased when melarsoprol is complexed to cyclodextrins. This lower concentration of free melarsen oxide could therefore account for the decreased cytotoxicity observed by Zirar *et al*. *in-vitro* when melarsoprol was complexed with the cyclodextrin HPβCD. As trypanosomes are more sensitive to melarsoprol than erythroleukemia (K562)

and myelomonocytic leukaemia (U937) cells lines, the free concentration of melarsen oxide although reduced, following the complexation of melarsoprol to HPβCD and RAMβCD, was still high enough to cause lysis of the trypanosomes. No difference was therefore detected in the present study between the IC_{50} of free melarsoprol and that of mel/HPβCD and mel/RAMβCD.

The remote, isolated, resource poor settings in which HAT occurs means that any new trypanocidal compound must be easy to administer. At present patients must be hospitalised while receiving treatment as all currently available drugs require parenteral administration. An oral formulation would eliminate the need for hospitalisation enabling patients to be treated in local health centres, freeing up limited resources. In this study the minimum curative dose of mel/HPβCD and mel/RAMβCD following oral administration was determined and compared to orally administered melarsoprol, cymelarsan and trimelarsen in a murine model of CNS stage *T. b. brucei* infection. Mel/HPβCD and mel/RAMβCD administered at a dose of 0.05mmol/kg, daily, for seven consecutive days, cured murine CNS stage *T. b. brucei* infection. Cymelarsan and trimelarsen given at an equivalent dose were unable to produce cures, while melarsoprol was able to cure only 33.3% of the animals. The cyclodextrins alone HPβCD and RAMβCD displayed no trypanocidal activity.

Melarsoprol is a very lipophillic compound (log P = 2.53) and as a result it is able to diffuse across biological membranes, including the blood-brain barrier (BBB) (Gibaud *et al.,* 2005). However, when melarsoprol is administered orally, very little of the compound is absorbed due to the compounds poor solubility and dissolution profile. In order for a drug to be absorbed from the gastrointestinal tract (GI), dissolution of the compound must occur followed by permeatation through the mucosal membrane (Carrier, Miller and Ahmed, 2007). The poor solubility of melarsoprol (S_0 = 6 mg/l) means dissolution of the compound is very slow (D_e = 24.6 ± 2.0% after 10 minutes at 37°C) and after 60 minutes only 60.3 ± 6.1% of the drug is dissolved (Gibaud *et al.,* 2005). As a result very little of the drug is absorbed from the GI tract. This means that the drug is unlikely to reach therapeutic levels within the CNS and chemotherapy will be of limited success.

The melarsoprol analogues cymelarsan and trimelarsen are water soluble. As a result, solubility and dissolution of the compounds should not be limiting factors in the absorption of the drugs from the GI tract as is the case with melarsoprol. One therefore might expect the oral bioavailability of cymelarsan and trimelarsen to be greater than melarsoprol. However, in the present study this was not the case. Cymelarsan and trimelarsen when administered orally failed to cure CNS stage *T. b. brucei* infection, while a cure rate of 33.3% was obtained with melarsoprol when administered at an equivalent dose. This suggests that cymelarsan and trimelarsen are poorly absorbed across biological membranes. Studies conducted by Watson and Robertson support this hypothesis (Robertson, 1963; Watson, 1965). In the studies the authors assessed the efficacy of trimelarsen to cure CNS stage *T. b. rhodesiense* and *T. b. gambiense* infections. Initial results from the studies showed promising results with trimelarsen appearing to be as effective as melarsoprol. However, subsequent follow up investigations conducted a number of months after completion of chemotherapy showed that a large majority of the patients had relapsed to parasitaemia. Watson reported treatment failure rates of 15.8% while Robertson observed a much higher relapse rate of 56.25% in patients with *T. b. rhodesiense* infections (Robertson, 1963; Watson, 1962; Watson, 1965). These results suggested poor penetration of trimelarsen across the BBB and as a result therapeutic concentrations of the compound could not be obtained in the CNS.

The complexation of melarsoprol to the cyclodextrins HPβCD and RAMβCD enhanced the inherent solubility of melarsoprol by a factor of 7.2 $x10^3$ (Gibaud *et al.,* 2005). This increased solubility means that there is a rapid dissolution of the complexes. The dissolution efficiency (D_e) of mel/RAMβCD was determined to be 96.7 $\pm$ 2.5% after 10 minutes and after 1 hour complete dissolution of the complex had occurred (Gibaud *et al.,* 2005). This increased rate of dissolution means that following complex dissociation melarsoprol rapidly permeates the mucosal membrane and is absorbed. As a result the oral bioavailability of the compound is increased. Uekama *et al.* reported similar observations following the complexation of diazepam with γ cyclodextrin (Uekama, Narisawa, Hirayama and Otagiri, 1983). The solubility of diazepam was increased by complexation and as a result the complex dissolved much more rapidly than the free drug. This enhanced dissolution rate led to an increase in the net amount of diazepam

permeating a cellophane membrane *in-vitro*. *In-vivo* the higher dissolution rate of the complex resulted in higher serum levels of diazepam being obtained following oral administration of the complex compared to the free drug alone, C_{max} = 1.05 ± 0.16 and 0.59 ± 0.08 µg/ml respectively. Increased oral bioavailability as a result of enhanced dissolution and solubility kinetics brought about by complex formation has also been reported for itraconazole (Willems, Van der Geest and de Beule, 2001), artemisinin (Wong and Yuen, 2001) and albendazole (Evrard, Chiap, DeTullio, Ghalmi *et al.*, 2002).

A second factor contributing to the increased oral bioavailability observed following complexation of melarsoprol is that the cyclodextrins act as carriers. The cyclodextrins effectively deliver the compound to the mucosal membrane. Once at the intestinal membrane, the membrane acts as a 'sink' causing dissociation of the complex based on a simple mass action principle (Stella *et al.*, 1999). Following dissociation of the complex at the intestinal membrane, the melarsoprol is free to diffuse across the membrane from where it enters the bloodstream (Figure 3-2). Undissociated complexes and the cyclodextrins themselves are not significantly absorbed and are mostly excreted unchanged in the faeces (Stella *et al.*, 1999).

The increased solubility and enhanced dissolution of melarsoprol as a result of complexation and the ability of the cyclodextrins to act as carriers, delivering the drug to the intestinal membrane all result in an increase in the oral bioavailability of melarsoprol. As a result the drug is able to penetrate into the CNS and cure CNS stage murine trypanosomiasis.

A single intravenous dose of 0.03mmol/kg mel/HPβCD resulted in an unsatisfactory cure rate of 16.7%. The low cure rate is unlikely to be due to the inability of the complex to penetrate the blood-brain barrier (BBB) as successful cure rates were obtained following oral administration of the complexes. The low cure rate is probably a result of the dose administered being too low for therapeutic levels to be obtained within the CNS. In the I.V. schedule the total amount of melarsoprol administered was only 0.478mg where as in the successful oral regime 5.6mg of melarsoprol was administered. This is nearly a 12 fold reduction in the amount of melarsoprol administered. For I.V. administration the dose is normally reduced compared to the oral dose as the

compound is delivered directly into the bloodstream but it is not usually reduced by such a large factor. Considering the low I.V. dose of mel/HPβCD administered, it is not surprising disappointing cure rates were obtained. The dose of mel/HPβCD can not be increased, as in a previous study, a dose of 0.038mmol/kg was found to kill 40% of the animals (Zirar *et al.,* 2007). One way, to raise the levels of melarsoprol reaching the CNS following I.V. administration of mel/HPβCD would be to lengthen the treatment schedule by administering the drug on a daily basis for a set period of time. However, as the drug/cyclodextrin complex is effective orally, there is little advantage in optimising a parenteral dosing regime where multiple injections are required. Mel/RAMβCD can not be administered I.V. as RAMβCD is nephrotoxic. Its high affinity for cholesterol results in the formation of cholesterol-inclusion complexes which crystallise within the kidney, resulting in nephrosis (Frank, Gray and Weaver, 1976) (Discussed in detail in chapter 1).

Hepatitis was observed within the liver parenchyma in animals from all treatment groups, twenty-one days after completion of chemotherapy. However, the alterations were not observed in every animal and were considered to be of little toxicological importance (personal communication, Prof. Hal Thompson, University of Glasgow). Mild treatment related alterations within the liver are a common occurrence following the administration of cyclodextrins. Gould and Scott reported an increase in the plasma concentration of the liver enzymes ALT, AST and GLDH in rats administered 4,500mg/kg HPβCD, a day, for seven days (Gould and Scott, 2005). However, in contrast to the present study these changes were not associated with any histopathology. This is despite the dose administered being 225 fold higher than in the present study. In the study conducted by Gould and Scott, liver pathology in the form of centrilobular swelling was only observed in rats administered HPβCD at doses greater than 2000mg/kg/day for a year (Gould and Scott, 2005). Discrepancies are commonly observed between studies investigating the oral toxicity of cyclodextrins. In one study, rats were administered HPβCD orally at a dose of 450mg/kg/day for one month (Gould and Scott, 2005). An increase in plasma liver enzymes was observed and plasma creatinine and triglyceride concentrations were also slightly reduced in males. However, in a second longer term study in which HPβCD was administered at a dose of 500mg/kg/day for a year in rats, no

toxicological effects were observed (Gould and Scott, 2005). One possible explanation for the discrepancies between studies investigating the toxicity of cyclodextrins is the route by which the cyclodextrins were administered. In some studies the cyclodextrins are administered by oral gavage directly into the stomach so the animal definitely receives the stated dose. However, in other studies, the cyclodextrins are fed by the diet. This means that some of the animals may receive a smaller dose of the cyclodextrin than stated, as the animals will consume varying quantities of the diet. If the taste of the diet has also been altered through the addition of the cyclodextrin this may also cause animals to consume less of the diet. Although hepatotoxicity was observed in the present study in mice administered 0.05mmol/kg (20mg/kg) HPβCD for seven days, in a study conducted in humans in which HPβCD was administered orally at doses up to 114mg/kg a day, for one to two weeks, no toxicological effects were observed (De Beule, 1996). Furthermore, HPβCD is included in the European Pharmacopoeia (Ph.Eur.) and the US food and drug administration's (FDA) list of inactive pharmaceutical ingredients (Loftsson and Duchene, 2007). This supports the hypothesis that the heptatoxicity observed in the present study is of no toxicological importance.

It can be concluded from these investigations that the *in-vitro* trypanocidal activity of melarsoprol is retained following complexation with HPβCD or RAMβCD. The melarsoprol cyclodextrin complexes mel/HPβCD and mel/RAMβCD display a superior activity in an *in-vivo* murine model of CNS stage *T. b. brucei* infection. The complexes are able to produce 100% cures while free melarsoprol is only able to produce a cure rate of 33.3%. The results from these initial experiments indicate that mel/HPβCD and mel/RAMβCD are promising oral candidates for the treatment of HAT and warrant further investigation.

Chapter 4: Detection of trypanosomes within the brain

4.1 Introduction

The previous chapter demonstrated that the melarsoprol cyclodextrin complexes mel/HPβCD and mel/RAMβCD can successfully cure CNS stage *T. b. brucei* infection following oral administration. However, the time-course of trypanosome elimination from the brain following this treatment regime is unknown. This chapter discusses the development of an in-situ hybridization technique and quantitative PCR (QPCR) assay to visualise the location of trypanosomes within the brain and to assess the number of trypanosomes present within the brain at set time points, before, during and after completion of the chemotherapy regime.

4.1.1 Location of trypanosomes in the brain

Since the early 1900's the ability of trypanosomes to establish a CNS infection has been recognised and many attempts have been made to visualise trypanosomes within paraffin embedded and frozen brain sections with limited success. Mott was one of the first to describe the histological changes that occur within the brain during trypanosome infection. However, trypanosomes were only observed sporadically within the brain parenchyma (Mott, 1906). Calwell also failed to detect any trypanosomes within the brains of 17 patients who had died as a result of *T. b. rhodesiense* infection (Calwell, 1937). The lack of trypanosomes within the brain was attributed to the patients receiving trypanocidal drugs prior to death and the poor fixation of the brain, resulting in degradation of the parasites before the specimens were examined (Calwell, 1937). One of the first descriptions on the location of trypanosomes within the brain was by Stevens and Moulton in deer mice (*Peromyscus maniculatus)* infected with *T. b. brucei* (Stevens and Moulton, 1977). Examination of the paraffin embedded brain sections under a light microscope revealed that the trypanosomes occurred in all areas of the brain but were found most frequently within the choroid plexus of the lateral ventricles. In the ventricles, the parasites were found within the choroidal capillaries, extravascularly but restricted to the choroid and in the ventricular space. The trypanosomes were only observed sporadically within the meninges and when present they were usually confined to the venules. Large numbers of trypanosomes were also

frequently observed within the hippocampus. A second study investigating the localisation of *T. b. rhodesiense* within the brains of mice found similar results to those reported by Stevens and Moulton (Fink and Schmidt, 1979). Two weeks after infection trypanosomes were observed within the connective tissue of the choroid plexus. As the infection progressed the number of trypanosomes present within the choroid plexus of the lateral ventricles increased with dense aggregates of trypanosomes frequently observed. At the terminal stage of infection large numbers of trypanosomes were present within the connective tissue of the villi of the choroid plexus and within the meningeal and cerebral vessels. Additionally, in a number of sections trypanosomes were observed within the brain tissue, in particular the cortex of the cerebrum, Ammon's horn and in the subcortical nuclei. It was therefore concluded that trypanosomes occur most frequently in areas of the brain where the vascular system is well developed (Fink and Schmidt, 1979).

It is difficult to detect trypanosomes within the brain parenchyma using conventional histopathology staining techniques, therefore, in an attempt to make the parasites within the brain tissue more visible Poltera *et al.* used an immunohistology technique (Poltera, Hochmann, Rudin and Lambert, 1980). Brain sections were incubated with fluorescently conjugated anti-trypanosomal antibodies purified from rabbits inoculated with trypanosomal lysate mixed with Freund's incomplete adjuvant. Using this method the trypanosomes showed a similar distribution to that reported by Stevens and Moulton (Stevens and Moulton, 1977). Trypanosomes were first located in the interstitium of the choroid plexus during the third or fourth week of infection with numbers increasing as the infection progressed. Two to three weeks after invasion of the choroid plexus small numbers of trypanosomes were found in the meninges, in particular in the lateral cerebral fissure, the perivascular spaces at the base of the brain and the pontocerebellar area. Electron microscopy conducted eight weeks after infection, revealed trypanosomes in the interstitium of the choroid plexus. However, no parasites were seen within the choroid ependyma (Poltera *et al.*, 1980).

An immunohistochemical approach was also used by Schultzberg *et al.* to visualise *T. b. brucei* trypanosomes in the nervous system of Sprague Dawley rats, BALB/c mice and deer mice (Schultzberg, Ambatsis, Samuelsson,

Kristensson *et al.*, 1988). Brain sections were incubated with antisera collected from rabbits infected with trypanosomes, followed by fluorescein isothiocyanate (FITC) labelled goat anti-rabbit antibodies. In addition, a peroxidase anti-peroxidase (PAP) method was used. Large numbers of trypanosomes were present in the choroid plexus stroma in both deer mice and rats, thirteen days after infection but at this point no trypanosomes were observed in the brain parenchyma (Schultzberg *et al.,* 1988). By 21 days post infection, trypanosomes were found in the stroma of trigeminal and spinal ganglia, in the median eminence, pineal gland and area postrema. Only small numbers of trypanosomes were observed in the brain parenchyma. By 33 days post-infection the number of parasites present within the brain parenchyma had increased and parasites were also observed in the choroid and ciliary body. A similar distribution was observed at days 49, 55 and 68 post-infection. By the terminal stage of infection in rats, the number of trypanosomes present within the brain parenchyma had increased dramatically.

An earlier invasion of the brain parenchyma by *T. b. brucei* was reported by Masocha *et al*. (Masocha, Robertson, Rottenberg, Mhlanga *et al.*, 2004). In this study, the distribution of *T. b. brucei* in relation to cerebral blood vessels was investigated in C57BL/6 mice by double immunolabelling (Masocha *et al.,* 2004). An anti-glucose transporter-1 antibody was used to mark endothelial cells, while a rabbit polyclonal anti-variant surface glycoprotein (anti-VSG) antibody was used to visualise trypanosomes. On day six post-infection, parasites were detected in the stroma of the choroid plexus and the circumventricular organs. At this time point parasites were confined to the lumen of intracerebral vessels and no trypanosomes were detected within the brain parenchyma. Thirteen days after infection trypanosomes were detected in the white matter and septal nuclei of the brain parenchyma. This is eight days earlier than in the study by Schultzberg *et al*. (Schultzberg *et al.,* 1988). By 20 days post-infection, large numbers of trypanosomes were detected within the brain parenchyma and only a small number were observed within the lumens of intracerebral vessels (Masocha *et al.,* 2004). One possible explanation for the earlier trypanosomal invasion of the brain observed by Masocha *et al*. is the animal model used in study. Masocha *et al*. conducted the experiment in C57BL/6 mice while Schultzberg *et al*. used Sprague Dawley rats, BALB/c mice and deer mice (Masocha, Rottenberg and

Kristensson, 2007; Schultzberg *et al.*, 1988). Although both authours used *T. b. brucei* trypanosomes, the time course of the infection varies between animal species thus explaining the difference between the two studies.

4.1.2 In-situ hybridization

Immunohistochemistry aids in the visualisation of trypanosomes within paraffin embedded and frozen brain sections but the methods previously reported in the literature use anti-trypanosomal antibodies raised in rabbits. The processes involved in the generation of anti-trypanosomal antibodies are time consuming and expensive and only limited quantities of antibodies can be produced. There is a need for a simpler, more reliable technique for the visualisation of trypanosomes within paraffin embedded/frozen brain sections. One possible option is in-situ hybridization.

In-situ hybridization allows the visualisation of specific nucleic acid sequences within preserved cells or tissue sections. The nucleic acid sequence is detected by a probe consisting of a complementary sequence to the target of interest. Depending on the intended target the probe can be a double stranded DNA probe, an RNA probe, a cDNA probe or a synthetic oligodeoxyribonucleotide probe (Hofler, 1990). Oligodeoxyribonucleotide probes are often favoured as they are easily synthesised at a low cost, and consistency and quality is guaranteed. The technique has been used to visualise many different infectious agents including varicella-zooster virus, herpes simplex, hepatitis B and Epstein-Barr virus as well as *T. cruzi* (Blum, Haase and Vyas, 1984; Hyman, Ecker and Tenser, 1983; Lane, Olivares-Villagomez, Vnencak-Jones, McCurley *et al.*, 1997; Sixbey, Nedrud, Raabtraub, Hanes *et al.*, 1984; Stroop, Rock and Fraser, 1984).

4.1.2.1 Detection of *Trypanosoma cruzi*

In-situ hybridization was used to visualise the location of *T. cruzi* amastigotes within paraffin embedded murine cardiac sections. Digoxigenin-labelled oligonucleotide probes were synthesised to three regions of the *T. cruzi* genome in order to increase the chances of the amastigotes being detected. The DNA sequences used were a 122 bp sequence present within the mini-repeats of the kinetoplast mini-circles, a 188 bp segment of a 195 bp tandomly repeating

sequence and a 177 bp region present within the open reading frame coding for a 160 KD protein (FL-160-1) located on the surface of the parasite, overlaying the flagellum (Degrave, Fragoso, Britto, van Heuverswyn *et al.*, 1988; Moser, Kirchhoff and Donelson, 1989; Van Voorhis, Schlekewy and Trong, 1991). Following the in-situ hybridization procedure the digoxigenin-labelled oligonucleotide probes were detected with an anti-digoxigenin-alkaline phosphatase antibody and 5-bromo-4-chloro-3-indolyl phosphate/nitro blue tetrazolium (NBT/BCIP) chromagen. All three oligonucleotide probes hybridised with the amastigote DNA present within the cardiac sections, allowing the location of the amastigotes to be visualised (Lane *et al.*, 1997). Single amastigotes could be detected with the oligonucleotide probe designed to a section of the 122 bp mini-circle sequence. This study demonstrates that in-situ hybridization is a sensitive and reliable technique by which to detect the location of kinetoplast parasites within paraffin embedded tissue sections.

4.1.3 Quantitative PCR (QPCR)

Although in-situ hybridization has the potential to locate trypanosomes within the brain it cannot accurately quantify the number of parasites within the brain. However, this could be achieved through the use of quantitative PCR (QPCR). There are many different forms of QPCR including SYBR green, Molecular Beacons, Scorpions and Taqman real-time PCR (Stratagene, 2004). Only the rationale of Taqman real-time PCR will be discussed in detail.

4.1.3.1 Principles of taqman real-time PCR

Taqman PCR takes advantage of the 5' exonuclease activity of taq polymerase in combination with a dual-labelled non-extendable fluorogenic oligonucleotide probe and specific oligonucleotide primers to quantify the number of copies of a gene present in a sample (Cardullo, Agrawal, Flores, Zamecnik *et al.*, 1988; Gibson, Heid and Williams, 1996; Holland, Abramson, Watson and Gelfand, 1991). The Taqman process is illustrated schematically in Figure 4-1. The oligonucleotide probe is labelled with two fluorescent dyes. One dye, positioned at the 5' end of the probe serves as the reporter while the second dye positioned at the 3' end acts as a quencher. The dyes FAM (6-carboxyfluorescein) and TAMRA (6-carboxy-tetramethyl-rhodamine) are frequently used as reporters and

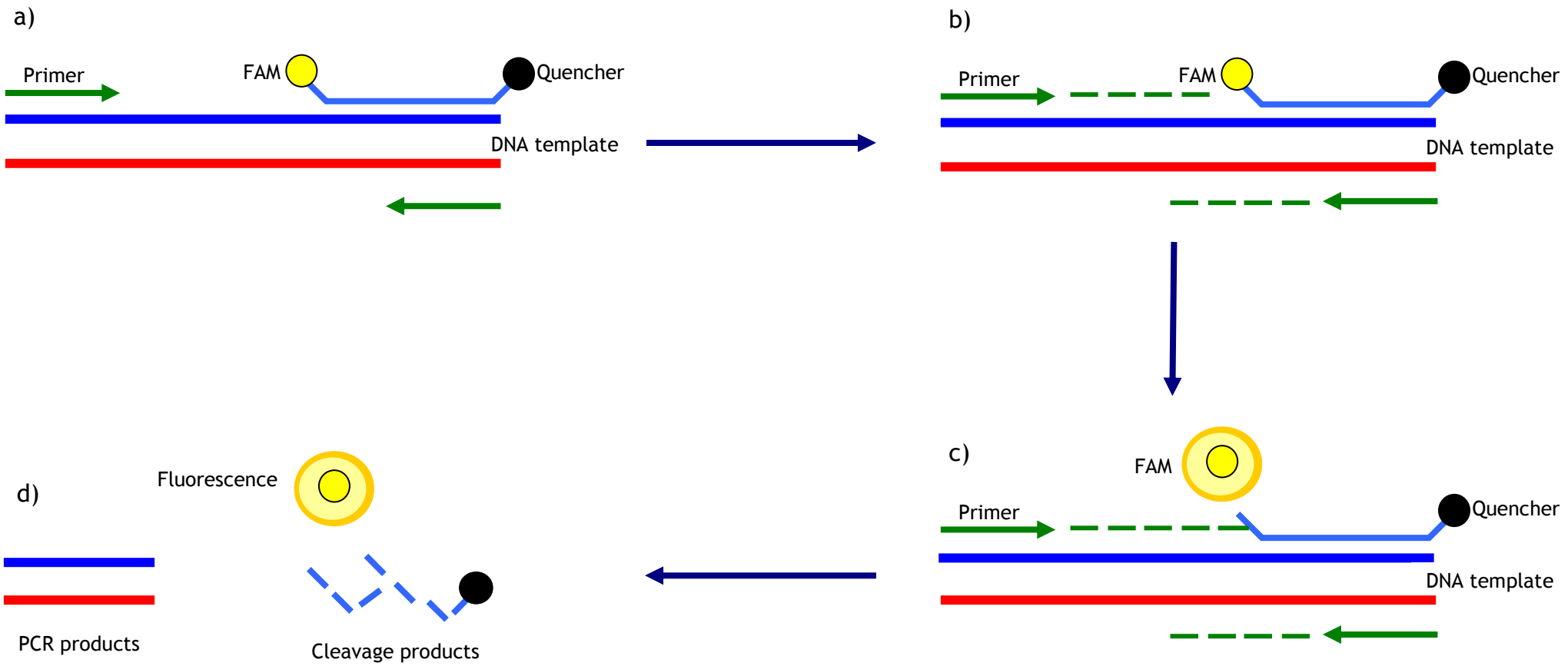

Figure 4-1: A schematic representation of the Taqman PCR reaction
a) The probe labelled with a reporter dye (FAM) and a quencher dye (TAMRA) anneals to the template DNA downstream to the primer. The close proximity of the reporter dye to the quencher dye means the fluorescence of the reporter dye is quenched and no fluorescence is detected. b) During the extension phase of the PCR reaction the primer is extended by the taq DNA polymerase. c) When the taq DNA polymerase comes into contact with the 5' end of the promoter, the probe is denatured and the reporter dye is cleaved. As the reporter dye is no longer in contact with the quencher dye, the fluorescence of the reporter dye is not quenched and fluorescence is detected. d) At the end of the PCR reaction PCR products, cleavage products and the free reporter dye are present.

quenchers respectively, but other dye combinations are available. When the probe is intact the close proximity of the two dyes means that the fluorescent emission of the reporter dye is quenched by the quencher dye and no fluorescence is detected. In the PCR reaction the probe anneals to the target sequence downstream from the forward primer. As the primer is extended the 5' end of the probe is encountered by the taq polymerase. The polymerase degrades the probe and in doing so the reporter dye is released. As the reporter dye is no longer in close proximity to the quencher, fluorescence is detected from the reporter dye. This relative increase in fluorescence can be monitored in real time throughout the PCR reaction and is proportional to the amount of DNA amplified in the PCR reaction and hence the quantity of target sequence present in the original sample.

The fluorescence of the quencher dye TAMRA varies very little during the course of the PCR reaction and so serves as an internal standard to which the change in fluorescence of the reporter dye is normalised. The fluorescence of the reporter dye is normalised to that of the quencher to give a value termed ΔRn, obtained using Equation 4-1:

$$\triangle Rn = (Rn^{+}) - (Rn^{-})$$

Equation 4-1: The equation used to calculate the change in reporter fluorescence normalised to that of the quencher
Rn^{+} = emission intensity of reporter/emission intensity of quencher at any given time. Rn^{-} = emission intensity of reporter/emission intensity of quencher measured prior to PCR amplification (Heid, Stevens, Livak and Williams, 1996).

The mean ΔRn value is subsequently plotted as a function of the cycle number in amplification plots (Figure 4-2). In the initial phases of the reaction the ΔRn value remains at base line level but as the reaction progresses the fluorescence intensity increases proportionally to the increase in amplicon concentration. Based on the variability of the base-line data a threshold fluorescence is set within the log phase of product accumulation. The point at which the amplification plot crosses the threshold is defined as the Ct value. The Ct value decreases linearly with increasing target quantity thus the value can be directly correlated to the concentration of the target DNA in the original sample.

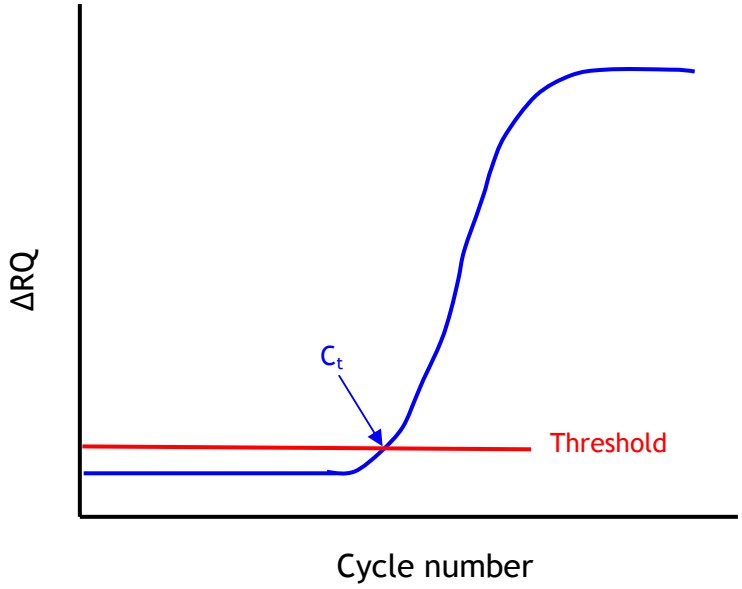

Figure 4-2: Amplification plots illustrating how the Ct value is calculated
The mean ΔRn value is plotted against the cycle number in order to produce amplification plots. A threshold level is set based on the variability of the baseline data. The point at which the amplification plot crosses the threshold is the Ct value.

4.1.3.2 Current uses of QPCR

4.1.3.2.1 Diagnostics

The accuracy and sensitivity of QPCR means it is often used as the 'gold standard' in the diagnosis of numerous infectious diseases. Using this technique an accurate and rapid diagnosis can be made and the lack of inter-assay variability, means results are reliable and reproducible (Bustin and Mueller, 2005). QPCR is frequently used to demonstrate the presence of viral nucleic acid within clinical samples. One example where QPCR is especially useful is in the diagnosis of HIV in babies born to infected mothers. Babies carry maternal antibodies for up to 15 months, therefore traditional antibody tests are not able to reliably determine the infection status of these children. QPCR assays allow the infection status of the children to be accurately determined and the viral load quantified (Fearon, 2005). The infection status of immunocompromised individuals, who do not mount an antibody response, can also be accurately determined by QPCR. Other infectious diseases, in which QPCR is frequently used to aid diagnosis include; *Toxoplasma gondii* (Lin, Chen, Kuo, Tseng *et al.*, 2001), Leishmania (Nicolas, Prina, Lang and Milon, 2002), West Nile virus (Tang, Hapip, Liu and Fang, 2006) and *Plasmodium falciparum* (Hermsen, Telgt, Linders, van de Locht *et al.*, 2001).

4.1.3.2.2 Assessing efficacy of chemotherapy

Quantitative PCR (QPCR) has been used to measure the rate of clearance of *Plasmodium spp* from the peripheral circulation following anti-malarial chemotherapy (Beshir, Hallett, Eziefula, Bailey *et al.*, 2010). Primers and a double-labelled fluorescent probe were designed to the Plasmodium tRNA methionine (PgMET) gene. This gene is present as a single copy in the species *P. vivax*, *P. falciparum*, *P. ovale. curtisi*, *P. ovale. wallikeri*, *P. malariae* and *P. knowlesi*. Blood samples were collected from malaria patients upon hospital admission and every 24 hours thereafter until parasites had been cleared from the peripheral circulation. DNA was extracted from the samples and the parasite density quantified by QPCR (Beshir *et al.,* 2010). Using this technique a decrease in parasite density was detected daily, in each sample as treatment took effect. The rates of parasite clearance obtained by QPCR were comparable to those obtained by microscopic examination of blood smears. Furthermore, QPCR proved to be more sensitive than the microscopic method, with limits of detection determined to be 5 and 50 parasites/µl of blood respectively (Beshir *et al.,* 2010). This study demonstrates that QPCR is a reliable and sensitive method for determining the rate of parasite clearance following chemotherapy.

4.1.4 Melarsoprol resistance

Treatment failures following melarsoprol chemotherapy have long been reported. In 1994, Pepin *et al.* reported a relapse rate of 6.2% in patients infected with *T. b. gambiense* following melarsoprol chemotherapy (Pepin, Milord, Khonde, Niyonsenga *et al.*, 1994). The relapse rate remained fairly constant until recently when drastic increases in the failure rate of melarsoprol were reported. Legros *et al.* reported a failure rate of 30.4% in patients with CNS stage *T. b. gambiense* in the Arua district of northern Uganda (Legros *et al.*, 1999). High treatment failure rates of 25% were also reported in Zaire by the Angolan National Institute for Combat and Control of trypanosomiasis (ICCT) (Burri and Keiser, 2001). The reasons for the sudden increase in the treatment failure rates observed following melarsoprol chemotherapy are currently unknown. Inter-patient and population variability in the pharmacokinetics of the compound, resulting in insufficient drug levels being obtained has been proposed

as a possible reason behind the increased failure rates (Burri and Keiser, 2001). The pharmacokinetics of melarsoprol in successfully treated and relapse patients was recently investigated (Burri and Keiser, 2001). No difference was observed in the pharmacological parameters measured between successfully treated patients and patients who relapsed, indicating that other mechanisms may lie behind the high treatment failure rates recently observed. As inter-patient variability was ruled out as a possible reason for the increased failure rates observed following melarsoprol chemotherapy, it was suggested that alterations within the parasite may be responsible (Brun, Schumacher, Schmid, Kunz *et al.*, 2001). The high treatment failure rates observed following melarsoprol chemotherapy mean that an alternative drug for the treatment of CNS-stage trypanosome infections is desperately needed.

Nifurtimox and eflornithine combination therapy (NECT) has recently been approved as a first line therapy for treatment of CNS stage *T. b. gambiense* infections. The treatment is gradually being distributed to the countries where *T. b. gambiense* is endemic, thereby solving the problem of melarsoprol resistance in *T. b. gambiense* infections (World Health Organisation, 2009). However, NECT therapy has not been assessed in patients with CNS stage *T. b. rhodesiense* infections, therefore melarsoprol remains as the first line drug (Priotto *et al.,* 2009). Melarsoprol refractory *T. b. rhodesiense* infections are treated with a combination of melarsoprol and the 5-nitrofuran nifurtimox (World Health Organisation, 1998). Adverse reactions following nifurtimox therapy are common and there is no standard treatment regime (Burri, Stich and Brun, 2004). There is therefore an urgent need for a trypanocide which is effective in melarsoprol resistant *T. b. rhodesiense* infections.

In this chapter we will attempt to use in-situ hybridization to determine the location of trypanosomes within the brain prior to mel/HPβCD and mel/RAMβCD chemotherapy. Furthermore, the rate of trypanosome clearance following complexed melarsoprol chemotherapy will be determined *in-vivo* in a melarsoprol sensitive *T. b. brucei* stabilate (GVR35/C1.9) as well as a *T. b. brucei* strain (GVR35/M14) demonstrating resistance to melarsoprol chemotherapy.

4.2 Methods

4.2.1 Melarsoprol resistant (GVR35/M14) T. b. brucei strain

The melarsoprol resistant *T. b. brucei* strain (GVR35/M14) was adapted specifically for this study to assess the activity of the melarsoprol cyclodextrin complexes mel/HPβCD and mel/RAMβCD against melarsoprol resistant *T. b. brucei* trypanosomes. The strain was originally developed from the melarsoprol sensitive GVR35 *T. b. brucei* strain by serial passage in mice subject to increasing doses of topical melarsoprol. The working stabilate GVR35/M14 is resistant to 9μM of melarsoprol.

4.2.2 Establishing infection with GVR35/M14

The working stabilate GVR35/M14 was initially passaged in a donor animal in order to obtain the number of trypanosomes required to inoculate large batches of experimental animals. A small section of the frozen GVR35/M14 stabilate was removed and diluted in phosphate glucose buffered saline (PGBS) pH 8 until a suspension containing 2 trypanosomes per field when viewed by light microscope at a magnification of 400 was obtained. This equates to approximately $2x10^4$ trypanosomes/0.1ml. A 0.2ml aliquot of the suspension was injected intraperitoneally into a female CD-1 mouse. The development of the parasitaemia in the animal was monitored by examination of a wet blood film prepared from tail blood as detailed in chapter 2. When the first parasitaemic peak was reached the animal was euthanised by exposure to increasing concentrations of carbon dioxide and exsanguinated by cardiac puncture. The blood was diluted in PBSG pH 8 as described above. A 0.1ml aliquot of the trypanosome suspension was then inoculated intraperitoneally into female CD-1 mice approximately 6 to 8 weeks in age and weighing 25 to 30 grams, in order to establish infection in the experimental animals.

4.2.3 Establishing infection with GVR35/C1.9

Female CD-1 mice, approximately 6 to 8 weeks in age and weighing 25 to 30 grams were injected intraperitoneally with $2x10^4$ *T. b. brucei* trypanosomes from

stabilate GVR35/C1.9. The full details regarding the preparation of the trypanosomes from the stabilate for inoculation are provided in chapter 2.

4.2.4 Confirmation of trypanosome infection

To confirm that the infection was successfully established in mice following inoculation of the stabilates GVR35/C1.9 and GVR35/M14 a wet blood film prepared from tail blood of each animal was examined under the microscope for the presence of trypanosomes. The level of parasitaemia observed in each animal was scored according to the system detailed in chapter 2.

4.2.5 Preparation of melarsoprol cyclodextrin complexes

The melarsoprol cyclodextrin complexes are supplied as fine white powders with the ratio of melarsoprol to cyclodextrin specified for each batch. Using the ratio, the amount of each complex required to give a melarsoprol concentration of 0.05mmol/kg was calculated. The corresponding amount of complex was weighed out on a fine balance and dissolved in sterile water. The solutions of each complex were freshly prepared each day immediately prior to administration. The full details of how the dose was calculated for each melarsoprol cyclodextrin complex are provided in chapter 2.

4.2.6 Administration of complexes

Prior to administration of the complexes each animal was weighed and the volume of complex to be administered determined using the table provided in chapter 2. To administer the melarsoprol cyclodextrin complexes the animals were appropriately restrained and a 20 gauge x 25mm gavage needle inserted directly into the oesophagus. The compounds were subsequently administered slowly and carefully directly into the stomach.

4.2.7 In-situ hybridization

4.2.7.1 Treatment schedule

Mel/HPβCD or mel/RAMβCD was administered at a dose of 0.05mmol/kg (melarsoprol concentration) once per day, for seven consecutive days, commencing on day 21 post-infection when a CNS stage infection is established in the animals. Immediately prior to chemotherapy commencing, six animals were sacrificed and served as untreated controls. Six further animals were sacrificed from each treatment group 24 hours and 7 days after completion of the treatment regimes (Figure 4-3).

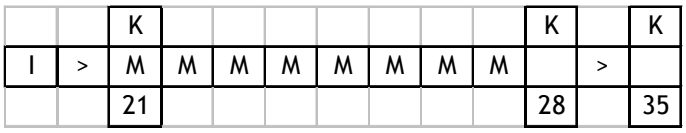

Figure 4-3: The treatment schedule used
Mel/HPβCD or mel/RAMβCD (M) was administered orally from day 21 post-infection, daily, for 7 consecutive days. Immediately prior to chemotherapy commencing on day 21 post-infection, 6 animals were sacrificed (K). Six further animals from each treatment group were sacrificed 24 hours and 7 days after the completion of the chemotherapy regime.

4.2.7.2 Collection of samples

Animals were sacrificed by CO_2 asphyxiation. The brain was carefully excised from the skull and placed into 4% neutral buffered formalin.

4.2.7.3 Preparation of samples for in-situ hybridization

The brain samples were removed from the neutral buffered formalin and processed to paraffin blocks. From the paraffin blocks 10µm thick sections were cut and placed onto 3-aminopropyltriethoxysilane (APES) coated slides. APES helps adhere the tissue sections to the slides thereby minimising tissue lost during the in-situ hybridization procedure (Maddox and Jenkins, 1987).

4.2.7.4 In-situ hybridization procedure

4.2.7.4.1 Oligonucleotide probe

Oligonucleotide probes are short nucleotide sequences, usually between 10 and 50 base pairs (bp) in length, which can be designed to a specific sequence (Leitch, Schwarzacher, Jackson and Leitch, 1994). They are often favoured over RNA and DNA probes in in-situ hybridization, as they are easily synthesised commercially, to a high specification, and purity, and various chromogenic labels can be incorporated. Two oligonucleotide probes were used in the in-situ hybridization protocol in this study (Table 4-1). The first PFR2, was designed to a region of the PFR2 gene encoding a 69 KDa paraflagella rod protein (Deflorin, Rudolf and Seebeck, 1994). A second probe was designed to a 177 bp repeat region present in the satellite DNA of *T. b. brucei* (Sloof, Bos, Konings, Menke *et al.*, 1983). A digoxigenin label was included at the 5' end of both probes to allow localisation of the probes within the tissue sections following the in-situ hybridization procedure. The probes were commercially synthesised by Eurofins MWG Operon.

Probe	Sequence
PFR 2	$_{2603}$cttgtcttctccttttttgtctctttccccct$_{2634}$
177 bp	$_{132}$gcaagtttgcaacgctgttctttagtg$_{158}$

Table 4-1: The sequence data for the oligonucleotide probes used in the in-situ hybridization procedure

4.2.7.4.2 Dewaxing and rehydration of the tissue sections

The paraffin embedded sections were dewaxed in 3 changes of histoclear for 5 minutes each. In order to rehydrate the sections, slides were passed through graded ethanol for 5 minutes at each concentration beginning with 100%, progressing on to 90% and finishing at 70%. Finally the slides were rinsed in RNase/DNase free water. To reduce non-specific probe hybridization with non-target sequences the sections were incubated in 0.2N HCl for 20 minutes. Residual HCl was removed from the sections by rinsing the sections in two changes of PBS for 5 minutes each time.

4.2.7.4.3 Permeabilisation of the tissue sections

To allow the probe to penetrate the tissue sections and reach the target sequence, the tissue must be permeabilised by exposure to proteases. The proteases digest the proteins that surround the target nucleic acid, thus making it more accessible to the probe (Leitch *et al.*, 1994). Permeabilisation of the tissue must be optimised as over digestion can lead to the target sequence and tissue morphology being lost, while under digestion can result in the probe being unable to access the target sequence. Permeabilisation of the brain sections was optimised by digesting the sections in varying concentrations of Proteinase K or pepsin (Table 4-2). The incubation temperature and length of incubation were also varied in order to determine the optimum digestion conditions. At the end of the digestion period, the proteases were deactivated, by rinsing the slides in either PBS buffer containing 2mg/ml glycine for 5 minutes for tissue sections incubated with Proteinase K or in 0.1M Tris-HCl, 0.15M NaCl (pH 7.5) for 3 minutes, for tissue sections incubated with pepsin. Finally slides were rinsed in PBS for 5 minutes.

<table>
<tr><th>Proteinase</th><th>Concentration</th><th>Incubation time</th><th>Incubation temperature</th></tr>
<tr><td rowspan="13">Proteinase K</td><td>0.125 µg/ml</td><td rowspan="2">5 minutes
7 minutes
10 minutes
15 minutes</td><td rowspan="11">37 °C</td></tr>
<tr><td>0.25 µg/ml</td></tr>
<tr><td>0.5 µg/ml</td><td rowspan="9">15 minutes</td></tr>
<tr><td>0.1 µg/ml</td></tr>
<tr><td>2 µg/ml</td></tr>
<tr><td>5 µg/ml</td></tr>
<tr><td>10 µg/ml</td></tr>
<tr><td>1 mg/ml</td></tr>
<tr><td>3 mg/ml</td></tr>
<tr><td>5 mg/ml</td></tr>
<tr><td>25 µg/ml</td><td>15 minutes</td><td rowspan="3">Room temperature</td></tr>
<tr><td>50 µg/ml</td><td rowspan="2">30 minutes</td></tr>
<tr><td>100 µg/ml</td></tr>
<tr><td rowspan="3">Pepsin</td><td>2 mg/ml</td><td rowspan="3">30 minutes</td><td rowspan="3">Room temperature</td></tr>
<tr><td>2.5 mg/ml</td></tr>
<tr><td>3 mg/ml</td></tr>
</table>

Table 4-2: The combination of enzyme concentrations, incubation times and temperatures used to identify the optimal degree of digestion for the tissue sections.

4.2.7.4.4 Fixation of tissue sections

The conditions endured by the tissue sections during the in-situ hybridization process are harsh, as a result tissue morphology can be lost during the procedure. In order to prevent the loss of tissue morphology and target sequence a fixative can be applied to the tissue sections. In this study the tissue sections were fixed with 4% paraformaldehyde for 5 minutes. Paraformaldehyde cross-links proteins within the tissue section thereby stabilising the section. However, care must be taken not to over expose the sections to the fixative, as this can decrease the permeability of the sections and prevent the probe accessing the target sequence.

4.2.7.4.5 Denaturation of the target sequence

The target sequence in this study was double stranded DNA therefore in order for the hybridization probe to be able to anneal to the sequence, the two strands of nucleic acid must be separated. Denaturation of the target sequence can be achieved by alkalis or heat. In this protocol denaturation of the target sequence was carried out at 90°C for 10 minutes by placing the slides on a hot plate. In order to prevent the tissue sections drying out during the denaturation process, the slides were covered in hybridization buffer consisting of 6 x SSC and 50% dextran sulphate.

4.2.7.4.6 Hybridization

During the hydridization step the probe anneals to the target sequence. The hybridization temperature for DNA:DNA hybrids is 37°C (Leitch *et al.*, 1994). Hybridization was carried out by placing the slides in a hybridization buffer consisting of 6 x SSC and 50% dextran sulphate and 2µg/ml of the oligonucleotide probe for 18 to 24 hours at 37°C in a humidified chamber.

4.2.7.4.7 Post-hydridization washes

In order to remove excess and weakly bound probe the slides were subject to a series of post-hybridization washes. During the post-hybridization washes, probe that is annealed to non-target molecules is removed, while the probe that is

annealed to the target sequence is maintained. A certain degree of mismatch will be present between the target sequence and probe. The degree of mismatch which is acceptable in the reaction is referred to as 'stringency'. Stringency can be controlled by adjusting the salt concentration of the post-hybridization washes. In high stringency conditions (low salt concentrations) only probes with a high degree of homology to the target sequence will form stable hybrids and be retained. In low stringency conditions (high salt concentrations) probes binding to sequences with only 70-90% homology to the target sequence will be retained, thus in low stringency conditions non-specific hybridization signals may be obtained. The degree of stringency which is acceptable for the reaction must be determined. In this protocol high-stringency post-hybridization washes were used. Slides were rinsed in 2 x SSC for 5 minutes at 37°C, followed by rinsing in 100mM Tris-HCl/150mM NaCl pH 7.4 (TBS) for 5 minutes.

4.2.7.4.8 Visualisation

The oligonucleotide probe contains a digoxigenin label therefore an anti-digoxigenin antibody labelled with alkaline phosphatase (fab fragments from sheep) was used as the primary antibody. The antibody was diluted 1:500 in a buffer containing TBS, 2% normal sheep serum (NSHS) and 0.3% Triton-X. The tissue sections were initially incubated in the buffer without the primary antibody for 30 minutes to prevent non-specific background staining. The buffer was subsequently removed from the tissue sections and replaced with the buffer containing the primary antibody. The tissue sections were incubated with the primary antibody for 2 hours in a humidified chamber at room temperature. Following incubation, unbound antibody was removed by rinsing the tissue sections in two changes of TBS for 20 minutes each time. Finally, the slides were washed in 100mM Tris pH 8.2-8.5 for 5 minutes.

A Vector© Red Alkaline Phosphatase Substrate Kit was used to visualise the primary antibody according to the manufactures instructions. Briefly a working solution of the substrate was prepared by adding 2 drops of reagent 1 to 5 ml of 100mM Tris-HCl pH 8.2-8.5 and mixing well. Two drops of reagent 2 were then added, the solution was mixed again and then 2 drops of reagent 3 added. To inhibit endogenous alkaline phosphatase activity, 5 drops of levamisol were added to the working solution. The tissue sections were incubated with the

substrate for 30 minutes at room temperature in a humidified chamber. As the substrate is light sensitive, the sections were developed in the dark. Excess substrate was removed by rinsing the tissue sections in 100mM Tris-HCl pH 8.2-8.5 for 5 minutes. Finally the tissue sections were rinsed in water, counter-stained with haematoxylin, dehydrated through a graded alcohol series, cleared in histoclear and permanently mounted using histomount.

4.2.7.4.9 Tyramide signal amplification system (TSA™ PerkinElmer)

To maximise the chance of visualising the location of the bound probe a Tyramide signal amplification (TSA™, PerkinElmer) system was used. The TSA system uses horse-radish peroxidise (HRP) to catalyse the deposition of biotin-labelled tyramide immediately adjacent to the immobilised HRP enzyme. The deposited tyramide is indirectly visualised by chromogenic techniques with a significant enhancement of the signal. The in-situ hybridization protocol detailed above was followed exactly up to the post-hybridization washing step, where the sections were rinsed in 2 x SSC for 5 minutes at 37°C. Following the post-hybridization washes, the TSA kit was introduced. Sections were incubated in TNB buffer (supplied with kit) for 30 minutes at room temperature. As the kit utilises HRP to catalyse the deposition of biotin-labelled tyramide, HRP had to be introduced into the sections. This was achieved by incubating the sections with a IgG monoclonal mouse anti-HRP-digoxigenin antibody at a dilution of 1:100 for 30 minutes at room temperature. As the oligonucleotide probe contains a digoxigenin label the antibody will bind to the probe present within the tissue sections forming a probe-antibody complex. Excess, unbound antibody was removed by rinsing the sections in 3 changes of TNT buffer for 5 minutes each time. The tissue sections were then incubated with the TSA biotin system for 10 minutes at room temperature in a humidified chamber. Following incubation the TSA biotin system was removed from the sections by washing in 3 changes of TNT buffer for 5 minutes each time.

A chromogenic method was used to visualise the deposited HRP. The sections were incubated with a streptavidin-HRP antibody (supplied with the TSA™ kit) diluted 1:100 in TNB buffer for 30 minutes in a humidified chamber at room temperature. Excess unbound antibody was removed by washing the sections in 3 changes of TNT buffer with each wash lasting 5 minutes. The deposited HRP was

visualised with a 3, 3'-diaminobenzidine (DAB) substrate kit according to the manufactures instructions. Briefly 2 drops of buffer stock solution were added to 5ml of distilled water and mixed well. Four drops of DAB stock solution were added and the solution mixed well. Finally 2 drops of hydrogen peroxide solution were added and the solution mixed again. Tissue sections were incubated with the substrate for 10 minutes at room temperature in a humidified chamber. Excess DAB substrate was removed by rinsing the tissue sections in water. The tissue sections were subsequently counter-stained with haematoxylin, dehydrated through a graded ethanol series, cleared in histoclear and permanently mounted using histomount.

4.2.8 Quantitative PCR

4.2.8.1 Treatment schedule

Mel/HPβCD or mel/RAMβCD was administered orally at a dose of 0.05mmol/kg (melarsoprol concentration) once per day for seven consecutive days, commencing on day 21 post-infection when a CNS infection is established in the animals. Immediately prior to chemotherapy commencing six animals were sacrificed and served as untreated controls. Twenty-four hours after the administration of each dose, six animals infected with GVR35/C1.9, the melarsoprol sensitive strain, and six animals infected with GVR35/M14, the melarsoprol resistant strain, were sacrificed from each treatment group. In addition, a further group from each parasite strain and treatment regime were sacrificed one week after completion of chemotherapy (Figure 4-4).

			K	K	K	K	K	K	K		K
I	>	M	M	M	M	M	M	M		>	
		21	22	23	24	25	26	27	28		35

Figure 4-4: The chemotherapy regime used in the quantitative PCR (QPCR) experiment
Female CD-1 mice were infected with $2x10^4$ *T. b. brucei* trypanosomes (I) from either the melarsoprol sensitive stabilate GVR35/C1.9 or the melarsoprol resistant stabilate GVR35/M14. On day 21 post-infection, when trypanosomes are known to be established within the CNS, chemotherapy (M) commenced. Animals were administered either mel/HPβCD or mel/RAMβCD orally, at a dose of 0.05 mmol/kg, daily, for seven consecutive days. Twenty-four hours after the administration of each dose six animals from each group were sacrificed (K). Animals were also sacrificed one week after completion of chemotherapy.

4.2.8.2 Collection of samples

Animals were sacrificed by CO_2 asphyxiation and the blood removed by cardiac puncture. Immediately following exsanguination the chest cavity of the animal was opened and the animal perfused through the left ventricle with 120ml of sterile normal saline. Following perfusion the brain was carefully excised from the skull and immediately snap frozen on solid CO_2 before being stored at -70°C. QPCR is an extremely sensitive technique therefore to prevent cross contamination occurring between samples a number of preventive measures were taken during sample collection. Prior to each animal being sacrificed all surfaces and instruments were thoroughly cleaned with hibiscrub and sprayed with RNase AWAY® solution in order to remove all traces of nucleic acid. Gloves and needles were also changed after the collection of each sample.

4.2.8.3 DNA extraction

DNA was extracted from the brain tissues using a Qiagen DNeasy® blood and tissue kit. The method provided with the kit was modified to suit our use. Before analysis the brain tissues were removed from the freezer and allowed to defrost at room temperature. Once thawed the brain was finely chopped with a sterile scalpel blade and placed in a 5ml bijoux. 3.6ml of ATL buffer was added to the tissue together with 400µl of 20mg/ml Proteinase K in order to lyse the tissue. The sample was vortexed for 10 seconds before being incubated in a 55°C water bath for 3 hours and 15 minutes with agitation every 30 minutes by vortexing. Thirty minutes before the end of the incubation period the sample was removed from the water bath and homogenised through a 20 gauge needle and then returned to the water bath to complete the digestion. After incubation, the sample was removed from the water bath and a 200µl aliquot transferred to a 1.5ml eppendorf tube. 200µl of AL buffer were added to the sample and mixed thoroughly by vortexing. 200µl of analytical grade ethanol were then added to the sample and mixed thoroughly again by vortexing. The sample was then transferred to a DNeasy mini-prep column. The column was centrifuged at 8,000rpm for one minute, the flow through discarded and the column placed in a new 2ml collection tube. 500µl of buffer AW1 were added to the column and the column centrifuged again at 8,000rpm for one minute. The flow through was

once again discarded, the column placed in a new 2ml collection tube and 500µl of buffer AW2 added to the column. The column was centrifuged at 14,000rpm for 3 minutes in order to dry the column. The flow through was once again discarded and the column placed in a new 2ml collection tube. 200µl of elution buffer (AE) were then added to the column and allowed to stand at room temperature for one minute before centrifugation at 8,000rpm for one minute to elute the DNA. The eluate containing the DNA was collected and the column placed in a new 2ml collection tube. The elution process was repeated to obtain the maximum quantity of DNA.

4.2.8.4 Quantification of DNA

The concentration of the DNA extracted from the brain samples was assessed by measuring the optical density of a 1:10 dilution of the original sample. This was prepared by adding 10µl of the DNA sample to 90µl of the elution buffer (AE) supplied with the Qiagen kit. The sample was placed in a disposable UV compatible plastic microcuvette and the optical density assessed. The spectrophotometer was zeroed using AE buffer as a blank. The optical density of the sample was then measured at wavelengths of 230 (OD_{230}), 260 (OD_{260}), 280 (OD_{280}) and 320nm (OD_{320}). The purity of the DNA sample was evaluated by calculating the OD_{260}/OD_{280} ratio. Pure DNA yields a ratio of 1.8 therefore a ratio of 1.6 or higher was considered to be acceptable purity for further analysis. Finally a 20µg/µl DNA solution was prepared by diluting the original sample in the appropriate volume of AE buffer.

4.2.8.5 Identification of gene of interest

To detect the presence of trypanosomes in samples by QPCR, a target gene needs to be identified which is highly conserved and which bares no significant sequence homology to any murine genes. Furthermore, to prevent the generation of false positive results, the gene must not persist in tissues once trypanosomes have been eliminated. In *T. b. brucei* the paraflagellar rod (PFR) is composed of two closely related proteins of 69 and 73 kDa (Deflorin, Rudolf and Seebeck, 1994). The 69 kDa protein, PFR-A is encoded by a locus containing four tandomly arranged identical genes (Deflorin, Rudolf and Seebeck, 1994). Sequence analysis revealed the presence of two closely linked and tandomly

repeated open reading frames (PFR-A and PFR-B) 800 base pairs (bp) in length and of identical nucleotide sequence. Outwith the open reading frames there is little sequence homology. The second 73 kDa protein comprising the PFR in *T. b. brucei* is encoded by a separate gene locus termed PFR C/D. The locus consists of four tandomly arranged very similar or identical genes (Deflorin, Rudolf and Seebeck, 1994). The gene product of the locus, protein PFR-C shares only a 62% amino acid sequence homology with the PFR-A protein.

Primers and a probe (Table 4-3) were designed to a section of the gene encoding the PFR-A protein outside of the open reading frames by Prof Dennis Grab, Johns Hopkins University (personal communication) and were synthesised by Eurofins MWG Operon. The probe was labelled with the reporter FAM at the 5' prime end and the quencher TAMRA at the 3' prime end.

Gene	Primers	Probe
PFR2	FW - $_{2564}$ccaaccgtgtgtttcctcct$_{2583}$ RV - $_{2636}$gaaaaggtgtcaaactactgccg$_{2658}$	$_{2603}$cttgtcttctccttttttgtctctttcccccct$_{2634}$

Table 4-3: Sequence data for the primers and probe used to identify *T. b. brucei* by QPCR analysis.

4.2.8.6 Generation of a plasmid containing the PFR2 gene

A 95bp section (2564 to 2658) of the PFR2 sequence (X14819) matching the regions spanned by the primers and probe was cloned via TOPO-TA into a pCR2.1 plasmid. This plasmid was commercially synthesised by Eurofins MWG operon.

4.2.8.7 Resuspension of plasmids

The commercially prepared, lyophilised plasmid, containing the PFR2 gene fragment, was resuspended in 10mM Tris pH 8.0, to give a plasmid concentration of 50ng/µl. Following resuspension the plasmid was stored at -80ºC.

4.2.8.8 Transformation of cells with PFR2 plasmid

DH5α competent cells were transformed according to the manufacturer's instructions.

The DH5α competent cells were removed from storage at -80ºC and allowed to thaw in wet ice. Upon thawing a 50µl aliquot of the cells was taken and placed in a 0.5ml DNA/RNA free eppendorf. 5µl of the 50ng/µl plasmid suspension were added and incubated on wet ice for 30 minutes. Following incubation the cells were subject to heatshock in a water bath at 42ºC for 30 seconds before being returned to wet ice for a further two minute incubation period. Subsequently, 950µl of LB broth were added to the cells before incubating for 1 hour at 37ºC. The culture was then removed and 100µl evenly spread over an LB/agar plate supplemented with 100µg/ml ampicillin and 50µg/ml kanamycin. The plate was incubated overnight at 37ºC.

The following day 5µl of ampicillin (100mg/ml) and 5µl of kanamycin (50mg/ml) were added to 5ml of LB broth to give final concentrations of 100µg/ml and 50µg/ml respectively. Using a sterile pick one colony was removed from the LB/agar plate and placed into the culture medium. The culture was mixed by gentle inversion before being incubated at 37ºC in an orbital incubator overnight.

4.2.8.9 Purification of the plasmid

Following growth of the transformed cells, the PFR2 plasmid was extracted using a High Pure Plasmid Isolation kit according to the manufacturer's instructions.

The culture was centrifuged at 3,000rpm for 5 minutes. The supernatant was removed and the cells resuspended in 250µl of suspension buffer. After gentle mixing, the suspension was incubated at room temperature for 5 minutes before being transferred to a 1.5ml eppendorf tube. 250µl of lysis buffer were added and the suspension gently mixed and incubated at room temperature for 5 minutes. Following incubation, 350µl of binding buffer were added, the solution carefully mixed and incubated on wet ice for a further 5 minutes. The suspension was centrifuged at 13,000rpm at 4ºC for 10 minutes. The supernatant

was carefully decanted and placed into a high pure filter column and the pellet discarded. The column was centrifuged at 13,000rpm at 4ºC for 1 minute and the flow through was discarded. 700µl of wash buffer II were then added and the column centrifuged at 13,000rpm for 1 minute. The flow through was once again discarded and the column membrane dried by centrifugation at 13,000rpm at 4ºC for 1 minute. The column was then placed in a 1.5ml eppendorf tube and 100µl elution buffer added directly to the membrane. After incubation for 1 minute at room temperature the column was centrifuged at 13,000rpm at 4ºC for 1 minute. The eluate was collected and the purified plasmid DNA quantified.

4.2.8.10 Quantification of purified plasmid DNA

The concentration of plasmid DNA in the eluate was assessed by measuring the optical density of a 1:50 dilution of the eluate. This was prepared by adding 20µl of the purified plasmid DNA to 980µl of sterile DNA/RNase free water. A 100µl aliquot of the dilution was placed in a plastic UV compatible disposable microcuvette and the optical density assessed as described previously.

4.2.8.11 Calculation of the plasmid copy number contained within the purified plasmid DNA

The number of copies of the plasmid and hence the number of copies of the PFR2 gene fragment within the purified plasmid DNA was calculated using an on-line calculator for determining the number of copies of a template (http://www.uri.edu/research/gsc/resources/cndna.html). The calculator uses Avogadro's number (6.022×10^{23}), the template length and the amount of template present in the sample in nano grams to calculate the number of copies of the template present within a sample (Equation 4-2). The total length of the plasmid containing the PFR2 gene fragment insert is 3995 base pairs and the amount of template present within the sample was determined by spectrophotometer analysis as discussed previously. These two values were entered into the calculator and the number of copies of the PFR2 gene fragment present within the sample calculated. The amount of DNA required to give 10^{10} copies of the PFR2 gene fragment was calculated and the purified plasmid DNA was diluted in 10mM Tris-HCl pH 8.5 (supplied with the High Pure Plasmid Isolation kit) to give 10^{10} copies of the PFR2 gene fragment in 5µl.

$$\text{Number of copies} = \frac{(\text{amount of template (ng)} \times 6.022 \times 10^{23})}{(\text{length of template (bp)} \times 650 \times 1 \times 10^{9})}$$

Equation 4-2: The equation used in order to calculate the number of copies of the PFR2 gene fragment present within the sample of purified DNA
The amount of template present (ng) within the sample is initially multiplied by Avogardro's number (6.022×10^{23}) to obtain the number of molecules of the template per gram. This number is then divided by the length of the template (bp), to obtain the number of copies of the template within the sample. The calculator assumes that one mole of a base pair weighs 650g, therefore to calculate the length of the template in nano grams, the length of the template in base pairs is multiplied by 650 and then 1×10^{9}.

4.2.8.12 Preparation of standard dilutions for the standard curve

The standard containing 10^{10}copies/5µl of the PFR2 gene was serially diluted with sterile DNase/RNase free water to give dilutions ranging from 10^{10} PFR2 copies/5µl down to 10^{1} copies/5µl. The range of dilutions used to construct the standard curve was 10^{5}, 10^{4}, 10^{3}, 10^{2} and 10^{1} copies/5µl. All standard dilutions were stored at -20 ºC until use.

4.2.8.13 Preparation of primers and probe

Stock solutions of primers and probes were diluted to 100pmol/µl in sterile DNase/RNase free water. Prior to use the stock solutions were further diluted in sterile DNase/RNase free water to give working concentrations of 10pmol/µl. All primers and probes were stored at -20ºC.

4.2.8.14 QPCR reaction

The number of copies of the PFR2 gene present in the brain following chemotherapy with complexed melarsoprol was quantified in each sample. The QPCR reaction consisted of 12.5µl Taqman Brilliant II master mix, 0.05pmol/µl (final concentration) of each primer, 0.1pmol/µl of the probe (final concentration), 5µl (100ng) of the template DNA and sterile DNase/RNase free water to make a final reaction volume of 25µl. Each sample was analysed in duplicate.

The QPCR reaction was performed in an Agilent MxPro 3005 thermocycler. After an initial denaturation step at 95°C for 10 minutes, the PCR cycles commenced.

The samples were denatured at 95°C for 15 seconds before the temperature was reduced to 60°C for 1 minute for annealing to occur before being raised to 72°C for 0.01 second for extension to take place. Fluorescence data was captured at the end of the extension phase in each cycle. The reaction consisted of 45 cycles.

4.2.8.15 Statistical analysis

All data was graphed in the software Graph Pad Prism version 5. Data were analysed using analysis of variance methods, in particular the General Linear Model procedure in Minitab 16. This provided a method for investigating significant main effect differences and interactions between factors such as time, drug and strain. As the data represented counts the [log(x+1)] transformation was applied prior to analysis to adjust for any zero counts. Significance was measured using the p-value of 5% significance level. Effect sizes were further investigated using 95% confidence intervals for the differences between means.

4.3 Results

4.3.1 In-situ hybridization

In-situ hybridization was used to visualise the location of *T. b. brucei* within paraffin embedded brain sections prior to, 24 hours and 7 days after completion of mel/HPβCD and mel/RAMβCD chemotherapy. Unfortunately despite attempts to optimise the in-situ hybridization reaction, no positive staining was observed.

4.3.2 QPCR

QPCR was used to assess the effect of mel/HPβCD and mel/RAMβCD chemotherapy on CNS parasite load, in a melarsoprol sensitive (GVR35/C1.9) and melarsoprol resistant (GVR35/M14) *T. b. brucei* strain. The parasite load within the CNS was quantified by measuring the number of copies of the PFR2 gene present within 100ng of DNA prepared from a sample containing approximately 25mg brain homogenate taken from a homogenate of the whole brain. There is only one copy of the PFR2 gene target sequence within the *T. b. brucei* genome therefore one copy of the gene is equivalent to one trypanosome (Deflorin, Rudolf and Seebeck, 1994).

4.3.2.1 *T. b. brucei* melarsoprol sensitive strain (GVR 35/C1.9)

4.3.2.1.1 The effect of mel/HPβCD treatment on CNS parasite load

Administration of the melarsoprol cyclodextrin complex mel/HPβCD results in a rapid reduction in the number of trypanosomes present within the brain (Figure 4-5, panel A). Immediately prior to treatment commencing on day 21 post-infection, high copy numbers of the PFR2 gene were present in the brain (mean 626 ± 82.8). Twenty-four hours after administration of the first dose of the complex a significant reduction ($P < 0.0001$) in the number of copies (68.1 ± 14.7) of the PFR2 gene was detected. This reduction continued after administration of a second dose of mel/HPβCD. The number of copies of the PFR2 gene detected in the brain after administration of the second dose was 13.13 ± 2.54, representing an 80.8% reduction compared to the numbers

detected after the first dose (P = 0.022). Administration of a third dose, resulted in a further decrease in the PFR2 copy number within the brain (4.32 ± 2.51) compared to 24 hours after the second dose (P = 0.023). By 24 hours after administration of the fourth dose, no copies of the PFR2 gene were detected within the brain. Summary statistics are given in Table 4-4.

4.3.2.1.2 The effect of mel/RAMβCD treatment on CNS parasite load

Immediately prior to chemotherapy commencing on day 21 post-infection, high copy numbers of the PFR2 gene were detected within the brain (626 ± 83) (Figure 4-5, panel B). Administration of one dose of mel/RAMβCD results in a rapid reduction in the number of copies of the PFR2 gene within the brain (66.2 ± 10.8, P < 0.0001). This reduction continued with the administration of a second dose of mel/RAMβCD (P = 0.0134). Twenty-four hours after the administration of a second dose, 10.61 ± 3.09 copies of the PFR2 gene were detected within the brain. This is a reduction of 84% compared to the numbers detected after administration of the first dose. The number of copies of the gene detected after administration of a third dose (6.13 ± 4.70) of the complex was significantly lower (P = 0.0001) than the number detected after the first dose of the complex. However, the number of copies of the gene detected after administration of the third dose of the complex was not significantly different to the number detected after the second dose (P = 0.1363). Administration of a fourth dose of mel/RAMβCD resulted in a significant reduction (P = 0.0173) in the number of copies of the PFR2 gene within the brain (1.27 ± 1.27), compared to the numbers detected after administration of the second dose. The number of copies of the gene detected after administration of the fourth and third doses of the complex were not significantly different from each other (P = 0.7409). By 24 hours after administration of the fifth dose, no copies of the PFR2 gene were detected. Summary statistics are detailed in Table 4-5.

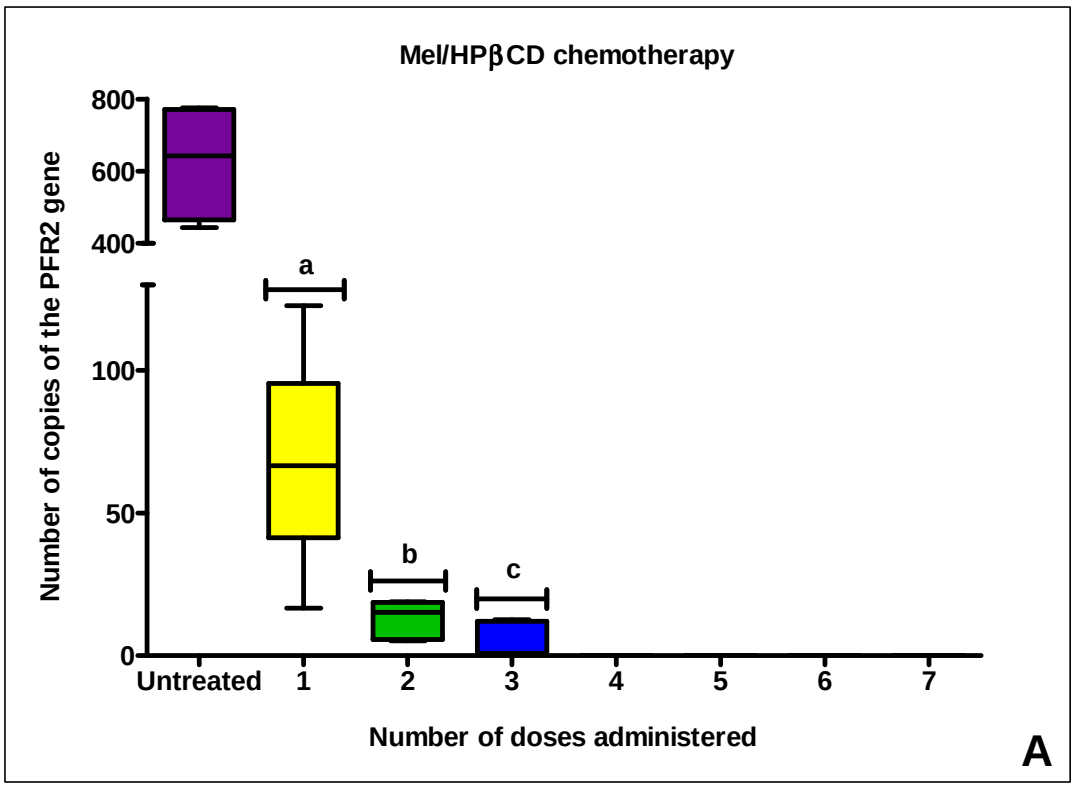

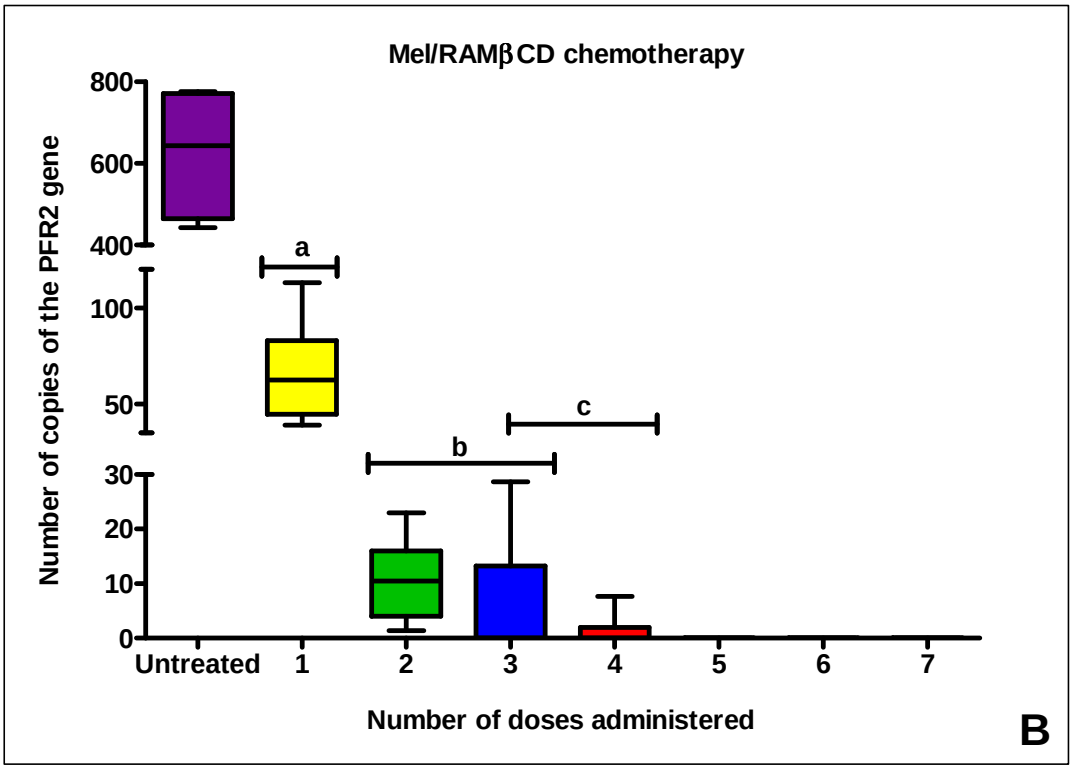

Figure 4-5: The number of copies of the PFR2 gene present within 100ng of DNA prepared from approximately 25mg of brain tissue taken from whole brain homogenate, of mice infected with *T. b. brucei* (GVR35/C1.9) following chemotherapy with A) Mel/HPβCD and B) Mel/RAMβCD.

The compounds were administered orally at a dose of 0.05mmol/kg, daily, for seven consecutive days, commencing on day 21 post-infection. The box plots show the median, interquartile range and minimum and maximum copy number detected after administration of each dose. Groups that do not share a letter are significantly different ($P < 0.05$).

4.3.2.1.3 Comparison of mel/HPβCD and mel/RAMβCD treatment

The melarsoprol cyclodextrin complexes contain the same drug but the cyclodextrin carrier differs. To assess if one cyclodextrin is more efficient at delivering melarsoprol to the brain and hence eliminating trypanosomes, the rate of parasite clearance of the two compounds was compared. No significant difference was detected between mel/HPβCD and mel/RAMβCD (P = 0.9835). Interaction plots (Figure 4-6), demonstrated parallel response lines and that there were no interactions between mel/HPβCD and mel/RAMβCD treatment and the number of copies of the PFR2 gene detected after administration of each dose (P = 0.813).

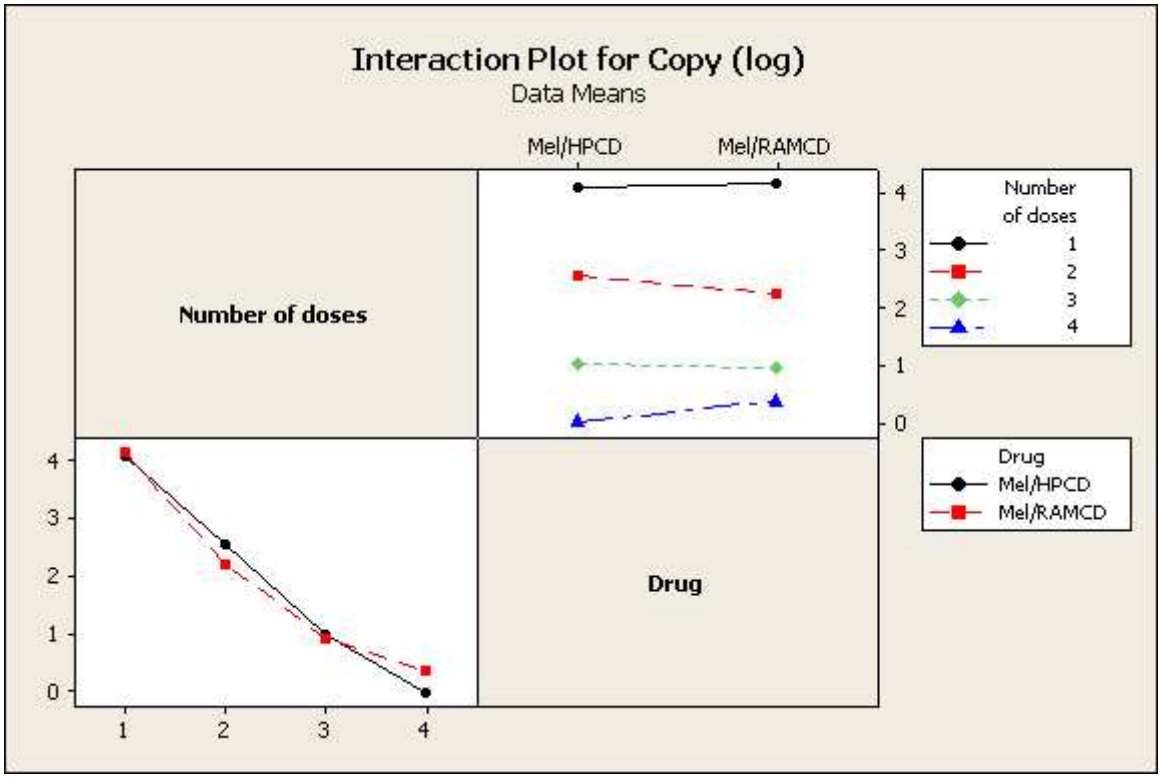

Figure 4-6: Interaction plots comparing the mean [log(x+1)] PFR2 copy number detected after administration of each dose of mel/HPβCD or mel/RAMβCD with number of doses
Mice were infected with the GVR35/C1.9 *T. b. brucei* melarsoprol sensitive stabilate. Chemotherapy commenced on day 21 post-infection. Mel/HPβCD or mel/RAMβCD was administered by oral gavage daily, for 7 consecutive days at a dose of 0.05mmol/kg. The number of copies of the PFR2 gene present within 100ng of DNA prepared from approximately 25mg of whole brain homogenate, 24 hours after administration of each dose was determined by QPCR. The interaction plots demonstrate that there are no interactions between mel/HPβCD and mel/RAMβCD treatment and the number of copies of the PFR2 gene detected after administration of each dose (P = 0.813).

Dose	1	2	3
2	P = 0.0220 (-2.860, -0.218)		
3	P = 0.0001 (-4.390, -1.748)	P= 0.0228 (-2.851, -0.2088)	
Mean ± SE n	68.1 ± 14.7 6	13.13 ± 2.54 6	4.32 ± 2.51 6

Table 4-4: Comparison of the number of copies of the PFR2 gene detected within 100ng of DNA prepared from approximately 25mg of whole brain homogenate from mice infected with melarsoprol sensitive *T. b. brucei* trypanosomes following mel/HPβCD chemotherapy

Mice were infected with *T. b. brucei* GVR35/C1.9. Mel/HPβCD chemotherapy commenced on day 21 post-infection. The compound was administered by oral gavage, daily for 7 consecutive days at dose of 0.05mmol/kg. The number of copies of the PFR2 gene present within 100ng of DNA prepared from approximately 25mg of whole brain homogenate, 24 hours after administration of each dose was determined by QPCR. The figures in the body of the table demonstrate the comparisons, in terms of statistical significance, between the number of copies of the PFR2 gene detected after administration of each dose, shown in the row and column headings. The p-values and 95% confidence intervals for differences are based on analysis using the logarithmic transformation [log(x + 1)] of the copy number. The mean copy number ± the standard error (mean ± SE) and the number of animals per group (n) are also shown. No copies of the PFR2 gene were detected after administration of the 4^{th}, 5^{th}, 6^{th} and 7^{th} dose of the complex. These values were therefore excluded as zero counts can bias the analysis.

Dose	1	2	3	4
2	P = 0.0134 (-3.507, -0.348)			
3	P = 0.0001 (-4.794, -1.635)	P = 0.1363 (-2.866, 0.2930)		
4	P < 0.0001 (-5.368, -2.209)	P = 0.0173 (-3.440, -0.2813)	P = 0.7409 (-2.154, 1.005)	
Mean ± SE n	66.2 ± 10.8 6	10.61 ± 3.09 6	6.13 ± 4.70 6	1.27 ± 1.27 6

Table 4-5: Comparison of the number of copies of the PFR2 gene detected within 100ng of DNA prepared from approximately 25mg of whole brain homogenate from mice infected with melarsoprol sensitive *T. b. brucei* trypanosomes following mel/RAMβCD chemotherapy

Mice were infected with *T. b. brucei* GVR35/C1.9. Mel/RAMβCD chemotherapy commenced on day 21 post-infection. The compound was administered by oral gavage, daily for 7 consecutive days at a dose of 0.05mmol/kg. The number of copies of the PFR2 gene present within 100ng of DNA prepared from approximately 25mg of whole brain homogenate, 24 hours after administration of each dose was determined by QPCR. The figures in the body of the table demonstrate the comparisons, in terms of statistical significance, between the number of copies of the PFR2 gene detected after administration of each dose, shown in the row and column headings. The p-values and 95% confidence intervals for differences are based on analysis using the logarithmic transformation [log(x + 1)] of the copy number. The mean copy number ± the standard error (mean ± SE) and the number of animals per group (n) are also shown. No copies of the PFR2 gene were detected following administration of the 5th, 6th and 7th dose of the complex. These values were therefore excluded as zero counts can bias the analysis.

4.3.2.2 *T. b. brucei* melarsoprol resistant strain (GVR35/M14)

4.3.2.2.1 The effect of mel/HPβCD treatment on CNS parasite load

Immediately prior to chemotherapy commencing on day 21 post-infection, high copies numbers of the PFR2 gene were detected in the brain (350 ± 107) (Figure 4-7, panel A). Twenty-four hours after administration of one dose of mel/HPβCD, there was a significant reduction (P = 0.0030) in the number of copies of the PFR2 gene (64.1 ± 11.5). Administration of a second dose, did not lead to a significant decrease (P = 0.9983) in the number of copies of the gene (49.83 ± 4.52). Following administration of a third dose of the complex, there was a significant reduction (P = 0.0004) in the number of copies of the PFR2 gene detected within the brain, 7.98 ± 2.71 copies were detected compared to 49.83 ± 4.52 copies after the second dose. This equates to a reduction of 83.4%. Administration of a fourth dose of the complex did not significantly reduce (P = 0.1640) the number of copies of the gene detected within the brain (2.95 ± 1.87) compared to the number detected after the third dose (7.98 ± 2.71). When animals were treated with a fifth dose of mel/HPβCD, a significant reduction (P < 0.0001) in the number of copies of the PFR2 gene (0.192 ± 0.192) was detected compared to after administration of 3 doses. However, this reduction was not significant when compared to the number of copies detected after 4 doses of the drug (P = 0.6770). The number of copies of the PFR2 gene detected after administration of six doses of the complex (0.508 ± 0.508) was significantly lower than the number detected after 3 doses (P = 0.0099). However, the number of copies of the gene present within the brain after six doses of the complex was not significantly lower than the number detected after four (P = 0.8154) or five doses (P = 0.9999). Twenty-four hours after administration of the seventh dose of mel/HPβCD, no copies of the PFR2 gene were detected. Summary statistics are detailed in Table 4-6.

4.3.2.2.2 The effect of mel/RAMβCD chemotherapy on CNS parasite load

High copy numbers of the PFR2 gene (350 ± 107) were detected in the brain immediately prior to chemotherapy commencing on day 21 post-infection (Figure 4-7, panel B). Administration of one dose of mel/RAMβCD significantly reduced

(P = 0.01) the number of copies of the gene (62.9 ± 26). This reduction continued following the administration of a second dose of the complex (13.07 ± 2.66), although the reduction was not significant (P = 0.2881) when compared to the number of copies detected after one dose. Following administration of a third dose of mel/RAMβCD, 4.34 ± 1.97 copies of the gene were detected. This is a significant reduction (P = 0.0022) when compared to the numbers detected after administration of one dose of the complex. When a fourth dose of the drug was administered to animals, a significant reduction (P = 0.0055) in the number of copies of the gene (2.65 ± 2.65) was detected compared to after administration of the second dose. However, the reduction in copy numbers detected after the fourth dose was not significant (P = 0.4813) when compared to the number of copies of the gene detected after 3 doses of the compound. The number of copies of the PFR2 gene detected after administration of a fifth dose (0.5668 ± 0.568) of mel/RAMβCD were significantly lower (P = 0.002) than the number detected after two doses of the complex. However, the number of copies of the gene detected after the fifth dose were not significantly different to the numbers detected after administration of the third (P = 0.2647) or fourth (P = 0.9932) doses of the complex. No copies of the PFR2 gene were detected 24 hours after administration of the sixth dose of mel/RAMβCD. Copies of the PFR2 gene (0.777 ± 0.777) were detected in one animal 24 hours after administration of the seventh dose of the complex. However, eight days after completion of mel/RAMβCD chemotherapy no copies of the gene were detected. Summary statistics are detailed in Table 4-7.

4.3.2.2.3 Comparison of mel/HPβCD and mel/RAMβCD treatment

To assess if one compound was more efficient at eliminating trypanosomes from the brain, the rate of parasite clearance of the two compounds was compared. A significant difference was detected between the two drugs (P = 0.0196). This was investigated further by individually comparing the number of copies of the PFR2 gene detected after administration of each dose of the two drugs against each other. A significant difference was detected between the two drugs, twenty-four hours after administration of the second dose (P = 0.001). In animals treated with mel/HPβCD a significantly higher number of copies of the PFR2

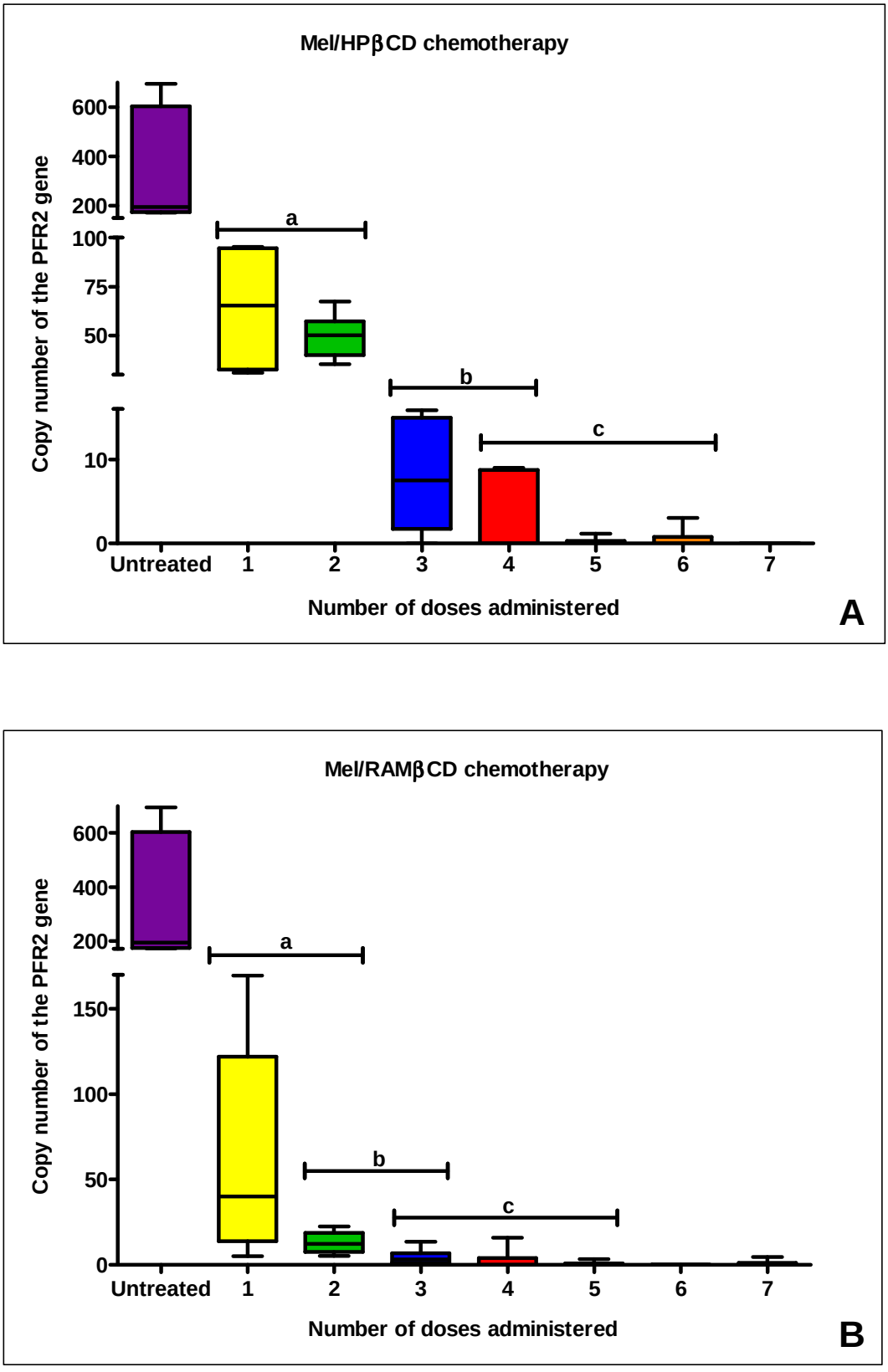

Figure 4-7: The number of copies of the PFR2 gene present within 100ng of DNA prepared from approximately 25mg of brain tissue taken from whole brain homogenate from mice infected with *T. b. brucei* (GVR35/M14) following chemotherapy with A) Mel/HPβCD and B) Mel/RAMβCD.

The compounds were administered orally at a dose of 0.05mmol/kg, daily, for seven consecutive days commencing on day 21 post-infection. The box plots illustrate the median, interquartile range and minimum and maximum copy number detected after administration of each dose. Groups that do not share a letter are significantly different ($P < 0.05$).

gene were detected (49.83 ± 4.52) compared to animals treated with mel/RAMβCD (13.07 ± 2.66). This was the only time point at which at significant difference was observed between the two drugs. Interaction plots (Figure 4-8), illustrate parallel response lines and that there were no interactions between mel/HPβCD and mel/RAMβCD treatment and the number of copies of the PFR gene detected after administration of each dose (P = 0.336).

4.3.2.3 Comparison of the melarsoprol sensitive and resistant strains

The rate of elimination of the PFR2 gene from the brain was compared between the melarsoprol sensitive (GVR35/C1.9) and melarsoprol resistant (GVR35/M14) strains for both drugs. A significant difference (P = 0.015) was observed between the two *T. b. brucei* strains. The PFR2 gene was eliminated more slowly in mice infected with the melarsoprol resistant strain (GVR35/M14) compared to the melarsoprol sensitive (GVR35/C1.9) strain. The two melarsoprol cyclodextrin compounds mel/HPβCD and mel/RAMβCD displayed an equivalent trypanocidal activity across the two strains, with no significant difference detected between the two drugs (P = 0.1013). Interaction plots (Figure 4-9) illustrate that there is no interaction between mel/HPβCD and mel/RAMβCD and the *T. b. brucei* strains (P = 0.096). Similarly the interaction between mel/HPβCD and mel/RAMβCD and the number of copies of the PFR2 gene detected after administration of each dose was not significant (P = 0.308) and there was no interaction between the number of copies of the PFR2 gene detected after administration of each dose and the *T. b. brucei* strains (P = 0.167).

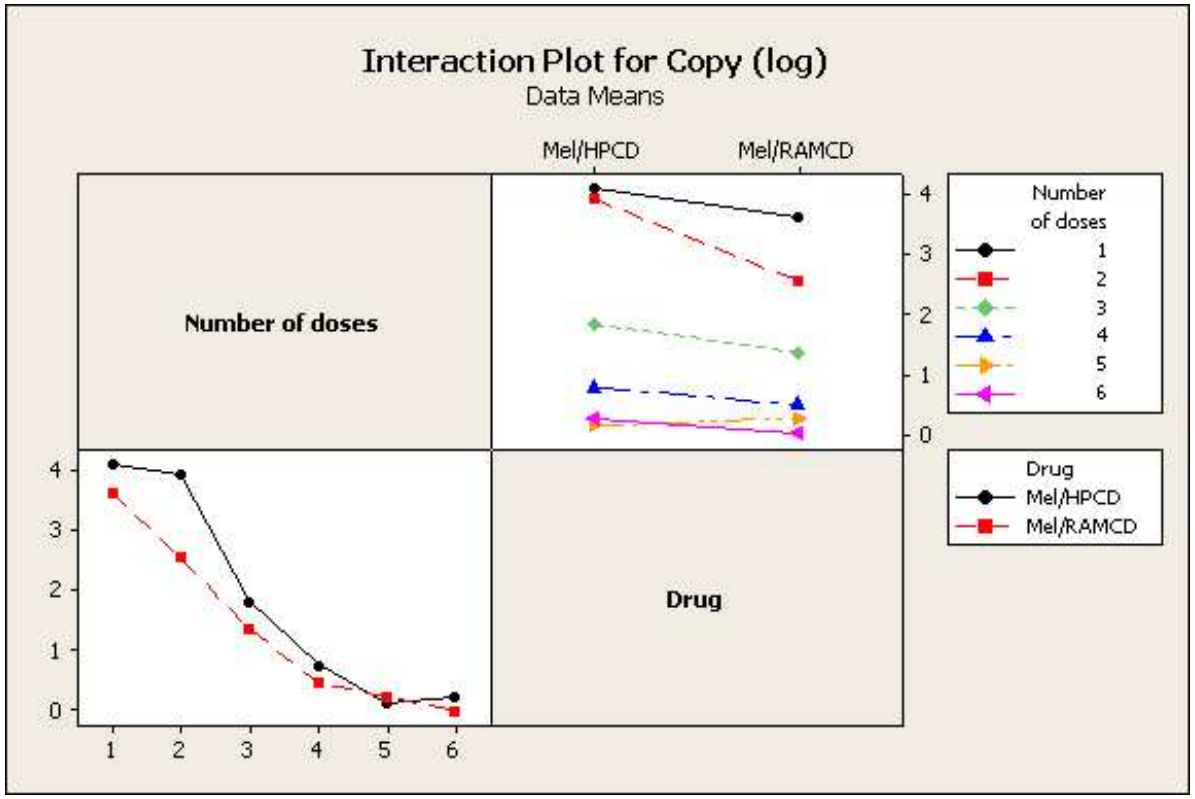

Figure 4-8: Interaction plots comparing the mean [log(x+1)] PFR2 copy number detected after administration of each dose of mel/HPβCD or mel/RAMβCD with number of doses

Mice were infected with the GVR35/M14 *T. b. brucei* melarsoprol resistant stabilate. Chemotherapy commenced on day 21 post-infection. Mel/HPβCD or mel/RAMβCD was administered by oral gavage, daily, for 7 consecutive days at a dose of 0.05mmol/kg. The number of copies of the PFR2 gene present within 100ng of DNA prepared from approximately 25mg of whole brain homogenate, 24 hours after administration of each dose was determined by QPCR. The interaction plots illustrate that there is no interaction between mel/HPβCD and mel/RAMβCD treatment and the number of copies of the PFR2 gene detected after administration of each dose (P = 0.336).

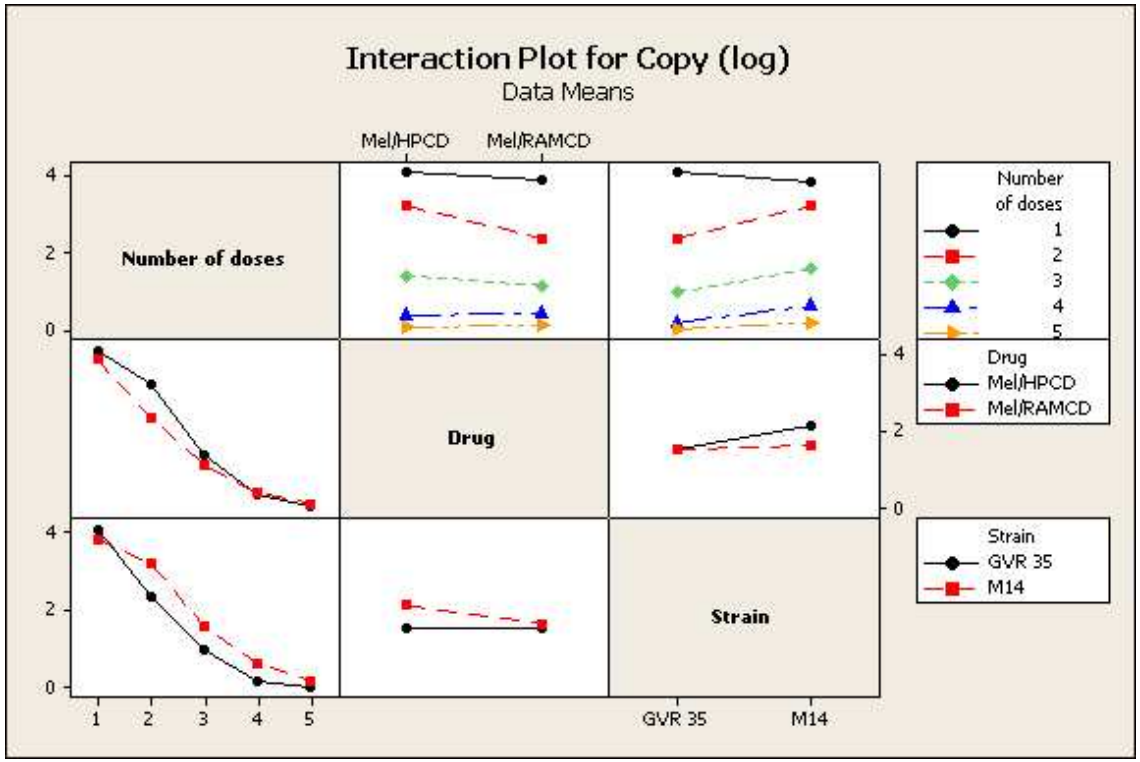

Figure 4-9: Interaction plots demonstrating the interactions in the mean [log(x+1)] PFR2 copy number detected between the two melarsoprol cyclodextrin complexes, mel/HPβCD and mel/RAMβCD and the number of doses and also between the melarsoprol sensitive (GVR35/C1.9) and resistant (GVR35/M14) *T. b. brucei* stabilates

Mice were infected with either the GVR35/C1.9 melarsoprol sensitive or GVR35/M14 *T. b. brucei* melarsoprol resistant stabilate. Chemotherapy commenced on day 21 post-infection. Mel/HPβCD or mel/RAMβCD was administered by oral gavage, daily, for 7 consecutive days at a dose of 0.05mmol/kg. The number of copies of the PFR2 gene present within 100ng of DNA prepared from approximately 25mg of whole brain homogenate, 24 hours after administration of each dose was determined by QPCR. Interaction plots illustrate that there is no interaction between mel/HPβCD and mel/RAMβCD and the *T. b. brucei* strains (P = 0.096). Similarly the interaction between mel/HPβCD and mel/RAMβCD and the number of copies of the PFR2 gene detected after administration of each dose was not significant (P = 0.308) and there was no interaction between the number of copies of the PFR2 gene detected after administration of each dose and the *T. b. brucei* strains (P = 0.167).

Dose	1	2	3	4	5	6
2	P = 0.9983 (-1.478, 1.124)					
3	P = 0.0001 (-3.566, -0.964	P = 0.0004 (-3.389, -0.787)				
4	P < 0.0001 (-4.625, -2.023)	P < 0.0001 (-4.447, -1.846)	P =0.1640 (-2.360, 0.2422)			
5	P < 0.0001 (-5.259, -2.658)	P < 0.0001 (-5.082, -2.480)	P = 0.0052 (-2.994, -0.3925)	P = 0.6770 (-1.936, 0.6662)		
6	P < 0.0001 (-5.154, -2.552)	P < 0.0001 (-4.976, -2.375)	P = 0.0099 (-2.889, -0.2870)	P = 0.8154 (-1.830, 0.7718)	P = 0.9999 (-1.195, 1.406)	
Mean ± SE n	64.1 ± 11.5 6	49.83 ± 4.52 6	7.98 ± 2.71 6	2.95 ± 1.87 6	0.192 ± 0.192 6	0.508 ± 0.508 6

Table 4-6: Comparison of the number of copies of the PFR2 gene detected within 100ng of DNA prepared from approximately 25mg of whole brain homogenate from mice infected with melarsoprol resistant *T. b. brucei* trypanosomes following mel/HPβCD chemotherapy

Mice were infected with *T. b. brucei* GVR35/M14. Mel/HPβCD chemotherapy commenced on day 21 post-infection. The compound was administered by oral gavage, daily for 7 consecutive days at dose of 0.05mmol/kg. The number of copies of the PFR2 gene present within 100ng of DNA prepared from approximately 25mg of whole brain homogenate, 24 hours after administration of each dose was determined by QPCR. The figures in the body of the table demonstrate the comparisons, in terms of statistical significance, between the number of copies of the PFR2 gene detected after administration of each dose, shown in the row and column headings. The p-values and 95% confidence intervals for differences are based on analysis using the logarithmic transformation [log(x + 1)] of the copy number. The mean copy number ± the standard error (mean ± SE) and the number of animals per group (n) are also shown. No copies of the PFR2 gene were detected following administration of the 7th dose of the complex. These values were therefore excluded from the analysis as zero counts can bias the analysis.

Dose	1	2	3	4	5
2	P = 0.2881 (-2.646, 0.492)				
3	P = 0.0022 (-3.839, -0.702)	P = 0.2008 (-2.762, 0.3752)			
4	P < 0.0001 (-4.721, -1.584)	P = 0.0055 (-3.644, -0.5068)	P = 0.4813 (-2.451, 0.6867)		
5	P < 0.0001 (-4.945, -1.808)	P = 0.0020 (-3.868, -0.7305)	P = 0.2647 (-2.674, 0.4630	P = 0.9932 (-1.792, 1.345)	
Mean ± SE n	62.9 ± 26.0 6	13.07 ± 2.66 6	4.34 ± 1.97 6	2.65 ± 2.65 6	0.568 ± 0.568 6

Table 4-7: Comparison of the number of copies of the PFR2 gene detected within 100ng of DNA prepared from approximately 25mg of whole brain homogenate from mice infected with melarsoprol resistant *T. b. brucei* trypanosomes following mel/RAMβCD chemotherapy

Mice were infected with *T. b. brucei* GVR35/M14. Mel/RAMβCD chemotherapy commenced on day 21 post-infection. The compound was administered by oral gavage, daily, for 7 consecutive days at dose of 0.05mmol/kg. The number of copies of the PFR2 gene present within 100ng of DNA prepared from approximately 25mg of whole brain homogenate, 24 hours after administration of each dose was determined by QPCR. The figures in the body of the table demonstrate the comparisons, in terms of statistical significance, between the number of copies of the PFR2 gene detected after administration of each dose, shown in the row and column headings. The p-values and 95% confidence intervals for differences are based on analysis using the logarithmic transformation [log(x + 1)] of the copy number. The mean copy number ± the standard error (mean ± SE) and the number of animals per group (n) are also shown. No copies of the PFR2 gene were detected in the majority of the animals following administration of the 6th and 7th doses of the complex. These values were therefore excluded from the analysis as zero counts can bias the analysis.

4.4 Discussion

In-situ hybridization is a valuable tool for directly visualising the location of genes of interest within tissues. Very little is known about the areas of the brain in which trypanosomes reside following their traversal of the blood-brain barrier (BBB). Previous studies have used direct microscopy or fluorescent anti-trypanosomal antibodies in order to visualise the trypanosomes within preserved brain sections (Poltera *et al.*, 1980; Schmidt and Bafort, 1985; Schultzberg *et al.*, 1988). However, both of these techniques have drawbacks. Direct microscopic visualisation of the trypanosomes is insensitive while the processes involved in the production of anti-trypanosomal antibodies are time consuming and problematic. The development of an in-situ hybridization assay would eliminate many of these problems and allow the direct visualisation of trypanosomes within paraffin embedded brain sections.

Despite numerous attempts to optimise the in-situ hybridization protocol no positive results were obtained. Several reasons could lie behind the failure to obtain positive staining for trypanosomes in the tissue sections. One possible explanation is that the target sequence was not accessible. In order for the oligonucleotide probe to be able to access the target sequence it must first penetrate through the tissue sections. To aid penetration of the probe, tissue sections are permeabilised with proteases which digest the proteins surrounding the target sequence. However, the permeabilisation step must be optimised. Over digestion can result in the target sequence been lost while in under digested tissues the target sequence remains inaccessible to the probe. The degree to which the tissue sections are digested can be controlled by varying the concentration of the proteases, the incubation temperature and time. In this study, various attempts were made to optimise the permeabilisation of the tissues. While optimising the permeabilisation step there was a concern that Proteinase K was over digesting the tissue sections leading to a loss of the target sequence. Over digestion is a common occurrence when Proteinase K is used to permeabilise tissue sections (Nuovo, 1994), it was therefore decided to use pepsin instead of Proteinase K to digest the tissues. Pepsin is widely used in in-situ hybridization to permeabilise tissue sections and excellent results have been reported following its use on formalin-fixed tissue sections (Roche, 2002). The

concentration of pepsin was varied along with the incubation time and temperature in an attempt to determine the optimal digestion conditions. However, despite all attempts to optimise the permeabilisation step positive staining for trypanosomes was still not obtained.

A second possible explanation for the lack of positive staining is that the target sequence of interest was present in numbers too low to be detected. The first oligonucleodtide probe used was designed to a section of the PFR2 gene, which encodes a paraflagellar rod protein (Deflorin, Rudolf and Seebeck, 1994). This gene was chosen as the target sequence as it is detected consistently and quantitatively in QPCR assays. However, trypanosomes only have one copy of the PFR2 gene (Schlaeppi, Deflorin and Seebeck, 1989). This does not pose a problem in QPCR as the target sequence is amplified during the reaction. However, in in-situ hybridization the target sequence is not amplified therefore if the target sequence is present in low numbers it could easily be missed by the probe. Furthermore, if the trypanosome is only partially within the plane of the tissue section, the target sequence could lie outside the section, meaning the trypanosome will not be detected by the probe.

The chances of detecting trypanosomes within the tissue sections could be increased by selecting a probe designed to a gene with a high copy number. A second probe was therefore designed to a section of a 177 bp repeat sequence found within the satellite DNA of *T. b. brucei* (Sloof, Menke, Caspers and Borst, 1983). Within the *T. b. brucei* genome, 15,000 copies of the 177 bp repeat are present, thus by using a probe directed to a section of this sequence the chances of detecting trypanosomes within the tissue sections should be increased (Wickstead, Ersfeld and Gull, 2003). This gene was also chosen as the target sequence since a probe designed to the equivalent gene in the American trypanosome *T. cruzi* was used successfully to detect the parasites within paraffin-embedded cardiac sections (Lane *et al.,* 1997).

In a further attempt to maximise the chances of detecting trypanosomes within the paraffin-embedded sections, a Tyramide Signal Amplification System (TSA™ PerkinElmer) was used. Immobilised HRP within the tissue sections converts the labelled tyramidine substrate into a short-lived extremely reactive intermediate. This intermediate interacts and covalently binds to electron rich regions of

adjacent proteins. The activated tyramide molecules only bind immediately adjacent to sites where the activating HRP is present. The subsequent detection of the tyramide labels by chromogenic methods yields a large amplification of the signal. The TSA™ system means that it should be possible to detected even low levels of signal. However, despite the use of a probe designed to a sequence with a high copy number and the amplification of the hybridization signal with a TSA™ system no positive staining for trypanosomes was observed.

The observation of African trypanosomes within paraffin-embedded brain sections by in-situ hybridization has not been described previously. All previous reports describing the localisation of trypanosomes within paraffin-embedded brain sections have involved the direct observation of the trypanosomes in haematoxylin stained sections by light microscopy (Fink and Schmidt, 1979; Stevens and Moulton, 1977) or the visualisation of trypanosomes with anti-trypanosomal antibodies previously raised in rabbits (Masocha *et al.,* 2004; Poltera *et al.,* 1980). However, the detection of trypanosomes by in-situ hybridization should be achievable. Lane *et al*. described the successful detection of the American trypanosome, *T. cruzi* within paraffin-embedded cardiac sections (Lane *et al.,* 1997). The methodology used in the study was adapted to suit the current investigation but positive staining for *T. b. brucei* was still not obtained. In-situ hybridization consists of numerous stages, all of which can be adjusted depending upon the tissue and target sequence. Unfortunately, there is not a standard protocol for all in-situ hybridization applications. Positive staining is achieved by systematically adjusting previously reported protocols step by step, in order to determine the optimum conditions for the tissue and target sequence of interest. In the current investigation, attempts were made to adapt previously reported protocols, to suit the needs of the study. However, due to time restrictions, optimisation of every stage in the protocol could not be carried out. With further investigation and optimisation of the protocol it should be possible to achieve positive staining for trypanosomes. By being able to visualise the location of trypanosomes within the brain, the regions where parasites first appear after infection could be identified. Furthermore, the location of trypanosomes in relation to areas of neuroinflammation or blood-brain barrier (BBB) damage could be investigated.

Although it was not possible to map the location of the parasites within the CNS in this investigation, QPCR was used to accurately quantify the number of copies of the PFR2 gene present within 100ng of DNA prepared from approximately 25mg of whole brain homogenate. The number of copies of the gene in the brain immediately prior to and following chemotherapy with the melarsoprol cyclodextrin complexes, mel/HPβCD and mel/RAMβCD was determined in a melarsoprol sensitive (GVR35/C1.9) and resistant (GRV35/M14) *T. b. brucei* strain.

The melarsoprol cyclodextrin complexes mel/HPβCD and mel/RAMβCD eliminate melarsoprol sensitive trypanosomes from the brain very quickly following administration. The PFR2 gene was not detected within the brain 24 hours after administration of the fourth dose of mel/HPβCD and fifth dose of mel/RAMβCD. Once eliminated from the brain, the gene did not reoccur. Unfortunately, in the present study it was not possible to determine the rate of trypanosome clearance from the brain following conventional melarsoprol chemotherapy, as the drug is very difficult to administer intravenously to mice. The rates of trypanosomal clearance, following conventional and complexed melarsoprol chemotherapy could not therefore be compared.

The speed at which the melarsoprol cyclodextrin complexes are able to eliminate trypanosomes from the brain may help prevent the development of the PTRE and hence reduce the toxicity of the drug. The PTRE currently occurs in up to 10% of all patients receiving melarsoprol chemotherapy of which 50% will die as a result of the complication. This gives melarsoprol an overall fatality rate of 5% which is unacceptably high (Kennedy, 2004; Pepin and Milord, 1994). The precise reasons for the development of the PTRE are not fully understood and a number of mechanisms have been proposed. Jennings *et al*. suggested that the PTRE occurs as a result of the compound eliminating trypanosomes from the circulation but not the brain (Jennings *et al.*, 1993; Jennings *et al.*, 1989). This allows the immune system to become focused on the parasites remaining in the brain causing a severe meningoencephalitis. The author further suggested that a rapidly curative treatment regime which simultaneously eliminates trypanosomes from the tissues and the brain may prevent the development of the PTRE. The theory was tested in an experiment in which mice infected with

T. b. brucei were treated with an aggressive or subcurative chemotherapy regime. Mice treated with the aggressive treatment regime received a combination of 5-nitroimidazole (40mg/kg) and mel Cy (5mg/kg), intraperitoneally, once a day, for two consecutive days. A single dose of diminazene aceturate (40mg/kg) was administered intraperitoneally to animals receiving the subcurative regime. The subcurative regime eliminated trypanosomes from the tissues but not the brain. Mice treated with the aggressive chemotherapy regime did not develop meningoencephalitis. In contrast, mice treated with the subcurative regime developed severe meningoencephalitis (Jennings *et al.*, 1993). The study concluded that the meningoencephalitis occurred as a result of the presence of living trypanosomes within the CNS and further indicated that if all the trypanosomes within the CNS were eliminated then the meningoencephalitis would not occur and any existing lesions would resolve. Complexed melarsoprol chemotherapy dramatically reduces the number of trypanosomes within the brain, twenty-four hours after administration of one dose of mel/HPβCD or mel/RAMβCD. By twenty-four hours after administration of 4 dose of mel/HPβCD or 5 doses of mel/RAMβCD, all trypanosomes were eliminated from the brain. These findings indicate that complexed melarsoprol acts in a rapid and aggressive manner. Therefore if the hypothesis suggested by Jennings *et al.* (1993) is correct, treatment of CNS-stage disease with mel/HPβCD or mel/RAMβCD should show a reduced incidence of the severe meningoencephalitis associated with contemporary trypanosome chemotherapy.

Previous *in-vivo* experiments (Chapter 3) determined the minimum curative dose of mel/HPβCD and mel/RAMβCD in a melarsoprol sensitive *T. b. brucei* strain to be seven daily doses of 0.05mmol/kg. However, the present studies indicate that all trypanosomes are cleared from the brain twenty-four hours after administration of four doses of mel/HPβCD or five doses of mel/RAMβCD, as evidenced by the absence of the PFR2 gene within the brain. This suggests that the treatment regime could be reduced from seven doses of 0.05mmol/kg to four doses of mel/HPβCD or five doses of mel/RAMβCD. Furthermore, the QPCR assay demonstrated low copy numbers of the PFR2 gene within the brain twenty-four hours after administration of three or four dose of mel/HPβCD and mel/RAMβCD respectively. It is not known if these numbers represent a viable

trypanosome population within the brain and this must be confirmed using the traditional *in-vivo* method of monitoring the animals for the development of a relapsed parasitaemia and brain transfer experiments. If the population is non-viable then it maybe possible to reduce the chemotherapy regime further still.

In addition to rapidly eliminating melarsoprol sensitive trypanosomes from the brain, the melarsoprol cyclodextrin complexes mel/HPβCD and mel/RAMβCD were also able to eliminate melarsoprol resistant trypanosomes. However, the rate of trypanosomal clearance was slower than for the sensitive strain. The PFR2 gene was not eliminated until twenty-four hours after administration of the seventh dose of mel/HPβCD and seven days after completion of mel/RAMβCD chemotherapy. However, less than one copy of the PFR2 gene was detected in the brain twenty-four hours after administration of a fifth dose of mel/HPβCD and mel/RAMβCD. When the number of copies of the PFR2 gene detected within the brain falls below one, it is possible that this does not represent a viable population of trypanosomes and the samples can therefore be classed as negative for the presence of the PFR2 gene. However, in order to confirm if the samples are truly negative, the animals would need to be monitored for the development of a relapsed parasitaemia.

The *T. b. brucei* melarsoprol resistant strain used in the study, GVR35/M14 was developed from the melarsoprol sensitive GVR35/C1.9 stabilate by serially treating mice with increasing sub-curative doses of topical melarsoprol and passaging the resulting stabilates. The final strain, GVR35/M14 was resistant to 9μM of melarsoprol. Following its development the GVR35/M14 strain was stored in liquid nitrogen. In this study the experimental animals were not infected directly with the GVR35/M14 stabilate. The stabilate was first passaged in a donor animal in order to obtain sufficient numbers of trypanosomes to infect large numbers of experimental animals. While being passaged in the donor animal and during the first 21 days of new infections the stabilate is not exposed to any trypanocidal compounds. There is therefore a concern that in the absence of any drug pressure the stabilate reverts back to a melarsoprol sensitive form. The GVR35/M14 stabilate is currently under investigation, in order to confirm that it has maintained a resistant phenotype in the absence of drug pressure. Until these studies are completed and the resistance profile of the stabilate

confirmed, no conclusions can be drawn regarding the activity of mel/HPβCD and mel/RAMβCD against *T. b. brucei* resistant strains.

This study demonstrates that QPCR is an effective method for assessing the rate of trypanosomal clearance from the brain following chemotherapy. The method allows the number of trypanosomes present in the brain to be accurately quantified, easily and quickly. The effectiveness of new chemotherapy regimes can be determined within a week of the regime ending. This is a significant improvement on the currently used *in-vivo* methods, which involve monitoring animals for the development of a parasitaemia for up to 120 days. These methods are time consuming, expensive and require large numbers of experimental animals. The use of QPCR to evaluate new treatment regimes would eliminate the need for large numbers of experimental animals and allow results to be obtained quicker, thus saving time and money. The PFR2 gene is a good gene candidate for quantifying the number of trypanosomes present within the brain as it is stable within samples and it does not persist in the brain following the elimination of trypanosomes.

This study is the first report of QPCR being used to assess the rate of trypanosomal clearance from the brain following chemotherapy but the method has already been successfully used in malaria patients to determine the rate of parasite clearance from the peripheral circulation following anti-malarial chemotherapy (Beshir *et al.*, 2010). In agreement with this study the authors found QPCR to be highly sensitive, allowing low numbers of parasites to be detected, which may be missed when examining blood smears by microscopy.

These investigations demonstrate that the melarsoprol cyclodextrin complexes mel/HPβCD and mel/RAMβCD are effective oral therapies for the treatment of melarsoprol sensitive CNS stage *T. b. brucei* infections. Administration of four doses of mel/HPβCD and five doses of mel/RAMβCD, orally, once per day at a dose of 0.05mmol/kg was sufficient to eliminate trypanosomes from the brain. This treatment regime is considerably shorter than the concise 10 day melarsoprol schedule currently used for the treatment of CNS stage *T. b. rhodesiense* infections. Furthermore, the oral bioavailability of the melarsoprol cyclodextrin complexes, means the problems and expenses associated with I.V.

administration of conventional melarsoprol are eliminated. Mel/HPβCD and mel/RAMβCD are therefore promising oral candidates for the treatment of CNS stage trypanosome infections.

Chapter 5: Visualisation of the changes in permeability of the blood-brain barrier following complexed melarsoprol chemotherapy

5.1 Introduction

The blood-brain barrier (BBB) is a specialised, highly organised structure, essential for normal brain function. However, in some diseases, the integrity of the BBB is compromised, resulting in CNS dysfunction and pathology. This chapter will investigate the effects of early CNS stage *T. b. brucei* infection on the integrity of the BBB using small bore magnetic resonance imaging (MRI) in conjunction with mel/HPβCD chemotherapy.

5.1.1 Barriers of the CNS

The exchange of molecules and solutes between the blood and the brain and its fluid spaces is regulated by three distinct barriers; the blood-brain barrier (BBB), the blood – CSF barrier and the arachnoid barrier.

5.1.1.1 The blood-brain barrier

The blood-brain barrier (BBB) is an integrated dynamic structure, separating the brain parenchyma from the bloodstream (Masocha, Rottenberg and Kristensson, 2007; Schlosshauer, 1993). It is located at the level of the cerebral capillary endothelial cells and is present in all areas of the brain, except the regions responsible for regulation of the autonomic nervous system and endocrine glands (Ballabh, Braun and Nedergaard, 2004). The BBB is the most extensive of the three CNS barriers and forms the greatest interface for blood-brain exchange, with a surface area of approximately $20m^2$ per 1.3kg brain (Nag and Begley, 2005).

The barrier is composed of tightly apposed vascular endothelial cells (Figure 5-1) characterised by their increased mitrochondrial content, lack of pinocytic vesicles and the presence of tight junctions (Chaudhuri, 2000). The tight junctions hold the endothelial cells of the BBB closely together, eliminating the gaps that usually occur between endothelial cells elsewhere in the body and restricting the paracellular passive diffusion of molecules (Chaudhuri, 2000; Enanga, Burchmore, Stewart and Barrett, 2002). Small lipophilic molecules such as O_2, CO_2 and ethanol are able to freely diffuse across the membranes but

larger hydrophobic molecules including glucose, are transported transcellularly by specialised transporters (Begley and Brightman, 2003). The endothelial basement membrane underlies the endothelial cells and separates the blood from the perivascular space. In close association with the endothelial cells are pericytes, also known as vascular smooth muscle cells. Vascular pericytes synthesise the major components of the basement membranes and provide essential structural support, helping to maintain the integrity of the tight junctions. The tight junctions are reinforced by the foot processes of astrocytes, a distinct type of glial cell essential in the maintenance of BBB integrity (Chaudhuri, 2000). The foot processes of the astrocytes are continuous with the parenchymal basement membrane which separates the perivascular space from the brain parenchyma. Together, the basement membranes, endothelial cells, astrocytes, pericytes, microglia cells and neurons constitute the neurovascular unit (NVU) (Choi and Kim, 2008; Persidsky, Ramirez, Haorah and Kanmogne, 2006). The NVU is the functional unit of the BBB and is essential for normal BBB function (Abbott, Ronnback and Hansson, 2006).

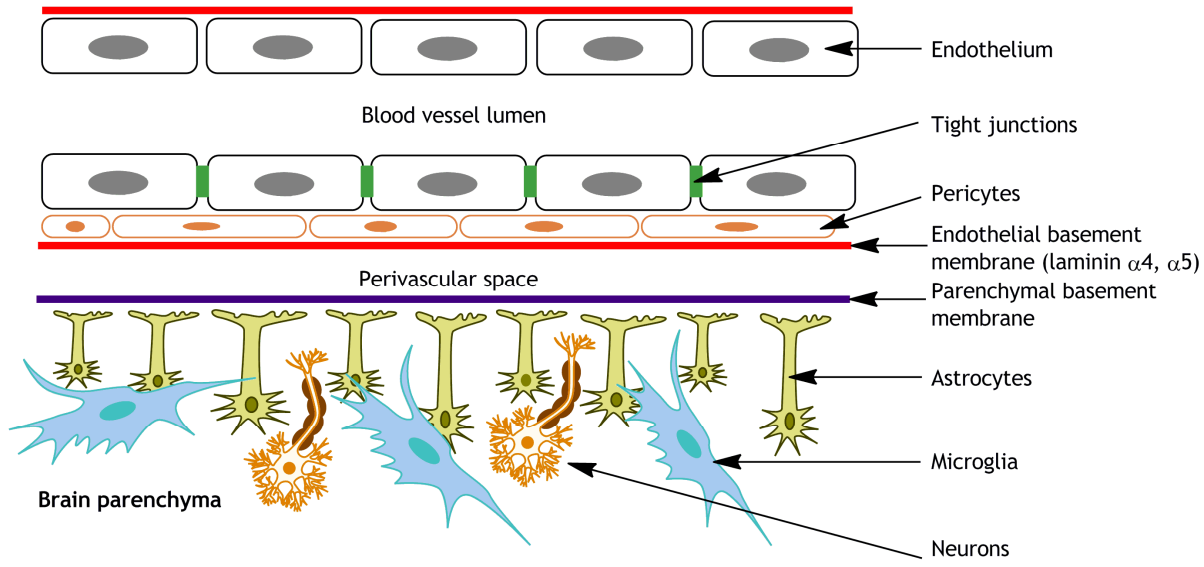

Figure 5-1: The blood-brain barrier
The blood-brain barrier (BBB) is composed of tightly apposed endothelial cells. Tight junctions are located between the endothelial cells, holding the cells together and severely restricting the paracellular diffusion of molecules. The tight junctions are reinforced by the foot processes of astrocytes. The astrocytes, together with the endothelial cells, basement membranes, neurons, pericytes and microglial cells constitute the neurovascular unit (NVU). The NVU is the functional unit of the BBB.

5.1.1.2 The blood–CSF barrier

The blood – CSF barrier is formed by the epithelial cells of the choroid plexus (Figure 5-2). The choroid plexus is a highly vascularised structure, containing an extensive capillary network enclosed by a single layer of cuboidal epithelium. The choroid plexus is situated within the lateral, third and fourth ventricles and is responsible for the production of CSF (Abbott, 2004). In order to produce CSF the endothelial cells need unrestricted access to blood-borne components. The endothelial cells in the choroid plexus are therefore fenestrated to allow the free movement of molecules. However, it is essential that the blood-borne components do not enter the ventricular space. To prevent the entry of blood-borne components into the ventricular space, tight junctions exist between the choroid plexus endothelial cells, forming the blood-CSF barrier.

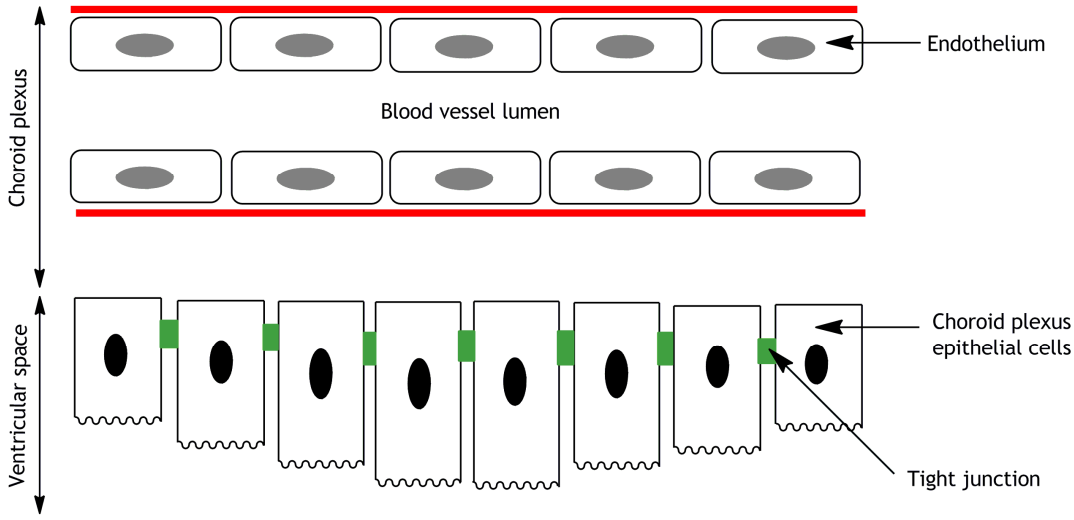

Figure 5-2: The blood-CSF barrier
The endothelial cells of the blood vessels within the choroid plexus are fenestrated, allowing the free movement of molecules. In order to prevent blood-borne components entering the ventricular space, tight junctions are present between the choroid plexus epithelial cells, forming the blood-CSF barrier.

5.1.1.3 Arachnoid barrier

The arachnoid barrier is the least studied and most complex of the three barriers (Figure 5-3). The arachnoid matter along with the pia and dura form the meninges (Haines, Harkey and Almefty, 1993). The collagenous external dura is the outer most layer and is in contact with the inner surface of the skull. Underlying the external dura is the meningeal dura which contains more

fibroblasts and less collagen than the external dura (Anderson, 1969). At the interface of the meningeal dura and the arachnoid lies a unique population of elongated, flattened fibroblasts known as border cells. The cells are characterised by a lack of extracellular collagen, sparse intercellular junctions and prominent extracellular spaces (Haines, Harkey and Almefty, 1993). Internal to the border cells is the arachnoid barrier. The barrier is composed of endothelial cells connected by tight junctions similar to those found in the brain parenchyma, although astrocytes are absent (Rodgers, 2010; Segal, 2000). They form an effective barrier, preventing the movement of fluid and large molecular weight substances between the subarachnoid space and the dura. Underlying the arachnoid barrier is a loosely organised population of fibroblasts, known as arachnoid trabeculae, which span the subarachnoid space (Haines, Harkey and Almefty, 1993). The subarachnoid space is a fluid filled compartment which separates the arachnoid from the pia matter (Haines, Harkey and Almefty, 1993). At the interface of the arachnoid barrier and subarachnoid space is a basement membrane. The basement membrane is composed of fenestrated endothelial cells with punctuate junctions, allowing CSF and molecules to freely diffuse across the cells (Segal, 2000). Internal to the subarachnoid space is the pia matter, composed of flattened fibroblasts. A final basement membrane separates the pia matter from the brain parenchyma (Haines, Harkey and Almefty, 1993).

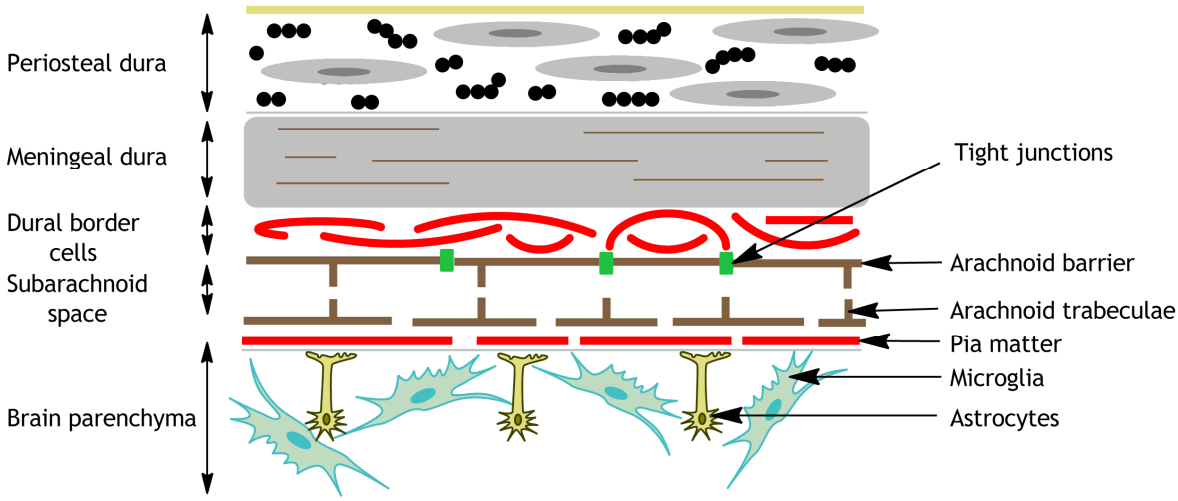

Figure 5-3: The arachnoid barrier
The arachnoid barrier is located between the dural border cells and the subarachnoid space. The barrier is composed of endothelial cells connected by tight junctions similar to those present in the brain parenchyma although astrocytes are absent. The barrier prevents the movement of fluid between the subarachnoid space and the dura.

5.1.2 Trypanosomes and the blood-brain barrier

5.1.2.1 Trypanosome traversal of the BBB

The mechanisms by which trypanosomes traverse the BBB and invade the CNS are currently unknown. In an attempt to understand the cellular and molecular events that occur immediately prior to trypanosome traversal of the BBB both *in-vitro* and *in-vivo* approaches have been followed.

5.1.2.1.1 In-vitro blood-brain barrier studies

The *in-vitro* model used to study the interaction between trypanosomes and the BBB is comprised of human brain microvascular endothelial cells (BMECs) which are seeded on top of tissue culture inserts pre-coated with type I collagen. Once confluency is reached the human BMECs form a continuous lining and act as a barrier between the upper and lower compartments of the well. The upper compartment represents the blood side of the BBB while the lower compartment represents the brain side (Grab, Nikolskaia, Kim, Lonsdale-Eccles *et al.*, 2004). Trypanosomes placed in the upper compartment (blood side) migrate through the mono-layer of human BMECs and enter the lower compartment (brain side). By taking transendothelial electrical resistance (TEER) measurements continuously throughout the experiment, the integrity of the human BMEC mono-layer can be assessed in real-time as the trypanosomes transverse the cells. In addition, washing and fixing of the human BMECs allows the point of trypanosomal traversal to be visualised microscopically.

Studies conducted using the *in-vitro* human BMEC model have shown that, prior to traversal of the BBB trypanosomes attach at or near to the periphery of endothelial cell tight junctions (Grab *et al.,* 2004). Preceding traversal of the barrier, oscillatory increases in Ca^{2+} are induced in the microvascular endothelial cells by the living parasites or their secretory products. These transient increases in Ca^{2+} were completely abolished when an irreversible cathepsin-L cysteine protease inhibitor was added to the culture. This suggests that parasite derived cysteine proteases are responsible for the calcium signalling events (Nikolskaia, de, Kim, Lonsdale-Eccles *et al.*, 2006). It was therefore proposed

that the trypanosomes induce Ca^{2+} signalling in the endothelial cells through secretion of cysteine proteases, in particular brucipain, and that these signalling events are essential in order for the parasites to penetrate the BBB (Nikolskaia *et al.*, 2006).

Following this discovery the search began for the molecular target of brucipain. Cysteine proteases are known to activate a class of G protein coupled receptors known as Protease Activated Receptors (PARs) (Grab, Garcia-Garcia, Nikolskaia, V, Kim, V *et al.*, 2009). The human BMECs express all four PARs and it has been shown previously that activation of PAR-1 and PAR-2 leads to Ca^{2+} mediated transmembrane signalling in human BMECs (Kim, Di Cello, Hillaire and Kim, 2004). Furthermore, in single cell studies, a PAR-2 agonist was able to induce Ca^{2+} signalling in greater than 60% of the human BMECs (Kim *et al.*, 2004). These findings substantiated the hypothesis that trypanosome derived cysteine proteases induce Ca^{2+} signalling in human BMECs through activation of PARs. In order to test the hypothesis further, expression of the PAR-2 gene (F2RL1) in the human BMECs was decreased by greater than 95% using RNA interference (RNA_i). Traversal of *T. b. rhodesiense* across the human BMEC mono-layer was decreased between 39 and 49% following silencing of the PAR-2 gene using this method. Furthermore, in human BMECs in which the PAR-2 gene had been silenced, normal TEER levels were maintained even in the presence of trypanosomes (Grab *et al.*, 2009). The results of these studies led Grab *et al.* to format a hypothesis suggesting that parasite proteases trigger PARs, leading to the release of Ca^{2+} from intracellular stores. The increase in intracellular calcium results in calmodulin (CaM) activation of myosin light chain kinase (MLCK), ultimately leading to rearrangement of the cytoskeleton and barrier dysfunction, and thereby allowing trypanosomes to traverse the BBB (Grab *et al.*, 2009).

5.1.2.1.2 In-vivo blood-brain barrier studies

In-vivo studies have also enabled the processes involved in trypanosome traversal across the blood-brain barrier to be unravelled. Work by Masocha *et al.* in a murine model of the disease found that trypanosomes were only able to penetrate regions of the endothelial basement membrane at sites where laminin $\alpha 4$ but not laminin $\alpha 5$ chains were present. Transmigration was inhibited at sites containing laminin $\alpha 5$ (Masocha, Rottenberg and Kristensson, 2007). The laminin

glycoprotein family form the major functional and structural component of all basement membranes. Laminins are heterotrimeric glycoproteins composed of α, β and γ chains (Timpl and Brown, 1994). To date 5 α, 4 β and 3 γ chains have been identified which can combine to form up to 15 different laminin isoforms (Colognato and Yurchenco, 2000). The α laminin chains represent the functionally active portion of each laminin as they form the cell-binding domains (Aumailley and Smyth, 1998; Tunggal, Smyth, Paulsson and Ott, 2000). The laminin isoforms present in the endothelial and parenchymal basement membranes vary. The endothelial basement membrane is composed of laminin α4 and α5 chains while the parenchymal basement membrane is composed of laminin α1 and α2 chains (Sixt, Engelhardt, Pausch, Hallmann *et al.*, 2001). In endothelial membranes the expression of laminins is regulated by proinflammatory cytokines such as IFN-γ, IL-12 and TNF-α (Sixt *et al.*, 2001). This led to the notion that proinflammatory cytokines could affect the ability of trypanosomes to penetrate the BBB and this hypothesis was investigated in IFN-γ knockout mice (IFN-$\gamma^{-/-}$) (Masocha *et al.*, 2004). In the IFN-γ knockout animals, extravasation of *T. b. brucei* from the cerebral blood vessels into the brain parenchyma was inhibited. Immunofluorescent staining revealed the expression of laminin α4 and α5 chains in the endothelial basement membrane of IFN-$\gamma^{-/-}$ mice was the same as that observed in wild type mice. Furthermore, the migration of *T. b. brucei* across the BBB was also reduced in recombinant activation gene-$1^{-/-}$ (RAG-$1^{-/-}$) mice and in the absence of IL-12, a major activator of IFN-γ (Masocha *et al.*, 2004). This suggested that penetration of trypanosomes into the brain parenchyma is dependent upon T cell derived IFN-γ. The mechanisms by which IFN-γ facilitates the migration of *T. b. brucei* across the BBB have still to be fully elucidated.

5.1.2.2 Breakdown of the blood-brain barrier during trypanosome infection

The effect of trypanosome infection and transmigration into the brain on the integrity of the BBB is not clear. In an initial study conducted by Philip *et al.*, utilising a rat model of the disease, BBB damage was assessed by monitoring the brain for the presence of a fluorescent dye following its injection into the jugular vein. Using this method an extensive and progressive breakdown of the

BBB was observed as the infection advanced (Philip, Dascombe, Fraser and Pentreath, 1994). Low levels of BBB damage were first observed on day 21 post-infection with damage localized to the thalamus and hypothalamus (Philip *et al.*, 1994). As the disease progressed damage to the BBB became more widespread with the rhodamine dye penetrating both the white and grey matter. However, there was large inter-animal variation in the level of BBB damage observed and there was no apparent correlation between areas of high BBB damage and the presence of parasites (Philip *et al.*, 1994). In a second study conducted by Mulenga *et al*. the effect of trypanosome traversal on the tight junctions of the BBB was investigated through visualisation of the tight junction markers occludin and ZO-1. The location of trypanosomes within the CNS in relation to the brain vascular endothelium, was also visualised using an anti-glucose transporter-1 (GLUT-1) antibody (Mulenga, Mhlanga, Kristensson and Robertson, 2001). No difference in the staining patterns of occludin and ZO-1 were detected between infected and control animals indicating that during infection there is no generalised loss of tight junction proteins. The majority of the parasites were confined to the blood vessels on day 12 post-infection, with only small numbers observed in the brain parenchyma. A similar parasite distribution was also observed on day 22 post-infection. As the infection progressed, the number of parasites within the brain parenchyma increased. At days 42, 45 and 55 post-infection, large accumulations of parasites were observed in the white matter and clustered around large vessels in the septal nuclei (Mulenga *et al.*, 2001). This suggests that the parasites within the brain parenchyma are mainly derived from parasites that have directly penetrated the cerebral vessels. Furthermore, the *T. b. brucei* parasites are able to penetrate the BBB with no permanent disruption of the tight junctions that are essential for barrier maintenance.

Histopathological investigations have provided insights into the morphological changes that occur at the BBB during trypanosome infection (Philip *et al.*, 1994). However, the data the studies provide is limited as only a small section of the brain can be visualised and processing of the tissues can lead to artefacts which could be wrongly attributed to the disease process. Furthermore, histopathology sections only provide a ‘snap shot’ of what is happening at the BBB at the point in time when the animal was sacrificed, they do not allow the changes in the BBB to be monitored over a period of time.

One method by which the integrity of the BBB can be studied in great detail, throughout the disease process is by magnetic resonance imaging (MRI).

5.1.3 Magnetic resonance imaging

MRI is a non-invasive, sensitive means of visualising the whole brain. It allows specific regions where BBB integrity is compromised to be identified and, as it is performed *in-vivo,* any changes observed in the BBB can be attributed solely to the disease process.

5.1.3.1 Principles of magnetic resonance imaging

The aim of MRI is to differentiate between adjacent tissues. To achieve this goal, a signal must be generated from each tissue. In MRI the signal is generated through a physical phenomenon known as nuclear magnetic resonance (NMR). NMR occurs when certain elements interact with a magnetic field (Lipton, 2008b). As hydrogen is the most abundant NMR compatible nucleus in human tissue, human MRI is focused almost entirely on the signal generated by the nuclei of hydrogen atoms (^1H) (Lipton, 2008b). A hydrogen atom consists of a nucleus containing a single positively charged proton which is orbited by a single negatively charged electron. Only the proton is of interest in MRI (Weishaupt, Kochli and Marincek, 2006b). The positive charge on the proton means it generates a magnetic field that is local to the nucleus, that behaves just like the magnetic field of a permanent magnet (Lipton, 2008b). In the absence of any external magnetic field the orientation of the nuclear magnetic field will be random. However, when an external magnetic field is applied, the nuclear magnetic field will align with that of the external field (Lipton, 2008b).

MRI relies on the generation of a moving magnetic field known as transverse magnetization (M_t). Transverse magnetization (M_t) is able to induce a voltage in a receiver coil. The voltage induced in the coil is directly proportional to M_t. Transverse magnetization (M_t) therefore provides a measurable signal which can be detected (Lipton, 2008d). At rest, no signal is generated as the net magnetization (NMV) of the sample is parallel to the external magnetic field (B_0) and no transverse magnetization (M_t) is generated. If the position of the NMV can be altered so that it lies at an angle to B_0, transverse magnetism will be

generated which can be measured. A flip of the NMV and hence generation of transverse magnetization (M_t) can be achieved by adding energy to the system (Lipton, 2008d).

The proton of the hydrogen atom can exist in two possible energy states, a lower energy state (E_1) and a higher energy state (E_2). In order to move between the energy states, energy must be emitted or absorbed. The laws of thermodynamics state that any system will exist in the lowest possible energy configuration, therefore in the resting state protons will be in the lower (E_1) energy state. The addition of energy results in the protons moving from the lower energy state (E_1) to the higher energy state (E_2). The transition between energy states results in a flip of the NMV and the generation of transverse magnetization (M_t) (Lipton, 2008b). Energy is introduced into the system by a second magnetic field (B_1), which is weaker than B_0 but rotates at the natural frequency of the protons (ω_0). The second magnetic field (B_1) delivers a radiofrequency (RF) pulse to the system which provides the energy required for the protons to move to the higher energy state (E_2), inducing a flip of the NMV and the generation of M_t (Lipton, 2008d). The E_2 configuration can only be maintained with the input of energy, therefore when the RF is shut off, the system returns to its lower (resting state) energy conformation (E_1) and the NMV returns to its original position, parallel to B_0 and transverse magnetization is lost. This return to resting state (M_0) is known as relaxation (Lipton, 2008c). During relaxation there is a recovery of longitudinal magnetization (M_z) and a loss of transverse magnetization (M_t). The rate of recovery of longitudinal magnetization (M_z) is represented by the time constant T1. T1 is the time required for 63% of the longitudinal magnetization (M_z) to be recovered. The loss of transverse magnetization (M_t) is represented by the time constant T2 and is the amount of time required for 63% of M_t to be lost. The loss of transverse magnetization occurs much more rapidly than the recovery of longitudinal magnetization, T2 is therefore always shorter than T1 (Lipton, 2008c). Tissues lose transverse magnetization and gain longitudinal magnetization at different rates. These differences in T1 and T2 mean the signal intensity obtained from each tissue varies, allowing the tissues to be distinguished (Lipton, 2008a; Weishaupt, Kochli and Marincek, 2006a). MRI can capture either the recovery of longitudinal magnetism (T1) or the loss of transverse magnetism (T2).

5.1.3.2 The use of contrast agents

Contrast agents are frequently used in MRI to increase the intensity of the signal obtained from a tissue, allowing the tissue and any areas of abnormality to be easily identified. The contrast agents used in MRI frequently contain the paramagnetic metal ion gadolinium chelated to a ligand. Currently used gadolinium based contrast agents include; gadopentetate dimeglumine (GdDTPA), gadoteridol (GdHP-DO3A), gadodiamide (GdDTPA-BMA) and gadoversetamide (GdDTPA-BMEA) (Runge, Muroff and Jinkins, 2001). Following I.V. administration the distribution of the contrast agent within the body varies depending upon the contrast agent administered. Extracellular contrast agents distribute in the vascular and interstitial spaces, while liver and lymph node specific contrast agents accumulate in liver cells and the lymph nodes respectively (Froehlich, 2006). In tissues which accumulate the contrast agent the rate of recovery of longitudinal magnetism (T_1) is shortened (Lipton, 2008a). As a result an increased signal intensity is detected on T_1 weighted images, allowing the tissue to be easily distinguished (Nelson and Runge, 1995). Contrast agents are unable to penetrate the blood-brain barrier (BBB) as they are strongly hydrophilic, therefore no signal enhancement is observed within the brain parenchyma (Froehlich, 2006). However, if the integrity of the BBB is compromised, the contrast agent is able to penetrate the barrier and an enhanced signal is detected in regions of the brain where the BBB is disrupted (Lipton, 2008a). Contrast agents therefore allow regions of the brain where the BBB is disrupted to be visualised and the degree of disruption to be quantified through the production of signal enhancement maps.

5.1.3.3 Magnetic resonance imaging of the CNS in disease

MRI has been extensively used to visualise the pathological changes in the brain and the BBB in numerous diseases. In the neurodegenerative disease, multiple sclerosis (MS), MRI is a vital tool in diagnosing and understanding the pathophysiological mechanisms of the disease as well as evaluating the efficacy of existing and novel treatment regimes.

5.1.3.3.1 Multiple sclerosis

Multiple sclerosis (MS) is an inflammatory demyelinating disease of the CNS, producing characteristic lesions known as 'plaques' in the white and gray matter, spinal cord and optic nerves (Rejdak, Jackson and Giovannoni, 2010). Patients display a wide range of neurological symptoms which can change as the disease progresses (Thompson, Toosy and Ciccarelli, 2010). Diagnosis of MS is primarily based on clinical evaluation (Lovblad, Anzalone, Dorfler, Essig *et al.*, 2010). MRI can aid in the diagnosis of MS as it enables lesions to be sensitively and accurately visualised and monitored over a period of time. As a result, when combined with clinical information, MRI enables an accurate and prompt diagnosis of MS to be made (Filippi and Rocca, 2007).

MRI analysis is also widely used in MS to monitor the efficacy of current and novel treatment regimes (Lovblad *et al.*, 2010; Sahraian and Eshaghi, 2010). Through conducting MRI scans prior to treatment and at regular intervals during and following completion of treatment, the ability of a compound to resolve existing lesions and to prevent the development of new ones can be assessed. If the MRI data shows that the treatment is having no effect then the treatment regime can be adjusted as necessary and then reassessed at a later time point. MRI is effective for monitoring the efficacy of chemotherapy in MS and has been shown to be 5 to 10 times more sensitive at detecting disease activity than conventional clinical assessments (Rovaris and Filippi, 2005).

5.1.3.3.2 Cerebral malaria

Cerebral malaria is a serious and often lethal complication of *Plasmodium falciparum* infection (Looareesuwan, Laothamatas, Brown and Brittenham, 2009). It is characterised by a diffuse encephalopathy accompanied by seizures and a loss of consciousness (Beales, Brabin, Dorman, Gilles *et al.*, 2000). The disease is associated with a high mortality rate, even with the administration of anti-malarial chemotherapy and supportive treatment. Patients who do recover are often left with long-term neurocognitive defects (Medana and Turner, 2006). Despite extensive investigations, the pathophysiology of cerebral malaria is still not fully understood. It is thought to arise due to a complex interplay of parasite and host factors. In an attempt to understand the pathophysiological

mechanisms of cerebral malaria, MRI has been utilised to visualise the changes that arise at the level of the BBB, in *in-vivo* models of the disease and in patients (Looareesuwan, Wilairatana, Krishna, Kendall *et al.*, 1995; Penet, Viola, Confort-Gouny, Le Fur *et al.*, 2005; Sibson, Blamire, Perry, Gauldie *et al.*, 2002; zur Muhlen, Sibson, Peter, Campbell *et al.*, 2008).

The pathophysiological alterations that occur within the brain of mice infected with *P. berhei* was investigated by Penet *et al*. (Penet *et al.,* 2005). MRI analysis revealed major alterations in the cerebral structure and vasculature. Vascular dysfunction was characterised by a breakdown of the BBB, a reduction in cerebral blood flow and severe arterial flow perturbations. In addition, a pronounced cerebral edema and inflammatory lesions within the parenchyma were observed (Penet *et al.,* 2005). From the study the authors concluded, that experimental cerebral malaria was an ischemic pathology, characterised by a severe edema (Penet *et al.,* 2005). In addition to enabling the alterations that occur within the brain during experimental cerebral malaria to be characterised, MRI is being increasingly used in patients to gain a better understand of the pathogenesis, and ultimately improve treatment of the disease. Looareesuwan *et al*. conducted a MRI study in 24 adults infected with *P. falciparum*, suffering from cerebral malaria (Looareesuwan *et al.,* 1995). MRI analysis revealed a swelling of the brain which was attributed to an increase in the volume of intracerebral blood. In contrast to the study conducted by *Penet et al*., in mice, cerebral edema was not observed in any of the patients. This difference between the two studies may be attributed to the different species of *Plasmodium* and host species investigated.

5.1.3.3.3 Human African trypanosomiasis

Large scale MRI studies on HAT patients are impossible to complete due to the isolated nature of the regions in which the disease occurs. The MRI studies that have been performed are restricted to individual case reports from patients treated out with Africa who contracted HAT before leaving the continent (Kager et al 2009, Hilde et al 2006, Gill et al 2002, Sabbah et al 1997). In one patient infected with the west African variant *T. b. gambiense*, hyperintensity was observed in both the periventricular white matter and midbrain along with an increased signal intensity in the basal ganglia. One year later, following

successful treatment with eflornithine, the hyperintensity in the basal ganglia and white matter had decreased but a moderate ventricular enlargement was still observed (Gill, Chatha and Carpio-O'Donovan, 2003). This is not the only study to report the persistence of lesions in the brain as detected by MRI following successful chemotherapy for HAT. In a woman infected with *T. b. gambiense* Kager *et al*. observed only minor improvements nine months after treatment despite the patient having improved both mentally and physically (Kager, Schipper, Stam and Majoie, 2009). Two years after successful treatment hyperintense signals were still observed in the corona radiate, the right cerebral white matter and the right basal nuclei. By four years post-treatment only remnants of the hyperintensity in the white matter and right basal nuclei remained. Persistence of lesions in the brain following successful chemotherapy for HAT are not restricted to infections with *T. b. gambiense*. Sabbah *et al*. reported MRI findings from a patient infected with the more acute east African variant *T. b. rhodesiense* (Sabbah, Brosset, Imbert, Bonardel *et al.*, 1997). Initial MRI analysis revealed a thickening of the meninges and subsequent imaging, midway through melarsoprol therapy, revealed a high signal intensity in the posterior limb of both internal capsules, middle cerebellar peduncles and the splenium of the corpus callosum. In addition, symmetrical, focal lesions were detected in the deep white matter of the internal capsules, cerebellum and corpus callosum. One year after successful melarsoprol treatment residual lesions in the left cerebellum remained.

In addition to being used to assess brain lesions in HAT patients, MRI has also proved useful in distinguishing between the PTRE and HAT induced encephalitis (Sabbah *et al.*, 1997). As discussed previously (Chapter 1) the PTRE is a serious complication of melarsoprol therapy, occurring in up to 10% of all patients treated with the drug, of which 50% will die as a result of the complication (Kennedy, 2004; Pepin and Milord, 1994). It is therefore important that the PTRE is rapidly and correctly diagnosed so that melarsoprol treatment can be suspended and supportive treatment administered. Sabbah *et al*. reported the use of MRI analysis to distinguish between the PTRE and HAT induced encephalitis in a patient infected with *T. b. rhodesiense* (Sabbah *et al.*, 1997). The patient received three, four day courses of melarsoprol, with a seven day, drug free interval between each course. Approximately one week after

completion of the second course of melarsoprol, the patient developed twitching, right hemiparesis, pyramidal syndrome, difficulty in swallowing and static and dynamic bilateral cerebellar syndrome. These symptoms and the timing of their appearance are suggestive of the PTRE. However, T2-weighted MRI analysis showed a symmetrical high signal intensity in the posterior limb of both internal capsules, middle cerebellar peduncles and the splenium of the corpus callosum. No brain oedema or focal lesions were observed (Sabbah *et al.,* 1997). These MRI findings are consistent with HAT induced encephalitis rather than the PTRE. As a result, the decision was made to continue melarsoprol treatment and the third course was administered to the patient. The patient subsequently recovered and MRI analysis one year later revealed all abnormalities with the exception of small residual foci in the left cerebellum had resolved. In a second case, a patient infected with *T. b. rhodesiense* and receiving melarsoprol therapy as three series of four injections of 3.6mg/kg/day, with a seven day drug free interval between each series, developed generalised tonic clonic seizures 23 hours after completion of the second treatment series (Checkley, Pepin, Gibson, Taylor *et al.*, 2007). MRI analysis revealed widespread bilateral abnormalities involving the supratentorial and infratentorial white matter. Multiple microhaemorrhages were also detected in some of these areas including the midbrain and brain stem using T2* scanning procedures. The PTRE was diagnosed and melarsoprol treatment suspended until the patients symptoms improved (Checkley *et al.,* 2007). These studies indicate the value of MRI in the diagnosis and management of the PTRE. However, despite its usefulness it is highly unlike that the technology will become available to the majority of HAT patients in sub-Saharan Africa.

The MRI studies reported in patients are very limited. In order to fully investigate the effect of trypanosome infection on the integrity of the BBB, small animal studies need to be completed. Recently the first MRI study in a murine model of CNS stage *T. b. brucei* infection was conducted by Rodgers and colleagues (Rodgers, McCabe, Gettinby, Bradley *et al.*, 2011). MRI scans were performed on mice prior to infection and 28 days after infection with *T. b. brucei* when a CNS infection is established. The use of a contrast agent enabled signal intensity maps to be generated and these were then compared to histological images in order for any relationship between areas of inflammation

and areas of BBB breakdown to be established. In infected animals, the percentage signal change detected following injection of the contrast agent was significantly higher than in uninfected animals, indicating a break down in the BBB (Rodgers *et al.,* 2011). Areas of increased signal intensity were detected throughout the brain and were not confined to the meninges, hippocampus or ventricles. No correlation was detected between areas of inflammation as observed by histology and the areas of increased signal intensity. This study demonstrated the integrity of the BBB is significantly compromised during early CNS stage *T. b. brucei* infection in mice. However, it is currently unknown if the integrity of the BBB is restored following successful chemotherapy.

Complexed melarsoprol can cure CNS stage *T. b. brucei* infection in mice following oral administration at a daily dose of 0.05mmol/kg for seven consecutive days. However, it has been shown in humans by MRI analysis that brain lesions persist long after completion of successful chemotherapy (Gill, Chatha and Carpio-O'Donovan, 2003; Kager *et al.,* 2009; Sabbah *et al.,* 1997). This chapter aims to use small bore MRI to investigate the level of BBB dysfunction present prior to the commencement of chemotherapy and to establish, through serial MRI, if BBB dysfunction resolves following successful chemotherapy with the melarsoprol cyclodextrin complex mel/HPβCD.

5.2 Methodology

5.2.1 Trypanosome infection

Female CD-1 mice aged approximately 6 to 8 weeks and weighing 25 to 30g were injected intraperitoneally with 2 x 10^4 *T. b. brucei* trypanosomes. The methodology detailing the preparation of the trypanosomes prior to inoculation is provided in chapter 2.

5.2.2 Confirmation of trypanosome infection

Prior to chemotherapy commencing it was confirmed that a trypanosome infection had been successfully induced in the animals by examining a wet blood film prepared from tail blood of each animal, under a microscope for the presence of trypanosomes. The level of parasitaemia in each animal was scored using the system detailed in chapter 2.

5.2.3 Preparation of complexed melarsoprol for administration

The melarsoprol cyclodextrin complex mel/HPβCD is provided as a fine white powder with the ratio of melarsoprol to cyclodextrin quantified for each batch. The ratio of melarsoprol to cyclodextrin for the complex used in this study was 1:17. Taking this ratio into account the amount of the mel/HPβCD complex required to give a melarsoprol dose of 0.05mmol/kg was calculated. The full details regarding the calculation of the dose are provided in chapter 2.

5.2.4 The treatment schedule employed

To determine the level of damage to the blood-brain barrier prior to chemotherapy commencing an MRI scan was performed on the mice at day 21 post-infection. At this point trypanosomes have penetrated the blood-brain barrier and a CNS stage infection is established in the animals. Following the recovery of the animals from the MRI procedure, mel/HPβCD was administered by oral gavage at a dose of 0.05mmol/kg, daily, for seven consecutive days, as previously described (chapter 2). MRI scans were subsequently performed on

days 28, 35 and 42 post-infection corresponding to 24 hours, 8 and 15 days after the completion of chemotherapy (Figure 5-4).

		S							S	S	S
I	>	M	M	M	M	M	M	M	>	>	>
		21							28	35	42

Figure 5-4: The treatment schedule employed in the MRI study
The animals were infected with 2 x10^4 *T. b. brucei* trypanosomes (I) on day 0. On day 21 post-infection an MRI scan (S) was performed on the animals. Following the recovery of the animals mel/HPβCD (M) was administered orally, at a dose of 0.05 mmol/kg, daily for 7 consecutive days. Subsequent MRI scans (S) were performed on days 28, 35 and 42 post-infection corresponding to 24 hours, 8 and 15 days after the completion of chemotherapy.

5.2.5 Magnetic resonance imaging

5.2.5.1 Preparation of animals

Animals were anaesthetised with 1-2% isofluorane delivered as a mixture of 70:30 $N_20:0_2$. In order to allow remote administration of the contrast agent a tail vein was cannulated with a 26 gauge x 19mm cannula. The animal was placed in a mouse cradle and restrained using tooth and ear bars to prevent movement. Throughout the procedure the body temperature of the animal was monitored by a rectal thermo probe and adjusted as necessary by an enclosed water circuit. Anaesthesia was maintained throughout the procedure and the level of anaesthesia monitored by observation of the respiration and heart rate.

5.2.5.2 Magnetic resonance imaging parameters

A Bruker Biospec 7T/30cm system equipped with an inserted gradient coil (121mm ID, 400mT/m) and a 72mm birdcage resonator was used to perform the MRI imaging. Brain images were obtained by using a surface coil placed directly above the animal's head. The scanning protocol consisted of a RARE (rapid acquisition with relaxation enhancement) T_1 weighted scan [effective TE (echo time) 76ms, TR (repetition time) 5362ms, 25 averages, matrix 176 x 176, FOV (field of view) 17.6 x 17.6 mm, 20 contiguous coronal slices of 0.4mm thickness] followed by a RARE T_2 weighted scan (effective TE 9ms, TR 8000ms, 25 averages, matrix 176x176, FOV 17.6 x 17.6 mm, 20 contiguous coronal slices of 0.4mm thickness). After completion of the RARE T_2 weighted scan the contrast agent

diethylenetriamine penta-acetic acid (Gd-DPTA Magnevist®) was administered in a volume of 0.1ml consisting of 50µl Gd-DPTA Magnevist® and 50µl of sterile water via the cannulated tail vein. Five minutes after administration of the contrast agent the T_1 weighted scan was repeated.

5.2.5.3 Analysis of magnetic resonance images

All magnetic resonance images were analysed using the software image J (http://rsbweb.nih.gov/ij/). Prior to analysis the pre and post contrast images were normalised by dividing each image by its respective reco map slope value. Signal enhancement maps were subsequently generated from the normalised pre and post contrast images using Equation 5-1:

$$\text{Signal change} = \frac{(\text{post contrast image} - \text{pre contrast image})}{\text{pre contrast image}} \times 100$$

Equation 5-1: The equation used to generate signal enhancement maps

In order to calculate the signal enhancement observed in each animal the entire brain and meninges were manually selected in each of the 20 coronal slices and the percentage signal change calculated for each slice.

5.2.6 Collection of samples for analysis of inflammatory reaction

Following the final MRI scan, 15 days after completion of mel/HPβCD chemotherapy, animals were culled by exposure to increasing levels of carbon dioxide. An additional group of mice was also sacrificed on day 21 post-infection and served as untreated controls. Following sacrifice the brain was carefully excised and placed in 4% neutral buffered formalin.

5.2.7 Preparation of samples for analysis of inflammatory reaction

The brain tissues were removed from the neutral buffered formalin and processed to paraffin blocks. From the paraffin blocks 3µm thick sections were cut and mounted onto glass microscope slides. The sections were stained with

haematoxylin and eosin (H&E) in order to assess the severity of the inflammatory reaction.

5.2.8 Analysis of inflammatory reaction

The H&E stained brain sections were examined under light microscopy at a magnification of 200 fold. The severity of the meningitis, the occurrence of and extent of perivascular cuffing and the degree of inflammatory cell infiltration of the brain parenchyma was assessed and graded in each section, using a neuropathological grading scale previously described (Kennedy, Rodgers, Jennings, Murray *et al.*, 1997). The criteria defining each neuropathological grade are described in Table 5-1. Briefly, a score of 0 represents normal histopathology, with no infiltration of inflammatory cells. Animals displaying a mild meningitis with a few inflammatory cells present in the meninges but no perivascular cuffing were assigned a grade 1 while mice displaying a moderate meningitis with perivascular cuffing of some of the vessels were graded as 2. As the inflammatory reaction progresses, the severity of the meningitis increases and perivascular cuffing becomes more apparent. The neuropil also becomes infiltrated with small populations of inflammatory cells. Animals displaying this level of inflammation were assigned a neuropathological score of 3. A grade of 4 was given to animals displaying a severe meningitis, with prominent perivascular cuffing of the vessels, accompanied by a severe encephalitis and the presence of numerous inflammatory cells in the neuropil. Each section was graded independently by two assessors in a blinded fashion.

5.2.9 Statistical analysis

Data was analysed using analysis of variance methods, in particular the General Linear Model (GLM) in Minintab 16. This provided a method for investigating significant main effect differences and interactions between factors such as uninfected animals, infected animals and treated animals. Significance was measured using the P-value at the 5% significance level. Effect sizes were further investigated using 95% confidence intervals for the differences between means.

	0	1	2	3	4
Meningitis	None	Mild	Moderate	Severe	Severe
Perivascular cuffing	None	None	Mild cuffing of some vessels	Prominent cuffing of some vessels	Prominent cuffing of most vessels
Encephalitis as defined by cellular activity in the neuropil	None	None	None	Moderate	Severe

Table 5-1: Neuropathological grading scale
This table details the criteria that define the neuropathological grading score associated with specific levels of the CNS inflammatory reaction. The severity scores are given horizontally along the top of the table; the parameters defining the specific scores are shown vertically (Kennedy *et al.,* 1997).

5.3 Results

5.3.1 MRI

The integrity of the BBB in mice infected with *T. b. brucei* was investigated on day 21 post-infection by MRI. Mel/HPβCD chemotherapy was then administered and the integrity of the BBB re-evaluated 24 hours, 8 and 15 days after completion of chemotherapy. Animals were serially scanned but in some cases it was not possible to complete all four scans on the same animal. Details of the scans completed on each animal are provided in Table 5-2.

5.3.1.1 Comparison of the signal change detected on day 21 post-infection and in uninfected animals

Analysis was completed using the scan data obtained from uninfected, untreated animals and infected animals, numbers 102, 103, 105 and 106, on day 21 post-infection, immediately prior to chemotherapy commencing (Table 5-2). The percentage signal change detected following injection of contrast agent in mice at 21 days post-infection (mean = 19.11 ± 0.955) was significantly higher ($P < 0.0001$) than that seen in uninfected control animals (mean = 7.11 ± 1.26). This represents a mean increase of 12% with 95% confidence interval [13.925, 10.080]. The difference in the percentage signal change between infected and uninfected animals can clearly be seen on the signal enhancement maps shown in Figure 5-5. The areas of bright colouration indicate regions where an increased signal is observed. In infected animals (Figure 5-5, panel b), an increased signal was observed in several regions of the brain including the cerebral cortex, hypothalamus, hippocampus and median essence. The ventricular region displayed the highest level of signal change. In contrast, minimal signal change was observed in uninfected control animals (Figure 5-5, panel a).

	101	102	103	105	106	107
Day 21 Post-infection (pre treatment)	X	√	√	√	√	X
24 hours after completion of chemotherapy	√	√	X	√	X	√
8 days after completion of chemotherapy	√	√	X	√	X	√
15 days after completion of chemotherapy	√	√	X	√	X	√

Table 5-2: The MRI scans completed in each animal
The information in the body of the table demonstrates if the MRI scan was completed in that animal. The animal number and details of the MRI scan are displayed in the column and row headings respectively. A '√' indicates the MRI scan was completed in the animal, while 'X' means the scan was not completed.

5.3.1.2 Comparison of the percentage signal change detected on day 21 post-infection and following completion of mel/HPβCD chemotherapy

Analysis was completed using the scan data obtained from animals 102 and 105 (Table 5-2) and uninfected, untreated animals. The percentage signal change detected prior to chemotherapy commencing on day 21 post-infection was compared to the levels detected 24 hours, 8 and 15 days after the completion of mel/HPβCD chemotherapy and also to normal uninfected, untreated mice (Figure 5-6, panel A). Twenty-four hours after completion of mel/HPβCD chemotherapy the percentage signal change detected was significantly lower (mean = 7.93 ± 0.455) than that seen prior to treatment commencing on day 21 post-infection (mean = 17.9 ± 1.62) ($P < 0.0001$). This represents a mean decrease of 10% with 95% confidence interval [6.862, 13.02]. The decrease in signal intensity can be visualised on signal enhancement maps (Figure 5-5). There is a decrease in the level of signal observed in the hypothalamus, thalamus, cerebral cortex and median essence. A hyperintensity can be seen in the ventricluar region although it is reduced compared to the level observed prior to treatment commencing. The percentage signal change detected twenty-four hours after the completion of mel/HPβCD treatment is not significantly different ($P = 0.9296$) to the level observed in uninfected, untreated control animals (7.1 ± 0.162). This indicates that by twenty-four hours after completion of mel/HPβCD chemotherapy the integrity of the BBB is restored. The percentage signal change observed within the brain eight days (9.2 ± 0.596) after the completion of mel/HPβCD treatment was significantly lower ($P=<0.0001$) than the level observed prior to treatment commencing on day 21 post-infection. However, the percentage signal change detected eight days (9.2±0.596) after treatment completion was not significantly different ($P=0.7622$) to the level observed twenty-four hours (7.9 ± 0.455) after completion of chemotherapy. Fifteen days after completion of mel/HPβCD chemotherapy the percentage signal change detected (6.6 ± 0.463) within the brain was significantly lower ($P < 0.0001$) than the level observed prior to treatment commencing on day 21 post-infection (17.87 ± 1.62). However, the percentage signal change observed fifteen days (6.6 ± 0.463) after completion of treatment was not significantly different to the level detected twenty-four hours

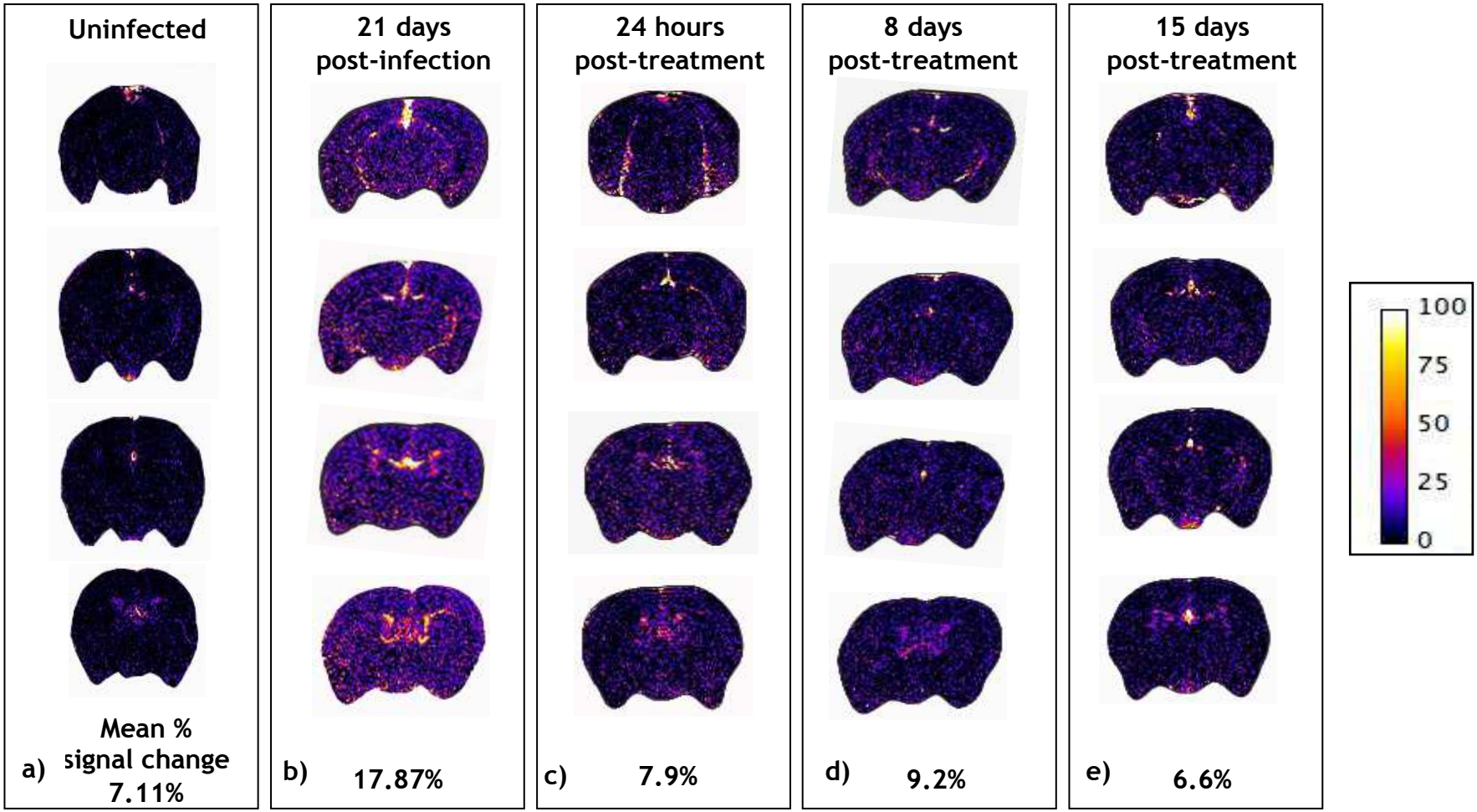

Figure 5-5: The signal enhancement maps generated following magnetic resonance imaging
Signal enhancement maps for four brain slices obtained from magnetic resonance imaging a) in an uninfected animal, b) 21 days after infection with *T. b. brucei* trypanosomes immediately prior to mel/HPβCD chemotherapy commencing. c) 24 hours after completion of the chemotherapy regime, d) 8 days after completion of treatment and e) 15 days after completion of the treatment regime. Mel/HPβCD was administered orally, daily, for 7 consecutive days at a dose of 0.05mmol/kg.

(P = 0.7370) and eight days after completion of the treatment regime (P = 0.1177). Summary statistics are detailed in Table 5-3.

5.3.1.3 Comparison of the percentage signal change detected 24 hours, 8 and 15 days after completion of mel/HPβCD chemotherapy

Analysis was completed using the scan data obtained from animals 101, 102, 105 and 107 (Table 5-2). The percentage signal change detected in the brain 24 hours, 8 and 15 days after completion of mel/HPβCD chemotherapy was compared to the level observed in untreated, uninfected animals (Figure 5-6, panel B). Twenty-four hours after the completion of mel/HPβCD chemotherapy the percentage signal change (8.510 ± 0.375) observed in the brain was significantly higher (P = 0.0254) than the level observed in untreated, uninfected control animals (P = 7.105 ± 0.339). Eight days after the completion of mel/HPβCD treatment, the percentage signal change (8.556 ± 0.361) was significantly higher (P = 0.0193) than the level observed in uninfected, untreated control animals (7.105 ± 1.62). However, the percentage signal change observed eight days (8.556 ± 0.362) after the completion of treatment was not significantly different (P = 0.9996) to the level observed twenty-four hours after completion of chemotherapy (8.510 ± 0.361). Fifteen days after the completion of mel/HPβCD therapy, the percentage signal change detected (7.103 ± 0.339) within the brain was not significantly different (P = 1.000) to the level observed in uninfected, untreated control animals (7.105 ± 1.62). The percentage signal change detected within the brain fifteen days after treatment completion was significantly lower than the level observed twenty-four hours (P = 0.0126) and eight days (P = 0.0091) after the completion of chemotherapy. Summary statistics are detailed in Table 5-4.

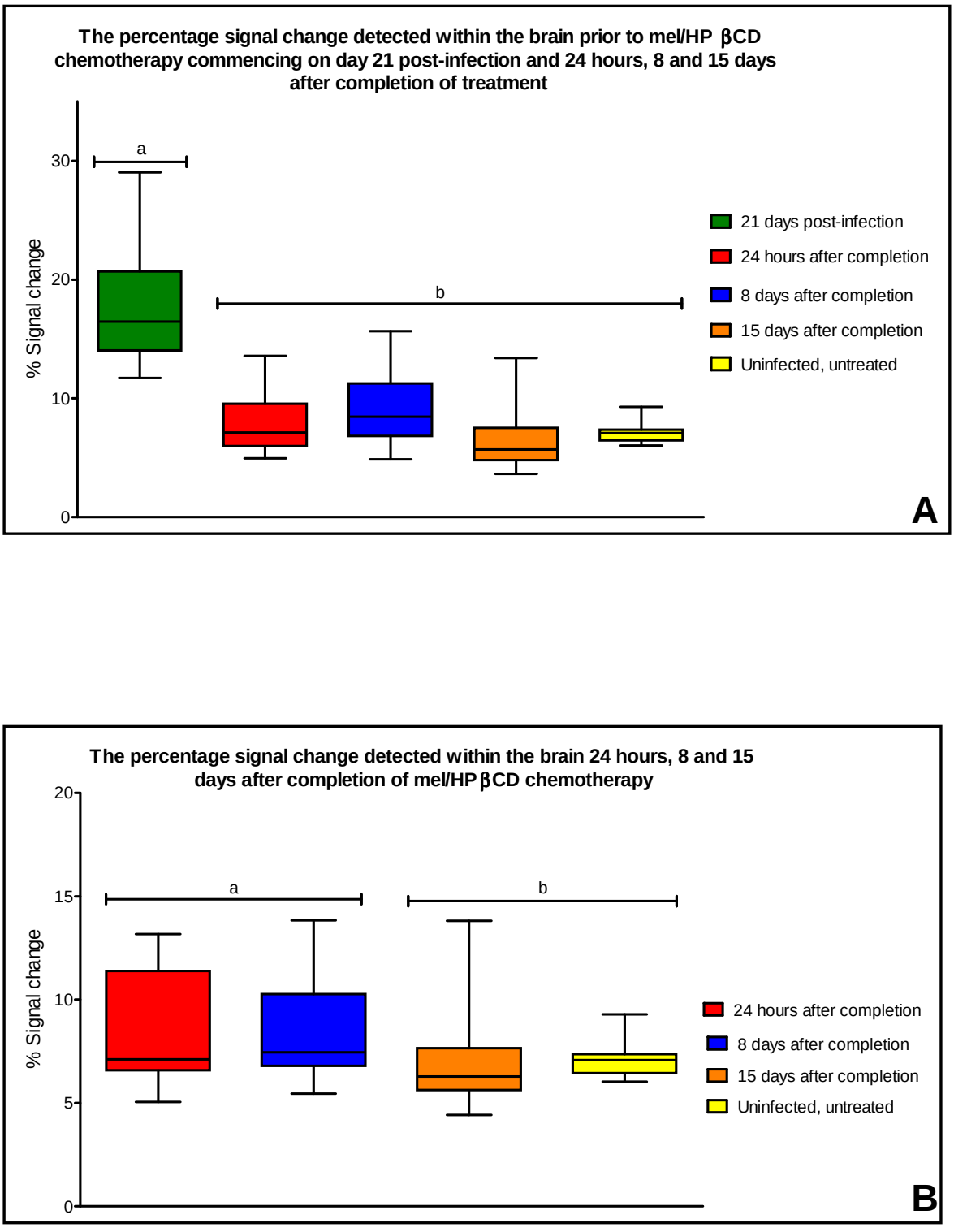

Figure 5-6: The percentage signal change detected by MRI in mice infected with *T. b. brucei*
A) Immediately prior to mel/HPβCD chemotherapy commencing on day 21 post-infection and 24 hours, 8 and 15 days after completion of treatment. B) 24 hours, 8 and 15 days after completion of mel/HPβCD chemotherapy. Mel/HPβCD was administered orally, daily, for 7 consecutive days at a dose of 0.05mmol/kg commencing on day 21 post-infection. The box plots illustrate the median, interquartile range and minimum and maximum percentage signal change detected at each time point. Groups which do not share a letter are significantly different $P < 0.05$.

5.3.2 Neuropathological reaction

The inflammatory reaction present in the brain on day 21 post-infection and 15 days after the completion of mel/HPβCD chemotherapy was scored using the neuropathological grading scale detailed in Table 5-1. On day 21 post-infection an early stage CNS infection is established and mice killed at this time point exhibited mild neuroinflammatory changes (Figure 5-7, panel A and C), with a neuropathology score of 1.5 ± 0.158 (n = 5). Inflammatory cells were apparent in the meninges and the Virchow robin spaces. An infiltration of inflammatory cells was also observed in the perivascular space surrounding some of the blood vessels in the hippocampus. The inflammatory cell infiltrate was composed of macrophages, lymphocytes and plasma cells. Fifteen days after the completion of mel/HPβCD chemotherapy the neuroinflammatory reaction present in the brain was significantly reduced (P = 0.0366) compared to animals killed on day 21 post-infection. A mean neuropathological score of 1.083 ± 0.083 (n = 6) was detected compared to 1.5 ± 0.158 (n = 5) on day 21 post-infection. This represents a mean decrease of 27.8% with 95% confidence interval [0.032, 0.801]. Fifteen days after the completion of mel/HPβCD chemotherapy mice exhibited very minor neuroinflammatory changes (Figure 5-7, panels B and D). A small number of inflammatory cells were apparent in the meninges and perivascular cuffing was observed sporadically around the blood vessels of the hippocampus.

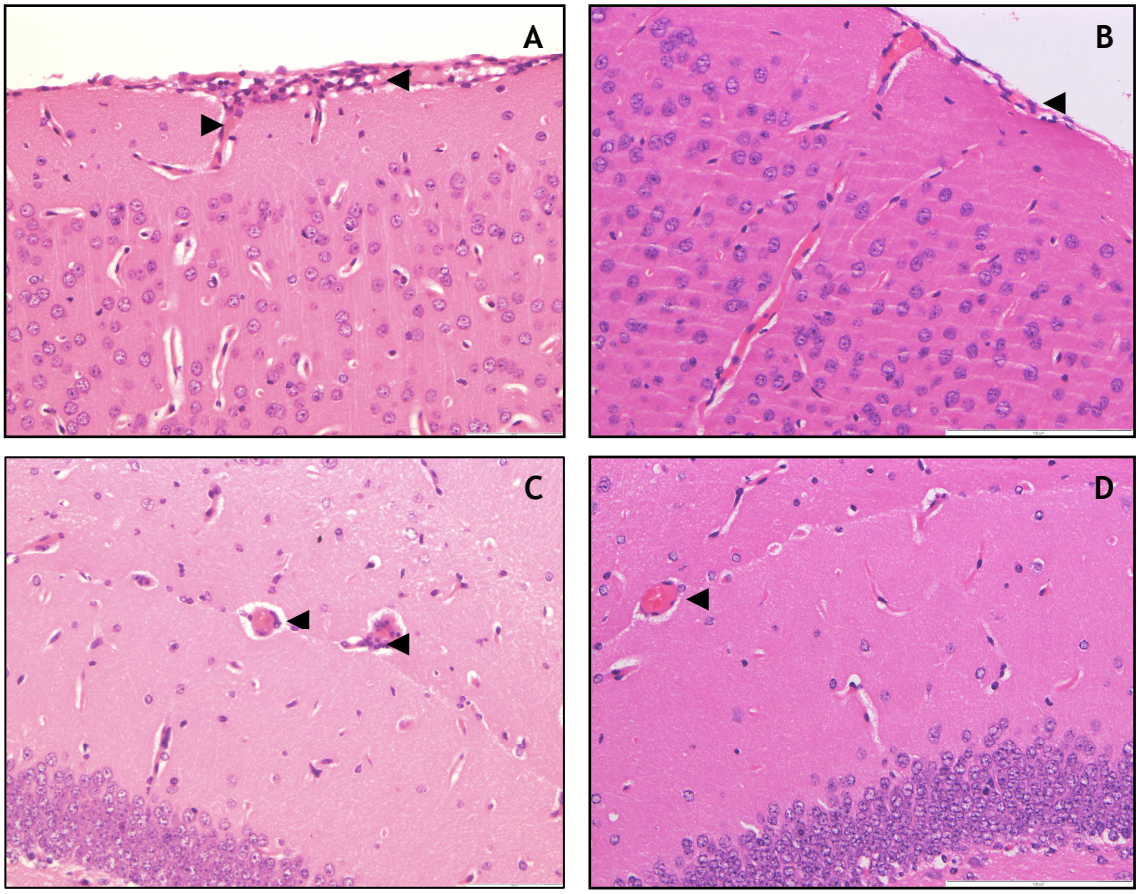

Figure 5-7: Coronal sections through the brain of a mouse 21 days after infection with *T. b. brucei* (A and C) and a mouse killed 15 days after completion of mel/HPβCD chemotherapy (B and D)

Mice were infected with *T. b. brucei* trypanosomes. A mouse (A and C) was killed on day 21 post-infection immediately prior to mel/HPβCD chemotherapy commencing. A second mouse (B and D) was administered mel/HPβCD at a dose of 0.05mmol/kg, daily, for 7 consecutive days commencing on day 21 post-infection. The animal was sacrificed 15 days after the completion of treatment. Infiltrating inflammatory cells (arrowheads) can been seen in the meninges of the cerebral cortex (A) and surrounding the blood vessels in the hippocampus (C) in the animal sacrificed on day 21 post-infection. In the animal sacrificed 15 days after completion of mel/HPβCD chemotherapy only small numbers of inflammatory cells (arrowheads) are observed within the meninges (B) and surrounding the blood vessels of the hippocampus (D).

	Untreated, uninfected	21 days post-infection, untreated	24 hours post-treatment	8 days post-treatment	15 days post-treatment
21 days post-infection, untreated	P < 0.0001 (7.951, 13.576)				
24 hours post-treatment	P = 0.9296 (-1.992, 3.633)	P < 0.0001 (-13.02, -6.862)			
8 days post-treatment	P = 0.2254 (-0.669, 4.956)	P < 0.0001 (-11.70, -5.539)	P = 0.7622 (-1.758, 4.404)		
15 days post-treatment	P = 0.9832 (-3.363, 2.261)	P < 0.0001 (-14.40, -8.234)	P = 0.7370 (-4.452, 1.709)	P = 0.1177 (-5.775, 0.3862)	
Mean ± SE N	7.1 ± 0.162 3	17.87 ± 1.62 2	7.93 ± 0.45 2	9.2 ± 0.60 2	6.55 ± 0.46 2

Table 5-3: Comparison of the percentage signal change detected within the brain, prior to mel/HPβCD chemotherapy commencing on day 21 post-infection and 24 hours, 8 and 15 days (corresponding to days 28, 35 and 42 post-infection respectively) after completion of the treatment regime and in uninfected, untreated animals

Mice were infected with *T. b. brucei* GVR35/C1.9. Immediately prior to treatment commencing on day 21 post-infection, animals were MRI scanned. Following recovery from the MRI procedure animals were administered mel/HPβCD orally at a dose of 0.05mmol/kg. Mel/HPβCD treatment continued for the next 6 days. Twenty-four hours, 8 and 15 days after administration of the last dose, corresponding to days 28, 35 and 42 post-infection respectively, the MRI scans were repeated. Each MRI scan consisted of 20 continuous coronal slices. The entire brain and meninges was manually selected in each slice and the percentage signal change calculated. The figures in the body of the table demonstrate the comparisons, in terms of statistical significance, between the groups shown in the row and column headings. The P-values and 95% confidence intervals are based on analysis using the percentage signal change for each slice. The mean signal change ± the standard error (mean ± SE) and the number of animals per group (n) are also shown.

	Untreated, uninfected	24 hours post- treatment	8 days post-treatment	15 days post-treatment
24 hours post-treatment	P = 0.0254 (0.123, 2.686)			
8 days post-treatment	P = 0.0193 (0.168, 2.732)	P = 0.9996 (-1.141, 1.2325)		
15 days post-treatment	P = 1.000 (-1.284, 1.280)	P = 0.0126 (-2.593, -0.2198)	P = 0.0091 (-2.639, -0.2657)	
Mean ± SE N	7.105 ± 1.62 3	8.510 ± 0.375 4	8.556 ± 0.361 4	7.103 ± 0.3339 4

Table 5-4: Comparison of the percentage signal change detected in the brain 24 hours, 8 and 15 days (corresponding to days 28, 35 and 42 post-infection respectively) after completion of mel/HPβCD chemotherapy to untreated, uninfected control animals

Mice were infected with *T. b. brucei* GVR35/C1.9. On day 21 post-infection mel/HPβCD chemotherapy commenced. The drug was administered orally, daily, for 7 consecutive days at a dose of 0.05mmol/kg. Twenty-four hours, 8 and 15 days (corresponding to days 28, 35 and 42 post-infection respectively) after completion of the treatment regime, animals were MRI scanned. Each MRI scan consisted of 20 continuous coronal slices. The entire brain and meninges was manually selected in each slice and the percentage signal change calculated. The figures in the body of the table demonstrate the comparisons, in terms of statistical significance, between the groups shown in the row and column headings. The P-values and 95% confidence intervals are based on analysis using the percentage signal change for each slice. The mean signal change ± the standard error (mean ± SE) and the number of animals per group (n) are also shown.

5.4 Discussion

Trypanosomes are able to penetrate the BBB and invade the CNS. However, the mechanisms by which the trypanosomes transverse the barrier and the point in infection at which BBB integrity is compromised remains unclear. The integrity of the BBB on day 21 post-infection in experimental murine *T. b. brucei* infection and the subsequent effect of a curative therapeutic regime with mel/HPβCD on the BBB was investigated by small bore MRI.

At day 21 post-infection, BBB dysfunction was already evident with the integrity of the barrier compromised. Damage to the BBB was particularly evident in the ventricular region. In agreement with the present study Philip *et al.* also reported an increase in BBB permeability in early CNS stage *T. b. brucei* infection (Philip *et al.,* 1994). In this study the penetration of rhodamine into the brain parenchyma was investigated at different time points during the course of the infection. On day 21 post-infection, low levels of dye were occasionally observed in the thalamus and hypothalamus, indicating that some damage to the BBB had occurred in these regions. In a study by Sanderson *et al.* the integrity of the BBB was investigated in BALB/c mice at 7, 14, 21, 28 and 35 days post-infection, by perfusing animals with [^{3}H] eflornithine and [^{14}C] sucrose and subsequently calculating the tissue radioactivity (Sanderson, Dogruel, Rodgers, Bradley *et al.*, 2008). Sucrose is incapable of penetrating the BBB therefore its presence in the brain means the integrity of the BBB has been compromised. No difference in the tissue [^{14}C] radioactivity levels were observed between uninfected and infected animals between days 7 and 21 post-infection, indicating that the integrity of the BBB was still intact up to day 21 post-infection. Dysfunction of the BBB was not observed until day 28 post-infection this is 7 days later than in the present study and the study by Philip *et al.* (Philip *et al.,* 1994). The discrepancies observed between the present study and that of Sanderson *et al.* may be due to the different animal models used in the two studies. The present study used the GVR35/C1.9 *T. b. brucei* model in CD-1 mice, which is very well characterised and established. CNS stage disease is reached between 14 and 21 days post-infection (Jennings and Gray, 1983). If the infection is allowed to run its natural course there is a gradual increase in the CNS involvement characterised by a diffuse encephalitis. The animals eventually

succumb to the infection around 30 days post-infection. The study by Sanderson *et al*. also used the GVR35/C1.9 *T. b. brucei* model but in BALB/c mice instead of CD-1 mice (Sanderson *et al.,* 2008). The disease progression in BALB/c mice is not as well characterised as in CD-1 mice. In BALB/c mice, a CNS infection is established from 11 days post-infection, which is earlier than in CD-1 mice (Jennings and Gray, 1983; Sanderson *et al.,* 2008). However, despite CNS stage disease establishing earlier in BALB/c mice, the time course of the infection is prolonged, with mice not succumbing to the infection until 38 days post-infection (Sanderson *et al.,* 2008). This is approximately 8 days later than in CD-1 mice. The shorter infection time course in CD-1 mice could mean that BBB damage occurs at an earlier point in the infection compared with BALB/c mice. This could explain why BBB dysfunction was observed at 21 days post-infection in this study but not in the study conducted by Sanderson *et al*.

A breakdown of the BBB during *T. b. brucei* infection in CD-1 mice has been previously reported by Rodgers *et al*. (Rodgers *et al.,* 2011). In the study the integrity of the BBB at day 28 post-infection, was investigated by small bore MRI analysis. As in the present study the integrity of the BBB was compromised, with a mean percentage signal change of 26.7% detected. This is 7.6% higher than the level detected in the present study. However, in the study conducted by Rodgers *et al*. the scan was performed at 28 days post-infection which is 7 days later than in the present study. The results from this study and the study by Rodgers *et al*. therefore suggest that there is a progressive breakdown of the BBB during *T. b. brucei* infection in CD-1 mice.

In addition to assessing the level of BBB dysfunction present at 21 days post-infection, the effect of mel/HPβCD chemotherapy on BBB function was also investigated. The melarsoprol cyclodextrin complex mel/HPβCD was able to reverse the BBB dysfunction induced by *T. b. brucei* infection. Twenty-four hours after completion of the chemotherapy regime normal BBB function had been restored. This is the first report of the use of MRI to investigate the effect of chemotherapy on BBB integrity in experimental trypanosomiasis. In the current study no persistence of the barrier changes detected by MRI on day 21 post-infection were observed following chemotherapy with the melarsoprol cyclodextrin complex mel/HPβCD. This is in contrast to the studies by Kager *et*

al. and Sabbah *et al*. who reported the presence of CNS lesions in patients treated for HAT, up to four years after completion of chemotherapy (Kager *et al.*, 2009; Sabbah *et al.*, 1997).

A possible explanation for the quick recovery of BBB integrity observed in the present study following the completion of mel/HPβCD chemotherapy is the speed at which trypanosomes were eliminated from within the brain. QPCR analysis has shown that by twenty-four hours after administration of the fourth dose of mel/HPβCD no copies of the PFR2 gene were detected within the brain (details contained in chapter 4). Furthermore, once the PFR2 gene has been eliminated from the brain it does not reoccur. By rapidly eliminating trypanosomes from the brain, further damage to the BBB is prevented and the BBB is able to begin repairing itself. In the present study BBB integrity was restored by twenty-four hours after completion of mel/HPβCD chemotherapy. As trypanosomes were eliminated by twenty-four hours after administration of the fourth dose, this means that for the three days immediately prior to the MRI scan being completed no trypanosomes were present within the brain, enabling restoration of the BBB to begin. Although no CNS lesions were detectable twenty-four hours after completion of mel/HPβCD chemotherapy by MRI analysis, histopathological examination of brain sections fifteen days after treatment completion, revealed a very mild meningitis. This indicates that although BBB function is rapidly restored following mel/HPβCD chemotherapy, the mild inflammatory changes within the brain take longer to resolve.

The speed at which the BBB is restored following the elimination of trypanosomes from the brain together with the persistence of the mild neuro-inflammatory reaction, suggest that that the BBB damage observed in *T. b. brucei* infection could be due directly to the presence of the parasites within the brain and not a secondary effect resulting from the ongoing inflammatory reaction. The integrity of the BBB was restored within three days of the trypanosomes being eliminated from the brain, despite the presence of an ongoing inflammatory reaction. If the inflammatory reaction was responsible for the breakdown of the BBB, the integrity of the BBB would remain compromised in the presence of the ongoing inflammatory reaction. However, this was not the case in the present study, the inflammatory reaction was still present within the

brain fourteen days after BBB function had been restored. This suggests that disruption of the BBB is due to the direct presence of either the parasites or their secretory products. This hypothesis is supported by the work of Nikolskaia *et al*. and Grab *et al*. in an *in-vitro* model of the BBB. Nikolskaia *et al*. and Grab *et al*. proposed that trypanosomes release cysteine proteases, especially brucipain, which activate protein activated receptors (PARs), triggering a release of intracellular calcium (Grab *et al.,* 2009; Nikolskaia *et al.,* 2006). The increase in intracellular calcium ultimatley leads to a rearrangement of the cell cytoskeleton and barrier dysfunction through calmodulin (CAM) activation of myosin light chain kinase (MLCK) (Grab *et al.,* 2009). If trypanosome cysteine proteases are responsible for the BBB damage observed during CNS stage trypanosomiasis then following the elimination of trypanosomes from the CNS, BBB function should be restored as cysteine proteases will no longer be released. In the present investigation the BBB was restored within three days of trypanosomes being eliminated from the brain thus supporting the hypothesis of Grab *et al.*, that trypanosome derived products are responsible for the breakdown in the BBB observed in trypanosome infections (Grab *et al.,* 2009).

This study is the first to describe the use of MRI to assess the effect of chemotherapy on the integrity of the BBB in experimental trypanosomiasis. However, in multiple sclerosis (MS) MRI is frequently used to evaluate existing and novel chemotherapy regimes (Fazekas, Soelberg-Sorensen, Comi and Filippi, 2007). In one such study, MRI analysis was used to demonstrate the ability of a new immunomodulating agent, fingolimod to reduce the number of lesions and disease activity in patients with relapsing MS (Kappos, Antel, Comi, Montalban *et al.*, 2006). In the study, 225 patients were enrolled and assigned, on a 1:1:1 ratio, to one of three treatment groups; placebo, 1.25mg fingolimod or 5mg fingolimod. The number of CNS lesions as detected on gadolinium enhanced T_1 weighted MRI images, was significantly lower in both fingolimod groups than in the placebo group (Kappos *et al.,* 2006). This study demonstrates the value of MRI in assessing and monitoring the effectiveness of chemotherapy regimes used in the treatment of CNS diseases. If MRI was widely available in HAT endemic regions, it could be used to monitor the effect of chemotherapy on the BBB and allow early detection of the PTRE. It could also establish if infection with trypanosomes results in long term CNS damage and mental impairment in

patients, as very little is known about the long term consequences of trypanosome infection. However, MRI analysis is unlikely to become available in the remote regions of sub-Saharan Africa where HAT occurs. All the MRI studies conducted to date have been in patients out with the African continent.

MRI technology is now becoming available within Africa, through its use in investigating the pathogenesis of cerebral malaria (Looareesuwan *et al.,* 2009). Recently one of the first public MRI facilities was opened in Malawi through the collaborative efforts of Michigan State University, the Queen Elizabeth Central Hospital, Malawi, and the University of Malawi College of Medicine (Latourette, Siebert, Barto, Marable *et al.*, 2010). However, the unit suffers from many operational difficulties, the main one being an unreliable electricity supply. Furthermore, all images need to be sent electronically to the Michigan State University for analysis (Latourette *et al.,* 2010). Development of further MRI facilities is unlikely due to the sizeable financial requirements. Moreover, operational and logistical requirements associated with managing such a facility would prevent the creation of additional MRI units in the more remote regions of sub-Saharan Africa. MRI is an invaluable tool for understanding the role of the BBB in the pathogenesis of HAT and for assessing the effect of anti-trypanocidal chemotherapy on the integrity of the BBB barrier (Braakman, van de Molengraft, Hubert and Boerman, 2006; Gill, Chatha and Carpio-O'Donovan, 2003; Kager *et al.,* 2009; Rodgers *et al.,* 2011; Sabbah *et al.,* 1997). However, it is highly unlikely that the technology will become available in the HAT endemic regions where it would be of greatest use.

This chapter has demonstrated through the use of small bore MRI, that the integrity of the BBB is compromised on day 21 post-infection in experimental *T. b. brucei* infection. The damage induced by the infection is fully reversible following administration of the melarsoprol cyclodextrin complex mel/HPβCD, orally for 7 consecutive days at 0.05 mmol/kg. The integrity of the BBB is fully restored by 24 hours after completion of treatment.

Chapter 6: Investigating the pharmacokinetic properties of complexed melarsoprol

6.1 Introduction

6.1.1 Pharmacokinetics of melarsoprol

Despite melarsoprol being used in the treatment of CNS stage HAT for over 60 years very little is known about the pharmacokinetic properties of the drug. Treatment schedules were initially introduced based on empirical data only. Over the years numerous assays have been developed in an attempt to understand the pharmacokinetic profile of the compound and to quantify the concentration of the drug reaching the CSF and brain.

6.1.1.1 Original bioassay

One of the first attempts to determine the concentration of melarsoprol in the plasma and CSF following administration was by Hawking (Hawking, 1962). Hawking developed a bioassay to determine the concentration of melarsoprol in biological fluids. The assay consisted of incubating trypanosomes in dilutions of serum taken from patients receiving melarsoprol therapy, for 24 hours and comparing the survival rate of the trypanosomes with that of trypanosomes incubated in known concentrations of melarsoprol. Samples were taken from patients receiving melarsoprol at doses ranging from 18mg to 180mg; 1, 6, 24, 48 and 62 hours after administration. The plasma concentration of melarsoprol one hour after administration of 180mg ranged from 0.98 to 1.15µg/ml. By six hours after administration the concentration had dropped to between 0.6 and 0.67µg/ml. The concentrations of melarsoprol in the cerebrospinal fluid (CSF) were only a fraction of those reached in the plasma. Six hours after administration of 180mg of melarsoprol the concentration detected in the CSF ranged from 7ng/ml to 10ng/ml. The assay was not validated and provided only a very basic estimation of the melarsoprol concentration in serum and CSF samples. One of the main problems Hawking faced when developing the bioassay was that culture conditions at the time only enabled trypanosomes to be kept in culture for 24 hours. As a result the exposure time of trypanosomes to compounds in the assay was severely limited, restricting the ability of the assay to accurately determine the melarsoprol content of samples.

6.1.1.2 ELISA

In an attempt to determine more accurately the melarsoprol concentration in plasma and CSF samples from patients who had received melarsoprol therapy Maes *et al*. developed a sensitive ELISA (Maes, Vanderveken, Hamers, Doua *et al.*, 1988). One of the first steps in the development of the assay was the production of high affinity antibodies against the drug molecule. In order to achieve this melarsoprol was conjugated with bovine serum albumin (BSA) and inoculated subcutaneously, in combination with Freund's complete adjuvant into rabbits. The anti-melarsoprol-BSA antibodies were subsequently collected from the rabbits and separated from the antisera by affinity chromatography. In order to obtain a melarsoprol calibration curve to which samples could be compared to, brain samples were spiked with standard solutions of melarsoprol. The standards were incubated with the antibodies, before being applied to a microtiter plate coated with a melarsoprol-ovalbumin (OVA) conjugate. The percentage specific antibody-binding inhibition was subsequently calculated for each standard and a calibration curve constructed. The melarsoprol concentration in patient serum samples was determined by incubating dilutions of the samples with the anti-melarsoprol antibodies in a plate coated with a melarsoprol-OVA conjugate. The percentage specific antibody-binding inhibition was calculated and the melarsoprol concentration within the sample determined by comparing the value obtained to those in the melarsoprol calibration curve (Maes *et al.,* 1988). The ELISA was capable of detecting melarsoprol concentrations of less than 0.25pmol/ml, but the assay was only validated on a small number of serum samples, collected from patients receiving melarsoprol. In one patient the melarsoprol concentration in the serum as determined by the ELISA method was found to be approximately 0.4µg/ml 60 minutes after administration of 3.6mg/kg of melarsoprol. This is considerably lower than the concentrations previously reported by Hawking (Hawking, 1962) but the lack of information regarding the total dose administered to patients, the time points at which samples were collected and the small number of samples examined makes it difficult to compare the results reported by Maes *et al*. using the ELISA to previous studies. Larger scale studies to determine the reliability and to validate the ELISA were never performed.

6.1.1.3 Long-term bioassay

Advances in culture methods and the development of axenic culture systems in 1985 made it possible to maintain trypanosomes in culture for a number of days without the need for sub-passaging (Baltz, Baltz, Giroud and Crockett, 1985). This meant that it was possible to develop a long-term bioassay in which trypanosomes could be exposed to drug concentrations for a prolonged period of time, thus over coming the problem of short drug expose times experienced by Hawking when initially developing a bioassay (Hawking, 1962). Utilising the new culture systems Burri and Brun developed a second bioassay based on the original Hawking method (Burri and Brun, 1992). In the assay *T. b. rhodesiense* trypanosomes were incubated with serial dilutions of melarsoprol for 72 hours at 37˚C. Following incubation the plate was examined under a microscope and the highest dilution of melarsoprol with less than five motile trypanosomes determined. This value was defined as the minimum inhibitory concentration (MIC) of melarsoprol. In order to validate the assay serum samples were collected from patients treated with I.V. melarsoprol. The melarsoprol was administered as series, of four increasing doses of 1.2, 2.4, 3.6 and 3.6mg/kg, with a 24 hour drug free period between each dose. Serum samples were collected 24 hours after administration of the last dose of the first series. Samples were serially diluted and incubated with *T. b. rhodesiense* trypanosomes for 72 hours at 37˚C. Once again the plate was examined under a microscope and the MIC determined. The melarsoprol content of the samples was calculated according to Equation 6-1:

$$C_X = MIC \times D \times 2^n$$

Equation 6-1: The equation used to calculate the melarsoprol content of samples analysed using the bioassay
Where C_x = Determined concentration in the investigated sample, MIC = Determined minimal inhibitory concentration of melarsoprol for the reference clone, D = The highest dilution of the sample, n = Steps of dilution to the first well with no living trypanosomes.

Using this procedure, serum samples prepared from two patients were found to contain melarsoprol concentrations of 1.4µg/ml and 3.6µg/ml. The melarsoprol concentration in CSF samples collected at the same time was considerably lower at 108ng/ml and 43ng/ml respectively. The lower detection limit of the assay was determined to be 9ng/ml. The parameter measured by the assay is

trypanocidal activity therefore it is not possible to distinguish whether the activity observed is due to melarsoprol or its metabolites. The assay is also unable to distinguish between trypanocidal drugs therefore it is important to know if the patient has received any other trypanocidal drugs prior to melarsoprol treatment.

Using the bioassay developed by Burri and Brun and atomic absorption spectrometry (AAS) Burri *et al*. conducted the first pharmacokinetic study on melarsoprol (Burri, Baltz, Giroud, Doua *et al.*, 1993). Serum and CSF samples were collected from patients receiving melarsoprol for the treatment of late stage *T. b. gambiense* infections in Daloa, Ivory Coast. The treatment protocol employed in the region is provided in Table 6-1. In four patients serum samples were collected 0.5, 1, 6 and 24 hours after injections 1, 2 and 4 of the treatment course. In addition, CSF samples were collected 24 hours after the last melarsoprol injection of treatment series 2 and 3. In 15 separate patients serum samples were collected 24, 48 and 72 hours after the last melarsoprol injection of each treatment series and 120 hours after the final injection of the treatment schedule. CSF samples were also collected 24 hours after the last dose in each treatment series and 120 hours after the final dose. The maximum serum concentration of melarsoprol after the fourth dose of the treatment series was found to be in the range of 5-6μg/ml. By 120 hours after administration of the last dose the concentration had dropped to 0.22 ± 0.08μg/ml. In between each treatment series the concentration of melarsoprol in the serum dropped to almost zero indicating that the drug is rapidly excreted and no accumulation occurs. The concentration of melarsoprol reaching the CSF was approximately 50 fold lower than that observed in the serum and varied significantly between patients. The maximum concentration recorded was 260ng/ml, 24 hours after administration of the final injection of the treatment schedule. The minimum concentration was below the level of detection of the assay. The study enabled some basic pharmacokinetic parameters to be calculated for melarsoprol. The mean terminal elimination half-life of melarsoprol ($t_{1/2}$) was estimated to be 35 hours with a volume of distribution ($V_{D\beta}$) of greater than 100l and a total clearance of approximately 50ml/min.

	Day of treatment	Drug	Dose
Series 1	1	Melarsoprol	1.2 mg/kg
	2	Melarsoprol	2.4 mg/kg
	3	Melarsoprol	3.6 mg/kg
	4	Melarsoprol	3.6 mg/kg
Series 2	14	Melarsoprol	1.2 mg/kg
	15	Melarsoprol	2.4 mg/kg
	16	Melarsoprol	3.6 mg/kg
	17	Melarsoprol	3.6 mg/kg
Series 3	27	Melarsoprol	1.2 mg/kg
	28	Melarsoprol	2.4 mg/kg
	29	Melarsoprol	3.6 mg/kg
	30	Melarsoprol	3.6 mg/kg

Table 6-1: The treatment protocol employed in the Daloa region, Ivory Coast
The above schedule was used for the treatment of *T. b. gambiense* CNS stage trypanosomiasis in the study conducted by (Burri *et al.,* 1993).

In a continuation of this study, a second pharmacokinetic investigation was conducted in uninfected vervet monkeys to compare two different treatment regimes (Burri, Onyango, Auma, Burudi *et al.*, 1994). One treatment group was given the established schedule, with serum samples taken 0.25, 0.5, 1, 3, 6, 12, 24, 48, 72 and 120 hours after the last injection of the first and third series and 0.25, 24, 48 and 120 hours after the last injection of the second series. In order to determine the trough levels of melarsoprol additional serum samples were taken 24 hours after administration of the first and second injections of each series. CSF samples were collected 24 hours after the first, second and third injection of series one and three, 24 and 48 hours after the third injection of series two and 120 hours after the very last injection of the treatment schedule. The second treatment group were administered melarsoprol at a dose of 2.2mg/kg daily for 10 days. Serum samples were collected 0.25, 0.5, 1, 3, 6, 12, 24, 48, 72 and 120 hours after the last injection. Additional serum samples were collected 24 hours after administration of the second injection for determination of trough levels. CSF samples were collected 24 hours after the first and second injection and 24, 72 and 120 hours after administration of the last injection.

The concentration of melarsoprol observed 0.25 hours after administration of the final dose of each series, in the group following the established treatment regime ranged from 1.7 to 3.1µg/ml (mean 2.2µg/ml) after the first, 2.4 to 3.6µg/ml (mean 2.6µg/ml) after the second and 3.1 to 3.8µg/ml (mean 3.3µg/ml) after the third series respectively. In the group receiving the alternate treatment regime serum concentration levels of melarsoprol 0.25 hours after administration of the final dose of the treatment schedule, ranged from 2.4 to 3.1µg/ml (mean 2.8µg/ml). In common with other studies it was found that, following I.V. administration, melarsoprol is rapidly cleared from the serum (Burri *et al.*, 1993; Hawking, 1962). Within six hours of administration serum levels had dropped from initial concentrations of around 3µg/ml to 0.3 to 0.7µg/ml. The terminal-half life of melarsoprol differed significantly between the two treatment groups being calculated at 25.8 to 32.6 hours for the established treatment group and 16.7 to 25.4 hours for the group receiving the alternate treatment regime. The serum concentrations were below the limit of detection by 120 hours after the last dose in both treatment regimes, confirming previous reports that melarsoprol does not accumulate within the body (Burri *et*

al., 1993). The total clearance (CL) of melarsoprol was found to be 2.9 to 4.0ml/min/kg (median 3.6ml/min/kg). In agreement with earlier studies, the concentration of melarsoprol in the CSF was found to be very low (55ng/ml) and despite the total amount of melarsoprol administered during the empirical regime being higher than in the alternate 10 day regime, higher CSF levels were not obtained (Burri *et al.,* 1993; Hawking, 1962). Although the bioassay developed by Burri and Brun allowed preliminary pharmacokinetic data on melarsoprol to be calculated for the first time, the assay is time consuming as every plate must be examined microscopically to determine the melarsoprol concentration within the sample (Burri *et al.,* 1993; Burri and Brun, 1992; Burri *et al.,* 1994). To over come this problem, an automated fluorescent biological assay was developed using Alamar blue® (Onyango, Burri and Brun, 2000).

6.1.1.4 Automated biological assay

Alamar blue® contains an oxidation-reduction (redox) indicator, which in its non-reduced state is deep blue in colour. Cellular proliferation reduces the indicator and a change in redox colour from blue to fluorescent red occurs. The extent of cellular proliferation is proportional to the intensity of the red colour (Ansar Ahmed, Gogal and Walsh, 1994). By measuring the level of fluorescence, the assay can be used to determine the viability of trypanosomes *in-vitro*, in the presence of varying concentrations of trypanocides (See chapter 3) (Raz *et al.,* 1997). Onyango *et al.* adapted the assay to determine the concentration of melarsoprol within serum and CSF samples (Onyango, Burri and Brun, 2000). In the assay, *T. b. rhodesiense* trypanosomes were incubated in three fold serial dilutions of the samples for 66 hours. Alamar blue® indicator was subsequently added and the plates incubated for a further 6 hours before the fluorescence was measured. The drug concentration within the sample was calculated according to Equation 6-2:

$$C_X = 1/D \times IC_{50}\text{det.} \times F$$

Equation 6-2: The equation used to calculate the melarsoprol content of samples analysed using the automated bioassay
Where C_x is the concentration of drug within the sample, D is the fraction of unknown drug sample required for 50% reduction of live parasites, IC_{50} det. is the IC_{50} of melarsoprol for the *T. b. rhodesiense* stabilate used in the study and F is the dilution factor in the first well (Onyango, Burri and Brun, 2000).

To validate the assay 108 serum and 37 CSF samples were spiked with melarsoprol at concentrations ranging from 17ng/ml to 2.2µg/ml for serum and 17ng/ml to 92ng/ml for CSF samples. The accuracy of the assay was determined to be 99.4% and 96.4% for serum and CSF samples respectively. The reproducibility of the assay, expressed as the average inter-day coefficient of variation was 9.9% for serum and 18.8% for CSF samples. The limit of detection of the assay was 4ng/ml for both serum and CSF samples (Onyango, Burri and Brun, 2000). The assay was only used to quantify the concentration of melarsoprol within spiked tissue samples, the ability of the assay to accurately determine the level of melarsoprol within patient samples was not evaluated. As in previous bioassays, the parameter measured was trypanocidal activity, which was expressed as melarsoprol concentration. It is not known if the trypanocidal activity observed is due to melarsoprol or its metabolites or even other trypanocides which the patients received prior to melarsoprol chemotherapy. In order for the active metabolites of melarsoprol to be identified and quantified, a more specific assay is required.

6.1.1.5 High performance liquid chromatography assay

The first method developed to separate and quantify the melaminophenyl arsenicals was a simple high performance liquid chromatography (HPLC) assay (Berger and Fairlamb, 2005). Solutions of trimelarsen (mel W), cymelarsan (mel Cy), melarsoprol and melarsen oxide were analysed individually and as a mixture containing 1.0nmol of each compound. All compounds produced sharp well defined peaks which were free from interference and showed no overlap. The limit of detection was less than 10pmol for each compound. To assess the ability of the HPLC method to detect melaminophenyl arsenicals in biological samples, foetal calf serum was spiked with a mixture of melarsen oxide, cymelarsan, trimelarsen and melarsoprol to give a final concentration of 100pmol of each compound per ml of serum. The arsenicals were extracted with an octadecylsilane solid-phase extraction cartridge. The recovery rates varied with each arsenical, melarsoprol and melarsen oxide were most successful with recovery rates of 65.2% and 61.5% respectively. In contrast, the recovery of cymelarsan and trimelarsen was poor with only 14.1% and 35.6% of each compound recovered respectively. Although the HPLC assay was the first to be

able to differentiate between the melaminophenyl arsenicals the poor recovery rate of the arsenicals from biological fluids and the 80 minute run time for each sample limits the assay's use in assessing the concentration of melarsoprol reaching tissues following administration. Both the method of extracting arsenicals from biological samples and the HPLC method itself therefore require optimisation.

Ericsson *et al*. developed a reverse-phase HPLC method for the determination of melarsoprol in plasma, whole blood, urine and cerebrospinal fluid (Ericsson, Schweda, Bronner, Rombo *et al.*, 1997). In order to evaluate the assay, plasma, whole blood and urine were spiked with concentrations of melarsoprol ranging from 11.3µmol/l to 625nmol/l. Extraction was performed in chloroform and acetonitrile followed by back extraction into phosphoric acid. The extraction recovery rates obtained were better than those previously reported by Berger and Fairlamb, with recovery rates of 86 ± 3%, 82 ± 2% and 75 ± 2% for plasma, CSF and urine respectively. A poor recovery rate was only observed in whole blood samples with only 34 ± 1% of the melarsoprol recovered. The assay was further evaluated on serum samples collected from patients suffering from CNS stage *T. b. gambiense*. Immediately after administration of 3.6mg/kg of melarsoprol concentrations ranging from 2 to 15µM were detected.

The melarsoprol concentrations detected by Ericsson *et al*. are substantially lower than those determined previously by Burri *et al*. using a bioassay approach (Burri *et al.,* 1993). A similar study conducted by Bronner *et al*. also detected concentrations of melarsoprol in the plasma by HPLC analysis that did not mirror those found previously using bioassays (Bronner, Brun, Doua, Ericsson *et al.*, 1998).

6.1.1.6 Comparing bioassay and HPLC approaches

In the study conducted by Bronner *et al*. plasma, urine and CSF samples were collected from eight patients suffering from CNS stage *T. b. gambiense* infection in Daloa, Côte d'Ivoire (Bronner *et al.,* 1998). The patients received three series of melarsoprol injections, with each series consisting of I.V. injections, once per day, for four days at increasing doses (Table 6-1). Each treatment series was separated by a 10 day drug free period. Plasma samples were collected before

the first injection, immediately after the fourth injection and 1, 24 hours and 5 days after the fourth injection. Urine and CSF samples were collected before treatment and 24 hours after the last dose. All samples were analysed by HPLC analysis and bioassay. Immediately after administration of the fourth injection the plasma concentration of melarsoprol, as detected by HPLC analysis, varied from 2,230 to 15,900nmol/l. By one hour after administration, the plasma concentration of melarsoprol had dropped considerably to between 0 and 1,780nmol/l and after 24 hours no melarsoprol was detected in the plasma (Bronner *et al.,* 1998). Analysis of the plasma samples by bioassay immediately after the fourth dose detected melarsoprol levels in the same order to those attained by HPLC analysis. However, 1 hour after the fourth dose the levels of melarsoprol in the plasma were 4 to 65 fold higher than those detected by HPLC and low levels of melarsoprol activity were still detected 24 hours and 5 days after the last dose by bioassay. Discrepancies were also observed in the concentrations of melarsoprol detected in the urine and CSF samples. The concentration in the urine was 40 to 260 fold higher when measured by bioassay compared to HPLC analysis and while no melarsoprol was detected in the CSF by HPLC analysis, the bioassay detected low levels in the range of 45 to 180nmol/l. The discrepancies observed between HPLC analysis and the bioassay are due to the different parameters each assay measures. HPLC analysis is only capable of detecting melarsoprol while the bioassay measures trypanocidal activity and cannot differentiate between trypanocidal compounds. The results obtained from the HPLC analysis suggest that following administration melarsoprol is rapidly metabolised to a number of active metabolites with trypanocidal activity (Bronner *et al.,* 1998).

6.1.2 Melarsoprol metabolites

The metabolites of melarsoprol were investigated in a study conducted by Keiser *et al*. (Keiser, Ericsson and Burri, 2000). Serum and CSF samples were collected from patients with CNS stage *T. b. gambiense* infection who had received melarsoprol therapy in the form of ten daily doses of 2.2mg/kg. Serum samples were collected 15 minutes before treatment commenced and then 1, 6 and 24 hours after administration of the last dose. CSF samples were collected 1, 6 and 24 hours after the first dose and 24, 48 and 72 hours after the final dose. The

pharmacokinetic profile of one known metabolite of melarsoprol, melarsen oxide was investigated in serum and CSF samples by HPLC analysis. In addition, the concentration of arsenic within the serum and CSF samples was analysed by atomic absorption spectrometry (AAS). The overall drug level within the samples was assessed by bioassay (Keiser, Ericsson and Burri, 2000). HPLC revealed maximum serum levels (C_{max}) of melarsen oxide within 15 minutes of administration, ranging from 461 to 848ng/ml, with an average of 636 ± 157ng/ml. At the same time point, comparable concentrations of arsenic were detected by AAS. The concentrations of arsenic within the serum samples ranged from 527 to 770ng/ml with a mean of 657 ± 90ng/ml. Melarsen oxide was rapidly cleared from the serum as by 8 hours after administration concentrations had fallen to between 7 and 11% of the C_{max} and by 24 hours after administration the level of melarsen oxide was below the limits of detection of the HPLC assay. The overall half-life of melarsen oxide was calculated to be 3.9 hours by HPLC. Arsenic as determined by AAS, was cleared more slowly from the serum than melarsen oxide. Eight hours after administration of melarsoprol, 256 to 139ng/ml (mean 182ng/ml) of arsenic was detected in the serum. By 24 hours after administration, the levels of arsenic within the serum had fallen, but were still detectable at 124 to 171ng/ml (mean 147ng/ml). The concentration of melarsoprol detected in the serum by bioassay, was greater than the levels of melarsen oxide and arsenic detected by HPLC and AAS respectively. Fifteen minutes after the administration of melarsoprol, the C_{max} was found to be 4,925ng/ml, this is 7.7 fold higher than the C_{max} of melarsen oxide. Eight hours after administration, the concentration of melarsoprol had dropped to between 998 and 1320ng/ml (mean 1140ng/ml). By 24 hours after administration of the drug, large concentrations of melarsoprol were still detectable within the serum by bioassay, concentrations ranged from 747 to 1070ng/ml (mean 855ng/ml). At the same time point no melarsen oxide was detectable by HPLC and only 124 to 171ng/ml of arsenic was detected by AAS. This suggests that following administration melarsoprol is rapidly metabolised to melarsen oxide which, in turn, is further transformed into one or more active metabolites (Keiser, Ericsson and Burri, 2000). At present the active metabolites of melarsen oxide are unknown.

6.1.3 Pharmacokinetics of complexed melarsoprol

The pharmacokinetic properties and tissue distribution of the melarsoprol cyclodextrin complex mel/HPβCD following I.V. administration has been investigated and compared to that of melarsoprol (Zirar, Astier, Muchow and Gibaud, 2008). CD-1 mice were administered a single dose of melarsoprol or mel/HPβCD at a dose of 0.038mmol/kg. Blood, liver, kidney and brain samples were taken 0.5, 30 minutes, 1, 5, 18, 24 and 48 hours after administration of the drug. The concentration of arsenic within the tissue was determined using a colorimetric method after digestion of the tissues with nitric acid and hydrogen peroxide (Zirar *et al.,* 2008).

Complexation of melarsoprol to HPβCD led to significant alterations in the pharmacokinetic properties of the compound. A reduction in the terminal half-life $t_{1/2}(\beta)$ of melarsoprol from 9.1 ± 5.7 to 2.6 ± 0.4 hours occurred. The volume of distribution was also greatly reduced from 338 ± 88ml for melarsoprol compared to 186 ± 38ml for melarsoprol complexed with HPβCD (Zirar *et al.,* 2008). In addition to the pharmacokinetic properties the tissue distribution profile of melarsoprol was also modified following insertion of the compound into the HPβCD cavity. The complexation of melarsoprol to HPβCD resulted in higher concentrations of the drug reaching the bone marrow, brain, liver and kidneys. The major target organ for the compound following its complexation to HPβCD was the brain with a C_{max} of 0.25μmol/g, in contrast when free melarsoprol was administered the major target organ was the bone marrow with a C_{max} of 1.64μmol/g. The reasons for the alteration in the tissue affinity of melarsoprol following its complexation are unknown but it is thought that it could occur as a result of the cyclodextrins being able to deliver the drug more efficiently to the biological membranes (Zirar *et al.,* 2008).

Only the pharmacokinetic properties of mel/HPβCD following I.V. administration were investigated by Zirar *et al.* (Zirar *et al.,* 2008). No information is available regarding the pharmacokinetics and tissue distribution of mel/HPβCD and mel/RAMβCD following oral administration. Therefore the aim of this chapter is to develop a gas chromatography mass spectrometry (GC-MS) method to allow the pharmacokinetic and tissue distribution profile of mel/HPβCD and

mel/RAMβCD following oral administration to be accurately determined. As it has recently been reported that there is an increase in the permeability of the blood-brain barrier during CNS stage *T. b. brucei* infection in mice (Rodgers *et al.*, 2011), the study will be conducted in normal and infected mice in order to assess if infection affects the pharmacokinetic and tissue distribution profiles of the compounds.

6.2 Methods

6.2.1 Establishing T. b. brucei infection

Female CD-1 mice aged approximately 6 to 8 weeks in age and weighing 25 to 30 grams were inoculated intraperitoneally with $2x10^4$ *T. b. brucei* GVR35/C1.9 trypanosomes. The methodology detailing the preparation of the trypanosomes prior to inoculation is provided in chapter 2.

6.2.2 Confirmation of trypanosome infection

To confirm that inoculation of *T. b. brucei* trypanosomes had led to the establishment of a trypanosome infection in the mice, a wet blood film of tail blood from each animal was examined under the microscope for the presence of trypanosomes. The level of parasitaemia observed in each animal was scored according to the system detailed in chapter 2.

6.2.3 Preparation of complexed melarsoprol for oral administration

The melarsoprol cyclodextrin complexes mel/HPβCD and mel/RAMβCD are supplied as fine white powders with the ratio of melarsoprol to cyclodextrin specified for each batch. Using the ratio, the amount of each complex required to give a melarsoprol concentration of 0.05mmol/kg was calculated. The corresponding amount of complex was weighed out on a fine balance and dissolved in sterile water. The solutions of each complex were freshly prepared each day immediately prior to administration. The full details as to how the dose was calculated for each melarsoprol cyclodextrin complex are provided in chapter 2.

6.2.4 Preparation of mel/HPβCD for intravenous administration

A 0.03mmol/kg solution of mel/HPβCD was prepared by the addition of 40.45mg of the complex to sterile pyrogen free saline. The full details regarding the calculation of the dose are provided in chapter 2.

6.2.5 Oral administration of complexed melarsoprol

Prior to the administration of the complexes each animal was weighed and the volume of complex to be administered determined using the table provided in chapter 2. To administer the melarsoprol cyclodextrin complexes, the animals were appropriately restrained and a 20 gauge x 25mm gavage needle inserted directly into the oesophagus. The compounds were subsequently administered slowly and carefully directly into the stomach.

6.2.6 Intravenous administration of mel/HPβCD

Animals were anaesthetised with isoflurane delivered as a mixture of 3% isoflurane and 50% oxygen. The animals were placed on a heat mat in order to dilate the caudal veins, and the compound administered into the tail vein using a 30 gauge insulin syringe. Anaesthesia was maintained throughout the procedure.

6.2.7 Treatment schedule

The pathogenesis and disease progression of *T. b. brucei* GVR35/C1.9 is well documented, with full details provided in chapter 2. Chemotherapy regimes commenced on day 21 post-infection, as at this time point the parasites are known to be established within the CNS and BBB breakdown has been demonstrated.

6.2.7.1 Oral administration

Mel/HPβCD or mel/RAMβCD was administered once, at a dose of 0.05mmol/kg. Animals were sacrificed at 5 minutes, 30 minutes, 1, 4, 8, 12 and 18 hours after administration of the compounds (Figure 6-1). At each time point three animals were killed. This protocol was also performed in groups of uninfected animals.

6.2.7.2 Intravenous administration

Mel/HPβCD was administered once at a dose of 0.03mmol/kg. Animals were sacrificed at 30 seconds, 5 minutes, 30 minutes, 1, 4, 8, 12 and 18 hours after

administration of the compound. At each time point 3 animals were killed. This protocol was also performed in groups of uninfected animals.

I	>	M	>	K	>	K	>	K	>	K	>	K	>	K	>	K
		21		5 min		30 min		1 hr		4 hr		8 hr		12 hr		18 hr

Figure 6-1: The oral treatment schedule employed
Mice were infected with $2x10^4$ *T. b. brucei* trypanosomes. On day 21 post-infection when CNS infection is known to be established chemotherapy commenced (M). Animals were administered one dose of mel/HPβCD or mel/RAMβCD at 0.05mmol/kg by oral gavage. Animals were subsequently killed (K) at the time points indicated. At each time point 3 animals were killed. This protocol was also performed in groups of uninfected animals.

I	>	M	>	K	>	K	>	K	>	K	>	K	>	K	>	K	>	K
		21		30s		5 min		30 min		1 hr		4 hr		8 hr		12 hr		18 hr

Figure 6-2: The intravenous treatment schedule employed
Mice were infected with $2x10^4$ *T. b. brucei* trypanosomes. On day 21 post-infection when CNS infection is known to be established chemotherapy commenced (M). Animals were administered one dose of mel/HPβCD at 0.03mmol/kg I.V. into the caudal tail vein. Animals were subsequently killed (K) at the time points indicated. At each time point 3 animals were killed. This protocol was also performed in groups of uninfected animals.

6.2.8 Collection of samples

Animals were sacrificed by CO_2 asphyxiation and the blood removed by cardiac puncture using a 25 gauge needle containing a bead of heprin. The blood was stored in a sterile 1.5ml eppendorf tube at 4°C. Immediately following exsanguination the chest cavity of the animal was opened and the animal perfused through the left ventricle with 120ml of sterile normal saline. Following perfusion the left kidney, spleen, liver and brain were carefully excised and placed in a 5ml bijoux. The tissues were immediately frozen on solid CO_2 before being stored at -70°C. In order to obtain plasma the whole blood was centrifuged at 13,500rpm at 15°C for 15 minutes. The separated plasma was subsequently collected and placed in a 1.5ml sterile eppendorf tube before being stored at -70°C.

6.2.9 Determining the arsenic content of tissue samples by gas chromatography mass spectrometry

6.2.9.1 Digestion of tissues

The tissue samples were removed from the freezer and allowed to defrost at room temperature before being weighed and placed in a digestion vial. 1ml of nitric acid (69%) was added to the tissue samples and the samples heated on a hot plate at 40°C for 30 minutes. The temperature of the samples was increased incrementally up to 100°C as described in Table 6-2. Once all the tissue was dissolved and a clear solution had formed, the samples were removed from the hotplate and cooled to room temperature. 2ml of hydrogen peroxide (30%) and 4ml of nitric acid (69%) were added to the samples and the samples returned to the hotplate for 30 minutes at 40°C. The temperature of the samples was increased up to 120°C, to completely digest all tissue elements. The temperature of the samples was then incrementally increased up to 300°C and the samples heated to dryness. The temperature increments and incubation periods are detailed in Table 6-3.

6.2.9.2 Resuspension of digestion residue

The dried tissue digest was resuspended in 1ml of 2M HCl. To ensure complete resuspension of the residue, the samples were sonicated in a water bath for 10 minutes. The suspension was then transferred to a 20ml headspace vial. The digestion vial was washed with 4ml of 2M HCl and the HCl subsequently transfer to the headspace vial. 100µl of a solution containing 10% potassium iodide (KI) and 10% ascorbic acid was added to the headspace vial, the vial was then sealed with a vial crimper and incubated at room temperature for 1 hour. 150µl of 5% sodium borohydride ($NaBH_4$) was then injected into the vial through the crimp cap and the sample analysed by gas chromatography mass spectrometry (GC-MS).

Temperature (°C)	Time (minutes)
40	30
60	30
80	60
100	Until tissue is digested

Table 6-2: The schedule used to digest the tissue samples
1ml of nitric acid (69%) was added to the tissue samples and the temperature of the samples gradually increased incrementally from 40℃ to 100° C.

Temperature (°C)	Time (minutes)
40	30
60	30
80	30
120	120
150	180
175	15
200	15
250	30
300	Until dry

Table 6-3: The schedule used to completely digest all tissue elements and heat the samples to dryness
After cooling to room temperature, 2ml of hydrogen peroxide (30%) and 4ml of nitric acid (69%) was added to the samples and the temperature increased from 40℃ to 150℃, to completely digest all the tissue elements. The temperature of the samples was subsequently increased to 300℃ and the samples heated to dryness.

6.2.9.3 Gas chromatography mass spectrometry analysis

A Thermoquest Trace GC 2000 series coupled with Fisons MD 800 mass spectrometer were used in the analysis. A Combi PAL autosampler was used for automated headspace analysis. Data was collected using Xcalibur software. Samples were incubated at 60°C for 3 minutes prior to injection. The carrier gas used was helium at a flow rate of 2ml/min. Injections were made in split mode at a ratio of 5:1 with an inlet temperature of 250°C. A Varian Factor FOUR™ VF-624 30m long with an internal diameter of 0.25mm and film thickness of 1.4µm

was used. The column temperature was first set at 35°C for 3 minutes then increased by a ramp of 10°C/min to 100°C. The MS signals were collected in SIM (singal ion) mode and electron impact (EI) for ionization. The signal monitored for quantification of arsine was the total response of the following ions (m/z) 74.85, 75.85, 76.85 and 77.85. The total run time was 16 minutes.

6.2.9.4 Assay validation

6.2.9.4.1 Constructing an arsenic standard curve

Solutions of arsenic (As) were prepared at concentrations of 1000, 750, 500, 250, 100, 50, 25, 10, 5 and 1ng/ml by dissolving the corresponding amount of As_2O_3 in HPLC grade H_2O. 1ml of each solution was added to 0.5g of normal rat brain tissue in a digestion vial. This was then digested and the residue resuspended and analysed by GC-MS as detailed above. The peak area was manually integrated for each concentration and plotted as a function of As concentration.

6.2.9.4.2 Determining the precision (repeatability) of the assay

The precision of the assay was determined using 5 replicates. Five, 25ng/ml solutions of As were prepared by dissolving the corresponding amount of As_2O_3 in HPLC grade H_2O. 1ml of the solution was added to 0.5g of normal rat brain tissue and digested and analysed by GC-MS as detailed above. The peak area of each replicate was manually integrated and the arsenic concentration calculated using the equation obtained from the arsenic calibration curve for concentrations ranging from 50ng to 5ng. The precision of the assay was determined as the average variation of the assay results obtained under identical conditions (repeatability) and expressed as the coefficient of variation.

6.2.9.4.3 Extraction recovery

The extraction recovery of the assay was determined using 7 replicates. Seven, 25ng/ml solutions of As were prepared by dissolving the corresponding amount of As_2O_3 in HPLC grade H_20. 1ml of the solution was added to a digestion vial and the solution digested and analysed by GC-MS as detailed above. The peak area of each replicate was manually integrated and the arsenic concentration

determined using the equation obtained from the arsenic calibration curve for concentrations ranging from 50ng to 5ng. The mean arsenic concentration was calculated and compared to that obtained from brain tissue spiked with 25ng/ml As to calculate the percentage recovery.

6.3 Results

6.3.1 Chromatograms

Brain tissue was spiked with a solution containing 250ng/ml of As. The sample was digested by wet-acid digestion and the arsenic content determined by GC-MS. An arsenic peak was detected at a retention time of 1.15 minutes (Figure 6-3). The peak was well defined and separated with minimal impurity peaks. To confirm that the peak obtained at 1.15 minutes was arsenic, the chromatogram was compared to one obtained from normal brain tissue, subjected to the same extraction procedure as the spiked brain tissue. No peak was detected at 1.15 minutes on the mass spectrometry chromatogram (Figure 6-4) confirming that the peak detected at 1.15 minutes in the spiked brain tissue was arsenic.

6.3.2 Calibration curve

A calibration curve was constructed using concentrations of As ranging from 1000ng to 1ng. The relationship between arsenic concentration and peak area was not linear across the whole concentration range tested. However, for arsenic concentrations between 1000ng and 100ng a linear relationship was present. A linear relationship was also present at lower arsenic concentrations, ranging from 50ng to 5ng. This effect is often seen when constructing a calibration curve covering a wide range of concentrations. Two arsenic calibration curves were therefore constructed in the present study. One curve was constructed for As concentrations ranging from 1000ng to 100ng (Figure 6-5) and a second curve included concentrations of As ranging from 50ng to 5ng (Figure 6-6). The standard curves were linear within the concentration ranges tested, and the correlation coefficients were 0.997 for As concentrations ranging from 1000ng to 100ng and 0.993 for As concentrations of 50ng to 5ng. At a concentration of 1ng/ml, the area of the arsenic peak could not be accurately calculated due to its low signal to noise ratio. The limit of quantification of the assay was therefore determined to be 5ng/ml.

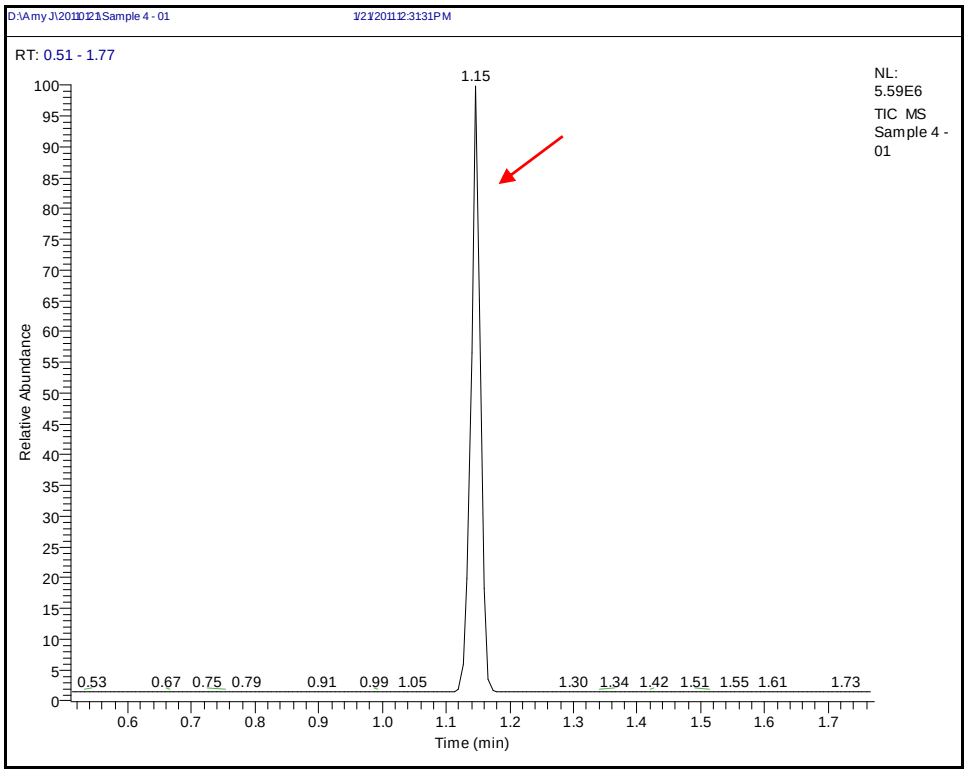

Figure 6-3: The chromatogram obtained from brain tissue spiked with 250ng As
The sample was digested by wet-acid digestion and the arsenic content of the sample analysed by GC-MS. A clear, well defined, separated peak, was detected at 1.15 minutes (red arrow), representing the concentration of arsenic within the sample.

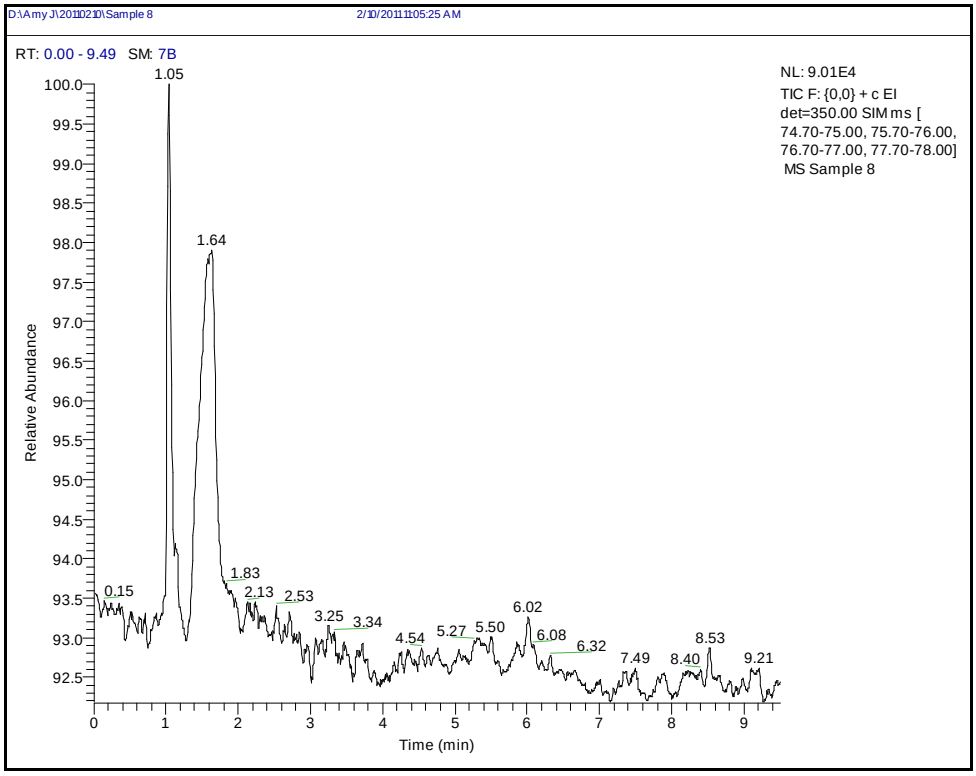

Figure 6-4: The chromatogram obtained from normal brain tissue
The sample was digested by wet acid digestion and the arsenic content of the sample determined by GC-MS. No peak was detected at 1.15minutes, confirming the peak detected at 1.15 minutes in the spiked brain tissue was arsenic.

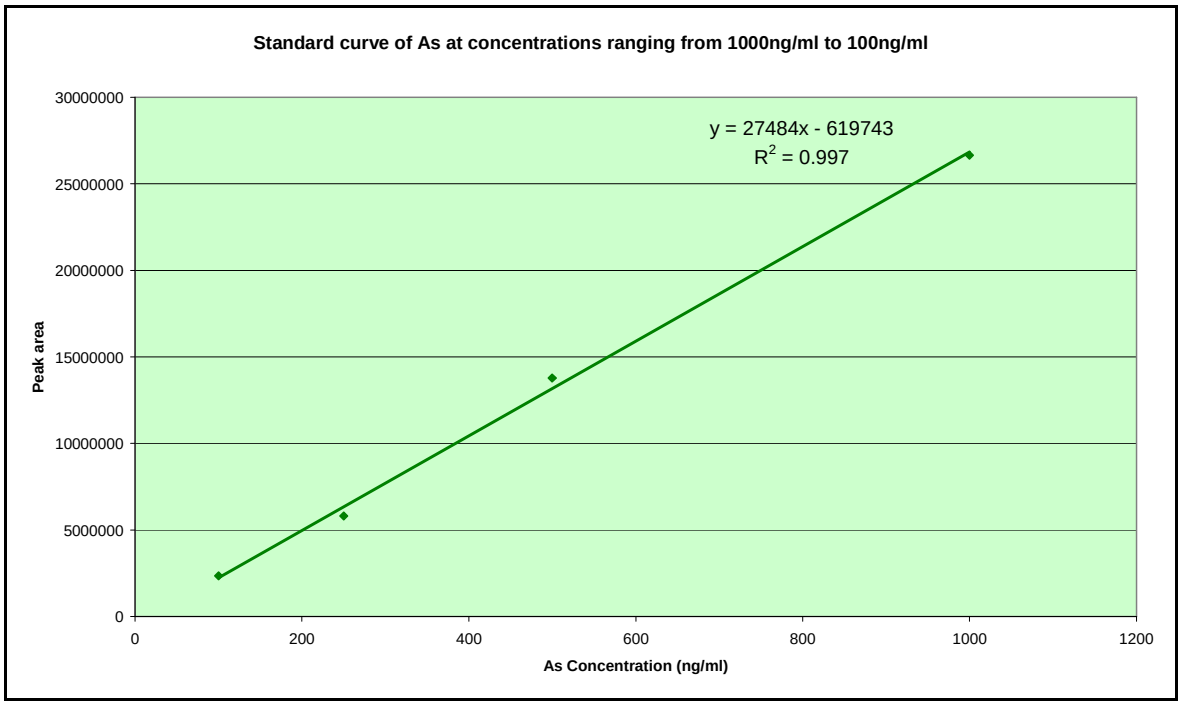

Figure 6-5: The As calibration curve for concentrations ranging from 1000ng/ml to 100ng/ml
0.5g of normal rat brain tissue was spiked with 1000, 500, 250 or 100ng/ml As. The tissue was digested by wet-acid digestion and the arsenic content of the sample evaluated by GC-MS. The peaks were manually integrated and the peak area plotted as a function of As concentration.

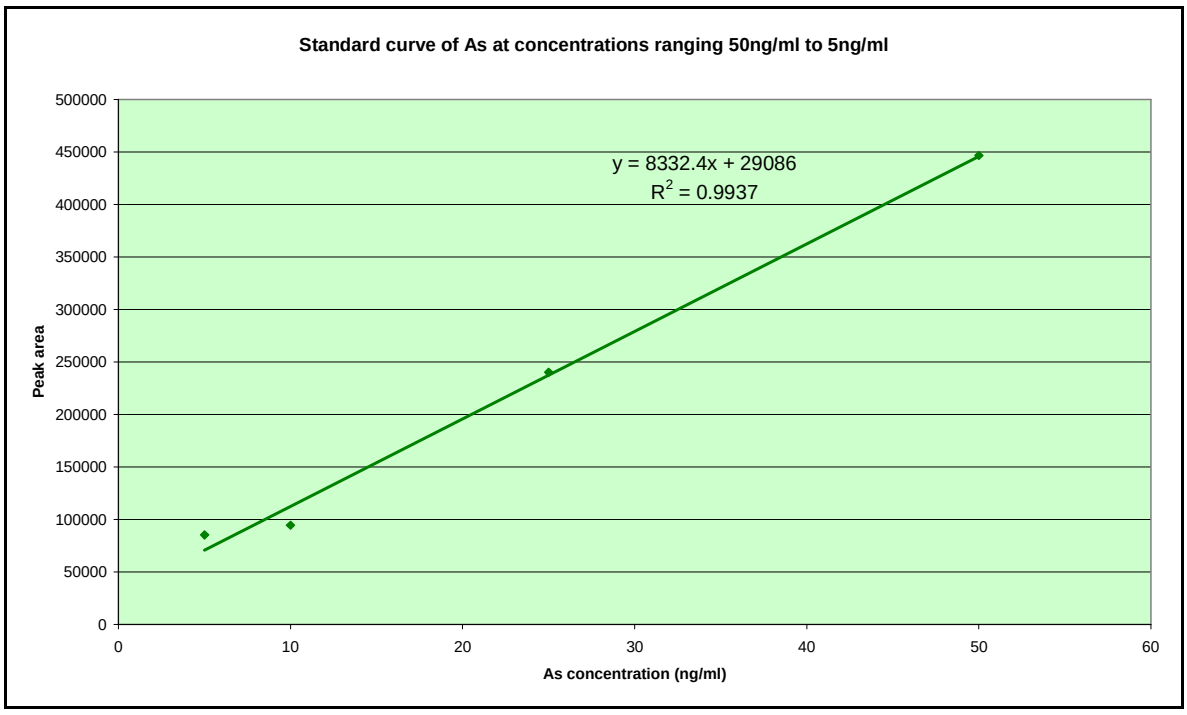

Figure 6-6: The As calibration curve for concentrations ranging from 50ng/ml to 5ng/ml
0.5g of normal rat brain tissue was spiked with 50, 25, 10 or 5ng/ml As. The tissue was digested by wet-acid digestion and the arsenic content of the sample evaluated by GC-MS. The peaks were manually integrated and the peak area plotted as a function of As concentration.

6.3.3 Precision of the assay

The arsenic content of five samples of normal rat brain spiked with 25ng/ml of As was determined by GC-MS (Table 6-4) and the precision of the assay calculated. The precision (repeatability) of the assay, expressed as the average inter-day coefficient of variation was 14.9%.

Sample	As concentration (ng/ml)	Peak area	Determined arsenic concentration (ng/ml)
1	25	300904	32.6
2	25	234775	24.7
3	25	217137	22.6
4	25	236304	24.9
5	25	234844	24.7

Table 6-4: The concentration of As detected by GC-MS in brain tissues spiked with 25ng/ml As
0.5g of normal rat brain tissue was spiked with 25ng/ml of As. The tissue was digested by wet-acid digestion and the arsenic content of the sample determined by GC-MS. The peak area of the samples was manually integrated and the arsenic content calculated using the equation obtained from the As calibration curve for concentrations ranging from 50ng to 5ng.

6.3.4 Extraction recovery

The arsenic content of 7 solutions containing 25ng/ml of As was determined by GC-MS (Table 6-5). The arsenic concentrations obtained were compared to those obtained from brain tissue spiked with 25ng/ml of As (Table 6-4) and the percentage extraction recovery of the assay calculated. The percentage extraction recovery of the assay, expressed as the percentage of arsenic recovered from spiked brain tissue compared to the arsenic solution alone was 87.5%.

Sample	As Concentration (ng/ml)	Peak area	Determined arsenic concentration (ng/ml)
1	25	353255	38.9
2	25	230405	24.2
3	25	257203	27.3
4	25	310906	33.8
5	25	270539	29.0
6	25	224701	23.5
7	25	285648	30.8

Table 6-5: The concentration of arsenic detected by GC-MS in solutions containing 25ng/ml of As
The samples were digested by wet-acid digestion and the arsenic content of the sample determined by GC-MS.The peak area of the samples was manually integrated and the arsenic content calculated using the equation obtained from the As calibration curve for concentrations ranging from 50ng to 5ng.

6.3.5 Concentration of arsenic within the brain

The concentration of arsenic within the brain following oral administration of 0.05mmol/kg mel/HPβCD was determined by GC-MS. An arsenic peak was detected in the brain samples taken 1 and 4 hours (Figure 6-7 and Figure 6-8 respectively) after the oral administration of mel/HPβCD but the peak area could not be integrated due to the presence of large interference peaks. No arsenic peak was detected in the samples taken 5 minutes, 30 minutes, 8, 12 and 18 hours after the oral administration of mel/HPβCD, as the arsenic content of the samples was below the limit of detection (<5ng/ml) of the assay. As no arsenic was detected within the brain following oral administration of mel/HPβCD it was concluded that it was unlikely arsenic would be detected in brain samples collected after oral administration of 0.05mmol/kg mel/RAMβCD. These samples were therefore not analysed.

6.3.6 Concentration of arsenic within the plasma

The concentration of arsenic within the plasma following I.V. administration of 0.03mmol/kg mel/HPβCD was determined by GC-MS. An arsenic peak was

detected in the plasma sample taken 30 seconds, after the administration of mel/HPβCD (Figure 6-9). The area of the peak was 62,314 corresponding to an arsenic concentration of 3.97ng. However, this is below the determined detection limit of the assay and therefore cannot be considered an accurate concentration. Arsenic was not detected in the plasma samples taken 5 minutes, 30 minutes, 1, 4, 8, 12 or 18 hours after the administration of mel/HPβCD. As the concentration of arsenic detected within the plasma immediately following the I.V. administration of 0.03mmol/kg mel/HPβCD was below the limit of detection of the assay it was concluded that it was unlikely arsenic would be detected in plasma samples collected after the oral administration of 0.05mmol/kg mel/HPβCD and mel/RAMβCD. These samples were therefore not analysed.

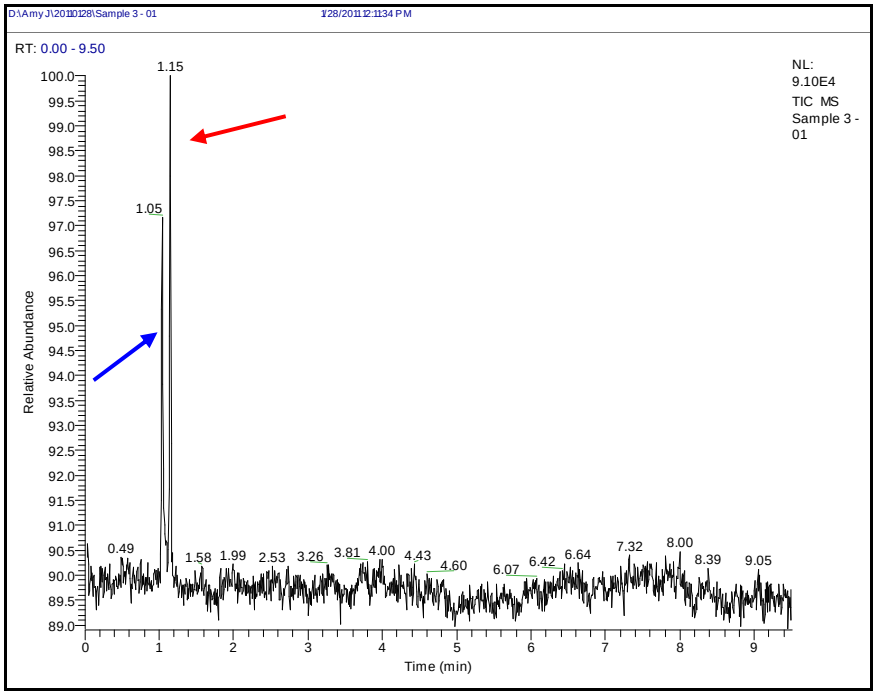

Figure 6-7: The chromatogram obtained from a brain sample taken 1 hour after the oral administration of 0.05mmol/kg mel/HPβCD

Mel/HPβCD was administered orally at a dose of 0.05mmol/kg and the brain removed 1 hour later. The brain was digested by wet-acid digestion and the arsenic content of the sample determined by GC-MS. An arsenic peak was detected (red arrow) but the peak area could not be calculated due to the presence of a large impurity peak (blue arrow).

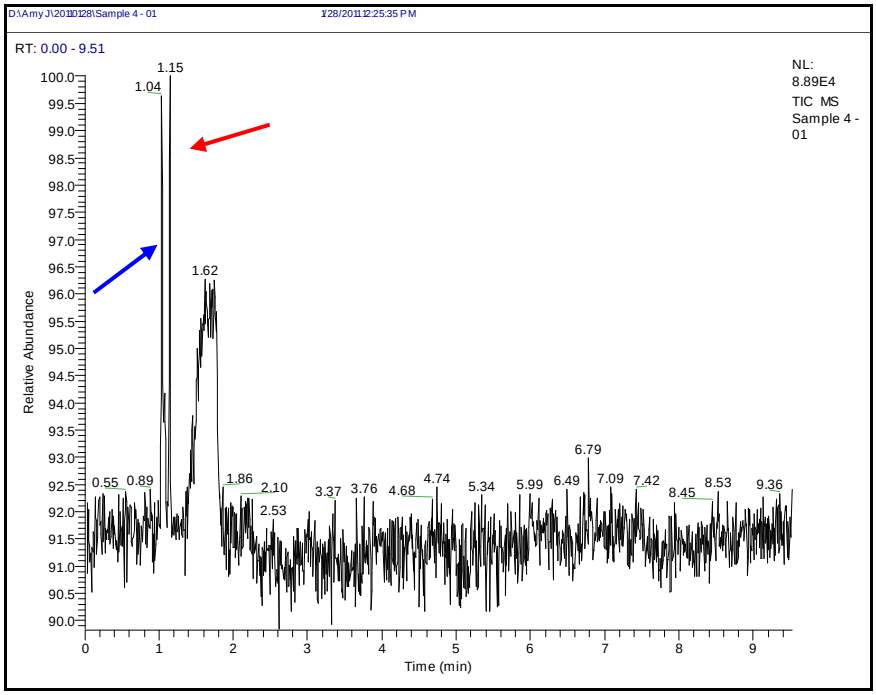

Figure 6-8: The chromatogram obtained from a brain sample taken 4 hours after the oral administration of 0.05mmol/kg mel/HPβCD

Mel/HPβCD was administered orally at a dose of 0.05mmol/kg and the brain removed 4 hours later. The brain was digested by wet-acid digestion and the arsenic content of the sample determined by GC-MS. An arsenic peak was detected (red arrow) but the peak area could not be calculated due to the presence of a large impurity peak (blue arrow).

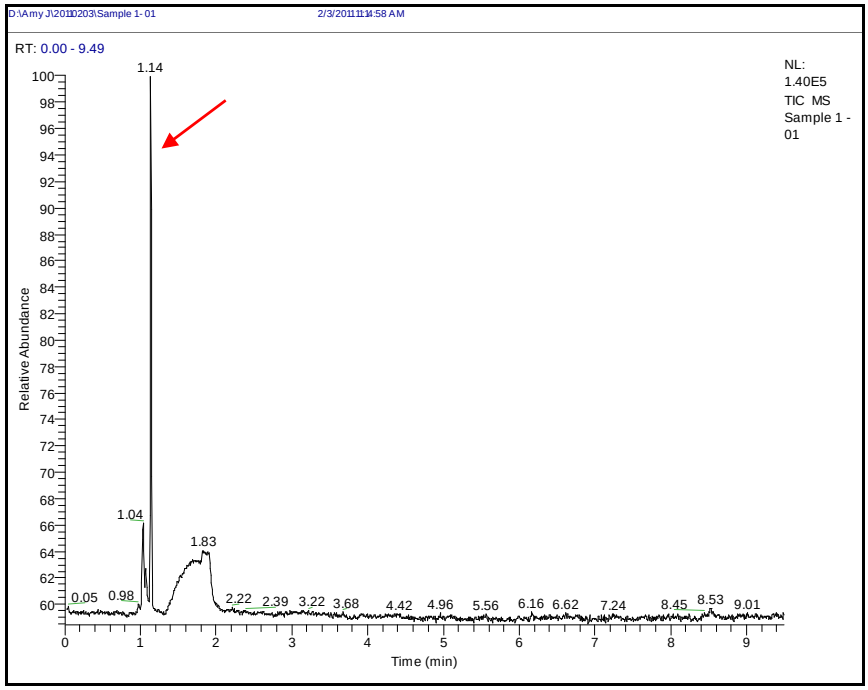

Figure 6-9: The chromatogram obtained from a plasma sample taken 30 seconds after the I.V. administration of 0.03 mmol/kg mel/HPβCD

Mel/HPβCD was administered I.V. at a dose of 0.03mmol/kg and blood removed by cardiac puncture after 30 seconds. The whole blood was centrifuged and the plasma collected. The plasma was digested by wet-acid digestion and the arsenic content of the sample determined by GC-MS. An arsenic peak was detected (red arrow).

6.4 Discussion

Melarsoprol has been used for the treatment of CNS stage trypanosomiasis for over 60 years, but very little is known about the drugs pharmacokinetic properties and tissue distribution. Previous pharmacokinetic investigations have used bioassays which quantify the trypanocidal activity of samples and compare it to known standards in order to estimate the concentration of melarsoprol within the samples (Burri *et al.*, 1993; Burri and Brun, 1992; Burri *et al.*, 1994). As the assay does not measure the drug directly, it is unable to differentiate between melarsoprol and its active metabolites. The trypanocidal activity observed is presumed to be solely due to the presence of melarsoprol. Attempts were made to distinguish between melarsoprol and its metabolites by high performance liquid chromatography (HPLC) (Berger and Fairlamb, 2005; Ericsson *et al.*, 1997; Keiser, Ericsson and Burri, 2000). The HPLC assay developed by Berger and Fairlamb was able to distinguish between melarsoprol, trimelarsen, cymelarsan and melarsen oxide (Berger and Fairlamb, 2005). However, the 80 minute run time prevented the analysis of large numbers of samples. To allow analysis of large numbers of clinical samples the assay was modified and the run time shortened by Ericsson *et al*. (Ericsson *et al.*, 1997). However, the only metabolite which could be detected was melarsen oxide, which was rapidly eliminated from the plasma within twenty-four hours of administration. Furthermore, discrepancies were detected between the HPLC assays and bioassay. While no melarsen oxide was detected in the plasma twenty-four hours after administration by HPLC, pronounced trypanocidal activity was detected by bioassay, indicating that melarsen oxide is further metabolised. In an attempt to resolve the discrepancies between HPLC and bioassays, the total arsenic content of samples was quantified by atomic absorption spectrometry (AAS) (Keiser, Ericsson and Burri, 2000). However, the limit of quantification of the assay was 50ng/ml. A sensitive, specific assay, which can accurately quantify the total arsenic content of samples, would allow the basic pharmacokinetic properties of melarsoprol to be determined.

In this study a gas chromatography mass spectrometry (GC-MS) assay was developed to quantify the total arsenic content of samples following chemotherapy with the melarsoprol cyclodextrin complexes, mel/HPβCD and

mel/RAMβCD. The limit of quantification of the assay was 5ng/ml. This is ten times lower than the limit of quantification of the atomic absorption spectrometry (AAS) assay previously described by Keiser *et al*. (Keiser, Ericsson and Burri, 2000). The limit of detection of the GC-MS assay is also nearly two fold lower than the limit of quantification of the bioassay developed by Burri and Brun (Burri and Brun, 1992). Only the automated bioassay developed by Onyango *et al*. and the HPLC assay developed by Berger and Fairlamb have lower limits of quantification, of 4ng/ml and 3.98pg/ml respectively. However, the HPLC assay is not suitable for the analysis of large numbers of clinical samples (Berger and Fairlamb, 2005; Onyango, Burri and Brun, 2000).

In this analysis the brain and plasma samples were digested by wet-acid digestion in nitric acid and hydrogen peroxide. The percentage recovery rate of arsenic from the brain samples using this methodology was found to be 87.5%. The extraction of arsenic by wet-acid digestion from brain samples has been previously reported by Zirar *et al*. (Zirar *et al.,* 2008). However, the recovery rate of the method was not stated, therefore no comparisons can be made between the recovery rates of the present study and that of Zirar *et al*. The extraction recovery rate obtained in the present study is similar to that reported by Ericsson *et al*. for plasma samples extracted in chloroform-acetonitrile and back extracted into phosphoric acid where a recovery rate of 86.3% was reported (Ericsson *et al.,* 1997). The recovery rate obtained in the present study was 22.3% higher than that previously reported by Berger *et al*. for plasma samples extracted over octadecylisilane cartridges (Berger and Fairlamb, 2005). Although direct comparisons cannot be made between the present study and those of Ericsson *et al*. and Berger *et al*. since they were conducted in different tissues, they indicate that the recovery rate obtained in the present study is within previously reported ranges for biological tissues. Unfortunately the percentage recovery rate of arsenic from plasma samples was not determined in the present study.

The precision (repeatability) of the GC-MS assay, expressed as the inter-day average coefficient of variation was 14.9% for brain samples. This value is similar to those previously reported by Onyango *et al*. for the automated biological assay (Onyango, Burri and Brun, 2000). The repeatability for plasma and CSF

samples using the automated bioassay was 9.9% and 18.8% respectively. Unfortunately, Onyango *et al*. did not assess the precision of the bioassay for brain samples and the repeatability of plasma samples using the GC-MS assay was not determined in the present study, so direct comparisons between the two assays cannot be made. Zirar *et al*. investigated the arsenic content of brain samples by a colorimetric method, but the precision of the assay was not reported (Zirar *et al.,* 2008).

The GC-MS assay was used in the present study to determine the arsenic content of brain and plasma samples following oral chemotherapy with the melarsoprol cyclodextrin complex mel/HPβCD. Arsenic was detected within the brain one and four hours after the administration of mel/HPβCD but the concentration could not be quantified due to the presence of large impurity peaks. Arsenic was not detected within the brain at any other time points investigated. It can therefore only be concluded that the concentration of arsenic within the brain following the oral administration of 0.05mmol/kg mel/HPβCD is below the limits of detection of the assay of 5ng/ml. Arsenic was detected in the plasma, 30 seconds after the intravenous administration of 0.03mmol/kg mel/HPβCD. At this time point 3.97ng of arsenic was detected. However, this value is below the 5ng/ml limit of quantification of the assay. No arsenic was detected within the plasma at any other time points sampled, therefore it can only be concluded that the concentration of arsenic within the plasma after I.V. administration of 0.03mmol/kg mel/HPβCD is less than 5ng/ml.

The detection of arsenic within the plasma and brain following intravenous administration of mel/HPβCD has been previously reported by Zirar *et al*. (Zirar *et al.,* 2008). In this study 0.038mmol/kg of mel/HPβCD was administered I.V. to mice. Plasma and brain tissue was collected 0.5, 30 minutes, 1, 5, 8, 18, 24 and 48 hours after administration of the compound. The samples were digested in nitric acid and hydrogen peroxide and the arsenic within the samples converted to arsine gas. The gas was bubbled through a solution of silver salt and the absorbance of the silver salt measured and compared to standards of known arsenic concentration in order to determine the arsenic content of the samples (Zirar *et al.,* 2008). The maximum concentration (C_{max}) of arsenic detected within the brain following the I.V. administration of 0.038mmol/kg of

mel/HPβCD was 0.25μmol/g. This is equivalent to 18.75μg of arsenic per gram of brain tissue. Assuming the average mouse brain weighs 0.5g, the total arsenic content of the brain was approximately 9.37μg. The maximum concentration (C_{max}) of arsenic obtained in the plasma following the intravenous administration of mel/HPβCD was not determined in the study.

In contrast to the study by Zirar *et al.*, arsenic was not detected within the brain in the present study following the oral administration of mel/HPβCD. One possible explanation for the discrepancy between the two studies is the route by which the melarsoprol cyclodextrin complex was administered. In the present study mel/HPβCD was administered orally, while Zirar *et al.* administered the compound intravenously. This means that in the present study the concentration of arsenic reaching the brain is likely to be lower, as the drug must first pass through the gastrointestinal tract and be absorbed across the mucosal membrane before entering the bloodstream and finally the brain. In contrast, when intravenously administered, the compound enters the bloodstream immediately and can pass directly into the brain, leading to high concentrations. This could account for our failure to detect arsenic within the brain following oral administration of the complexes but it does not explain why arsenic could only be detected within the plasma 30 seconds after the I.V. administration of mel/HPβCD but at no other time points. One possible explanation for the difference in the plasma concentration of arsenic detected in the present study and that of Zirar *et al.* is the different assays used to quantify the total arsenic content of the samples (Zirar *et al.*, 2008). In the present study GS-MS was used to quantify the total arsenic content of the plasma samples. The only ion the assay measures is arsenic therefore the technique is very sensitive and specific. The limit of detection of the assay is 5ng/ml. In contrast, Zirar *et al.* used a colorimetric method (Zirar *et al.*, 2008). The arsenic within the samples was reduced under acidic conditions by the addition of zinc, generating arsine gas. The arsine was bubbled through a solution of silver salt of diethyldithiocarbamate in pyridine and the absorbance of the solution measured to quantify the arsenic content of the samples. Zirar *et al.* did not state the limit of detection of the assay but other studies using a similar method have quoted the limit of detection of the assay to be 100ng/ml (Baghel, Singh, Pandey and Sekhar, 2007; Dhar, Zheng, Rubenstone and van Geen, 2004; Talmi and

Bostick, 1975). This is 20 fold lower than the GS-MS assay. The colorimetric method is not able to accurately quantify the arsenic content of samples, as the zinc power used within the assay to generate arsine gas also contains arsenic. The concentration of arsenic measured by the colorimetric method is therefore not solely from the samples (Baghel *et al.*, 2007; Jacobs and Nagler, 1942). This could account for why arsenic was detected in the plasma samples in the study conducted by Zirar *et al*. but not in the present study.

In a previous study in which the arsenic content of human plasma samples was determined by atomic absorption spectrometry (AAS) following the intravenous administration of melarsoprol, 147ng/ml of arsenic was still detected twenty-four hours after administration of the drug (Keiser, Ericsson and Burri, 2000). However, the dose of melarsoprol administered in the study was considerably larger than the dose given in the present study. In the study by Keiser *et al*. patients were administered 2.2mg/kg of melarsoprol (Keiser, Ericsson and Burri, 2000). For a 50kg patient this is equivalent to 110mg of melarsoprol. In the present study, mice were administered 0.03mmol/kg of mel/HPβCD this is equivalent to 11.94mg/kg of melarsoprol. A mouse weighing 40g would therefore receive 0.478mg of melarsoprol. This is 230 fold less than the dose administered to patients in the study conducted by Keiser *et al*. (Keiser, Ericsson and Burri, 2000). Immediately after administration of 2.2mg/kg of melarsoprol Keiser *et al*. detected 657ng/ml of arsenic within the plasma (Keiser, Ericsson and Burri, 2000). In the present study, 3.97ng/ml of arsenic was detected in the plasma 30 seconds after the administration of mel/HPβCD. This is approximately 165.5 times lower than that detected in humans. In humans, by one hour after administration of 2.2mg/kg melarsoprol, the concentration of arsenic within the plasma had decreased to 417ng/ml (Keiser, Ericsson and Burri, 2000). Extrapolating this value down to mice, the arsenic concentration within the plasma 1 hour after administration of 0.03mmol/kg mel/HPβCD would be approximately 2.5ng/ml. This is below the limit of quantification of the GC-MS assay and thus could explain why arsenic was only detected thirty seconds after the intravenous administration of mel/HPβCD in the present study. In order to detect the concentration of arsenic within murine tissues following the administration of the melarsoprol cyclodextrin complexes, mel/HPβCD and

mel/RAMβCD, an assay with a greater degree of sensitivity is required. One possible option is inductively coupled plasma mass spectrometry (ICP-MS).

ICP-MS was developed over 20 years ago by the Houk and Gray research groups (Date and Gray, 1981; Houk, Fassel, Flesch, Svec *et al.*, 1980). It is a sensitive, accurate, and precise tool, by which to determine the total concentration of an element within a sample (Kawabata, Inoue, Takahashi and Endo, 1994). Ito *et al*. used dynamic reaction cell (DRC)-ICP-MS to quantify the total concentration of arsenic within whole blood, collected from patients who had a total arsenic urine concentration of greater than 50μg/ml (Ito, Palmer, Steuerwald and Parsons, 2010). The whole blood was lysed and diluted 1:49 with a reagent containing nitric acid and Triton®-X and the total arsenic content determined by DRC-ICP-MS. The total concentration of arsenic detected within the samples ranged from 1.4 and 8.0μg/L. The limit of quantification of the assay was 300pg/ml (Ito *et al.*, 2010). This is 16.7 times more sensitive than the GC-MS assay described in the present study. The ability of ICP-MS to detect arsenic when present within the pico gram range in samples, means that it should be possible to detect the extremely low concentration of arsenic present within murine tissues, following oral or intravenous administration of mel/HPβCD and mel/RAMβCD, using this technique. Only the total concentration of arsenic within a sample can be quantified by ICP-MS but if the technique is coupled with a separation assay such as chromatography, it is possible to determine the species of the element present within the sample (B'Hymer and Caruso, 2004). Mandal *et al*. coupled ICP-MS with high performance liquid chromatography (HPLC) to separate eight species of arsenic (Mandal, Ogra and Suzuki, 2001). The species which could be separated using the technique included, arsenocholine, arsenobetaine, dimethylarsinic acid (DHA^{V}), dimethylarsinous acid (DMA^{III}), monomethylarsonic acid (MMA^{V}), monomethylarsonous acid (MMA^{III}), arsenite (As^{III}) and arsenate (As^{V}). The limits of detection ranged from 0.14 to 0.33ng/ml. The technique was used to quantify the concentration and species of arsenic present within plasma samples collected from residents of an arsenic affected district in West Bengal, India (Mandal, Ogra, Anzai and Suzuki, 2004). Four species of arsenic, were detected in the plasma samples at concentration ranging from 1.28ng/ml to 2.56ng/ml. Ito *et al*. also used liquid chromatography (LC) coupled with ICP-MS to determine the species of arsenic within whole

blood, collected from patients with total urine arsenic concentrations greater than 50µg/l (Ito *et al.*, 2010). The technique was able to separate five species of arsenic, arsenite (As^{III}), arsenate (As^{V}), monomethylarsonic acid (MMA^{V}), dimethylarsinic acid (DHA^{V}) and arsenobetaine (AsB). The analysis was completed in twelve minutes and the limit of detection for each species was <0.3ng/ml (Ito *et al.*, 2010). The studies conducted by Mandal *et al*. and Ito *et al*. demonstrate that ICP-MS when coupled with chromatography techniques enables the quantity and species of arsenic contained within biological samples to be accurately quantified (Ito *et al.*, 2010; Mandal *et al.*, 2004). ICP-MS coupled with chromatography, would enable the species of arsenic present within murine tissues following the administration of mel/HPβCD and mel/RAMβCD to be accurately determined and quantified. Furthermore, the technique would enable the full pharmacokinetic profile of the melarsoprol cyclodextrin complexes to be determined and the metabolic fate of melarsoprol, following administration to be elucidated.

From these investigations it can be concluded that gas chromatography mass spectrometry (GC-MS) is an accurate and sensitive method for quantifying the total amount of arsenic, present within brain samples when the concentration of arsenic is above 5ng/ml. The concentration of arsenic present within the brain and plasma of mice administered the melarsoprol cyclodextrin complexes, mel/HPβCD and mel/RAMβCD is below 5ng/ml, for both oral and intravenous administration. The concentration of arsenic within the tissues could therefore not be determined by GC-MS. In order to quantify the total amount of arsenic present within tissues following administration of mel/HPβCD and mel/RAMβCD a more sensitive assay is required. Inductively coupled plasma mass spectrometry (ICP-MS) is one option.

Chapter 7: General Discussion

7.1 The trypanocidal activity of mel/HPβCD and mel/RAMβCD

The melarsoprol cyclodextrin complexes mel/HPβCD and mel/RAMβCD were developed with the aim of reducing the toxicity of melarsoprol and providing an orally administrable formulation of the drug. This investigation has demonstrated that the trypanocidal activity of melarsoprol is retained, following its complexation with the cyclodextrins HPβCD and RAMβCD. Initial studies investigating the drug's efficacy *in-vitro* against wild type *T. b. brucei* trypanosomes demonstrated that the IC_{50} of the complexed molecules was comparable to that of contemporary melarsoprol.

When the activity of the drugs was investigated *in-vivo*, both mel/HPβCD and mel/RAMβCD were able to produce 100% cure rates in a murine model of CNS stage *T. b. brucei* infection, when administered orally, for seven consecutive days, at a dose of 0.05mmol/kg. In contrast, melarsoprol, when administered at the same dose and by the same route, produced cure rates of only 33.3%. This indicates that the cyclodextrins HPβCD and RAMβCD increase the oral bioavailability of melarsoprol. An increase in bioavailability of the compound occurs, as the cyclodextrins act as carriers, delivering the drug directly to the intestinal membrane. Once at the intestinal membrane, dissociation of the complexes occurs due to a simple mass action principle and the drug is absorbed across the intestinal mucosa (Stella *et al.,* 1999). An increase in the oral bioavailability of poorly soluble drugs, by complexation is frequently reported. The oral bioavailability of the antimalarial artemisinin was improved, with no concurrent loss in activity by complexation with β and γ cyclodextrin (Wong and Yuen, 2001). In this study artemisinin, artemisinin/β or artemisinin/γ were administered at equivalent doses to healthy volunteers. The plasma drug levels obtained after administration of the two complexes were two fold higher than those obtained following administration of the compound alone. This indicates that the rate and extent of artemisinin absorption is increased by complexation with β and γ cyclodextrins (Wong and Yuen, 2001).

Administration of seven daily doses of mel/HPCD or mel/RAMβCD at a dose of 0.05mmol/kg produced 100% cure rates in a murine model of CNS stage *T. b. brucei* infection. However, quantitative taqman PCR analysis demonstrated that all trypanosomes were eliminated from the brain, twenty-four hours after the administration of four doses of mel/HPβCD or five doses of mel/RAMβCD. This suggests that it may be possible to reduce the regime from seven doses to four daily doses of mel/HPβCD or five daily doses of mel/RAMβCD. This treatment regime is shorter than the currently used concise 10 day melarsoprol schedule for the treatment of CNS stage *T. b. gambiense* infections. During the current concise 10 day schedule the total amount of melarsoprol administered to patients is 1080mg for a 50kg patient (Burri *et al.,* 1993). In the current study, the melarsoprol cyclodextrin complexes were administered at a daily dose of 0.05mmol/kg. This is equivalent to 19.9mg/kg of melarsoprol a day. In order to obtain a human equivalent dose from an animal dose, the dose must be normalised to the body surface area. This means that to convert the dose administered to mice in the present study to a human equivalent dose, the dose must be divided by twelve (U.S.Department of Health and Human Services, 2005). This means that the dose administered to humans would be 4.2μmol/kg. This is equivalent to 1.67mg/kg of melarsoprol a day. During a four day course of mel/HPβCD the total amount of melarsoprol which would be administered to a 50kg patient would be 334mg, while for a five day course of mel/RAMβCD the total amount of melarsoprol given would be 417.5mg. This is 3.2 and 2.6 fold lower, respectively, than the total amount of melarsoprol currently administered during the concise 10 day schedule. By reducing the total amount of melarsoprol which is administered to patients, the safety profile of the drug may be improved.

Melarsoprol is a highly toxic drug with a number of adverse reactions associated with its administration. The main side effect resulting from the administration of melarsoprol is a post-treatment reactive encephalopathy (PTRE), which occurs in up to 10% of patients, administered the drug, of which 50% die as a result of the complication. This gives melarsoprol an overall fatality rate of 5% (Kennedy, 2004; Pepin and Milord, 1994). Numerous mechanisms have been proposed to explain the occurrence of the PTRE. Pepin and Milord suggested it results from the formation of inclusion complexes and the release of trypanosomal antigens

which bind to glial cells and become a target for antibodies and T lymphocytes (Pepin and Milord, 1991). However, Jennings *et al*. suggested an alternative mechanism. Jennings *et al*. proposed that administration of melarsoprol results in a rapid clearance of trypanosomes from the bloodstream but not the CNS. As a result the trypanosomes within the brain become the sole focus of the immune system resulting in an exacerbation of the pre-existing meningoencephalitis (Jennings *et al.,* 1989). Based on this theory, Jennings and colleagues suggested that aggressive treatment schedules which simultaneously eliminate trypanosomes from the CNS and bloodstream could prevent the development of the PTRE. This hypothesis was tested in a study in which mice were administered either a subcurative or an aggressive treatment regime (Jennings *et al.,* 1993). Meningoencephalitis was not observed in animals receiving the aggressive chemotherapy regime, while mice administered the subcurative regime, developed severe meningoencephalitis. The findings of this study supported the original hypothesis of Jennings *et al*. (Jennings *et al.,* 1989). Quantitative taqman PCR (QPCR) experiments conducted during the present study indicate that complexed melarsoprol is a rapid and aggressive treatment regime. Twenty-four hours after the administration of one dose of mel/HPβCD or mel/RAMβCD there is over a nine fold reduction in the number of copies of the PFR2 gene detected within the brain. Therefore if the hypothesis suggested by Jennings *et al*. (1989) is correct, treatment of CNS stage disease with mel/HPβCD or mel/RAMβCD should result in a reduced incidence of the PTRE, associated with the intravenous administration of contemporary melarsoprol. Thus the toxicity of melarsoprol should be reduced by complexation with the cyclodextrins HPβCD and RAMβCD. However, in order to confirm this hypothesis the time course of trypanosome elimination from the brain following the I.V. administration of contemporary melarsoprol would have to be investigated. In the present study this was not possible as administration of multiple doses of contemporary melarsoprol I.V. to mice is not viable as the propylene glycol solvent in which the drug is dissolved causes severe necrosis in the tissues adjacent to the injection site precluding further drug administration. The rate of elimination of the PFR2 gene following complexed melarsoprol or contemporary melarsoprol chemotherapy could therefore not be directly compared in the present study.

The PTRE is not exclusively associated with HAT patients as it has also been observed in patients with acute promyelocytic leukaemia (APL) who were given melarsoprol (Soignet *et al.*, 1999). Melarsoprol was administered I.V. as three series, of three doses of escalating concentration. An initial dose of 1mg/kg was given on day 1, followed by 2mg/kg on day 2 and 3.6mg/kg on day 3. During the second week of treatment three out of the eight patients developed generalised seizures. It was suggested that the CNS toxicity observed was due to a direct toxic effect of the drug (Soignet *et al.*, 1999). During complexed melarsoprol chemotherapy the total dose of melarsoprol administered to patients would be reduced compared to the concise 10 day schedule of contemporary melarsoprol. If arsenical toxicity is responsible for the PTRE, reducing the total amount of melarsoprol which is administered to patients should result in a reduced incidence of the PTRE. Furthermore, when the melarsoprol cyclodextrin complexes are administered, the melarsoprol is gradually released over a prolonged period of time from the cyclodextrin cavity. Patients are therefore not exposed to a 'bolus' of the drug as is the case with the I.V. administration of contemporary melarsoprol. This controlled and sustained release of melarsoprol obtained with complexed melarsoprol should therefore reduce the toxicity of the drug and prevent the occurrence of the PTRE.

Development of the PTRE is not the only problem associated with the administration of contemporary melarsoprol. The poor solubility of the drug means it must be dissolved in the solvent propylene glycol. This means administration of the drug is very painful and extreme care must be taken when administering the drug intravenously as if the solution leaks into the tissues surrounding the vein severe necrosis can occur (World Health Organisation, 1998). As the drug has to be administered intravenously patients must be hospitalised for the entire duration of the treatment regime. This places an enormous strain on the hospitals which have very limited resources and also on the patients' families who must accompany the patients to the hospital. Complexed melarsoprol is orally administrable therefore the problems associated with the intravenous administration of contemporary melarsoprol therapy are instantly eliminated. Furthermore, due to being orally administrable, patients could receive treatment at their local health centre by community health workers thereby relieving the pressure on hospitals. The

complexes could be provided pre-packaged, with the dose clearly indicated, so patients could take the drugs themselves. A similar scheme is currently in operation for the treatment of malaria. A presumptive diagnosis of malaria is made by specially trained members of the community. Patients are then given a course of pre-packed antimalarials based on their weight, which they can take within their own home. The packaging is clearly designed so that the patient knows which tablets to take each day (Hopkins, Talisuna, Whitty and Staedke, 2007). However, although the scheme has increased the access to antimalarial treatment, patient compliance is often a problem. In one study conducted in Ghana, Nigeria and Uganda, the percentage of children receiving the correct dose and completing the treatment regime, ranged from 74 to 97% (Ajayi, Browne, Garshong, Bateganya *et al.*, 2008). If patients do not complete the specified treatment regime, parasites will be exposed to subcurative drug levels, which could lead to the development of resistance. Treatment failures following melarsoprol chemotherapy of 30% have already been reported in certain regions of Uganda (Legros *et al.,* 1999). Drug resistance is therefore a real threat in the treatment of HAT and measures would have to be taken to ensure that patients received the correct dose and completed the full chemotherapy regime.

The only oral trypanocide currently in clinical development is the nitroimidazole fexinidazole (Torreele *et al.,* 2010). *In-vitro* the IC_{50} of fexinidazole against *T. b. rhodesiense* trypanosomes was 48 to 82ng/ml. In contrast, the IC_{50} of the melarsoprol cyclodextrin complexes mel/HPβCD and mel/RAMβCD against *T. b. brucei* trypanosomes was 8.6ng/ml and 3.50ng/ml respectively. However, the *in-vitro* trypanocidal activity of fexinidazole and the melarsoprol cyclodextrin complexes cannot be directly compared due to the different parasite strains used in the two studies. In an *in-vivo* murine model of CNS stage *T. b. brucei* infection, mel/HPβCD and mel/RAMβCD produced 100% cure rates when administered orally, at a dose of 0.05mmol/kg (19.9mg/kg), daily, for seven consecutive days. Fexinidazole, in the same model was only able to cure 87.5% of the animals, when administered orally at a dose of 200mg/kg, daily, for five days (Torreele *et al.,* 2010). If equivalent figures are seen in the treatment of human trypanosomiasis this means that for every 100 patients treated with fexinidazole 12 will relapse and will have to receive alternative treatment. Fexinidazole entered phase I clinical trials in September 2009 in order to

establish the drug's pharmacokinetics and tolerability in healthy African volunteers. If successful, the compound is expected to progress to phase II clinical trials. However, despite the initial promising data, there is no guarantee that fexinidazole will successfully complete all stages of the clinical trials and be approved for the treatment of HAT. It is therefore important to have other drug candidates in development. Based on the findings from the current investigation, the melarsoprol cyclodextrin complexes mel/HPβCD and mel/RAMβCD are two possible candidates.

7.2 The effect of mel/HPβCD chemotherapy on the integrity of the blood-brain barrier

In the present investigation the ability of mel/HPβCD chemotherapy to rapidly restore the integrity of the blood-brain barrier (BBB) was demonstrated. The BBB is disrupted during trypanosome infection but the exact mechanism as to how trypanosomes traverse the barrier and invade the CNS remains unclear. Mulenga *et al*. demonstrated that trypanosome traversal of the BBB was not associated with a loss of tight junction proteins (Mulenga *et al.,* 2001). However, in a MRI study conducted by Rodgers *et al.*, at 28 days post-infection in mice infected with *T. b. brucei,* the integrity of the BBB was found to be compromised (Rodgers *et al.,* 2011). Histological examination revealed, minimal inflammatory cell infiltration of the meninges and perivascular space, furthermore, there was no correlation between the areas of meningoencephalitis and regions of BBB breakdown (Rodgers *et al.,* 2011). In the present investigation a mild inflammatory reaction was still present within the brain 14 days after the integrity of the BBB had been restored. This finding suggests that the breakdown in the BBB observed in trypanosome infections, is not due to the presence of a CNS inflammatory reaction. The rapid restoration of the BBB following the elimination of trypanosomes from the CNS, observed in the present study, suggests that either the trypanosomes directly, or their secretory products, disrupt the BBB. The work of Grab *et al*. and Nikolskaia *et al*. in an *in-vitro* model of the BBB supports this hypothesis (Grab *et al.,* 2009; Nikolskaia *et al.,* 2006). Grab *et al*. proposed that trypanosomes release cysteine proteases in particular, brucipain, which triggers the release of intracellular calcium through the activation of protease activated receptors (PARs). Calmodulin (CaM)

activation of myosin light chain kinase (MLCK), subsequently leads to a rearrangement of the cytoskeleton and barrier dysfunction (Grab *et al.*, 2009; Nikolskaia *et al.*, 2006). Following the elimination of trypanosomes from the CNS, the integrity of the BBB should be restored as parasite derived cysteine proteases will no longer be released. In the current investigations, the melarsoprol cyclodextrin complexes, mel/HPβCD and mel/RAMβCD, rapidly eliminated trypanosomes from the brain, thus preventing further release of trypanosome derived cysteine proteases and damage to the BBB. The BBB was thus able to repair itself and barrier function was restored. In order to gain concrete evidence that the release of trypanosome derived cysteine proteases are responsible for the BBB damage observed in trypanosome infection, further investigations are required. One possible option is to develop a murine model in which expression of the PARs genes has been decreased. If activation of PARs by trypanosome derived cysteine proteases is responsible for the BBB damage observed in trypanosome infections, the level of BBB disruption should be reduced in mice in which PARs expression has been decreased.

7.3 Future work

The investigations in the present study demonstrate that the melarsoprol cyclodextrin complexes mel/HPβCD and mel/RAMβCD are promising oral candidates for the treatment of CNS stage trypanosome infections. However, if the complexes are to progress into clinical trials, further investigations are required. In order for complexed melarsoprol to be considered for clinical trials the pharmacokinetics of the complexes must be determined. In the present study the pharmacokinetics of the complexes was investigated by gas chromatography mass spectrometry (GC-MS). However, the total concentration of arsenic reaching the plasma and brain following oral administration of the complexes appears to be within the sub-nanogram range. The limit of detection of arsenic using the GC-MS technique is 5ng/ml, a more sensitive technique is therefore required to determine the pharmacokinetic properties of the melarsoprol cyclodextrin complexes. As discussed in chapter 6, one possible option is inductively coupled plasma mass spectrometry (ICP-MS). ICP-MS is a highly sensitive technique, able to detect arsenic concentrations in the picogram range. Furthermore, if the method is coupled with a separation technique such

as chromatography, the species of arsenic present within the samples could be determined (B'Hymer and Caruso, 2004). This would provide important insights into the metabolic fate of melarsoprol following its administration, as currently very little is known about the active metabolites of melarsoprol.

Mel/HPβCD and mel/RAMβCD were able to cure murine CNS stage *T. b. brucei* infection when administered daily, for seven consecutive days, at a dose of 0.05mmol/kg. Subsequent quantitative taqman PCR (QPCR) analysis revealed all trypanosomes were eliminated from the CNS twenty-four hours after the administration of four doses of mel/HPβCD or five doses of mel/RAMβCD. This indicates that the number of doses of the complexes could be reduced from seven to four doses of mel/HPβCD and five doses mel/RAMβCD. However, QPCR analysis also revealed that very low copy numbers of the PFR2 gene were present within the brain after the administration of three doses of each complex. It is not known if this represents a viable population of trypanosomes. Further, *in-vivo* experiments are required in order to determine if the trypanosomes present within the brain after administration of three doses of the complexes can sustain the infection. If the trypanosomes are not viable it would enable the treatment regime to be reduced even further.

In the present study the integrity of the blood brain barrier (BBB) was restored by twenty-four hours after the completion of mel/HPβCD chemotherapy. However, the exact point during the chemotherapy regime, at which barrier function is restored, is currently unknown. Serial MRI scanning twenty-fours after the administration of each dose of the complex would enable the point during the chemotherapy regime at which the integrity of the BBB is restored to be identified. This could then be compared to the number of trypanosomes present within the brain at that time point to establish if any correlation exists between the restoration of barrier function and the presence of trypanosomes within the CNS. Only the effect of mel/HPβCD chemotherapy on the BBB was investigated in the present study but the investigations could also be conducted for mel/RAMβCD to establish if there is any difference between the two complexes in their ability to restore BBB function.

The PTRE is a serious adverse reaction associated with melarsoprol treatment. The mechanisms behind the occurrence of the PTRE are poorly understood with numerous hypotheses proposed including, subcurative chemotherapy, arsenical toxicity and autoimmune mechanisms (Hunter, Murray, Jennings, Adams *et al.*, 1992; Jennings *et al.*, 1989; Pepin, Milord, Khonde, Niyonsenga *et al.*, 1995; Soignet *et al.*, 1999). Recent analysis of cytokine levels within the CSF and plasma of late stage HAT patients has revealed that the degree of meningoencephalitis maybe regulated by pro and counter inflammatory cytokines. Lejon *et al.* found elevated levels of IL-6, IL-8 and IL-10 in the CSF of late stage *T. b. gambiense* patients (Lejon, Lardon, Kenis, Pinoges *et al.*, 2002). The counter inflammatory cytokine IL-10 was also significantly increased in the plasma and CSF of late stage *T. b. rhodesiense* patients. However, following successful completion of chemotherapy the cytokine level was comparable to that observed in uninfected patients (MacLean, Odiit and Sternberg, 2001). In order to investigate further the effect of successful chemotherapy on the levels of pro and counter inflammatory cytokines within the brain, quantitative taqman PCR could be utilised to quantify the cytokines present within the brain during complexed melarsoprol chemotherapy. Furthermore, the cytokine levels could be compared with the number of trypanosomes present within the brain and regions of neuroinflammation, to determine if any correlation existed.

7.4 Conclusions

The main findings which can be drawn from the present study are:

- The trypanocidal activity of melarsoprol is retained following its complexation with the cyclodextrins HPβCD and RAMβCD.

- The cyclodextrins HPβCD and RAMβCD increase the oral bioavailability of melarsoprol.

- The melarsoprol cyclodextrin complexes mel/HPβCD and mel/RAMβCD are able to cure CNS stage murine *T. b. brucei* infection when administered orally, daily, at a dose of 0.05mmol/kg, for seven consecutive days. Melarsoprol, cymelarsan and trimelarsen, when administered at an

equivalent dose, following the same treatment regime produced unsatisfactory cure rates.

- The human equivalent dose of mel/HPβCD and mel/RAMβCD is lower than the melarsoprol dosage currently administered to patients during the concise 10 day schedule.

- Mel/HPβCD and mel/RAMβCD are rapidly trypanocidal, with all trypanosomes eliminated from the brain by twenty-four hours after administration of four doses of mel/HPβCD and five doses of mel/RAMβCD. Thus indicating the potential for further reductions in the dosage required for successful chemotherapy.

- The integrity of the blood-brain barrier (BBB) as determined by MRI analysis is fully restored by twenty-four hours after administration of the seventh dose of mel/HPβCD.

- The rapid restoration of BBB function following the elimination of trypanosomes from the brain, suggests that trypanosomes either directly or through the release of secretory products may cause the BBB damage observed in trypanosome infections.

- No signs of the PTRE were observed in animals following administration of mel/HPβCD and mel/RAMβCD indicating that the neurotoxicity of melarsoprol may be reduced following complexation with HPβCD and RAMβCD.

- The melarsoprol cyclodextrin complexes mel/HPβCD and mel/RAMβCD are well tolerated in the mouse, following oral administration with no adverse treatment related reactions detected.

In conclusion the melarsoprol cyclodextrin complexes mel/HPβCD and mel/RAMβCD are promising oral candidates for the treatment of CNS stage trypanosome infections. At present chemotherapy of CNS stage trypanosome

infections is reliant on either nifurtimox eflornithine combination therapy (NECT) for the treatment of *T. b. gambiense* infections or melarsoprol for the treatment of *T. b. rhodesiense* infections. Melarsoprol is extremely toxic with an overall fatality rate of 5%. Although NECT therapy is associated with less adverse reactions than melarsoprol, eflornithine must be administered by slow intravenous administration every twelve hours for seven days. This places a considerable strain on hospitals which have limited resources and also on patients' families who must accompany the patients to hospital. A drug which is orally administrable would eliminate the need for patients to be hospitalised, thus alleviating the strain on hospitals and patients' families. Furthermore, an orally available drug can be administered by the patients themselves, freeing up essential doctors and nurses. Currently, only one orally administrable drug, fexinidazole, is in clinical trials. It is essential that other orally available drugs are developed so that treatment of HAT does not become dependant on one drug.

The melarsoprol cyclodextrin complexes mel/HPβCD and mel/RAMβCD are promising oral candidates for the treatment of HAT. The complexes are highly trypanocidal, orally administrable, well tolerated and consist of short treatment regimes. These are essential characteristics that a compound must posses if it to be considered as a potential new trypanocide. With further toxicological and pharmacokinetic studies it should be possible for the melarsoprol cyclodextrin complexes, mel/HPβCD and mel/RAMβCD, to enter into clinical trials. This would represent a huge breakthrough in the search for new trypanocides and could revolutionise the treatment of HAT.

Appendix 1

Calculation of the oral dose of complexed melarsoprol

The amount of complex required to provide a melarsoprol dose of 0.05mmol/kg was calculated. 0.05mmol/kg is equivalent to:

- 0.05mmol/1000g
- 0.05µmol/1g

The dose was prepared per 10g of body weight, 10g is therefore equivalent to 0.5µmols of melarsoprol. For ease of administration the 0.5µmols was prepared in a volume of 0.1ml which is equivalent to:

- 5µmols/ml
- 5mmols/l

To prepare a dose of 0.05mmol/kg, 5mmols of melarsoprol is required per litre:

- 1M melarsoprol = 398g/l
- 1000mM = 398g/l
- 1mM = 0.398g/l
- 5mM = 1.99g/l
- 5mM = 0.00199g/ml
- 5mM = 2mg/ml

To prepare a melarsoprol solution of 0.05mmol/kg, 2mg of melarsoprol per ml is required. The ratio of melarsoprol to cyclodextrin within the complexes as determined by HPLC analysis is 1:17 for mel/HPβCD and 1:14 for mel/RAMβCD. This ratio has to be taken into account when calculating the amount of each complex required to obtain a melarsoprol dose of 0.05mmol/kg:

- 0.05mmol/kg of mel/HPβCD = 2x17 = 34mg/ml
- 0.05mmol/kg of mel/RAMβCD = 2x14 = 28mg/ml

To obtain a dose of 0.05mmol/kg 34mg/ml of mel/HPβCD and 28mg/ml of mel/RAMβCD is therefore required.

Calculation of the intravenous dose of mel/HPβCD

The amount of melarsoprol required to provide a dose of 0.03mmol/kg was calculated. 0.03mmol/kg is equivalent to:

- 0.03mmol/1000g
- 0.03µmols/1g

The dose was prepared per 10g of bodyweight, 10g is therefore equivalent to 0.3µmols of melarsoprol. For ease of administration 0.3µmols was prepared in a volume of 0.05ml which is equivalent to:

- 6µmols/ml
- 6mmols/l

To prepare a dose of 0.03mmol/kg, 6mmols of melarsoprol per l is required:

- 1M melarsoprol = 398g/l
- 1000mM = 398g/l
- 1mM = 0.398g/l
- 6mM = 2.388g/l
- 6mM = 0.002388g/ml
- 6mM = 2.388mg/ml

To prepare a dose of 0.03mmol/kg, 2.388mg of melarsoprol per ml is required. The ratio of cyclodextrin to melarsoprol in the mel/HPβCD complex is 1:17. This ratio must be taken into account when calculating the amount of mel/HPβCD required to obtain a dose of 0.03mmol/kg:

- 2.388 x 17 = 40.6mg/ml

40.6mg/ml of mel/HPβCD is therefore required to provide a dose of 0.03mmol/kg.

Appendix 2

Alamar blue®

Alamar blue	12.5mg

Dissolve the Alamar blue® in 100ml of 1 x PBS and mix well. Filter sterilise the solution with a 0.22µm syringe filter in an aseptic environment. Store at 4°C, protected from the light for up to 2 months.

LB/Agar

LB broth	5g
Agar	5g

Dissolve the LB broth and agar in 250ml of distilled water. Sterilise the solution by autoclaving.

Phosphate buffered saline (PBS)

Di-sodium hydrogen phosphate (anhydrous)	1.48g
Potassium di-hydrogen phosphate (anhydrous)	0.43g
Sodium chloride	7.2g

Add salts to 800ml of distilled water with constant stirring. Adjust the pH to 7.4 and make the total volume up to 1 litre with distilled water.

Phosphate glucose buffer saline (PGBS)

Stock buffer (without glucose)

Di-sodium hydrogen phosphate anhydrous	13.48g
Sodium dihydrogen phosphate anhydrous	0.622g
NaCl	4.25g

Dissolve salts in 1l of distilled water and adjust the pH to 8.0

Working solution

Dilute the stock buffer 6:4 in distilled water and add 15g/l glucose

TNB blocking buffer (for use in TSA™ biotin system)

Solution A

Tris (Mw = 121.1) 121.14g

Dissolve in 1l of distilled water and adjust the pH to 7.5

Solution B

NaCl 87.66g

Dissolve in 1l of distilled water

Working solution

Mix 10ml of solution A with 10ml of solution B. Gradually add 500µl of blocking reagent (supplied in kit) while continually stirring. Make up to a final volume of 100ml with distilled water and gradually heat the solution to 60°C while continually stirring in order to completely dissolve the blocking reagent.

TNT wash buffer (for use in TSA™ biotin system)

Solution A

Tris (Mw = 121.1) 121.14g

Dissolve in 1l of distilled water and adjust the pH to 7.5

Solution B

NaCl 87.66g

Dissolve in 1l of distilled water

Working solution

Mix 100ml of solution A with 100ml of solution B. Add 500µl of Tween 20 and make up to a final volume of 1l with distilled water.

0.2M phosphate buffer

Solution A

Sodium dihydrogen phosphate	6.24g

Dissolve in 100ml of distilled water

Solution B

Disodium hydrogen phosphate	5.66g

Dissolve in 100ml of distilled water

Working solution

Mix 9.5ml of solution A with 40.5ml of solution B and make up to 100ml with distilled water, adjust the pH to 7.4.

4% paraformaldehyde

Paraformaldehyde	1g

Dissolve paraformaldehyde in 10ml of distilled water at 60°C with constant stirring. Once dissolved, cool the solution and add 12.5ml 0.2M phosphate buffer (see above). Adjust the pH to 7.3 and the total volume to 25ml with distilled water. Store at 4°C for up to 24 hours or at -20°C for longer periods.

10mM Tris pH 8.0

Tris (Mw = 121.1)	1.214g

Dissolve the salt in 800ml of distilled water. Adjust the pH to 8.0 by the addition of HCl and make up the final volume to 1l with distilled water.

20x SSC (Salt Sodium Citrate)

Sodium chloride	175.3g
Sodium citrate	88.2g

Dissolve the salts in 800ml of distilled water. Adjust the pH to 7.0 and make up the final volume to 1l with distilled water. Differing strengths of SSC can be prepared by dilution of the x20 stock with distilled water.

100mm Tris/150mm NaCl pH 7.5 (TBS)

Solution A

Tris (Mw = 121.1)	121.4g

Dissolve in 1l of distilled water.

Solution B

NaCl	87.66g

Dissolve in 1l of distilled water

Working solution

Mix 100ml of solution A with 100ml of solution B and add 750ml of distilled water. Adjust the pH to 7.5 and make up to the final volume of 1l with distilled water.

Appendix 3

Source of chemicals

Alamar Blue	Sigma Aldrich
Ampicillin	Sigma Aldrich
Anti-digoxigenin antibody Fab Fragments from sheep	Roche
BCIP/NBT Alkaline Phosphatase Substrate kit (5-bromo-4-chloro-3-indolyl phosphate/nitroblue tetrazolium)	Vector Laboratories
Crimp cap two part tin and Blue aluminium with silicone/PTFE liner 20mm	Speck and Burke Analytical
DAB(3,3' diaminobenzidine) Substrate kit	Vector Laboratories
Dextran sulphate	Sigma Aldrich
DH5α competent cells	Invitrogen
DNA/RNase free water	Sigma Aldrich
GdDPTA magnevist®	Bayer Health Care Pharmaceuticals
Headspace Vial (Vial crimp top 20ml)	Speck and Burke Analytical
Heparin	Martindale Pharmaceuticlas
HCl	Fisher Scientific
High Pure Plasmid Isolation kit	Roche
Histoclear	Raymond A Lamb

HMI-9 + 10% FCS + β-mercaptoethanol	Invitrogen
HPβCD	Sigma Aldrich
Hydrogen peroxide (30%)	VWR
Injectable saline	Martindale Pharmaceuticals
Kanamycin	Sigma Aldrich
L-Ascorbic acid	BDH Limited
LB broth	Sigma Aldrich
Levamisole solution	Vector Laboratories
Mouse monoclonal [HRP.21H8] to Digoxigenin (HRP) antibody	Abcam
Nitric acid	VWR
Paraformaldehyde	Sigma Aldrich
Pepsin	Sigma Aldrich
Potassium iodide	Sigma Aldrich
Proteinase K	Applichem Gmbh
Qiagen DNeasy® DNeasy blood and tissue kit	Qiagen
RAMβCD	Sigma Aldrich
RNase Away® solution	VWR
Sodium borohydride	Sigma Aldrich

Sterile H_2O	Baxter Health Care
Sterile normal saline	Baxter Health Care
Taqman Brilliant II master mix	Agilent
Tyramide signal amplification system (TSA™)	PerkinElmer
Vector Red Alkaline Phosphatase substrate kit	Vector laboratories

References

References

Abbott,N.J. (2004) Evidence for bulk flow of brain interstitial fluid: significance for physiology and pathology. *Neurochemistry International* **45**, 545-552.

Abbott,N.J., Ronnback,L., and Hansson,E. (2006) Astrocyte-endothelial interactions at the blood-brain barrier. *Nature Reviews Neuroscience* **7**, 41-53.

Abelian,V.A., Afyan,K.B., Avakian,Z.G., Melkumyan,A.G., and Afrikian,E.G. (1995) Cyclomaltodextrin glucotransferases from thermophilic actinomycetes. *Biochemistry-Moscow* **60**, 1223-1229.

Adams,J.H., Haller,L., Boa,F.Y., Doua,F., Dago,A., and Konian,K. (1986) Human African Trypanosomiasis (*T b gambiense*) - A Study of 16 Fatal Cases of Sleeping Sickness with Some Observations on Acute Reactive Arsenical Encephalopathy. *Neuropathology and Applied Neurobiology* **12**, 81-94.

Ajayi,I., Browne,E., Garshong,B., Bateganya,F., Yusuf,B., Agyei-Baffour,P., Doamekpor,L., Balyeku,A., Munguti,K., Cousens,S., and Pagnoni,F. (2008) Feasibility and acceptability of artemisinin-based combination therapy for the home management of malaria in four African sites. *Malaria Journal* **7**, 6-15.

Albers,E. and Muller,B.W. (1995) Cyclodextrin derivatives in pharmaceutics. *Critical Reviews in Therapeutic Drug Carrier Systems* **12**, 311-337.

Alibu,V.P., Richter,C., Voncken,F., Marti,G., Shahi,S., Renggli,C.K., Seebeck,T., Brun,R., and Clayton,C. (2006) The role of *Trypanosoma brucei* MRPA in melarsoprol susceptibility. *Molecular and Biochemical Parasitology* **146**, 38-44.

Aman,M., Reuscher,H., Wimmer,T., and Hirsenkorn,R. (1995) Rational design of cyclodextrin derivatives benefits that pay off in applications. Anaheim California

Anderson,D.R. (1969) Ultrastructure of Meningeal Sheaths - Normal Human and Monkey Optic Nerves. *Archives of Ophthalmology* **82**, 659-674.

Anderson,V.R. and Curran,M.P. (2007) Nitazoxanide - A review of its use in the treatment of gastrointestinal infections. *Drugs* **67**, 1947-1967.

Ansar Ahmed,S., Gogal,J., and Walsh,J.E. (1994) A new rapid and simple non-radioactive assay to monitor and determine the proliferation of lymphocytes: an alternative to [3H]thymidine incorporation assay. *Journal of Immunological Methods* **170**, 211-224.

Apted (1970a) Clinical Manifestations and Diagnosis of Sleeping Sickness. In: "The African Trypanosomiases." Ed. Mulligan. George Allen and Unwin LTD. London. pp661-683.

Apted (1970b) Treatment of Human Trypanosomiasis. In: "The African Trypanosomiases." Ed. Mullerhorvath. George Allen and Unwin LTD. London. pp684-725.

Atouguia and Kennedy (2000) Neurological aspects of human African trypanosomiasis in Infectious Diseases of the Nervous System. Ed. Davis and Kennedy P.G.E. Butterworth-Heinemann. Oxford. pp321-372.

Atouguia,J.M., Jennings,F.W., and Murray,M. (1995) Successful treatment of experimental murine *Trypanosoma brucei* infection with topical melarsoprol gel. *Transactions of the Royal Society of Tropical Medicine and Hygiene* **89**, 531-533.

Aumailley,M. and Smyth,N. (1998) The role of laminins in basement membrane function. *Journal of Anatomy* **193**, 1-21.

B'Hymer,C. and Caruso,J.A. (2004) Arsenic and its speciation analysis using high-performance liquid chromatography and inductively coupled plasma mass spectrometry. *Journal of Chromatography A* **1045**, 1-13.

Bacchi,C.J., Nathan,H.C., and Hutner,S.H. (1980) Polyamine Metabolism - A Potential Therapeutic Target in Trypanosomes. *Science* **210**, 332-334.

Bafort,J.M., Schutte,C.H.J., and Gathiram,V. (1986) Specificity of the Testryp Catt Card Agglutination-Test in A Non-Sleeping-Sickness Area of Africa. *South African Medical Journal* **69**, 541-542.

Baghel,A., Singh,B., Pandey,P., and Sekhar,K. (2007) A rapid field detection method for arsenic in drinking water. *Analytical Sciences* **23**, 135-137.

Bahl,H., Burchhardt,G., Spreinat,A., Haeckel,K., Wienecke,A., Schmidt,B., and Antranikian,G. (1991) Alpha-Amylase of Clostridium-Thermosulfurogenes Em1 - Nucleotide-Sequence of the Gene, Processing of the Enzyme, and Comparison to Other Alpha-Amylases. *Applied and Environmental Microbiology* **57**, 1554-1559.

Bailey,J.W. and Smith,D.H. (1992) The Use of the Acridine-Orange Qbc(R) Technique in the Diagnosis of African Trypanosomiasis. *Transactions of the Royal Society of Tropical Medicine and Hygiene* **86**, 630-630.

Ballabh,P., Braun,A., and Nedergaard,M. (2004) The blood-brain barrier: an overview: Structure, regulation, and clinical implications. *Neurobiology of Disease* **16**, 1-13.

Baltz,T., Baltz,D., Giroud,C., and Crockett,J. (1985) Cultivation in A Semi-Defined Medium of Animal Infective Forms of *Trypanosoma brucei*, *Trypanosoma equiperdum*, *Trypanosoma evansi*, *Trypanosoma rhodesiense* and *T gambiense*. *Embo Journal* **4**, 1273-1277.

Barone,J.A., Moskovitz,B.L., Guarnieri,J., Hassell,A.E., Colaizzi,J.L., Bierman,R.H., and Jessen,L. (1998) Enhanced bioavailability of itraconazole in hydroxypropyl-beta-cyclodextrin solution versus capsules in healthy volunteers. *Antimicrobial Agents and Chemotherapy* **42**, 1862-1865.

Barrett,M.P. (2010) Potential new drugs for human African trypanosomiasis: some progress at last. *Current Opinion in Infectious Diseases* **23**, 603-608.

Barrett,M.P., Boykin,D.W., Brun,R., and Tidwell,R.R. (2007) Human African trypanosomiasis: pharmacological re-engagement with a neglected disease. *British Journal of Clinical Pharmacology* **152**, 1155-1171.

Barrett,S.V. and Barrett,M.P. (2000) Anti-sleeping Sickness Drugs and Cancer Chemotherapy. *Parasitology Today* **16**, 7-9.

Barry and Carrington (2004) Antigenic Variation. In: "The trypanosomiases." Ed. Maudlin, Holmes, and Miles M.A. CABI Publishing. Trowbridge. pp25-37.

Barry,J.D., Marcello,L., Morrison,L.J., Read,A.F., Lythgoe,K., Jones,N., Carrington,M., Blandin,G., Bohme,U., Caler,E., Hertz-Fowler,C., Renauld,H., El Sayed,N., and Berriman,M. (2005) What the genome sequence is revealing about trypanosome antigenic variation. *Biochemical Society Transactions* **33**, 986-989.

Beales,P.F., Brabin,B., Dorman,E., Gilles,H.M., Loutain,L., Marsh,K., Molyneux,M.E., Olliaro,P., Schapira,A., Touze,J.E., Hien,T.T., Warrell,D.A., White,N., and WHO (2000) Severe falciparum malaria. *Transactions of the Royal Society of Tropical Medicine and Hygiene* **94**, S1-S90.

Begley,D.J. and Brightman,M.W. (2003) Structural and functional aspects of the blood-brain barrier. *Progress in Drug Research, Vol 61* **61**, 39-78.

Bekers,O., Uijtendaal,E.V., Beijnen,J.H., Bult,A., and Underberg,W.J.M. (1991) Cyclodextrins in the Pharmaceutical Field. *Drug Development and Industrial Pharmacy* **17**, 1503-1549.

Bellofatto,V., Fairlamb,A.H., Henderson,G.B., and Cross,G.A.M. (1987) Biochemical-Changes Associated with Alpha-Difluoromethylornithine Uptake and Resistance in *Trypanosoma brucei*. *Molecular and Biochemical Parasitology* **25**, 227-238.

Bellringer,M.E., Smith,T.G., Read,R., Gopinath,C., and Olivier,P. (1995) [beta]-Cyclodextrin: 52-Week toxicity studies in the rat and dog. *Food and Chemical Toxicology* **33**, 367-376.

Bentivoglio,M., Grassi-Zucconi,G., Olsson,T., and Kristensson,K. (1994) *Trypanosoma brucei* and the nervous system. *Trends in Neurosciences* **17**, 325-329.

Berger,B.J. and Fairlamb,A.H. (2005) High-performance liquid chromatographic method for the separation and quantitative estimation of anti-parasitic melaminophenyl arsenical compounds. *Transactions of the Royal Society of Tropical Medicine and Hygiene* **88**, 357-359.

Berriman,M., Ghedin,E., Hertz-Fowler,C., Blandin,G., Renauld,H., Bartholomeu,D.C., Lennard,N.J., Caler,E., Hamlin,N.E., Haas,B., Bohme,W., Hannick,L., Aslett,M.A., Shallom,J., Marcello,L., Hou,L.H., Wickstead,B., Alsmark,U.C.M., Arrowsmith,C., Atkin,R.J., Barron,A.J., Bringaud,F., Brooks,K., Carrington,M., Cherevach,I., Chillingworth,T.J., Churcher,C., Clark,L.N., Corton,C.H., Cronin,A., Davies,R.M., Doggett,J., Djikeng,A., Feldblyum,T., Field,M.C., Fraser,A., Goodhead,I., Hance,Z., Harper,D., Harris,B.R., Hauser,H., Hostetter,J., Ivens,A., Jagels,K., Johnson,D., Johnson,J., Jones,K., Kerhornou,A.X., Koo,H., Larke,N., Landfear,S., Larkin,C., Leech,V., Line,A., Lord,A., Macleod,A., Mooney,P.J., Moule,S., Martin,D.M.A., Morgan,G.W., Mungall,K., Norbertczak,H., Ormond,D., Pai,G., Peacock,C.S., Peterson,J., Quail,M.A., Rabbinowitsch,E., Rajandream,M.A., Reitter,C., Salzberg,S.L., Sanders,M., Schobel,S., Sharp,S., Simmonds,M., Simpson,A.J., Talton,L., Turner,C.M.R., Tait,A., Tivey,A.R., Van Aken,S., Walker,D., Wanless,D., Wang,S.L., White,B., White,O., Whitehead,S., Woodward,J., Wortman,J., Adams,M.D., Embley,T.M., Gull,K., Ullu,E., Barry,J.D., Fairlamb,A.H., Opperdoes,F., Barret,B.G., Donelson,J.E., Hall,N., Fraser,C.M., Melville,S.E., and El Sayed,N.M. (2005) The genome of the African trypanosome *Trypanosoma brucei*. *Science* **309**, 416-422.

Beshir,K.B., Hallett,R.L., Eziefula,A.C., Bailey,R., Watson,J., Wright,S.G., Chiodini,P.L., Polley,S.D., and Sutherland,C.J. (2010) Measuring the efficacy of anti-malarial drugs in vivo: quantitative PCR measurement of parasite clearance. *Malaria Journal* **9**, 312-319.

Binder,F., Huber,O., and Bock,A. (1986) Cyclodextrin-Glycosyltransferase from Klebsiella-Pneumoniae M5A1 - Cloning, Nucleotide-Sequence and Expression. *Gene* **47**, 269-277.

Bisser,S., Lejon,V., Preux,P.M., Bouteille,B., Stanghellini,A., Jauberteau,M.O., Buscher,P., and Dumas,M. (2002) Blood-cerebrospinal fluid barrier and intrathecal immunoglobulins compared to field diagnosis of central nervous system involvement in sleeping sickness. *Journal of the Neurological Sciences* **193**, 127-135.

Bitonti,A.J., McCann,P.P., and Sjoerdsma,A. (1986) Necessity of antibody response in the treatment of African trypanosomiasis with [alpha]-difluoromethylornithine. *Biochemical Pharmacology* **35**, 331-334.

Biwer,A., Antranikian,G., and Heinzle,E. (2002) Enzymatic production of cyclodextrins. *Applied Microbiology and Biotechnology* **59**, 609-617.

Blum,H.E., Haase,A.T., and Vyas,G.N. (1984) Molecular Pathogenesis of Hepatitis-B Virus-Infection - Simultaneous Detection of Viral-Dna and Antigens in Paraffin-Embedded Liver Sections. *Lancet* **2**, 771-775.

Blum,J. and Burri,C. (2002) Treatment of late stage sleeping sickness caused by *T.b. gambiense*: a new approach to the use of an old drug. *Swiss Medical Weekly* **132**, 51-56.

Braakman,H.M., van de Molengraft,F.J., Hubert,W.W., and Boerman,D.H. (2006) Lethal African trypanosomiasis in a traveler: MRI and neuropathology. *Neurology* **66**, 1094-1096.

Brener,Z. (1979) Present Status of Chemotherapy and Chemoprophylaxis of Human Trypanosomiasis in the Western Hemisphere. *Pharmacology & Therapeutics* **7**, 71-90.

Brewster,M.E., Estes,K.S., and Bodor,N. (1990) An Intravenous Toxicity Study of 2-Hydroxypropyl-Beta-Cyclodextrin, A Useful Drug Solubilizer, in Rats and Monkeys. *International Journal of Pharmaceutics* **59**, 231-243.

Brewster,M.E., Neeskens,P., and Peeters,J. (2007) Solubilization of itraconazole as a function of cyclodextrin structural space. *Journal of Inclusion Phenomena and Macrocyclic Chemistry* **57**, 561-566.

Brewster,M.E., Simpkins,J.W., Hora,M.S., Stern,W.C., and Bodor,N. (1989) The Potential Use of Cyclodextrins in Parenteral Formulations. *Journal of Parenteral Science and Technology* **43**, 231-240.

Brewster,M.E. and Loftsson,T. (2007) Cyclodextrins as pharmaceutical solubilizers. *Advanced Drug Delivery Reviews* **59**, 645-666.

Bridges,D.J., Gould,M.K., Nerima,B., Maser,P., Burchmore,R.J.S., and de Koning,H.P. (2007) Loss of the High-Affinity Pentamidine Transporter Is Responsible for High Levels of Cross-Resistance between Arsenical and Diamidine Drugs in African Trypanosomes. *Molecular Pharmacology* **71**, 1098-1108.

Bronner, Brun, Doua, Ericsson, Burri, Keiser, Miezan, Boa, Rombo, and Gustafsson (1998) Discrepancy in plasma melarsoprol concentrations between HPLC and bioassay methods in patients with *T. gambiense* sleeping sickness indicates that melarsoprol is metabolized. *Tropical Medicine & International Health* **3**, 913-917.

Bronner,U., Ericsson,O., Nordin,J., Wikstrom,I., Abdi,Y.A., Hall,J.E., Tidwell,R.R., and Gustafsson,L.L. (1995) Metabolism Is An Important Route of Pentamidine Elimination in the Rat - Disposition of C-14 Pentamidine and Identification of Metabolites in Urine Using Liquid Chromatography-Tandem Mass-Spectrometry. *Pharmacology & Toxicology* **77**, 114-120.

Bronner,U., Gustafsson,L.L., Doua,F., Ericsson,O., Miezan,T., Rais,M., and Rombo,L. (1995) Pharmacokinetics and Adverse Reactions After A Single-Dose of Pentamidine in Patients with *Trypanosoma gambiense* Sleeping Sickness. *British Journal of Clinical Pharmacology* **39**, 289-295.

Bruce (1895) Preliminary report on the tsetse fly disease or nagana in Zululand. Bennet & Davis. Durban.

Bruce,D. and Nabarro,D. (1903) Can the Uganda tsetse fly carry the trypanosome found in sleeping sickness from animal to animal? *Reports of the Sleeping Sickness Comission* **1**, 11-88.

Bruce,D., Nabarro,D., and Grieg,E.D.W. (1903) Further report of sleeping sickness in Uganda. *Reports of the Sleeping Sickness Comission* **4**, 3-87.

Bruce,S.-G.D. (1914) Classification of the African Trypanosomes pathogenic to man and domestic animals. *Transactions of the Royal Society of Tropical Medicine and Hygiene* **8**, 1-22.

Brun,R., Schumacher,R., Schmid,C., Kunz,C., and Burri,C. (2001) The phenomenon of treatment failures in Human African Trypanosomiasis. *Tropical Medicine & International Health* **6**, 906-914.

Buchanan,J.C.R. (1929) Some clinical aspects of *trypanosomiasis rhodesiensis*. *Transactions of the Royal Society of Tropical Medicine and Hygiene* **23**, 81-88.

Burri,C., Baltz,T., Giroud,C., Doua,F., Welker,H.A., and Brun,R. (1993) Pharmacokinetic Properties of the Trypanocidal Drug Melarsoprol. *Chemotherapy* **39**, 225-234.

Burri,C. and Blum,J. (1996) A case of reactive encephalopathy after treatment with suramin of first stage sleeping sickness. *Tropical Medicine & International Health* **1**, A36-A37.

Burri,C. and Brun,R. (1992) An *in vitro* bioassay for quantification of melarsoprol in serum and cerebrospinal fluid. *Tropical Medicine and Parasitology* **43**, 223-225.

Burri,C. and Keiser,J. (2001) Pharmacokinetic investigations in patients from northern Angola refractory to melarsoprol treatment. *Tropical Medicine & International Health* **6**, 412-420.

Burri,C., Nkunku,S., Merolle,A., Smith,T., Blum,J., and Brun,R. (2000) Efficacy of new, concise schedule for melarsoprol in treatment of sleeping sickness caused by *Trypanosoma brucei gambiense*: a randomised trial. *Lancet* **355**, 1419-1425.

Burri,C., Onyango,J.D., Auma,J.E., Burudi,E.M., and Brun,R. (1994) Pharmacokinetics of melarsoprol in uninfected vervet monkeys. *Acta Tropica* **58**, 35-49.

Burri,C. and Brun,R. (2003) Eflornithine for the treatment of human African trypanosomiasis. *Parasitology Research* **90**, S49-S52.

Burri, Stich, and Brun (2004) Current Chemotherapy of Human African Trypanosomiasis. In: "The Trypanosomiases." Ed. Maudlin, Holmes, and Miles M.A. CABI Publishing. Trowbridge. pp403-419.

Buscher and Lejon (2004) Diagnosis of Human African Trypanosomiasis. In: "The Trypanosomiases." Ed. Maudlin, Holmes, and Miles M.A. CABI Publishing. Trowbridge. pp203-218.

Bustin,S.A. and Mueller,R. (2005) Real-time reverse transcription PCR (qRT-PCR) and its potential use in clinical diagnosis. *Clinical Science* **109**, 365-379.

Calwell,H.G. (1937) The pathology of the brain in rhodesian trypanosomiasis. *Transactions of the Royal Society of Tropical Medicine and Hygiene* **30**, 611-621.

Cardullo,R.A., Agrawal,S., Flores,C., Zamecnik,P.C., and Wolf,D.E. (1988) Detection of nucleic acid hybridization by nonradiative fluorescence resonance energy transfer. *Proceedings of the National Academy of Sciences of the United States of America* **85**, 8790-8794.

Carrier,R.L., Miller,L.A., and Ahmed,I. (2007) The utility of cyclodextrins for enhancing oral bioavailability. *Journal of Controlled Release* **123**, 78-99.

Carter,N.S., Berger,B.J., and Fairlamb,A.H. (1995) Uptake of Diamidine Drugs by the P2 Nucleoside Transporter in Melarsen-Sensitive and -Resistant *Trypanosoma brucei brucei*. *Journal of Biological Chemistry* **270**, 28153-28157.

Carter,N.S. and Fairlamb,A.H. (1993) Arsenical-resistant trypanosomes lack an unusual adenosine transporter. *Nature* **361**, 173-176.

Cartledge,J.D., Midgely,J., and Gazzard,B.G. (1997) Itraconazole solution: Higher serum drug concentrations and better clinical response rates than the capsule formulation in acquired immunodeficiency syndrome patients with candidosis. *Journal of Clinical Pathology* **50**, 477-480.

Castellani,A. (1903) On the discovery of a species of Trypanosoma in the cerebro-spinal fluid of cases of sleeping sickness. *Proceedings of the Royal Society of London.Series B, Containing Papers of a Biological Character* **71**, 501-508.

Chappuis,F., Loutan,L., Simarro,P., Lejon,V., and Buscher,P. (2005a) Options for Field Diagnosis of Human African Trypanosomiasis. *Clinical Microbiology Reviews* **18**, 133-146.

Chappuis,F., Udayraj,N., Stietenroth,K., Meussen,A., and Bovier,P. (2005b) Eflornithine Is Safer than Melarsoprol for the Treatment of Second Stage *Trypanosoma brucei gambiense* Human African Trypanosomiasis. *Clinical Infectious Diseases* **41**, 748-751.

Chaudhuri,J.D. (2000) Blood brain barrier and infection. *Medical Science Monitor* **6**, 1213-1222.

Checkley,A.M., Pepin,J., Gibson,W.C., Taylor,M.N., Jager,H.R., and Mabey,D.C. (2007) Human African trypanosomiasis: diagnosis, relapse and survival after severe melarsoprol-induced encephalopathy. *Transactions of the Royal Society of Tropical Medicine and Hygiene* **101**, 523-526.

Chello,P.L. and Jaffe,J.J. (1972) Comparative Properties of Trypanosomal and Mammalian Thymidine Kinases. *Comparative Biochemistry and Physiology* **43**, 543-&.

Choi,Y.K. and Kim,K.W. (2008) Blood-neural barrier: its diversity and coordinated cell-to-cell communication. *Bmb Reports* **41**, 345-352.

Clarke,R.J., Coates,J.H., and Lincoln,S.F. (1988) Inclusion Complexes of the Cyclomalto-Oligosaccharides (Cyclodextrins). *Advances in Carbohydrate Chemistry and Biochemistry* **46**, 205-249.

Colognato,H. and Yurchenco,P.D. (2000) Form and function: The laminin family of heterotrimers. *Developmental Dynamics* **218**, 213-234.

Coussement,W., Vancauteren,H., Vandenberghe,J., Vanparys,P., Teuns,G., Lampo,A., and Marsboom,R. (1990) Toxicological Profile of Hydroxypropyl Beta-Cyclodextrin (Hp Beta-Cd) in Laboratory-Animals. *Minutes of the Fifth International Symposium on Cyclodextrins* 522-524.

Cox,F.E. (2004) History of sleeping sickness (African trypanosomiasis). *Infectious Disease Clinics of North America* **18**, 231-245.

Cox (1993) Parasitic Protozoa. In: "Modern Parasitology." Ed. Cox. Blackwell Science Ltd. Oxford. pp1-23.

Cramer (1954) Einschlussverbindungen. Springer-verlag. Berlin.

Cramer,F. (1956) Inclusion Compounds. *Angewandte Chemie-International Edition* **68**, 115-120.

Culwick,A.T. and Fairbairn,H. (1947) Polymorphism in *Trypanosoma simiae* and the Morphology of the Metacyclic Forms. *Transactions of the Royal Society of Tropical Medicine and Hygiene* **41**, 415-418.

Date,A.R. and Gray,A.L. (1981) Plasma Source-Mass Spectrometry Using An Inductively Coupled Plasma and A High-Resolution Quadrupole Mass Filter. *Analyst* **106**, 1255-1267.

De Beule,K. (1996) Proceedings of the 8th international Symposium on Cyclodextrins. Szejtli, J. Editions de Sante Paris

de Koning,H.P. (2008) Ever-increasing complexities of diamidine and arsenical crossresistance in African trypanosomes. *Trends in Parasitology* **24**, 345-349.

de Koning,H.P. and Jarvis,S.M. (2001) Uptake of pentamidine in *Trypanosoma brucei brucei* is mediated by the P2 adenosine transporter and at least one novel, unrelated transporter. *Acta Tropica* **80**, 245-250.

De Raadt,P. (2005) The history of sleeping sickness. http://www.who.int/trypanosomiasis_african/country/history/en/print.html

Deflorin,J., Rudolf,M., and Seebeck,T. (1994) The major components of the paraflagellar rod of *Trypanosoma brucei* are two similar, but distinct proteins which are encoded by two different gene loci. *Journal of Biological Chemistry* **269**, 28745-28751.

Degrave,W., Fragoso,S.P., Britto,C., van Heuverswyn,H., Kidane,G.Z., Cardoso,M.A.B., Mueller,R.U., Simpson,L., and Morel,C.M. (1988) Peculiar sequence organization of kinetoplast DNA minicircles from *Trypanosoma cruzi*. *Molecular and Biochemical Parasitology* **27**, 63-70.

Delespaux,V. and de Koning,H.P. (2007) Drugs and drug resistance in African trypanosomiasis. *Drug Resistance Updates* **10**, 30-50.

Denise,H. and Barrett,M.P. (2001) Uptake and mode of action of drugs used against sleeping sickness. *Biochemical Pharmacology* **61**, 1-5.

Dhar,R.K., Zheng,Y., Rubenstone,J., and van Geen,A. (2004) A rapid colorimetric method for measuring arsenic concentrations in groundwater. *Analytica Chimica Acta* **526**, 203-209.

Donaubauer,H.H., Fuchs,H., Langer,K.H., and Bar,A. (1998) Subchronic intravenous toxicity studies with gamma-cyclodextrin in rats. *Regulatory Toxicology and Pharmacology* **27**, 189-198.

Doua,F., Miezan,T.W., Singaro,J.R.S., Yapo,F.B., and Baltz,T. (1996) The efficacy of pentamidine in the treatment of early-late stage *Trypanosoma brucei gambiense* trypanosomiasis. *American Journal of Tropical Medicine and Hygiene* **55**, 586-588.

Drake,S., Lampasona,V., Nicks,H.L., and Schwarzmann,S.W. (1985) Pentamidine Isethionate in the Treatment of Pneumocystis-Carinii Pneumonia. *Clinical Pharmacy* **4**, 507-516.

Duggan,A.J. and Hutchins,M.P. (1966) Sleeping Sickness in Europeans - A Review of 109 Cases. *Journal of Tropical Medicine and Hygiene* **69**, 124-131.

Dukes,P., Gibson,W.C., Gashumba,J.K., Hudson,K.M., Bromidge,T.J., Kaukus,A., Asonganyi,T., and Magnus,E. (1992) Absence of the Litat-1.3 (Catt Antigen) Gene in *Trypanosoma-brucei-gambiense* Stocks from Cameroon. *Acta Tropica* **51**, 123-134.

Dutton,J.E. (1902) Preliminary note upon a trypanosome occurring in the blood of man. *Thompson Yates Lab Reports* **4**, 455-468.

Enanga,B., Burchmore,R.J.S., Stewart,M.L., and Barrett,M.P. (2002) Sleeping sickness and the brain. *Cellular and Molecular Life Sciences (CMLS)* **59**, 845-858.

Enyaru,J.C.K., Matovu,E., Akol,M., Sebikali,C., Kyambadde,J., Schmidt,C., Brun,R., Kaminsky,R., Ogwal,L.M., and Kansiime,F. (1998) Parasitological detection of *Trypanosoma brucei gambiense* in serologically negative sleeping-sickness suspects from north-western Uganda. *Annals of Tropical Medicine and Parasitology* **92**, 845-850.

Enyaru,J.C.K., Odiit,M., Winyi-Kaboyo,R., Sebikali,C.G., Matovu,E., Okitoi,D., and Olaho-Mukani,W. (1999) Evidence for the occurrence of *Trypanosoma brucei rhodesiense* sleeping sickness outside the traditional focus in south-eastern Uganda. *Annals of Tropical Medicine and Parasitology* **93**, 817-822.

Ericsson,O., Schweda,E.K., Bronner,U., Rombo,L., Friden,M., and Gustafsson,L.L. (1997) Determination of melarsoprol in biological fluids by high-performance liquid chromatography and characterisation of two stereoisomers by nuclear magnetic resonance spectroscopy. *Journal of Chromatography B Biomedical Sciences and Applications* **690**, 243-251.

Evans,D.A. and Ellis,D.S. (1983) Recent Observations on the Behavior of Certain Trypanosomes Within Their Insect Hosts. *Advances in Parasitology* **22**, 1-42.

Evans,G. (1881) On a horse disease in India known as 'Surra' probably due to a haematozoon. *Vet J Ann Comp Pathol* **13**, 1-10.

Evrard,B., Chiap,P., DeTullio,P., Ghalmi,F., Piel,G., Van Hees,T., Crommen,J., Losson,B., and Delattre,L. (2002) Oral bioavailability in sheep of albendazole from a suspension and from a solution containing hydroxypropyl-beta-cyclodextrin. *Journal of Controlled Release* **85**, 45-50.

Fairlamb,A.H. and Bowman,I.B.R. (1977) *Trypanosoma-brucei* - Suramin and Other Trypanocidal Compounds Effects on Sn-Glycerol-3-Phosphate Oxidase. *Experimental Parasitology* **43**, 353-361.

Fairlamb,A.H. and Cerami,A. (1992) Metabolism and Functions of Trypanothione in the Kinetoplastida. *Annual Review of Microbiology* **46**, 695-729.

Fairlamb,A.H., Smith,K., and Hunter,K.J. (1992) The interaction of arsenical drugs with dihydrolipoamide and dihydrolipoamide dehydrogenase from arsenical resistant and sensitive strains of *Trypanosoma brucei brucei*. *Molecular and Biochemical Parasitology* **53**, 223-231.

Fairlamb,A.H., Henderson,G.B., and Cerami,A. (1989) Trypanothione is the Primary Target for Arsenical Drugs against African Trypanosomes. *Proceedings of the National Academy of Sciences* **86**, 2607-2611.

Farazi,T.A., Waksman,G., and Gordon,J.I. (2001) The biology and enzymology of protein N-myristoylation. *Journal of Biological Chemistry* **276**, 39501-39504.

Fazekas,F., Soelberg-Sorensen,P., Comi,G., and Filippi,M. (2007) MRI to monitor treatment efficacy in multiple sclerosis. *Journal of Neuroimaging* **17**, 50S-55S.

Fearon,M. (2005) The laboratory diagnosis of HIV infections. *Canadian Journal of Infectious Diseases and Medical Microbiology* **16**, 26-30.

Fiedler,G., Pajatsch,M., and Bock,A. (1996) Genetics of a novel starch utilisation pathway present in *Klebsiella oxytoca*. *Journal of Molecular Biology* **256**, 279-291.

Filippi,M. and Rocca,M.A. (2007) Conventional MRI in Multiple Sclerosis. *Journal of Neuroimaging* **17**, 3S-9S.

Fink,E. and Schmidt,H. (1979) Meningoencephalitis in Chronic *Trypanosoma brucei rhodesiense* Infection of the White-Mouse. *Tropenmedizin und Parasitologie* **30**, 206-211.

Forde,R.M. (1902) Some clinical notes on an European patient in whose blood a trypanosome was observed. *Journal of Tropical Medicine* **5**, 261-263.

Frank,D.W., Gray,J.E., and Weaver,R.N. (1976) Cyclodextrin Nephrosis in Rat. *American Journal of Pathology* **83**, 367-382.

Frearson,J.A., Brand,S., McElroy,S.P., Cleghorn,L.A.T., Smid,O., Stojanovski,L., Price,H.P., Guther,M.L.S., Torrie,L.S., Robinson,D.A., Hallyburton,I., Mpamhanga,C.P., Brannigan,J.A., Wilkinson,A.J., Hodgkinson,M., Hui,R., Qiu,W., Raimi,O.G., van Aalten,D.M.F., Brenk,R., Gilbert,I.H., Read,K.D., Fairlamb,A.H., Ferguson,M.A.J., Smith,D.F., and Wyatt,P.G. (2010) N-myristoyltransferase inhibitors as new leads to treat sleeping sickness. *Nature* **464**, 728-U100.

Freudenberg,K. and Jacobi,R. (1935) Uber Schardingers Dextrine aus Starke. *Justus Liebigs Annalen der Chemie* **518**, 102-108.

Friedheim,E.A.H. (1949) Mel-B in the Treatment of Human Trypanosomiasis. *American Journal of Tropical Medicine* **29**, 173-180.

Friedheim,E.A.H. and De Jongh,R.T. (1959) Mel W, a new trypanosomicidal agent derived from mel B. *Transactions of the Royal Society of Tropical Medicine and Hygiene* **53**, 262-269.

Frijlink,H.W., Franssen,E.J., Eissens,A.C., Oosting,R., Lerk,C.F., and Meijer,D.K. (1991) The effects of cyclodextrins on the disposition of intravenously injected drugs in the rat. *Pharmaceutical Research* **8**, 380-384.

Froehlich (2006) MR Contrast Agents. In: "How Does MRI Work? An Introduction to the Physics and Function of Magnetic Resonance Imaging." Ed. Weishaupt, Kochli, and Marincek. Springer. Berlin. pp103-128.

Fromming and Szejtli (1994) Cyclodextrin Derivatives. In: "Cyclodextrins in Pharmacy." Ed. Fromming and Szejtli. Kluwer Academic Publishers. Netherlands. pp19-32.

Gelfand,M. (1947) Transitory Neurological Signs in Sleeping Sickness. *Transactions of the Royal Society of Tropical Medicine and Hygiene* **41**, 255-258.

Gergely,V., Sebestyen,G., and Virag,S. (1982) Proceedings of the 1st International Symposium on Cyclodextrins. 109-Reidel Dordrecht

Ghoda,L., Phillips,M.A., Bass,K.E., Wang,C.C., and Coffino,P. (1990) Trypanosome Ornithine Decarboxylase Is Stable Because It Lacks Sequences Found in the Carboxyl Terminus of the Mouse Enzyme Which Target the Latter for Intracellular Degradation. *Journal of Biological Chemistry* **265**, 11823-11826.

Gibaud,S., Zirar,S.B., Mutzenhardt,P., Fries,I., and Astier,A. (2005) Melarsoprol-cyclodextrins inclusion complexes. *International Journal of Pharmaceutics* **306**, 107-121.

Gibson,U.E., Heid,C.A., and Williams,P.M. (1996) A novel method for real time quantitative RT-PCR. *Genome Research* **6**, 995-1001.

Gibson,W., Peacock,L., Ferris,V., Williams,K., and Bailey,M. (2008) The use of yellow fluorescent hybrids to indicate mating in *Trypanosoma brucei*. *Parasites & Vectors* **1**, 4-19.

Gilis,P.M.V., De Conde,V.F.V., Vandecruys,R.P.G., and [Anon] (2003) Pellets having a core coated with an antifungal and a polymer. Janssen Pharmaceutical, N. V. US 6663901

Gill,D.S., Chatha,D.S., and Carpio-O'Donovan,R. (2003) MR imaging findings in African trypansomiasis. *American Journal of Neuroradiology* **24**, 1383-1385.

Gould,S. and Scott,R.C. (2005) 2-Hydroxypropyl-[beta]-cyclodextrin (HP-[beta]-CD): A toxicology review. *Food and Chemical Toxicology* **43**, 1451-1459.

Grab,D., Garcia-Garcia,J., Nikolskaia,O., V, Kim,Y., V, Brown,A., Pardo,C., Zhang,Y., Becker,K., Wilson,B., Lima,A., Scharfstein,J., and Dumler,J. (2009) Protease activated receptor signaling is required for African trypanosome traversal of human brain microvascular endothelial cells. *PLos Neglected Tropical Diseases* **3**, e479-

Grab,D.J., Nikolskaia,O., Kim,Y.V., Lonsdale-Eccles,J.D., Ito,S., Hara,T., Fukuma,T., Nyarko,E., Kim,K.J., Stins,M.F., Delannoy,M.J., Rodgers,J., and Kim,K.S. (2004) African trypanosome interactions with an *in vitro* model of the human blood-brain barrier. *Journal of Parasitology* **90**, 970-979.

Grant,E.M. (2000) Optimizing the bioavailability of itraconazole. *Connecticut Medicine* **64**,

Greenwood,B.M. and Whittle,H.C. (1980) The pathogenesis of sleeping sickness. *Transactions of the Royal Society of Tropical Medicine and Hygiene* **74**, 716-725.

Grunberg,E. and Tisworth,E.H. (1973) Chemotherapeutic Properties of Heterocyclic-Compounds - Monocyclic Compounds with 5-Membered Rings. *Annual Review of Microbiology* **27**, 317-346.

Haines,D.E., Harkey,H.L., and Almefty,O. (1993) The Subdural Space - A New Look at An Outdated Concept. *Neurosurgery* **32**, 111-120.

Hall,B.S., Bot,C., and Wilkinson,S.R. (2011) Nifurtimox Activation by Trypanosomal Type I Nitroreductases Generates Cytotoxic Nitrile Metabolites. *Journal of Biological Chemistry* **286**, 13088-13095.

Haller,L., Adams,H., Merouze,F., and Dago,A. (1986) Clinical and Pathological Aspects of Human African Trypanosomiasis (*Trypanosoma gambiense*) with Particular Reference to Reactive Arsenical Encephalopathy. *American Journal of Tropical Medicine and Hygiene* **35**, 94-99.

Hansen,M.B., Nielsen,S.E., and Berg,K. (1989) Re-examination and further development of a precise and rapid dye method for measuring cell growth/cell kill. *Journal of Immunological Methods* **119**, 203-210.

Hawking,F. (1962) Estimation of the concentration of melarsoprol (Mel B) and Mel W in biological fluids by bioassay with trypanosomes *in vitro*. *Transactions of the Royal Society of Tropical Medicine and Hygiene* **56**, 354-363.

Hawking,F. (1978) Suramin: with special reference to onchocerciasis. *Advances in Pharmacology and Chemotherapy* **15**, 289-322.

Hawking,F. and Greenfield,J.G. (1941) Two autopsies on rhodesiense sleeping sickness; Visceral lesions and significance of changes in cerebrospinal fluid. *Transactions of the Royal Society of Tropical Medicine and Hygiene* **35**, 155-164.

Hedges (1992) Cyclodextrin: Production, Properties, and Applications. In: "Starch Hydrolysis Products." Ed. Schenk and Habeda. VCH. New York. pp319-333.

Heid,C.A., Stevens,J., Livak,K.J., and Williams,P.M. (1996) Real time quantitative PCR. *Genome Research* **6**, 986-994.

Herder,S., Simo,G., Nkinin,S., and Njiokou,F. (2002) Identification of trypanosomes in wild animals from Southern Cameroon using the polymerase chain reaction (PCR). *Parasite-Journal de la Societe Francaise de Parasitologie* **9**, 345-349.

Hermsen,C.C., Telgt,D.S.C., Linders,E.H.P., van de Locht,L.A.T.F., Eling,W.M.C., Mensink,E.J.B.M., and Sauerwein,R.W. (2001) Detection of *Plasmodium falciparum* malaria parasites *in vivo* by real-time quantitative PCR. *Molecular and Biochemical Parasitology* **118**, 247-251.

Hide,G., Welburn,S.C., Tait,A., and Maudlin,I. (1994) Epidemiological relationships of *Trypanosoma brucei* stocks from south east Uganda: evidence for different population structures in human infective and non-human infective isolates. *Parasitology* **109**, 95-111.

Higuchi and Connons (1965)In: "Advances in Analytical Chemistry and Instrmentation vol 4." Ed. Reilly C.N. Wiley-Interscience. New York. pp117-212.

Hirayama and Uekama (1987) Cyclodextrins and their Industrial Uses. Ed. Duchene. Editions de Sante. Paris.

Hirayama,F. and Uekama,K. (1999) Cyclodextrin-based controlled drug release system. *Advanced Drug Delivery Reviews* **36**, 125-141.

Hoare,C.A. (1964) Morphological and Taxonomic Studies on Mammalian Trypanosomes. X. Revision of the Systematics. *Journal of Eukaryotic Microbiology* **11**, 200-207.

Hoare (1970a) Systematic Description of the Mammalian Trypanosomes of Africa. In: "The Africa Trypanosomiases." George Allen and Unwin LTD. London. pp24-59.

Hoare (1970b) The Mammalian Trypanosomes of Africa. In: "The African Trypanosomiases." Ed. Mulligan. George Allen and Unwin LTD. London. pp3-23.

Hoare (1972) The Trypanosomes Of Mammals. Blackwell Scientific Publications. Oxford.

Hofler (1990) Principles of in situ hybridization. In: "In Situ Hybridization Principles and Practice." Ed. Polak and McGee. Oxford University Press Inc. New York. pp15-29.

Holland,P.M., Abramson,R.D., Watson,R., and Gelfand,D.H. (1991) Detection of specific polymerase chain reaction product by utilizing the 5'----3' exonuclease activity of Thermus aquaticus DNA polymerase. *Proceedings of the National Academy of Sciences of the United States of America* **88**, 7276-7280.

Hopkins,H., Talisuna,A., Whitty,C., and Staedke,S. (2007) Impact of home-based management of malaria on health outcomes in Africa: a systematic review of the evidence. *Malaria Journal* **6**, 134-143.

Horikoshi,K. (1979) Production and Industrial Applications of Beta-Cyclodextrin. *Process Biochemistry* **14**, 26-

Houk,R.S., Fassel,V.A., Flesch,G.D., Svec,H.J., Gray,A.L., and Taylor,C.E. (1980) Inductively Coupled Argon Plasma As An Ion-Source for Mass-Spectrometric Determination of Trace-Elements. *Analytical Chemistry* **52**, 2283-2289.

Hunter,C.A., Murray,M., Jennings,F., Adams,J.H., and Kennedy,P.G.E. (1992) Subcurative chemotherapy and fatal post-treatment reactive encephalopathies in African trypanosomiasis. *Lancet* **339**, 956-958.

Hyman,R.W., Ecker,J.R., and Tenser,R.B. (1983) Varicella-Zoster Virus-Rna in Human Trigeminal Ganglia. *Lancet* **2**, 814-816.

Irie,T., Kuwahara,S., Otagiri,M., Uekama,K., and Iwamasa,T. (1983) Reduction in the Local Tissue Toxicity of Chlorpromazine by Beta-Cyclodextrin Complexation. *Journal of Pharmacobio-Dynamics* **6**, 790-792.

Irie,T., Otagiri,M., Sunada,M., Uekama,K., Ohtani,Y., Yamada,Y., and Sugiyama,Y. (1982) Cyclodextrin-induced hemolysis and shape changes of human erythrocytes *in vitro*. *Journal of Pharmacobio-Dynamics* **5**, 741-744.

Irie,T., Sunada,M., Otagiri,M., and Uekama,K. (1983) Protective Mechanism of Beta-Cyclodextrin for the Hemolysis Induced with Phenothiazine Neuroleptics *In vitro*. *Journal of Pharmacobio-Dynamics* **6**, 408-414.

Irie,T. and Uekama,K. (1997) Pharmaceutical applications of cyclodextrins .3. Toxicological issues and safety evaluation. *Journal of Pharmaceutical Sciences* **86**, 147-162.

Iten,M., Mett,H., Evans,A., Enyaru,J.C.K., Brun,R., and Kaminsky,R. (1997) Alterations in ornithine decarboxylase characteristics account for tolerance of *Trypanosoma brucei rhodesiense* to D,L-alpha-difluoromethylornithine. *Antimicrobial Agents and Chemotherapy* **41**, 1922-1925.

Ito,K., Palmer,C.D., Steuerwald,A.J., and Parsons,P.J. (2010) Determination of five arsenic species in whole blood by liquid chromatography coupled with inductively coupled plasma mass spectrometry. *Journal of Analytical Atomic Spectrometry* **25**, 1334-1342.

Jacobs,M. and Nagler,J. (1942) Colorimetric Microdetermination of Arsenic. *Industrial & Engineering Chemistry Analytical Edition* **14**, 442-444.

Jaffe,J.J., Meymaria,E., and Mccormac,J.J. (1972) Comparative Properties of Schistosomal and Filarial Dihydrofolate Reductases. *Biochemical Pharmacology* **21**, 719-&.

Jamonneau,V., Truc,P., Garcia,A., Magnus,E., and Buscher,P. (2000) Preliminary evaluation of LATEX/*T-b. gambiense* and alternative versions of CATT/*T-b. gambiense* for the serodiagnosis of Human African Trypanosomiasis of a population at risk in Cote d'Ivoire: considerations for mass-screening. *Acta Tropica* **76**, 175-183.

Janssens,P.G. and Demuynck,A. (1977) Clinical-Trials with Nifurtimox in African Trypanosomiasis. *Annales de la Societe Belge de Medecine Tropicale* **57**, 475-480.

Jenni,L., Marti,S., Schweizer,J., Betschart,B., Le Page,R.W.F., Wells,J.M., Tait,A., Paindavoine,P., Pays,E., and Steinert,M. (1986) Hybrid formation between African trypanosomes during cyclical transmission. *Nature* **322**, 173-175.

Jennings,F. (1976) The anaemias of parasitic infections. *Pathophysiology of parasitic infection (Proc.7th Internat.Conf.World Ass.Adv.Vet.Parasit., Thessaloniki, Greece, 14-16 July, 1975)*. 41-67.

Jennings,F.W. (1987) Chemotherapy of late-stage trypanosomiasis: the effect of the nitrothiazole compounds. *Transactions of the Royal Society of Tropical Medicine and Hygiene* **81**, 616-

Jennings,F.W. (1992) Relative efficacy of melarsen oxide compared with mel Cy (Cymelarsan«) when used in combination with difluoromethylornithine in the treatment of trypanosomiasis of the central nervous system. *Transactions of the Royal Society of Tropical Medicine and Hygiene* **86**, 257-258.

Jennings,F.W. (1993) Combination chemotherapy of CNS trypanosomiasis. *Acta Tropica* **54**, 205-213.

Jennings,F.W. and Gray,G.D. (1983) Relapsed parasitaemia following chemotherapy of chronic *T. brucei* infections in mice and its relation to cerebral trypanosomes. *Contributions to Microbiology and Immunology* **7**, 147-154.

Jennings,F.W., Hunter,C.A., Kennedy,P.G.E., and Murray,M. (1993) Chemotherapy of *Trypanosoma brucei* infection of the central nervous system: the use of a rapid chemotherapeutic regimen and the development of post-treatment encephalopathies. *Transactions of the Royal Society of Tropical Medicine and Hygiene* **87**, 224-226.

Jennings,F.W., McNeil,P.E., Ndungu,J.M., and Murray,M. (1989) Trypanosomiasis and Encephalitis - Possible Etiology and Treatment. *Transactions of the Royal Society of Tropical Medicine and Hygiene* **83**, 518-519.

Jennings,F.W. and Urquhart,G.M. (1983) The Use of the 2 Substituted 5-Nitroimidazole, Fexinidazole (Hoe 239) in the Treatment of Chronic *T-brucei* Infections in Mice. *Zeitschrift fur Parasitenkunde-Parasitology Research* **69**, 577-581.

Jones,P.M. and George,A.M. (2005) Multidrug resistance in parasites: ABC transporters, P-glycoproteins and molecular modelling. *International Journal for Parasitology* **35**, 555-566.

Joshi,P.P., Shegokar,V.R., Powar,R.M., Herder,S., Katti,R., Salkar,H.R., Dani,V.S., Bhargava,A., Jannin,J., and Truc,P. (2005) Human trypanosomiasis caused by *Trypanosoma evansi* in India: The first case report. *American Journal of Tropical Medicine and Hygiene* **73**, 491-495.

Kager,P.A., Schipper,H.G., Stam,J., and Majoie,C.B. (2009) Magnetic resonance imaging findings in human African trypanosomiasis: a four-year follow-up study in a patient and review of the literature. *American Journal of Tropical Medicine and Hygiene* **80**, 947-952.

Kappos,L., Antel,J., Comi,G., Montalban,X., O'Connor,P., Polman,C.H., Haas,T., Korn,A.A., Karlsson,G., and Radue,E.W. (2006) Oral Fingolimod (FTY720) for Relapsing Multiple Sclerosis. *New England Journal of Medicine* **355**, 1124-1140.

Kawabata,K., Inoue,Y., Takahashi,H., and Endo,G. (1994) Determination of arsenic species by inductively coupled plasma mass spectrometry with ion chromatography. *Applied Organometallic Chemistry* **8**, 245-248.

Keiser,J. and Burri,C. (2000) Physico-chemical properties of the trypanocidal drug melarsoprol. *Acta Tropica* **74**, 101-104.

Keiser,J., Ericsson,O., and Burri,C. (2000) Investigations of the metabolites of the trypanocidal drug melarsoprol[ast]. *Clinical Pharmacology and Therapeutics* **67**, 478-488.

Kellersberger,E.R. (1933) African Sleeping Sickness: A Review of 9000 Cases from a Central African Clinic. *American Journal of Tropical Medicine and Hygiene* **s1-13**, 211-236.

Kennedy,P.G. (2004) Human African trypanosomiasis of the CNS: current issues and challenges. *Journal of Clinical Investigation* **113**, 496-504.

Kennedy,P.G. (2008) The continuing problem of human African trypanosomiasis (sleeping sickness). *Annals of Neurology* **64**, 116-126.

Kennedy,P.G., Rodgers,J., Jennings,F.W., Murray,M., Leeman,S.E., and Burke,J.M. (1997) A substance P antagonist, RP-67,580, ameliorates a mouse meningoencephalitic response to *Trypanosoma brucei brucei*. *Proceedings of the National Academy of Sciences* **94**, 4167-4170.

Kennedy,P.G.E., Rodgers,J., Bradley,B., Hunt,S.P., Gettinby,G., Leeman,S.E., De Felipe,C., and Murray,M. (2003) Clinical and neuroinflammatory responses to meningoencephalitis in substance P receptor knockout mice. *Brain* **126**, 1683-1690.

Killickkendrick,R. and Godfrey,D.G. (1963) Bovine Trypanosomiasis in Nigeria .2. Incidence Among Some Migrating Cattle, with Observations on Examination of Wet Blood Preparations As A Method of Survey. *Annals of Tropical Medicine and Parasitology* **57**, 117-126.

Kim,Y.V., Di Cello,F., Hillaire,C.S., and Kim,K.S. (2004) Differential Ca2+ signaling by thrombin and protease-activated receptor-1-activating peptide in human brain microvascular endothelial cells. *American Journal of Physiology - Cell Physiology* **286**, C31-C42.

Kinghorn,A. and Yorke,W. (1912) On the transmission of human trypanosomes by *Glossina morsitans* Westw., and on the occurrence of human trypanosomes in game. *Annals of Tropical Medicine and Parasitology* **6**, 1-23.

Kleine (1909) Positive infection experiments with *Trypanosoma brucei* by using *Glossina palpalis*. *Deutsche Medizinische Wochenschrift* **35**, 469-470.

Klokouzas,A., Shahi,S., Hladky,S.B., Barrand,M.A., and van Veen,H.W. (2003) ABC transporters and drug resistance in parasitic protozoa. *International Journal of Antimicrobial Agents* **22**, 301-317.

Kobayashi (1996) Cyclodextrin producing enzyme (CGTase). In: "Progress in Biotechnology
Enzymes for Carbohydrate Engineering." Ed. Kwan-Hwa Park. Elsevier. pp23-41.

Koten,J.W. and De Raadt,P. (1969) Myocarditis in *Trypanosoma rhodesiense* infections. *Transactions of the Royal Society of Tropical Medicine and Hygiene* **63**, 485-489.

Kuzoe,F.A.S. (1993) Current situation of African trypanosomiasis. *Acta Tropica* **54**, 153-162.

Lane,J.E., Olivares-Villagomez,D., Vnencak-Jones,C.L., McCurley,T.L., and Carter,C.E. (1997) Detection of *Trypanosoma cruzi* with the Polymerase Chain Reaction and in Situ Hybridization in Infected Murine Cardiac Tissue. *American Journal of Tropical Medicine and Hygiene* **56**, 588-595.

Larsen,K.L., Duedahl-Olesen,L., Christensen,H.J.S., Mathiesen,F., Pedersen,L.H., and Zimmermann,W. (1998) Purification and characterisation of cyclodextrin glycosyltransferase from *Paenibacillus* sp. F8. *Carbohydrate Research* **310**, 211-219.

Latourette,M., Siebert,J., Barto,R., Marable,K., Muyepa,A., Hammond,C., Potchen,M., Kampondeni,S., and Taylor,T. (2010) Magnetic Resonance Imaging Research in Sub-Saharan Africa: Challenges and Satellite-Based Networking Implementation. *Journal of Digital Imaging* 1-10.

Legros,D., Evans,S., Maiso,F., Enyaru,J.C., and Mbulamberi,D. (1999) Risk factors for treatment failure after melarsoprol for *Trypanosoma brucei gambiense* trypanosomiasis in Uganda. *Transactions of the Royal Society of Tropical Medicine and Hygiene* **93**, 439-442.

Leitch, Schwarzacher, Jackson, and Leitch (1994) In Situ Hybridization. BIOS Scientific Publishers Limited. Oxford.

Lejon,V., Lardon,J., Kenis,G., Pinoges,L., Legros,D., Bisser,S., N'Siesi,X., Bosmans,E., and Buscher,P. (2002) Interleukin (IL)-6, IL-8 and IL-10 in serum and CSF of *Trypanosoma brucei gambiense* sleeping sickness patients before and after treatment. *Transactions of the Royal Society of Tropical Medicine and Hygiene* **96**, 329-333.

Lejon,V., Reiber,H., Legros,D., Dje,N., Magnus,E., Wouters,I., Sindic,C.J.M., and Buscher,P. (2003) Intrathecal immune response pattern for improved diagnosis of central nervous system involvement in trypanosomiasis. *Journal of Infectious Diseases* **187**, 1475-1483.

Leuner,C. and Dressman,J. (2000) Improving drug solubility for oral delivery using solid dispersions. *European Journal of Pharmaceutics and Biopharmaceutics* **50**, 47-60.

Levine,R.A., Wardlaw,S.C., and Patton,C.L. (1989) Detection of Hematoparasites Using Quantitative Buffy Coat Analysis Tubes. *Parasitology Today* **5**, 132-134.

Lin,M.H., Chen,T.C., Kuo,T.T., Tseng,C.C., and Tseng,C.P. (2001) Real-time PCR for quantitative detection of *Toxoplasma gondii*. *Journal of Clinical Microbiology* **38**, 4121-4125.

Lina,B.A.R. and Bar,A. (1998) Subchronic oral toxicity studies with gamma-cyclodextrin in rats. *Regulatory Toxicology and Pharmacology* **27**, 178-188.

Lina,B.A.R. and Bar,A. (2004a) Subchronic (13-week) oral toxicity study of alpha-cyclodextrin in dogs. *Regulatory Toxicology and Pharmacology* **39**, S27-S33.

Lina,B.A.R. and Bar,A. (2004b) Subchronic oral toxicity studies with alpha-cyclodextrin in rats. *Regulatory Toxicology and Pharmacology* **39**, S14-S26.

Lipton (2008a) Image Contrast: T1, T2, T2*, and Proton Density. In: "Totally Accessible MRI: A User's Guide to Principles, Technology and Applications." Ed. Lipton. Springer. New York. pp38-46.

Lipton (2008b) Laying the Foundation: Nuclear Magnetism, Spin, and the NMR Phenomenon. In: "Totally Accessible MRI: A User's Guide to Principles, Technology and Applications." Ed. Lipton. Springer. New York. pp3-18.

Lipton (2008c) Relaxation: What Happens Next? In: "Totally Accessible MRI: A User's Guide to Principles, Technology and Applications." Ed. Lipton. Springer. New York. pp27-37.

Lipton (2008d) Rocking the Boat: Resonance, Excitation, and Relaxation. In: "Totally Accessible MRI: A User's Guide to Principles, Technology and Applications." Ed. Lipton. Springer. New York. pp19-26.

Loftsson,T. and Brewster,M.E. (1996) Pharmaceutical applications of cyclodextrins .1. Drug solubilization and stabilization. *Journal of Pharmaceutical Sciences* **85**, 1017-1025.

Loftsson,T., Brewster,M.E., and Masson,M. (2004) Role of Cyclodextrins in Improving Oral Drug Delivery. [Article]. *American Journal of Drug Delivery* **2**, 261-275.

Loftsson,T. and Duchene,D. (2007) Cyclodextrins and their pharmaceutical applications. *International Journal of Pharmaceutics* **329**, 1-11.

Loftsson,T., Jarho,P., Masson,M., and Jarvinen,T. (2005) Cyclodextrins in drug delivery. *Expert Opinion on Drug Delivery* **2**, 335-351.

Looareesuwan,S., Laothamatas,J., Brown,T.R., and Brittenham,G.M. (2009) Cerebral Malaria: A New Way Forward with Magnetic Resonance Imaging (MRI). *American Journal of Tropical Medicine and Hygiene* **81**, 545-547.

Looareesuwan,S., Wilairatana,P., Krishna,S., Kendall,B., Vannaphan,S., Viravan,C., and White,N.J. (1995) Magnetic-Resonance-Imaging of the Brain in Patients with Cerebral Malaria. *Clinical Infectious Diseases* **21**, 300-309.

Lovblad,K.O., Anzalone,N., Dorfler,A., Essig,M., Hurwitz,B., Kappos,L., Lee,S.K., and Filippi,M. (2010) MR Imaging in Multiple Sclerosis: Review and Recommendations for Current Practice. *American Journal of Neuroradiology* **31**, 983-989.

Lumsden,W.H.R., Kimber,C.D., Evans,D.A., and Doig,S.J. (1979) *Trypanosoma brucei* - Miniature Anion-Exchange Centrifugation Technique for Detection of Low Parasitemias - Adaptation for Field Use. *Transactions of the Royal Society of Tropical Medicine and Hygiene* **73**, 312-317.

Lundkvist,G.B., Kristensson,K., and Bentivoglio,M. (2004) Why Trypanosomes Cause Sleeping Sickness. *Physiology* **19**, 198-206.

MacLean,L., Odiit,M., and Sternberg,J.M. (2001) Nitric Oxide and Cytokine Synthesis in Human African Trypanosomiasis. *Journal of Infectious Diseases* **184**, 1086-1090.

Maddox,P.H. and Jenkins,D. (1987) 3-Aminopropyltriethoxysilane (APES): a new advance in section adhesion. *Journal of Clinical Pathology* **40**, 1256-1257.

Maes,L., Vanderveken,M., Hamers,R., Doua,F., and Cattand,P. (1988) The monitoring of trypanocidal treatment with a sensitive ELISA method for measuring melarsoprol levels in serum and in cerebrospinal fluids. *Annales de la Societe Belge de Medecine Tropicale* **68**, 219-231.

Magnus,E., Van Meirvenne,N., and Vervoort,T. (1978) Card-Agglutination Test with Stained Trypanosomes (Catt) for Serological Diagnosis of *T b gambiense* Trypanosomiasis. *Annales de la Societe Belge de Medecine Tropicale* **58**, 169-176.

Mamont,P.S., Duchesne,M.C., Grove,J., and Bey,P. (1978) Anti-Proliferative Properties of Dl-Alpha-Difluoromethyl Ornithine in Cultured-Cells - Consequence of Irreversible Inhibition of Ornithine Decarboxylase. *Biochemical and Biophysical Research Communications* **81**, 58-66.

Mandal,B.K., Ogra,Y., and Suzuki,K.T. (2001) Identification of dimethylarsinous and monomethylarsonous acids in human urine of the arsenic-affected areas in West Bengal, India. *Chemical Research in Toxicology* **14**, 371-378.

Mandal,B.K., Ogra,Y., Anzai,K., and Suzuki,K.T. (2004) Speciation of arsenic in biological samples. *Toxicology and Applied Pharmacology* **198**, 307-318.

Manson-Bahr,P.E.C. and Charters,A.D. (1963) Myocarditis in African trypanosomiasis. *Transactions of the Royal Society of Tropical Medicine and Hygiene* **57**, 119-121.

Maser,P. and Kaminsky,R. (1998) Identification of three ABC transporter genes in *Trypanosoma brucei* spp. *Parasitology Research* **84**, 106-111.

Maser,P., Sutterlin,C., Kralli,A., and Kaminsky,R. (1999) A nucleoside transporter from *Trypanosoma brucei* involved in drug resistance. *Science* **285**, 242-244.

Masocha,W., Robertson,B., Rottenberg,M.E., Mhlanga,J., Sorokin,L., and Kristensson,K. (2004) Cerebral vessel laminins and IFN-gamma define *Trypanosoma brucei brucei* penetration of the blood-brain barrier. *Journal of Clinical Investigation* **114**, 689-694.

Masocha,W., Rottenberg,M.E., and Kristensson,K. (2007) Migration of African trypanosomes across the blood-brain barrier. *Physiology & Behavior* **92**, 110-114.

Massussi,J.A., Massussi,J.A., Mbida Mbida,J.A., Djieto-Lordon,C., Njiokou,F., LaveissiΦre,C., and van der Ploeg,J.D. (2010) Diversity and spatial distribution of vectors and hosts of *T. brucei gambiense* in forest zones of, Southern Cameroon: Epidemiological implications. *Acta Tropica* **114**, 44-48.

Matovu,E., Stewart,M.L., Geiser,F., Brun,R., Maser,P., Wallace,L.J.M., Burchmore,R.J., Enyaru,J.C.K., Barrett,M.P., Kaminsky,R., Seebeck,T., and de Koning,H.P. (2003) Mechanisms of Arsenical and Diamidine Uptake and Resistance in *Trypanosoma brucei*. *Eukaryotic Cell* **2**, 1003-1008.

Matsuda,K., Mera,Y., Segawa,Y., Uchida,I., Yokomine,A., and Takagi,K. (1983) Acute toxicity of study of gamma cyclodextrin in mice and rats. *Oyo Yakuri (Pharmacometrics)* **26**, 287-291.

Matsui,Y. and Mochida,K. (1979) Binding Forces Contributing to the Association of Cyclodextrin with Alcohol in An Aqueous-Solution. *Bulletin of the Chemical Society of Japan* **52**, 2808-2814.

Matzuzawa,M., Kawano,M., Nakamura,N., and Horikoshi,K. (1975) Improved Method for Preparation of Schardinger Beta-Dextrin on A Industrial Scale by Cyclodextrin Glycosyl Transferase of An Alkalophilic Bacillus Sp (Atcc21783). *Starke* **27**, 410-413.

Maudlin,I. (2006) African trypanosomiasis. *Annals of Tropical Medicine and Parasitology* **100**, 679-701.

Medana,I.M. and Turner,G.D.H. (2006) Human cerebral malaria and the blood-brain barrier. *International Journal for Parasitology* **36**, 555-568.

Melville, Majiwa, and Tait (2004) The African Trypanosome Genome. In: "The Trypanosomiases." Ed. Maudlin, Holmes, and Miles M.A. CABI Publishing. Trowbridge. pp39-57.

Miezan,T.W., Meda,H.A., Doua,F., Yapo,F.B., and Baltz,T. (1998) Assessment of central nervous system involvement in gambiense trypanosomiasis: value of the cerebro-spinal white cell count. *Tropical Medicine & International Health* **3**, 571-575.

Miles, Yeo, and Gaunt (2004) Epidemiology of American Trypanosomiasis. In: "The Trypanosomiases." Ed. Maudlin I, Holmes, and Miles M.A. CABI Publishing. Trowbridge. pp243-267.

Miyazawa,I., Ueda,H., Nagase,H., Endo,T., Kobayashi,S., and Nagai,T. (1995) Physicochemical Properties and Inclusion Complex-Formation of Delta-Cyclodextrin. *European Journal of Pharmaceutical Sciences* **3**, 153-162.

Moens,F., Dewilde,M., and Ngato,K. (1984) Clinical-Trial of Nifurtimox in Human African Trypanosomiasis. *Annales de la Societe Belge de Medecine Tropicale* **64**, 37-43.

Moser,D.R., Kirchhoff,L.V., and Donelson,J.E. (1989) Detection of *Trypanosoma cruzi* by DNA amplification using the polymerase chain reaction. *Journal of Clinical Microbiology* **27**, 1477-1482.

Mosi,R., He,S.M., Uitdehaag,J., Dijkstra,B.W., and Withers,S.G. (1997) Trapping and characterization of the reaction intermediate in cyclodextrin glycosyltransferase by use of activated substrates and a mutant enzyme. *Biochemistry* **36**, 9927-9934.

Mott (1906) Histological observations on sleeping sickness and other trypanosome infections. John Bale, sons & danielsson LTD.

Mulenga,C., Mhlanga,J.D., Kristensson,K., and Robertson,B. (2001) *Trypanosoma brucei brucei* crosses the blood-brain barrier while tight junction proteins are preserved in a rat chronic disease model. *Neuropathology and Applied Neurobiology* **27**, 77-85.

Nag and Begley (2005) Blood-brain barrier, exchange of metabolites and gases. In: "Pathology and Genetics. Cerebrovascular Diseases." Ed. Kalimo. Neuropath Press. Basel. pp22-29.

Nagai and Ueda (1996) Aspects of Drug Formulation with Cyclodextrins. In: "Comprehensive Supramolecular Chemistry Vol 3: Cyclodextrins." Ed. Szejtli and Osa. Elsevier Science. Oxford. pp441-450.

Nambu,N., Kikuchi,K., Kikuchi,T., Takahashi,Y., Ueda,H., and Nagai,T. (1978) Pharmaceutical Interaction in Dosage Forms and Processing .11. Influence of Inclusion of Non-Steroidal Anti-Inflammatory Drugs with Beta-Cyclodextrin on the Irritation to Stomach of Rats Upon Oral-Administration. *Chemical & Pharmaceutical Bulletin* **26**, 3609-3612.

Nare,B., Wring,S., Bacchi,C., Beaudet,B., Bowling,T., Brun,R., Chen,D., Ding,C., Freund,Y., Gaukel,E., Hussain,A., Jarnagin,K., Jenks,M., Kaiser,M., Mercer,L., Mejia,E., Noe,A., Orr,M., Parham,R., Plattner,J., Randolph,R., Rattendi,D., Rewerts,C., Sligar,J., Yarlett,N., Don,R., and Jacobs,R. (2010) Discovery of novel orally bioavailable oxaborole 6-carboxamides that demonstrate cure in a murine model of late-stage central nervous system african trypanosomiasis. *Antimicrobial Agents and Chemotherapy* **54**, 4379-4388.

Nelson,K.L. and Runge,V.M. (1995) Basic Principles of Mr Contrast. *Topics in Magnetic Resonance Imaging* **7**, 124-136.

Newberne,P.M., Conner,M.W., and Estes,P. (1988) The Influence of Food Additives and Related Materials on Lower Bowel Structure and Function. *Toxicologic Pathology* **16**, 184-197.

Newstead,R. (1911) A revision of the Tsetse-flies (Glossina), based on a study of the male genital armature. *Bulletin of Entomological Research* **2**, 9-36.

Nicolas,L., Prina,E., Lang,T., and Milon,G. (2002) Real-time PCR for detection and quantitation of Leishmania in mouse tissues. *Journal of Clinical Microbiology* **40**, 1666-1669.

Nikolskaia,O.V., de,A.L.A., Kim,Y.V., Lonsdale-Eccles,J.D., Fukuma,T., Scharfstein,J., and Grab,D.J. (2006) Blood-brain barrier traversal by African trypanosomes requires calcium signaling induced by parasite cysteine protease. *Journal of Clinical Investigation* **116**, 2739-2747.

Nishijo,J. and Nagai,M. (1991) Inclusion complex of 8-anilinonaphthalene-1-sulfonate with beta-cyclodextrin. *Journal of Pharmaceutical Sciences* **80**, 58-62.

Noireau,F., Gouteux,J.P., and Duteurtre,J.P. (1987) Catt Test Diagnostic-Value in Mass-Screening of Human Sleeping Sickness in Congo. *Bulletin de la Societe de Pathologie Exotique* **80**, 797-803.

Nuovo (1994) PCR in situ hybridization protocols and Applications. Raven Press. New York.

Ohtani,Y., Irie,T., Uekama,K., Fukunaga,K., and Pitha,J. (1989) Differential-Effects of Alpha-Cyclodextrins, Beta-Cyclodextrins and Gamma-Cyclodextrins on Human-Erythrocytes. *European Journal of Biochemistry* **186**, 17-22.

Onyango,J.D., Burri,C., and Brun,R. (2000) An automated biological assay to determine levels of the trypanocidal drug melarsoprol in biological fluids. *Acta Tropica* **74**, 95-100.

Orlando,J. and Arroz,L. (1987) Melarsoprol and reactive encephalopathy in *Trypanosoma brucei rhodesiense*. *Transactions of the Royal Society of Tropical Medicine and Hygiene* **81**, 192-192.

Ormerod (1970) Pathogenesis and Pathology of Trypanosomiasis in Man. In: "The African Trypanosomiases." Ed. Mulligan. George Allen and Unwin LTD. London. pp587-601.

Peeters,J., Neeskens,P., Tollenaere,J.P., Van Remoortere,P., and Brewster,M.E. (2002) Characterization of the interaction of 2-hydroxypropyl-beta-cyclodextrin with itraconazole at pH 2, 4, and 7. *Journal of Pharmaceutical Sciences* **91**, 1414-1422.

Pegg,A.E. and Mccann,P.P. (1982) Polyamine Metabolism and Function. *American Journal of Physiology* **243**, C212-C221.

Penet,M.F., Viola,A., Confort-Gouny,S., Le Fur,Y., Duhamel,G., Kober,F., Ibarrola,D., Izquierdo,M., Coltel,N., Gharib,B., Grau,G.E., and Cozzone,P.J. (2005) Imaging Experimental Cerebral Malaria *In Vivo*: Significant Role of Ischemic Brain Edema. *Journal of Neuroscience* **25**, 7352-7358.

Pentreath,V.W. (1989) Neurobiology of sleeping sickness. *Parasitology Today* **5**, 215-218.

Pepin,J. and Meda,H.A. (2001) The epidemiology and control of human African trypanosomiasis. *Advances in Parasitology* **49:71-132.**, 71-132.

Pepin,J., Milford,F., Meurice,F., Ethier,L., Loko,L., and Mpia,B. (1992) High-Dose Nifurtimox for Arseno-Resistant *Trypanosoma brucei gambiense* Sleeping Sickness - An Open Trial in Central Zaire. *Transactions of the Royal Society of Tropical Medicine and Hygiene* **86**, 254-256.

Pepin,J. and Milord,F. (1991) African trypanosomiasis and drug-induced encephalopathy: risk factors and pathogenesis. *Transactions of the Royal Society of Tropical Medicine and Hygiene* **85**, 222-224.

Pepin,J. and Milord,F. (1994) The treatment of human African trypanosomiasis. *Advances in Parasitology* **33:1-47.**, 1-47.

Pepin,J., Milord,F., Khonde,A., Niyonsenga,T., Loko,L., and Mpia,B. (1994) Gambiense trypanosomiasis: frequency of, and risk factors for, failure of melarsoprol therapy. *Transactions of the Royal Society of Tropical Medicine and Hygiene* **88**, 447-452.

Pepin,J., Milord,F., Khonde,A.N., Niyonsenga,T., Loko,L., Mpia,B., and De Wals,P. (1995) Risk factors for encephalopathy and mortality during melarsoprol treatment of *Trypanosoma brucei gambiense* sleeping sickness. *Transactions of the Royal Society of Tropical Medicine and Hygiene* **89**, 92-97.

Pepin,J., Milord,F., Mpia,B., Meurice,F., Ethier,L., Degroof,D., and Bruneel,H. (1989) An Open Clinical-Trial of Nifurtimox for Arseno-Resistant *Trypanosoma brucei gambiense* Sleeping Sickness in Central Zaire. *Transactions of the Royal Society of Tropical Medicine and Hygiene* **83**, 514-517.

Pepin,J., Guern,C., Ethier,L., Milord,F., Mpia,B., and Mansinsa,D. (1989) Trial of prednisolone for prevention of melarsoprol-induced encephalopathy in gambiense sleeping sickness. *Lancet* **333**, 1246-1250.

Persidsky,Y., Ramirez,S.H., Haorah,J., and Kanmogne,G.D. (2006) Blood-brain Barrier: Structural Components and Function Under Physiologic and Pathologic Conditions. *Journal of Neuroimmune Pharmacology* **1**, 223-236.

Philip,K.A., Dascombe,M.J., Fraser,P.A., and Pentreath,V.W. (1994) Blood-brain barrier damage in experimental African trypanosomiasis. *Annals of Tropical Medicine and Parasitology* **88**, 607-616.

Phillips,M.A. and Wang,C.C. (1987) A *Trypanosoma brucei* Mutant Resistant to Alpha-Difluoromethylornithine. *Molecular and Biochemical Parasitology* **22**, 9-17.

Picozzi,K., Fevre,E.M., Odiit,M., Carrington,M., Eisler,M.C., Maudlin,I., and Welburn,S.C. (2005) Sleeping sickness in Uganda: a thin line between two fatal diseases. *British Medical Journal* **331**, 1238-1241.

Pitha,J., Rao,C.T., Lindberg,B., and Seffers,P. (1990) Distribution of Substituents in 2-Hydroxypropyl Ethers of Cyclomaltoheptaose. *Carbohydrate Research* **200**, 429-435.

Pitha,J., Szabo,L., and Fales,H.M. (1987) Reaction of cyclodextrins with propylene oxide or with glycidol: Analysis of product distribution. *Carbohydrate Research* **168**, 191-198.

Pitha,J. and Szente,L. (1983) Rescue from hypervitaminosis A or potentiation or retinoid toxicity by different modes of cyclodextrin administration. *Life Sciences* **32**, 719-723.

Poltera,A.A. (1980) Immunopathological and chemotherapeutic studies in experimental trypanosomiasis with special reference to the heart and brain. *Transactions of the Royal Society of Tropical Medicine and Hygiene* **74**, 706-715.

Poltera,A.A. (1985) Pathology of human African trypanosomiasis with reference to experimental African trypanosomiasis and infections of the central nervous system. *British Medical Bulletin* **41**, 169-174.

Poltera,A.A., Cox,J.N., and Owor,R. (1976) Pancarditis Affecting Conducting System and All Valves in Human African Trypanosomiasis. *British Heart Journal* **38**, 827-837.

Poltera,A.A., Hochmann,A., Rudin,W., and Lambert,P.H. (1980) *Trypanosoma brucei brucei*: a model for cerebral trypanosomiasis in mice--an immunological, histological and electronmicroscopic study. *Clinical and Experimental Immunology* **40**, 496-507.

Priotto,G., Kasparian,S., Mutombo,W., Ngouama,D., Ghorashian,S., Arnold,U., Ghabri,S., Baudin,E., Buard,V., Kazadi-Kyanza,S., Ilunga,M., Mutangala,W., Pohlig,G., Schmid,C., Karunakara,U., Torreele,E., and Kande,V. (2009) Nifurtimox-eflornithine combination therapy for second-stage African *Trypanosoma brucei gambiense* trypanosomiasis: a multicentre, randomised, phase III, non-inferiority trial. *Lancet* **374**, 56-64.

Qi,Q. and Zimmermann,W. (2005) Cyclodextrin glucanotransferase: from gene to applications. *Applied Microbiology and Biotechnology* **66**, 475-485.

Rassi Jr,A., Rassi,A., and Marin-Neto,J.A. (2010) Chagas disease. *Lancet* **375**, 1388-1402.

Raz,B., Iten,M., GretherBuhler,Y., Kaminsky,R., and Brun,R. (1997) The Alamar Blue(R) assay to determine drug sensitivity of African trypanosomes (*T b rhodesiense and T b gambiense*) *in vitro*. *Acta Tropica* **68**, 139-147.

Rejdak,K., Jackson,S., and Giovannoni,G. (2010) Multiple sclerosis: a practical overview for clinicians. *British Medical Bulletin* **95**, 79-104.

Resh,M.D. (2006) Trafficking and signaling by fatty-acylated and prenylated proteins. *Nature Chemical Biology* **2**, 584-590.

Robertson,D.H. (1963) A trial of mel W in the treatment of *Trypanosoma rhodesiense* sleeping sickness. *Transactions of the Royal Society of Tropical Medicine and Hygiene* **57**, 274-289.

Roche (2002) DIG Application Manual for Nonradioactive In Situ Hydridization. Ed. Eisel, Grunewald-Janho, and Kruchen. Roche Diagnostics GmbH. Germany.

Rodgers,J. (2010) Trypanosomiasis and the brain. *Parasitology* **137**, 1995-2006.

Rodgers,J., McCabe,C., Gettinby,G., Bradley,B., Condon,B., and Kennedy,P.G.E. (2011) Magnetic Resonance Imaging to Assess Blood-Brain Barrier Damage in Murine Trypanosomiasis. *American Journal of Tropical Medicine and Hygiene* **84**, 344-350.

Rodgers,J., Stone,T.W., Barrett,M.P., Bradley,B., and Kennedy,P.G.E. (2009) Kynurenine pathway inhibition reduces central nervous system inflammation in a model of human African trypanosomiasis. *Brain* **132**, 1259-1267.

Rovaris,M. and Filippi,M. (2005) Defining the response to multiple sclerosis treatment: the role of conventional magnetic resonance imaging. *Neurological Sciences* **26**, S204-S208.

Ruiz,J.A., Simarro,P.P., and Josenando,T. (2002) Control of human African trypanosomiasis in the Quicama focus, Angola. *Bulletin of the World Health Organization* **80**, 738-745.

Runge,V.M., Muroff,L.R., and Jinkins,J.R. (2001) Central nervous system: review of clinical use of contrast media. *Topics in Magnetic Resonance Imaging* **12**, 231-263.

Sabbah,P., Brosset,C., Imbert,P., Bonardel,G., Jeandel,P., and Briant,J.F. (1997) Human African trypanosomiasis: MRI. *Neuroradiology* **39**, 708-710.

Saenger,W., Noltemeyer,M., Manor,P.C., Hingerty,B., and Klar,B. (1976) Topography of Cyclodextrin Inclusion Compounds .9. Induced-Fit-Type Complex-Formation of Model Enzyme Alpha-Cyclodextrin. *Bioorganic Chemistry* **5**, 187-195.

Sahraian,M.A. and Eshaghi,A. (2010) Role of MRI in diagnosis and treatment of multiple sclerosis. *Clinical Neurology and Neurosurgery* **112**, 609-615.

Sanderson,L., Dogruel,M., Rodgers,J., Bradley,B., and Thomas,S.A. (2008) The blood-brain barrier significantly limits eflornithine entry into *Trypanosoma brucei brucei* infected mouse brain. *Journal of Neurochemistry* **107**, 1136-1146.

Sands,M., Kron,M.A., and Brown,R.B. (1985) Pentamidine - A Review. *Reviews of Infectious Diseases* **7**, 625-634.

Santucci,L., Fiorucci,S., Chiucchiu,S., Sicilia,A., Bufalino,L., and Morelli,A. (1992) Placebo-controlled comparison of piroxicam-beta-cyclodextrin, piroxicam, and indomethacin on gastric potential difference and mucosal injury in humans. *Digestive Diseases and Sciences* **37**, 1825-1832.

Schardinger,F. (1903) Uber thermophile Bakterien aus verschiedenen Speisen und Milch. *Zeitschrift fur Lebensmitteluntersuchung und -Forschung A* **6**, 865-880.

Schlaeppi,K., Deflorin,J., and Seebeck,T. (1989) The major component of the paraflagellar rod of *Trypanosoma brucei* is a helical protein that is encoded by two identical, tandemly linked genes. *Journal of Cell Biology* **109**, 1695-1709.

Schlosshauer,B. (1993) The Blood-Brain-Barrier - Morphology, Molecules, and Neurothelin. *Bioessays* **15**, 341-346.

Schmid,C., Nkunku,S., Merolle,A., Vounatsou,P., and Burri,C. (2004) Efficacy of 10-day melarsoprol schedule 2 years after treatment for late-stage gambiense sleeping sickness. *Lancet* **364**, 789-790.

Schmid,C., Richer,M., Bilenge,C.M.M., Josenando,T., Chappuis,F., Manthelot,C.R., Nangouma,A., Doua,F., Asumu,P.N., Simarro,P.P., Burri,C., and Impamel,I.S. (2005) Effectiveness of a 10-day melarsoprol schedule for the treatment of late-stage human African trypanosomiasis: Confirmation from a multinational study (IMPAMEL II). *Journal of Infectious Diseases* **191**, 1922-1931.

Schmid (1996) Preparation and Industrial Production of Cyclodextrins. In: "Comprehensive Supramolecular Chemistry." Ed. Szejtli and Osa. Pergamon. Oxford. pp41-56.

Schmidt,H. and Bafort,J.M. (1985) African Trypanosomiasis - Treatment-Induced Invasion of Brain and Encephalitis. *American Journal of Tropical Medicine and Hygiene* **34**, 64-68.

Schultzberg,M., Ambatsis,M., Samuelsson,E.B., Kristensson,K., and Van Meirvenne,N. (1988) Spread of *Trypanosoma brucei* to the nervous system: early attack on circumventricular organs and sensory ganglia. *Journal of Neuroscience Research* **21**, 56-61.

Segal,M.B. (2000) The choroid plexuses and the barriers between the blood and the cerebrospinal fluid. *Cellular and Molecular Neurobiology* **20**, 183-196.

Seiler,K.U., Szathmary,S., Huss,H.J., Decoster,R., and Junge,W. (1990) Safety Profile and Intravenous Tolerance of Hydroxypropyl Beta-Cyclodextrin After Increasing Single Dose. *Minutes of the Fifth International Symposium on Cyclodextrins* 518-521.

Shahi,S.K., Krauth-Siegel,R.L., and Clayton,C.E. (2002) Overexpression of the putative thiol conjugate transporter TbMRPA causes melarsoprol resistance in *Trypanosoma brucei*. *Molecular Microbiology* **43**, 1129-1138.

Shimpi,S., Chauhan,B., and Shimpi,P. (2005) Cyclodextrins: application in different routes of drug administration. *Acta Pharmaceutica* **55**, 139-156.

Sibson,N.R., Blamire,A.M., Perry,V.H., Gauldie,J., Styles,P., and Anthony,D.C. (2002) TNF-alpha reduces cerebral blood volume and disrupts tissue homeostasis via an endothelin- and TNFR2-dependent pathway. *Brain* **125**, 2446-2459.

Simarro,P.P., Louis,F.J., and Jannin,J. (2003) [Sleeping sickness, forgotten illness: what are the consequences in the field?]. *Medecine Tropicale: revue du Corps de sante colonial* **63**,

Simarro,P.P., Ruiz,J.A., Franco,J.R., and Josenando,T. (1999) Attitude towards CATT-positive individuals without parasitological confirmation in the African Trypanosomiasis (*T.b. gambiense*) focus of Quicama (Angola). *Tropical Medicine & International Health* **4**, 858-861.

Simarro,P.P., Jannin,J., and Cattand,P. (2008) Eliminating Human African Trypanosomiasis: Where Do We Stand and What Comes Next? *PLoS Medicine* **5**, e55-

Sin,K.A., Nakamura,A., Kobayashi,K., Masaki,H., and Uozumi,T. (1991) Cloning and Sequencing of A Cyclodextrin Glucanotransferase Gene from Bacillus-Ohbensis and Its Expression in Escherichia-Coli. *Applied Microbiology and Biotechnology* **35**, 600-605.

Singh,D.K. and Lippman,S.M. (1998) Cancer chemoprevention - Part 2: Hormones, nonclassic antioxidant natural agents, NSAIDs, and other agents. *Oncology-New York* **12**, 1787-1800.

Sixbey,J.W., Nedrud,J.G., Raabtraub,N., Hanes,R.A., and Pagano,J.S. (1984) Epstein-Barr Virus-Replication in Oropharyngeal Epithelial-Cells. *New England Journal of Medicine* **310**, 1225-1230.

Sixt,M., Engelhardt,B., Pausch,F., Hallmann,R., Wendler,O., and Sorokin,L.M. (2001) Endothelial Cell Laminin Isoforms, Laminins 8 and 10, Play Decisive Roles in T Cell Recruitment across the Blood Brain Barrier in Experimental Autoimmune Encephalomyelitis. *Journal of Cell Biology* **153**, 933-946.

Sloof,P., Bos,J.L., Konings,A.F., Menke,H.H., Borst,P., Gutteridge,W.E., and Leon,W. (1983) Characterization of satellite DNA in *Trypanosoma brucei* and *Trypanosoma cruzi*. *Journal of Molecular Biology* **167**, 1-21.

Sloof,P., Menke,H.H., Caspers,M.P., and Borst,P. (1983) Size fractionation of *Trypanosoma brucei* DNA: localization of the 177-bp repeat satellite DNA and a variant surface glycoprotein gene in a mini-chromosomal DNA fraction. *Nucleic Acids Research* **11**, 3889-3901.

Smith,J.M., Smith,N.H., O'Rourke,M., and Spratt,B.G. (1993) How clonal are bacteria? *Proceedings of the National Academy of Sciences of the United States of America* **90**, 4384-4388.

Soignet,S.L., Tong,W.P., Hirschfeld,S., and Warrell,J. (1999) Clinical study of an organic arsenical, melarsoprol, in patients with advanced leukemia. *Cancer Chemotherapy and Pharmacology* **44**, 417-421.

Steiger,R.F. (1973) On the Ultrastructure of *Trypanosoma brucei* in the Course of Its Life Cycle and Some Related Aspects. *Acta Tropica* **30**, 64-168.

Stella,V.J., Rao,V.M., Zannou,E.A., and Zia,V. (1999) Mechanisms of drug release from cyclodextrin complexes. *Advanced Drug Delivery Reviews* **36**, 3-16.

Stephens,J.W.W. and Fantham,H.B. (1910) On the Peculiar Morphology of a Trypanosome from a Case of Sleeping Sickness and the Possibility of Its Being a New Species (*T. rhodesiense*). *Proceedings of the Royal Society of London.Series B, Containing Papers of a Biological Character* **83**, 28-33.

Sternberg,J., Turner,C.M.R., Wells,J.M., Ranford-Cartwright,L.C., Lepage,R.W.F., and Tait,A. (1989) Gene exchange in African trypanosomes: frequency and allelic segregation. *Molecular and Biochemical Parasitology* **34**, 269-280.

Stevens,D.R. and Moulton,J.E. (1977) Experimental Meningoencephalitis in *Trypanosoma brucei* Infection of Deer Mice (Peromyscus-Maniculatus) - Light, Immunofluorescent, and Electron-Microscopic Study. *Acta Neuropathologica* **38**, 173-180.

Stevens and Brisse (2004) Systematics of Trypanosomes of medical and Veterinary Importance. In: "The Trypanosomiases." Ed. Maudlin, Holmes, and Miles M.A. CABI Publishing. Trowbridge. pp1-23.

Stover,C.K., Warrener,P., VanDevanter,D.R., Sherman,D.R., Arain,T.M., Langhorne,M.H., Anderson,S.W., Towell,J.A., Yuan,Y., McMurray,D.N., Kreiswirth,B.N., Barry,C.E., and Baker,W.R. (2000) A small-molecule nitroimidazopyran drug candidate for the treatment of tuberculosis. *Nature* **405**, 962-966.

Stratagene (2004) Introduction to Quantitative PCR: Methods and Application Guide. Stratagene. California.

Stroop,W.G., Rock,D.L., and Fraser,N.W. (1984) Localization of Herpes-Simplex Virus in the Trigeminal and Olfactory Systems of the Mouse Central Nervous-System During Acute and Latent Infections by In situ Hybridization. *Laboratory Investigation* **51**, 27-38.

Szejtli (1988) Cyclodextrin Technology. Kluwer Academic Publishers. Dordrecht.

Szejtli (1996) Chemistry, Physical and Biological Properties of Cyclodextrins. In: "Comprehensive Supramolecular Chemistry." Ed. Szejtli and Osa. Pergamon. Oxford. pp5-40.

Szejtli,J. (1998) Introduction and General Overview of Cyclodextrin Chemistry. *Chemical Reviews* **98**, 1743-1754.

Szejtli (1999) Inclusion of Guest Molecules, Selectivity and Molecular Recognition by Cyclodextrins. In: "Comprehensive Supramolecular Chemistry." Ed. Szejtli and Osa. Pergamon. Oxford. pp189-203.

Szejtli,J. (2004) Past, present, and future of cyclodextrin research. *Pure and Applied Chemistry* **76**, 1825-1845.

Szejtli,J. and Sebestyen,G. (1979) Resorption, Metabolism and Toxicity Studies on the Peroral Application of Beta-Cyclodextrin. *Starke* **31**, 385-389.

Szente,L. and Szejtli,J. (1999) Highly soluble cyclodextrin derivatives: chemistry, properties, and trends in development. *Advanced Drug Delivery Reviews* **36**, 17-28.

Tait,A. (1980) Evidence for diploidy and mating in trypanosomes. *Nature* **287**, 536-538.

Takano,T., Fukuda,M., Monma,M., Kobayashi,S., Kainuma,K., and Yamane,K. (1986) Molecular-Cloning, Dna Nucleotide Sequencing, and Expression in Bacillus-Subtilis Cells of the Bacillus-Macerans Cyclodextrin Glucanotransferase Gene. *Journal of Bacteriology* **166**, 1118-1122.

Talmi,Y. and Bostick,D.T. (1975) Determination of Arsenic and Arsenicals. *Journal of Chromatographic Science* **13**, 231-237.

Tang,Y.L., Hapip,C.A., Liu,B., and Fang,C.T. (2006) Highly sensitive TaqMan RT-PCR assay for detection and quantification of both lineages of West Nile virus RNA. *Journal of Clinical Virology* **36**, 177-182.

Thompson,A.J., Toosy,A.T., and Ciccarelli,O. (2010) Pharmacological management of symptoms in multiple sclerosis: current approaches and future directions. *Lancet Neurology* **9**, 1182-1199.

Thompson,D.O. (1997) Cyclodextrins--enabling excipients: their present and future use in pharmaceuticals. *Critical Reviews in Therapeutic Drug Carrier Systems* **14**, 1-104.

Tibayrenc,M., Kjellberg,F., and Ayala,F.J. (1990) A clonal theory of parasitic protozoa: The population structures of Entamoeba, Giardia, Leishmania, Naegleria, Plasmodium, Trichomonas and Trypanosoma and their medical and taxonomical consequences. *Proceedings of the National Academy of Sciences of the United States of America* **87**, 2414-2418.

Til,H.P. and Bar,A. (1998) Subchronic (13-week) oral toxicity study of gamma-cyclodextrin in dogs. *Regulatory Toxicology and Pharmacology* **27**, 159-165.

Timpl,R. and Brown,J.C. (1994) The Laminins. *Matrix Biology* **14**, 275-281.

Tokumura,T., Nanba,M., Tsushima,Y., Tatsuishi,K., Kayano,M., Machida,Y., and Nagai,T. (1986) Enhancement of Bioavailability of Cinnarizine from Its Beta-Cyclodextrin Complex on Oral-Administration with Deuterium-L-Phenylalanine As A Competing Agent. *Journal of Pharmaceutical Sciences* **75**, 391-394.

Tokumura,T., Tsushima,Y., Tatsuishi,K., Kayano,M., Machida,Y., and Nagai,T. (1985) Evaluation of Bioavailability Upon Oral-Administration of Cinnarizine-Beta-Cyclodextrin Inclusion Complex to Beagle Dogs. *Chemical & Pharmaceutical Bulletin* **33**, 2962-2967.

Tokumura,T., Ueda,H., Tsushima,Y., Kasai,M., Kayano,M., Amada,I., and Nagai,T. (1984) Physicochemical Approach to Biopharmaceutical Phenomena .41. Inclusion Complexes of Cinnarizine with Beta-Cyclodextrin in Aqueous-Solution and in the Solid-State. *Chemical & Pharmaceutical Bulletin* **32**, 4179-4184.

Tomono,K., Gotoh,H., Okamura,M., Ueda,H., Saitoh,T., and Nagai,T. (1988) Effect of Beta Cyclodextrin and Its Derivatives on the Photostability of Photosensitive Drugs. *Yakuzaigaku* **48**, 322-325.

Torreele,E., Bourdin,T.B., Tweats,D., Kaiser,M., Brun,R., Mazue,G., Bray,M.A., and Pecoul,B. (2010) Fexinidazole - a new oral nitroimidazole drug candidate entering clinical development for the treatment of sleeping sickness. *PLos Neglected Tropical Diseases* **4**, e923-

Tunggal,P., Smyth,N., Paulsson,M., and Ott,M.C. (2000) Laminins: Structure and genetic regulation. *Microscopy Research and Technique* **51**, 214-227.

U.S. Department of Health and Human Services (2005) Guidance for Industry: Estimating the Maximum Safe Starting Dose in Initial Clinical Trials for Therapeutics in Adult Healthy Volunteers. 1-30. Centre for Drug Evaluation and Research (CDER)

Uekama,K. (1985) Pharmaceutical Applications of Methylated Cyclodextrins. *Pharmacy International* **6**, 61-65.

Uekama,K., Fujinaga,T., Hirayama,F., Otagiri,M., Kurono,Y., and Ikeda,K. (1982) Effects of Cyclodextrins on the Acid-Hydrolysis of Digoxin. *Journal of Pharmacy and Pharmacology* **34**, 627-630.

Uekama,K., Irie,T., Sunada,M., Otagiri,M., Iwasaki,K., Okano,Y., Miyata,T., and Kase,Y. (1981a) Effects of Cyclodextrins on Chlorpromazine-Induced Hemolysis and Central Nervous-System Responses. *Journal of Pharmacy and Pharmacology* **33**, 707-710.

Uekama,K., Irie,T., Sunada,M., Otagiri,M., and Tsubaki,K. (1981b) Protective Effects of Cyclodextrins on Drug-Induced Hemolysis Invitro. *Journal of Pharmacobio-Dynamics* **4**, 142-144.

Uekama,K., Narisawa,S., Hirayama,F., and Otagiri,M. (1983) Improvement of Dissolution and Absorption Characteristics of Benzodiazepines by Cyclodextrin Complexation. *International Journal of Pharmaceutics* **16**, 327-338.

Uekama,K. and Otagiri,M. (1987) Cyclodextrins in Drug Carrier Systems. *Critical Reviews in Therapeutic Drug Carrier Systems* **3**, 1-40.

Uekama,K., Hirayama,F., and Irie,T. (1998) Cyclodextrin Drug Carrier Systems. *Chemical Reviews* **98**, 2045-2076.

Uitdehaag,J.C., Mosi,R., Kalk,K.H., van der Veen,B.A., Dijkhuizen,L., Withers,S.G., and Dijkstra,B.W. (1999) X-ray structures along the reaction pathway of cyclodextrin glycosyltransferase elucidate catalysis in the alpha-amylase family. *Nature Structural and Molecular Biology* **6**, 432-436.

Uitdehaag,J.C.M., Kalk,K.H., van der Veen,B.A., Dijkhuizen,L., and Dijkstra,B.W. (1999) The Cyclization Mechanism of Cyclodextrin Glycosyltransferase (CGTase) as Revealed by a +¦-Cyclodextrin-CGTase Complex at 1.8-+à Resolution. *Journal of Biological Chemistry* **274**, 34868-34876.

van der Veen,B.A., Uitdehaag,J.C.M., Dijkstra,B.W., and Dijkhuizen,L. (2000) Engineering of cyclodextrin glycosyltransferase reaction and product specificity. *Biochimica et Biophysica Acta (BBA) - Protein Structure and Molecular Enzymology* **1543**, 336-360.

Van Hoof,L., Henrard,C., and Peel,E. (1944) Pentamidine in the prevention and treatment of trypanosomiasis. *Transactions of the Royal Society of Tropical Medicine and Hygiene* **37**, 271-280.

Van Schaftingen,E., Opperdoes,F.R., and Hers,H.-G. (1987) Effects of Various Metabolic Conditions and of the Trivalent Arsenical Melarsen Oxide on the Intracellular Levels of Fructose 2 6-Bisphosphate and of Glycolytic Intermediates in *Trypanosoma-brucei*. *European Journal of Biochemistry* **166**, 653-662.

Van Voorhis,W.C., Schlekewy,L., and Trong,H.L. (1991) Molecular mimicry by *Trypanosoma cruzi*: the F1-160 epitope that mimics mammalian nerve can be mapped to a 12-amino acid peptide. *Proceedings of the National Academy of Sciences of the United States of America* **88**, 5993-5997.

Vanpeer,A., Woestenborghs,R., Heykants,J., Gasparini,R., and Gauwenbergh,G. (1989) The Effects of Food and Dose on the Oral Systemic Availability of Itraconazole in Healthy-Subjects. *European Journal of Clinical Pharmacology* **36**, 423-426.

Vansterkenburg,E.L.M., Coppens,I., Wilting,J., Bos,O.J.M., Fischer,M.J.E., Janssen,L.H.M., and Opperdoes,F.R. (1993) The Uptake of the Trypanocidal Drug Suramin in Combination with Low-Density Lipoproteins by *Trypanosoma brucei* and Its Possible Mode of Action. *Acta Tropica* **54**, 237-250.

Vickerman (1970) Ultrastructure of Trypanosoma and Relation to Function. In: "The African Trypanosomiases." Ed. Mulligan. George Allen and Unwin LTD. London. pp60-66.

Vickerman,K., Tetley,L., Hendry,K.A.K., and Turner,C.M.R. (1988) Biology of African Trypanosomes in the Tsetse-Fly. *Biology of the Cell* **64**, 109-119.

Vickerman,K. (1985) Developmental cycles and biology of pathogenic trypanosomes. *British Medical Bulletin* **41**, 105-114.

Villiers,A. (1891) Sur la fermentation de la f´ecule par l'action du ferment

butyrique. *Comptes Rendus Hebdomadaires des Seances de l'Academie des Science* **112**, 536-538.

Voogd,T.E., Vansterkenburg,E.L.M., Wilting,J., and Janssen,L.H.M. (1993) Recent Research on the Biological-Activity of Suramin. *Pharmacological Reviews* **45**, 177-203.

Wang,C.C. (1995) Molecular Mechanisms and Therapeutic Approaches to the Treatment of African Trypanosomiasis. *Annual Review of Pharmacology and Toxicology* **35**, 93-127.

Watson,H.J. (1962) Mel W: A field trial in the treatment of *Trypanosoma gambiense* sleeping sickness. *Transactions of the Royal Society of Tropical Medicine and Hygiene* **56**, 231-235.

Watson,H.J. (1965) Mel W: Final report on a field trial in the treatment of *Trypanosoma gambiense* sleeping sickness. *Transactions of the Royal Society of Tropical Medicine and Hygiene* **59**, 163-170.

Weishaupt, Kochli, and Marincek (2006a) Image Contrast. In: "How Does MRI Work? An Introduction to the Physics and Function of Magnetic Resonance Imaging." Ed. Weinshenker, Kochli, and Marincek. Springer. Berlin. pp11-20.

Weishaupt, Kochli, and Marincek (2006b) Spin and Nuclear Magnetic Resonance Phenomenon. In: "How Does MRI Work? An Introduction to the Physics and Function of Magnetic Resonance Imaging." Ed. Weishaupt, Kochli, and Marincek. Springer. Berlin. pp1-5.

Welage,L.S., Carver,P.L., Revankar,S., Pierson,C., and Kauffman,C.A. (1995) Alterations in gastric acidity in patients infected with human immunodeficiency virus. *Clinical Infectious Diseases* **21**, 1431-1438.

Welburn,S.C., Fevre,E.M., Coleman,P.G., Odiit,M., and Maudlin,I. (2001) Sleeping sickness: a tale of two diseases. *Trends in Parasitology* **17**, 19-24.

Wenzler,T., Boykin,D.W., Ismail,M.A., Hall,J.E., Tidwell,R.R., and Brun,R. (2009) New Treatment Option for Second-Stage African Sleeping Sickness: *In Vitro* and *In Vivo* Efficacy of Aza Analogs of DB289. *Antimicrobial Agents and Chemotherapy* **53**, 4185-4192.

Wickstead,B., Ersfeld,K., and Gull,K. (2003) Repetitive Elements in Genomes of Parasitic Protozoa. *Microbiology and Molecular Biology Reviews* **67**, 360-375.

Willems,L., Van der Geest,R., and de Beule,K. (2001) Itraconazole oral solution and intravenous formulations: a review of pharmacokinetics and pharmacodynamics. *Journal of Clinical Pharmacy and Therapeutics* **26**, 159-169.

Williamson (1970) Review of Chemotherapeutic and Chemoprophylactic Agents. In: "The African Trypanosomiases." Ed. Mulligan. George Allen and Unwin LTD. London. pp125-221.

Willson,M., Callens,M., Kuntz,D.A., Perie,J., and Opperdoes,F.R. (1993) Synthesis and Activity of Inhibitors Highly Specific for the Glycolytic-Enzymes from *Trypanosoma-brucei*. *Molecular and Biochemical Parasitology* **59**, 201-210.

Wind,R.D., Uitdehaag,J.C.M., Buitelaar,R.M., Dijkstra,B.W., and Dijkhuizen,L. (1998) Engineering of cyclodextrin product specificity and pH optima of the thermostable cyclodextrin glycosyltransferase from Thermoanaerobacterium thermosulfurigenes EM1. *Journal of Biological Chemistry* **273**, 5771-5779.

Wong,J.W. and Yuen,K.H. (2001) Improved oral bioavailability of artemisinin through inclusion complexation with beta- and gamma-cyclodextrins. *International Journal of Pharmaceutics* **227**, 177-185.

Woo,P. (1970) The haemocrit centrifuge technique for the diagnosis of African trypanosomiasis. *Acta Tropica* **27**,

Woo,P.T.K. (1971) Evaluation of the Hematocrit Centrifuge and Other Techniques for the Field Diagnosis of Human Trypanosomiasis and Filariasis. *Acta Tropica* **28**, 298-303.

World Health Organisation (1986) Epidemiology and control of African trypanosomiasis. *Report of a WHO Expert Committee, Technical Report Series* **739**, 1-125.

World Health Organisation (1987) Principles for the Safety Assessment of Food Additives and Contaminants in Food. *Environmental Health Criteria* **70**, 1-174.

World Health Organisation (1998) Control and surveillance of African trypanosomiasis. Technical Report Series No 881 Geneve

World Health Organisation (2004) Global Burden of Disease (GBD) 2004 update. *World Health Organisation* http://www.who.int/healthinfo/global_burden_disease/GBD_report_2004update_AnnexA.pdf

World Health Organisation (2009) WHO includes combination of eflornithine and nifurtimox in its Essential List of Medicines for the treatment of human African trypanosomiasis. *World Health Organisation* http://www.who.int/neglected_diseases/disease_management/drug_combination/en/index.html

World Health Organisation (2010) Human African trypanosomiasis: number of new cases drops to historically low level in 50 years. http://www.who.int/neglected_diseases/integrated_media/integrated_media_hat_june_2010/en/index.html

Yeates,C. (2003) DB-289 Immtech International. *Idrugs* **6**, 1086-1093.

Zillmann,S., Konstantinov,M., Berger,M., and Braun,R. (1996) Improved performance of the anion-exchange centrifugation technique for studies with human infective African trypanosomes. *Acta Tropica* **62**, 183-187.

Zillmann,U. and Albiez,E.J. (1986) The Testryp Catt (Card Agglutination-Test for Trypanosomiasis) - A Field-Study on Gambiense Sleeping Sickness in Liberia. *Tropical Medicine and Parasitology* **37**, 390-392.

Zirar,S.B., Astier,A., Muchow,M., and Gibaud,S. (2008) Comparison of nanosuspensions and hydroxypropyl-beta-cyclodextrin complex of melarsoprol: Pharmacokinetics and tissue distribution in mice. *European Journal of Pharmaceutics and Biopharmaceutics* **70**, 649-656.

Zirar,S.B., Gibaud,S., Camut,A., and Astier,A. (2007) Pharmacokinetics and tissue distribution of the antileukaemic organoarsenicals arsthinol and melarsoprol in mice. *Journal of Organometallic Chemistry* **692**, 1348-1352.

zur Muhlen,C., Sibson,N.R., Peter,K., Campbell,S.J., Wilainam,P., Grau,G.E., Bode,C., Choudhury,R.P., and Anthony,D.C. (2008) A contrast agent recognizing activated platelets reveals murine cerebral malaria pathology undetectable by conventional MRI. *Journal of Clinical Investigation* **118**, 1198-1207.